Assigning functions to Hfq-dependent small RNAs in the model pathogen *Salmonella* Typhimurium

Dissertation

zur Erlangung des naturwissenschaftlichen Doktorgrades
der Bayerischen Julius-Maximilians-Universität Würzburg

vorgelegt von

Kathrin Sophie Fröhlich

aus Ulm

Würzburg 2012

Eingereicht am: 02.10.2012

Mitglieder der Promotionskommission:

Vorsitzender: Prof. Dr. Wolfgang Rössler

1. Gutachter: Prof. Dr. Jörg Vogel

2. Gutachter: Prof. Dr. Thomas Rudel

3. Gutachter: Prof. Dr. Gerhart Wagner

Tag des Promotionskolloquiums: 25.01.2013

Summary

Non-coding RNAs constitute a major class of regulators involved in bacterial gene expression. A group of riboregulators of heterogeneous size and shape referred to as small regulatory RNAs (sRNAs) control *trans*- or *cis*-encoded genes through direct base-pairing with their mRNAs. Although mostly inhibiting their target mRNAs, several sRNAs also induce gene expression. An important co-factor for sRNA activity is the RNA chaperone, Hfq, which is able to rearrange intramolecular secondary structures and to promote annealing of complementary RNA sequences. In addition, Hfq protects unpaired RNA from degradation by ribonucleases and thus increases sRNA stability. Co-immunoprecipitation of RNA with the Hfq protein, and further experimental as well as bioinformatical studies performed over the last decade suggested the presence of more than 150 different sRNAs in various *Enterobacteria* including *Escherichia coli* and *Salmonellae*. So-called core sRNAs are considered to fulfill central cellular activities as deduced from their high degree of conservation among different species. Approximately 25 core sRNAs have been implicated in gene regulation under a variety of environmental responses. However, for the majority of sRNAs, both the riboregulators' individual biological roles as well as modes of action remain to be elucidated. The current study aimed to define the cellular functions of the two highly conserved, Hfq-dependent sRNAs, SdsR and RydC, in the model pathogen *Salmonella* Typhimurium.

SdsR had been known as one of the most abundant sRNAs during stationary growth phase in *E. coli*. Examination of the conservation patterns in the *sdsR* promoter region in combination with classic genetic analyses revealed SdsR as the first sRNA under direct transcriptional control of the alternative σ factor σ^S. In *Salmonella*, over-expression of SdsR down-regulates the synthesis of the major porin OmpD, and the interaction site in the *ompD* mRNA coding sequence was mapped by a 3'RACE-based approach. At the post-transcriptional level, expression of *ompD* is controlled by three additional sRNAs, but SdsR plays a specific role in porin regulation during the stringent response.

Similarly, RydC, the second sRNA adressed in this study, was initially discovered in *E. coli* but appeared to be conserved in many related γ-proteobacteria. An interesting aspect of this Hfq-dependent sRNAs is its secondary structure involving a pseudo-knot configuration, while the 5' end remains single stranded. A transcriptomic approach combining RydC pulse-expression and scoring of global mRNA changes on microarrays was employed to identify the targets of this sRNA. RydC specifically activated expression of the longer of two versions of the *cfa* mRNA encoding for the phospholipid-modifying enzyme cyclopropane fatty acid synthase. Employing its conserved single-stranded 5' end, RydC acts as a positive regulator and masks a recognition site of the endoribonuclease, RNase E, in the *cfa* leader.

Zusammenfassung

Die bakterielle Genexpression wird unter anderem maßgeblich von nicht-kodierenden RNAs bestimmt. Kleine regulatorische RNAs (sRNAs) sind eine bezüglich Größe und Struktur heterogene Gruppe von Riboregulatoren, die ihre *in cis* oder *in trans*-kodierten Zielgene mittels direkter Basenpaarungen kontrollieren. Während der Großteil der sRNAs reprimierend wirkt, konnte für einige RNAs gezeigt werden, dass sie die Expression ihres Zieltranskripts verstärken. Ein wichtiger Kofaktor für die regulatorische Funktion der sRNAs ist das RNA-Chaperon Hfq, welches sowohl die Umfaltung intramolekularer Sekundärstrukturen ermöglicht, als auch die Ausbildung von Basenpaarungen zwischen komplementären RNA-Sequenzen steuert. Zusätzlich schützt Hfq nicht-gepaarte RNAs vor dem Abbau durch Ribonukleasen, und trägt damit zur Stabilität der Moleküle bei. Durch Ko-Immunopräzipitation mit Hfq sowie in weiteren experimentellen als auch bioinformatischen Studien konnten im letzten Jahrzehnt in diversen Enterobakterien, wie z.B. auch *Escherichia coli* und *Salmonellae*, mehr als 150 verschiedene sRNAs bestimmt werden. Von so genannten "core sRNAs" (Kern-sRNAs) wird aufgrund ihres hohen Grades an Konservierung in unterschiedlichen Spezies angenommen, dass sie zentrale Funktionen erfüllen. Etwa 25 core sRNAs agieren unter verschiedenen Umweltbedingungen als Regulatoren. Ihre exakte biologische Rolle, sowie ihre Funktionsweise sind jedoch größtenteils noch unbekannt. In der vorliegenden Arbeit wurden die beiden konservierten, Hfq-abhängigen sRNAs, SdsR und RydC, im Modellpathogen *Salmonella* Typhimurium charakterisiert.

SdsR war als eine der abundantesten sRNAs der stationären Phase in *E. coli* beschrieben worden. Durch Auswertung der Konservierungsmuster der *sdsR* Promotorsequenz sowie klassische genetische Analyse konnte SdsR als erste sRNA unter direkter Kontrolle des alternativen σ Faktors σ^S bestimmt werden. In *Salmonella* führt die Überexpression von SdsR zur Reprimierung des Membranporins OmpD, und die Bindestelle von SdsR auf dem *ompD* Transkript wurde mittels einer auf 3'-RACE basierenden Methode ermittelt. Obwohl die Expression von *ompD* auf post-transkriptionaler Ebene von drei weiteren sRNAs kontrolliert wird, konnte eine spezische Regulation des Porins durch SdsR während Aminosäure-Hungerung gezeigt werden.

Auch RydC, die zweite in dieser Studie analysierte sRNA, wurde zunächst in *E. coli* beschrieben und ist aber auch in weiteren γ-Proteobakterien konserviert. Interessanterweise enthält die Sekundärstruktur dieser Hfq-abhängigen sRNA einen Pseudoknoten, während das 5'-Ende ungepaart ist. Die Zielgene von RydC wurden mittels einer Transkriptomanalyse bestimmt, in der die Änderung der Häufigkeitsverteilung aller mRNAs nach kurzzeitiger Überexpression der sRNA auf Microarrays untersucht wurde. RydC bewirkte die spezifische Aktivierung des längeren von insgesamt zwei Versionen der *cfa* mRNA, die für eine Cyclopropan-fettsäuresynthase kodiert, ein Enzym das zur Modifikation von Phospholipiden dient. Eine

Basenpaarung über das freie 5'-Ende der sRNA RydC führt zur Aktivierung der *cfa*-Expression, und maskiert eine Erkennungssequenz der Endoribonuklease, RNase E, innerhalb des Transkripts.

Index

1 Introduction 1

1.1 Gene expression regulation in bacteria 1
1.2 Base-pairing small RNAs 2
1.2.1 sRNA-mediated repression of gene expression 3
1.2.2 Activation of gene expression by sRNAs 5
1.3 Proteins required for the regulatory function of sRNAs 8
1.3.1 The RNA chaperone Hfq 8
1.3.2 The major ribonuclease RNase E 10
1.4 The model pathogen *Salmonella* Typhimurium 11
1.5 Identification and functional characterization of sRNAs in *Salmonella* 12
1.6 Aim of the study 14

2 Characterization of the conserved σ^S-dependent small RNA SdsR in *Salmonella* ..16

2.1 SdsR is highly abundant in stationary phase cells 16
2.2 SdsR expression depends on the alternative σ factor σ^S 18
2.3 SdsR exhibits σ^S-dependent regulation under stress 22
2.4 The influence of SraC on SdsR expression 25
2.5 SdsR represses synthesis of the major porin OmpD 28
2.6 Requirement of the SdsR 5’ end for *ompD* regulation 30
2.7 SdsR regulates *ompD* mRNA post-transcriptionally 32
2.8 Coding-sequence targeting of *ompD* mRNA by SdsR 32
2.9 SdsR requires RNase E for *ompD* mRNA decay 34
2.10 A 3’RACE-based approach to target site identification 36
2.11 Validation of the SdsR binding site on *ompD* mRNA 37
2.12 The *ompD* translation initiation site is not refractory to sRNA targeting 39
2.13 Overlapping and specific regulation of *ompD* expression by SdsR and RybB sRNAs 41
2.14 Concluding remarks 43

3 The conserved 5’ end of RydC sRNA activates one of two isoforms of *cfa* mRNA..44

3.1 RydC sRNA is constitutively expressed in *Salmonella* 44
3.2 The molecular architecture of RydC sRNA determines its stability 46
3.3 Transcriptome-based identification of RydC targets 50
3.4 The *cfa* mRNA is positively regulated by RydC 53
3.5 RydC selectively activates the longer of two *cfa* mRNA isoforms 54
3.6 RydC and *cfa* promoter architectures are conserved 56
3.7 Identification of the RydC binding site on *cfa* mRNA 58

3.8 The 5’ end of RydC is sufficient to activate *cfa* expression 60
3.9 A 5’ inhibitory element within the long *cfa* mRNA 61
3.10 Processing of the *cfa* mRNA in the presence of RydC 65
3.11 Involvement of ribonucleases in RydC-mediated regulation of *cfa* 67
3.12 Reconstitution of RNase E-mediated cleavage of *cfa* mRNA *in vitro* 71
3.13 The role of RydC in induction of *cfa* under different stress conditions 74
3.14 Transcriptional regulation of *rydC* 76
3.15 Concluding remarks 80

4 Appendices 81

4.1 Global transcriptome analysis of five enterobacterial species 81
4.2 On the necessity of 5' end determination 89
4.3 Supplementary figures 93

5 Discussion 95

5.1 Post-transcriptional control by small RNAs 95
5.2 Identification of bacterial sRNAs 96
5.2.1 SdsR is highly conserved among Enterobacteria 97
5.2.2 The RydC pseudoknot: form follows function 100
5.3 Integration of core sRNAs into cellular networks 101
5.3.1 SdsR is directly controlled by the alternative σ factor σ^S 101
5.3.2 SdsR regulates expression of the major porin OmpD 103
5.3.3 Transcriptional control of RydC 105
5.3.4 Physiological consequences of RydC-mediated *cfa* activation 107
5.4 The mechanisms employed by Hfq-dependent sRNAs 109
5.4.1 SdsR represses *ompD* by binding within the deep coding sequence 110
5.4.2 RydC activates *cfa* mRNA 112
5.5 Identification of sRNA binding sites 115
5.5.1 RydC interacts with a conserved sequence stretch within the *cfa* 5’ UTR 115
5.5.2 A 3'RACE approach to identify the SdsR binding site on *ompD* mRNA 115
5.6 Conclusions and perspective 117

6 Material and Methods 118

6.1 General equipment 118
6.2 Consumables 119
6.3 Chemicals and commercially available systems 119
6.4 Enzymes and size markers 121
6.5 Purified proteins and antibodies 122

6.6 Synthetic oligonucleotides 122
6.7 Bacterial strains and plasmids 125
6.8 Media and media stocks 134
6.9 Media supplements 135
6.10 Buffers and solutions 136
6.11 Sterilization 139
6.12 Microbiological Methods 140
6.12.1 Standard growth conditions 140
6.12.2 Growth under SPI-1-inducing conditions 140
6.12.3 Growth under SPI-2-inducing conditions 140
6.12.4 Growth in M9 minimal medium 140
6.12.5 Induction of heat-shock 140
6.12.6 Induction of osmotic shock 140
6.12.7 Induction of amino acid starvation 140
6.12.8 Induction of envelope stress 140
6.12.9 Induction of acetate stress 141
6.12.10 Transformation of chemically competent *E. coli* 141
6.12.11 Transformation of electrocompetent *E. coli* 141
6.12.12 P1 transduction 141
6.12.13 Transformation of *Salmonella* 141
6.12.14 P22 transduction 142
6.12.15 One-step integration into the chromosome 142
6.12.16 Construction of *Salmonella* chromosomal *rydC'::lacZ*$^{+}$ reporter fusions 143
6.12.17 Construction of a *E.coli* chromosomal P*rydC'::lacZ*$^{+}$ reporter fusion 143
6.12.18 Screening for transcriptional regulators by transposon insertion 143
6.12.19 Determination of lacZ activity (β-galactosidase assay) 144
6.13 Molecular biological methods 144
6.13.1 Determination of concentration of nucleic acids 144
6.13.2 Preparation of plasmid DNA 144
6.13.3 Polymerase chain reaction (PCR) 144
6.13.4 Agarose gel electrophoresis of DNA 145
6.13.5 Restriction digest and DNA ligation 145
6.14 RNA techniques 146
6.14.1 RNA purification using TRIzol 146
6.14.2 Hot Phenol method for RNA purification 146
6.14.3 RNA purification using SV Total RNA Isolation System 146
6.14.4 DNase I digest 147
6.14.5 5'RACE 147
6.14.6 3'RACE 148
6.14.7 Quantitative RT-PCR 148
6.14.8 Denaturing PAGE 149

6.14.9 Native PAGE 149
6.14.10 Northern blot analysis 149
6.14.11 Generation of radiolabelled DNA oligonucleotides for RNA detection 150
6.14.12 Generation of radiolabelled RNA transcripts (riboprobes) for RNA detection 150
6.14.13 Determination of RNA stability 150
6.14.14 Primer extension analysis 150
6.14.15 *In vitro* transcription and 5' end-labelling of RNA 151
6.14.16 Determination of sRNA *in vivo* copy number 152
6.14.17 Electrophoretic mobility shift assay (EMSA) 152
6.14.18 *In vitro* structure probing 152
6.14.19 30S toeprint analysis 153
6.14.20 *In vitro* RNase E cleavage assay 153
6.15 Transcriptome analyses 154
6.15.1 Microarray experiments 154
6.15.2 Whole transcriptome sequencing 155
6.16 Protein techniques 156
6.16.1 Preparation of total protein samples 156
6.16.2 One-dimensional SDS-PAGE 156
6.16.3 Western blot analysis 156
6.17 Bioinformatic tools 157
6.17.1 Sequence retrieval 157
6.17.2 Alignments 157
6.17.3 Hybrid predictions 157
6.17.4 Secondary structure predictions 158
6.17.5 Melting temperature oligos 158
6.17.6 Software 158

7 References 159

8 Abbreviation index 173

9 List of Figures 175

10 List of Tables 177

11 Curriculum vitae 178

12 Publications 179

13 Acknowledgements 180

Erklärung 181

1 Introduction

1.1 Gene expression regulation in bacteria

Bacteria are highly adaptive organisms which effectively sense and respond to intra- and extracellular stimuli. Tight control of gene expression is a prerequisite to govern the complex regulatory networks triggered when cells encounter environmental changes.

Signals provoking changes in gene expression are often communicated at the level of DNA by transcription factors binding in a sequence-specific manner at promoter elements. In *E. coli*, ~300 genes are predicted to encode for this type of regulatory proteins which function as activators or repressors of transcription depending on whether they increase or prevent RNA polymerase (RNAP) association at the cognate promoter (Perez-Rueda & Collado-Vides, 2000).

A variety of regulatory RNAs have been identified in recent years to additionally act as potent modulators of gene expression. RNA was originally only considered an information-carrying biopolymer connecting the genome with the proteome. However, up to 10-15% of the compact bacterial genomes are transcribed into non-coding RNAs (Westhof, 2010) which include the abundant classes of transfer RNAs (tRNAs), ribosomal RNAs (rRNAs) as well as some non-coding RNAs performing important housekeeping functions (Wassarman et al, 1999). In addition, a highly heterogeneous group of non-coding RNAs serves as regulatory molecules that impact on gene expression (Waters & Storz, 2009). The class of regulatory RNAs includes elements within the 5' leaders of mRNAs that affect expression of the downstream ORF as well as small RNAs which can either modulate the activity of interacting proteins, or exert their regulatory function by base-pairing to cognate target transcripts.

The most basic principle of RNA-mediated gene control are so-called riboswitches and RNA thermometers in both of which the regulatory element is transcribed as a part of the protein-encoding sequence that it governs. In riboswitches, expression is controlled through the formation of alternative, mutually exclusive secondary structures as a consequence of small molecule binding within the 5’ untranslated region (UTR) of a transcript. The association of sugars, amino acids, nucleotides or uncharged tRNAs within the so-called “aptamer domain” induces a conformational change of the “expression platform” which in turn can result in the abortion or elongation of transcription or translation, respectively, of the downstream open reading frame (ORF)(Grundy & Henkin, 2004).

Similar to riboswitches, “RNA thermometers” regulate translation initiation of the downstream ORF. Often located in the 5’ UTR of heat-shock proteins or virulence factors, RNA thermometers fold in a temperature-sensitive and not in a ligand-specific manner: A hairpin structure occluding the RBS and thus preventing ribosome association at low temperatures can melt in a zipper-like manner with increasing temperature (Kortmann & Narberhaus, 2012).

A prominent class of regulatory RNAs in bacteria is small regulatory RNAs (sRNAs). sRNAs vary dramatically in both size (50-400 nt) and secondary structure, and act at all levels of gene expression (Papenfort & Vogel, 2010; Waters & Storz, 2009).

The majority of characterized sRNAs function through direct base-pairing interactions with their cognate target mRNAs and are discussed below (Fröhlich & Vogel, 2009).

In contrast, several sRNAs bind to and alter the activity of a protein factor by mimicking the structure of the default binding partner. RNAs of the CsrB/CsrC family, for example, counteract the activity of the CsrA effector protein which acts as a translational repressor. With multiple binding sites for the regulatory protein, CsrB/CsrC-like RNAs can effectively sequester CsrA and thus increase translation of the formerly repressed mRNAs (Babitzke & Romeo, 2007).

In contrast, 6S RNA does not exert its activity post-transcriptionally but rather influences the transcriptional process itself. 6S is a highly structured RNA containing a single-stranded central bulge (Barrick et al, 2005; Trotochaud & Wassarman, 2005). This distinct secondary structure resembles the conformation of DNA within an open promoter complex during transcription initiation. Mimicking the melted promoter DNA, 6S can specifically titrate RNAP holoenzyme associated with σ^{70} from its DNA binding sites (Wassarman, 2007).

1.2 Base-pairing small RNAs

So-called *cis*-acting sRNAs are located in the same genetic locus on the opposite strand of their mRNA target and thus by default have the potential for extensive base-pairing. Most *cis*-acting sRNAs have been identified in association with plasmids, transposable elements and phages (Brantl, 2007). In plasmids, antisense RNAs can provide mechanisms to prevent plasmid loss at cell division but also to restrict replication as is the case for the first sRNA characterized, RNAI, produced by the plasmid ColE1 (Tomizawa et al, 1981). ColE1 replication initiation by DNA polymerase I requires a pre-primer, RNAII, to associate with the DNA and adopt a distinct secondary structure which is cleaved to result in a mature primer. In the presence of the *cis*-encoded RNAI, RNAII maturation, and thus plasmid replication, is prevented by the formation of an inhibitory kissing complex between the two RNAs. This specific base-pairing is stabilized by the plasmid-encoded protein Rom (Brenner & Tomizawa, 1989). Due to extensive complementarity with the target, the function of most *cis*-encoded sRNAs is not dependent on auxiliary protein factors.

In addition to plasmid-borne RNAs, several *cis*-encoded sRNAs are located within the bacterial chromosome. In *E. coli*, base-pairing of the Hfq-associated sRNA GadY to the *cis*-encoded *gadXW* mRNA stimulates cleavage of the transcript and gives rise to a more stable mRNA species (Opdyke et al, 2004; Tramonti et al, 2002).

A large number of *trans*-encoded sRNAs (*i.e.* those riboregulators which are encoded in genomic loci unrelated to their target genes) require the RNA chaperone, Hfq, for both

intracellular stability as well as effective target base-pairing (Vogel & Luisi, 2011). Hfq-associated RNAs are considered as the largest class of post-transcriptional regulators in model bacteria such as *Salmonella* (Chao et al, 2012; Kröger et al, 2012). A typical enterobacterial sRNA is transcribed from a free-standing gene and harbours a structured 3' end followed by a poly(U)-stretch facilitating ρ-independent termination. Additionally the molecule comprises domains mediating interactions with the Hfq chaperone and the target mRNA (Storz et al, 2011). Notwithstanding exceptions (e.g. OxyS/*fhlA* mRNA, and CyaR/*ompX* mRNA which pair via kissing loop-interactions (Argaman & Altuvia, 2000; Johansen et al, 2008; Papenfort et al, 2008)), base-pairing between sRNAs and their cognate target mRNA is generally conferred through single-stranded, conserved sequence elements (Beisel et al, 2012; Peer & Margalit, 2011). These interactions can be as short as 6 bp for the SgrS/*ptsG* mRNA couple in *E. coli* (Kawamoto et al, 2006) and are referred to as "seed-pairing" (Papenfort et al, 2010) due to their reminiscence of target recognition by eukaryotic microRNAs (miRNAs). Interestingly, several sRNAs govern large post-transcriptional networks and employ a single seed sequence to target multiple transcripts. For example, GcvB sRNA of *Salmonella* was demonstrated to pair more than 20 mRNAs via a G/U rich element (Sharma et al, 2007; Sharma et al, 2011). The majority of these targets are involved in amino acid uptake, and thus GcvB governs a physiological response similar to a protein transcription factor, but at the post-transcriptional level. Likewise, the conserved sRNAs RybB, OxyS, FnrS and RyhB are integral components of cellular reactions to membrane perturbation, oxidative stress, anaerobicity or iron starvation, respectively (Storz et al, 2011).

Bacterial sRNAs exert their regulatory roles via a plethora of different mechanisms. Although the majority of regulation is negative and occurs at the level of translation initiation (Aiba, 2007), sRNAs can also function by altering the stability of their target mRNA and as activators of gene expression (Fröhlich & Vogel, 2009). Noteworthy, the RNA hybrids that underlie either positive or negative regulation of an involved mRNA are principally similar. For example, RyhB sRNA can act as both a repressor of *sodB* mRNA and an activator of *shiA* translation (Masse & Gottesman, 2002; Prevost et al, 2007), and the Vibrio Qrr sRNAs use a single sequence stretch to promote *vca0939* expression and to down-regulate *luxO*/*hapR* mRNA, respectively (Hammer & Bassler, 2007; Lenz et al, 2004).

1.2.1 sRNA-mediated repression of gene expression

The first described trans-encoded sRNA, MicF, was serendipitously discovered as a regulator of outer membrane porin (Omp) F (Mizuno et al, 1984) and acts through a common mechanism. As the sRNA binds within or adjacent to the region recognized by the 30S ribosomal subunit, *i.e.* SD and AUG start codon, it serves as a physical roadblock to prevent formation of the translation initiation complex (Fig. 1.1 A). 30S ribosomes occupy a region covering residues -35 to +19

relative to the translational start site (Hüttenhofer & Noller, 1994) but interestingly, sRNAs can effectively prevent translation initiation when base-pairing as far as 70 nt upstream or 15 nt downstream the AUG (Bouvier et al, 2008; Holmqvist et al, 2010). Similarly, sRNAs can also impair initiation of protein synthesis of short leader peptides, and consequently inhibit expression of the translationally coupled ORFs as observed for the repression of fur by RyhB sRNA (Vecerek et al, 2007). The primary consequence of sRNA binding is translational repression of the target and thus, a reduction in protein levels (Morita et al, 2006). Subsequently, in the absence of ribosomes the silenced mRNA becomes rapidly degraded by ribonucleolytic attack and as determined in *E. coli* for RyhB sRNA, the riboregulator can likewise be destabilized when bound to the target (Masse et al, 2003; Prevost et al, 2011). The principle of "coupled degradation" of sRNA/mRNA hybrids could allow bacteria to quickly shut-down an sRNA-mediated response as soon as the triggering cue is removed, and to prevent the establishment of a full response if stress signals appear only transiently (Aiba, 2007; Beisel & Storz, 2011).

Recent studies have unraveled further mechanisms of negative regulation by sRNAs base-pairing upstream of the region relevant for translation initiation (Fig. 1.1 B/C). *E. coli* Spot42 represses *sdhC* translation initiation by directing the RNA chaperone Hfq to a site in the vicinity of the start codon where it competes directly with 30S ribosomal subunits. Contrary to the default mechanism of translational repression, the sRNA is itself not involved in occlusion of the ribosome and only acts as a recruitment factor for Hfq (Desnoyers & Masse, 2012). Using yet another mechanism, GcvB sRNA reduces translation of several target mRNAs by recognizing C/A rich sequences within the 5' UTR that serve as translation enhancer elements (Sharma et al, 2007). Likewise, IstR-1 sRNA binds to *tisB* mRNA far upstream in the 5' UTR and translation is inhibited through masking of a ribosome standby-site; in contrast to all previous examples, this latter regulation occurs independent of the major RNA binding protein, Hfq (Darfeuille et al, 2007).

Apart from interfering with translation, several sRNAs act by stimulating the decay of their cognate mRNA targets (Fig. 1.1 D). *Salmonella* MicC sRNA base-pairs the *ompD* transcript downstream the 20th codon and thus, is unable to repress its translation. Instead, it promotes rapid mRNA decay by recruiting the major endoribonuclease, RNase E, which cleaves immediatedly downstream the MicC binding site (Pfeiffer et al, 2009).

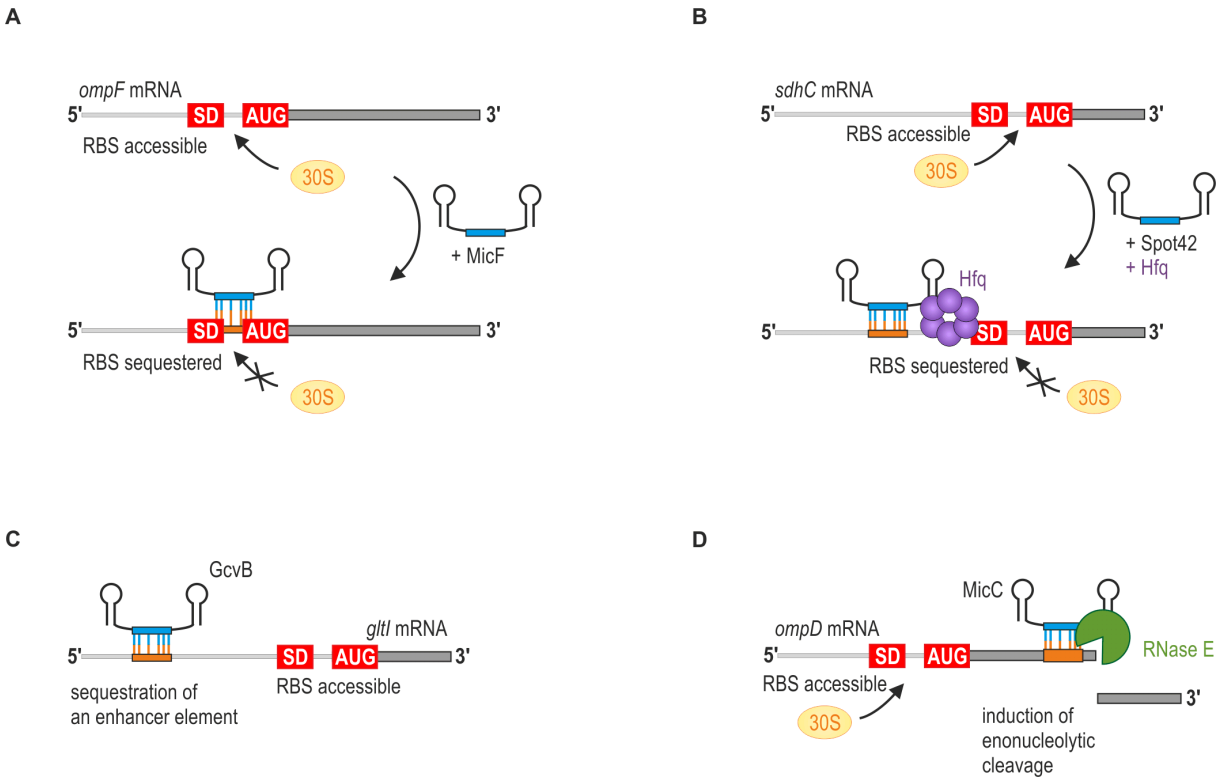

Figure 1.1 Post-transcriptional repression of gene expression by sRNAs.

(A) Binding of MicF sRNA within the region relevant for translation initiation prevents ribosome association on the mRNA. (B) While the binding site of Spot42 within the 5' UTR of *sdhC* mRNA is too far upstream to interfere with translation of the target itself, concomitant recruitment of Hfq and redirection of the chaperone close to the SD site results in inhibition of ribosome binding. (C) GcvB sRNA represses translation of *gltI* mRNA by sequestration of an enhancer element within the 5' UTR. (D) MicC base-pairs within the deep CDS of *ompD* and recruits RNase E. Binding of the sRNA induces the endonucleolytic cleavage of *ompD* mRNA in proximity to the binding site.

1.2.2 Activation of gene expression by sRNAs

Although negative regulation of mRNAs has been observed more frequently, several different mechanisms by which sRNAs can directly or indirectly promote target gene expression in various bacterial species have been described (Fröhlich & Vogel, 2009).

The most common mechanism by which direct base-pairing of an sRNA to an mRNA activates its expression is referred to as the "anti-antisense mechanism". Some transcripts feature hairpin structures occluding regions essential for translation initiation, *i.e.* the ribosome binding site (RBS). While these sites often imply *cis*-encoded regulation by RNA thermometers or riboswitches, their activation can also depend on sRNAs acting in *trans* (Fröhlich & Vogel, 2009). First observed for the 514 nt long RNAIII in *Staphylococcus aureus* promoting *hla* mRNA translation (Morfeldt et al, 1995), most insight into the exact mechanism of regulation was

gained from studying the translation of *rpoS* mRNA coding for the major stress σ factor σ^S. Three differentially expressed sRNAs, namely DsrA, RprA and ArcZ, can stimulate σ^S synthesis in response to cold shock, envelope stress and aerobic conditions, respectively, by disruption of an inhibitory stem-loop structure within the *rpoS* 5' leader (Majdalani et al, 2001; Majdalani et al, 1998; Mandin & Gottesman, 2010). In this alternative conformation, ribosomes can enter on the transcript and, as a consequence of enhanced translation, the mRNA is stabilized (Fig. 1.2 A). The very same mechanism plays a pivotal role in several additional sRNA/mRNA pairs in various organisms including *Vibrio* Qrr sRNAs/*vca0939* mRNA or *E. coli* GlmZ/*glmS* mRNA (Hammer & Bassler, 2007; Urban et al, 2007). In addition, sRNA-mediated activation of expression can occur through the regulation of translationally-coupled leader peptides: In *Pseudomonas*, PhrS sRNA interferes with an inhibitory secondary structure to induce translation of the leader peptide encoded within the *pqsR* 5' UTR which consequently also results activates the main transcript (Sonnleitner et al, 2011).

An alternative mechanism was recently described for the activation of *colA* mRNA by VR-RNA in the Gram-positive pathogen *Clostridium* (Fig. 1.2 B). VR-RNA not only antagonizes the formation of a self-inhibitory structure burying the translation initiation site of the *colA* transcript, but the sRNA also induces an endonucleolytic cleavage within the 5' UTR giving rise to a shorter and, importantly, more stable version of the mRNA (Obana et al, 2010).

FasX, a *Streptococcus pyogenes* sRNA, can likewise prevent endonucleolytic decay and consequent stabilization of its target *ska* mRNA by base-pairing to its very 5' UTR. The formed hybrid blocks the contact point of transcript decay and converts the single-stranded end into a stabilizing stem-loop-like structure (Fig. 1.2 C) (Ramirez-Pena et al, 2010).

A distinct case is the indirect activation of *ybfMN* expression through the elimination of an inhibitory riboregulator (Fig. 1.2 D). Under standard growth conditions, the constitutively expressed MicM is in large excess over *ybfMN* mRNA and represses its translation (Rasmussen et al, 2009). Importantly, MicM does not undergo coupled degradation together with its target but is recycled (Overgaard et al, 2009). In the presence of inducing chitosugars cells express the *chbBCARFG* chitobiose operon which harbours a sequence complementary to MicM and is able to tether the sRNA. Importantly, a conformational change resulting from the interaction renders MicM more susceptible to ribonucleolytic attack, and the repressor is eventually cleared. Thus, *chbBCARFG* mRNA functions as a molecular trap for MicM, and indirectly triggers the translation of *ybfMN* mRNA (Figueroa-Bossi et al, 2009; Overgaard et al, 2009).

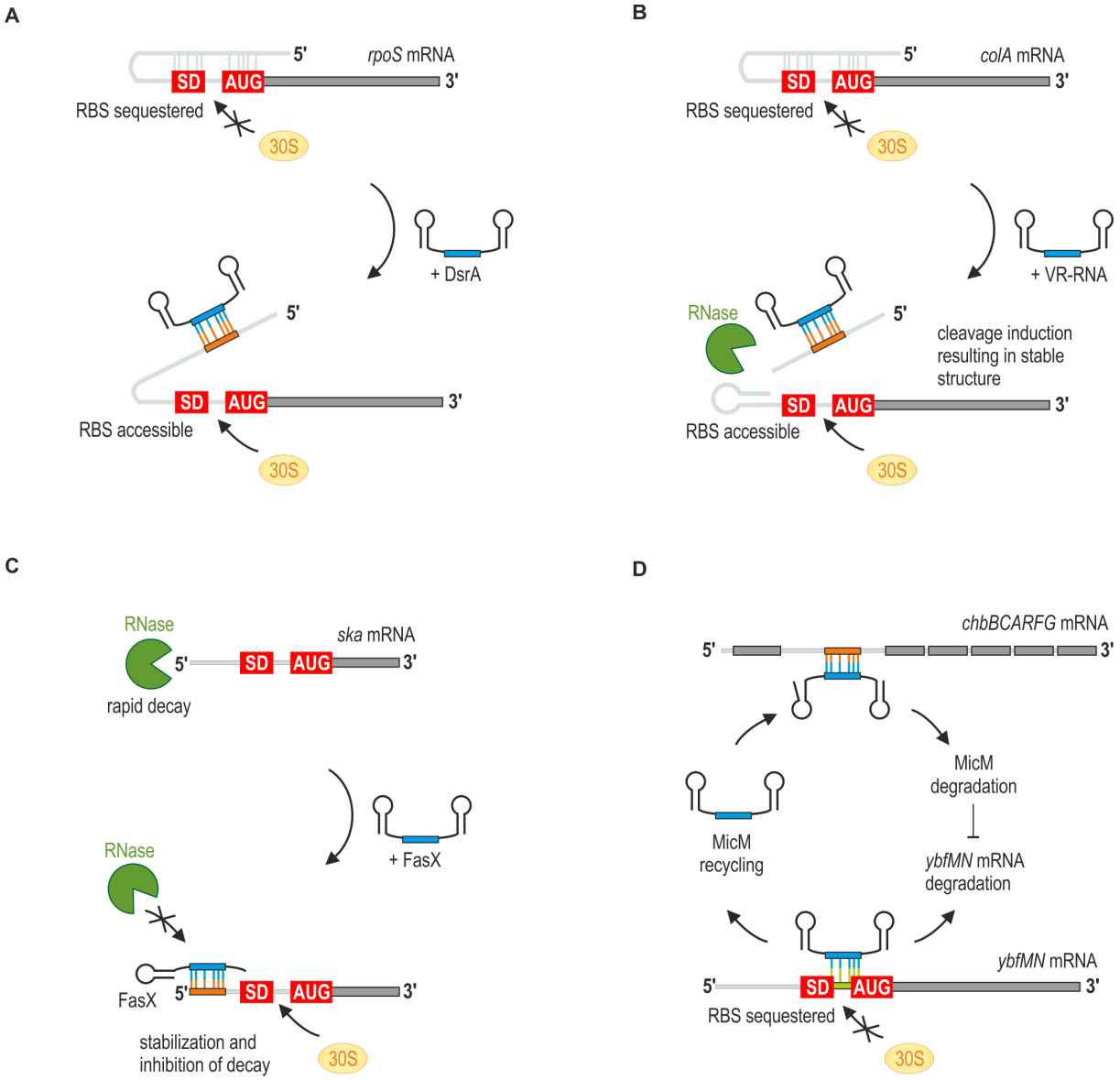

Figure 1.2 Mechanisms of target gene activation by sRNAs.

(A) Translation efficiency can be severely limited due to hairpins within the 5' UTR sequestering the region around SD and AUG as it is the case for *rpoS* mRNA. Binding of DsrA sRNA within the leader can alleviate the inhibitory structure and unmask the RBS to allow translation. (B) VR-RNA binds to the 5' UTR of *colA* mRNA and induces an endonucleolytic cleavage resulting in an mRNA species of higher stability. (C) By masking the very 5' end of *ska* mRNA in a stem-loop-like structure, FasX inhibits endonucleolytic decay of its target. (D) The constitutively expressed MicM sRNA represses the translation of *ybfMN* mRNA without being consumed through coupled degradation. The presence of chitosugars induces expression of the *chbBCAFRG* operon harbouring a MicM binding site within the *chbBC* intergenic region. Trapping MicM by the chitobiose operon RNA results in sRNA degradation and consequent de-repression of *ybfMN* (based on (Fröhlich & Vogel, 2009)).

1.3 Proteins required for the regulatory function of sRNAs

1.3.1 The RNA chaperone Hfq

One of the few commonalities among the heterogeneous class of sRNAs in Gram-negative bacteria is the association with the RNA binding protein Hfq. As a co-factor of regulatory RNAs Hfq governs one of the most complex post-transcriptional networks known to date (Chao et al, 2012). Its importance in gene expression regulation was however not evident when Hfq was first described in the late 1960s as a host factor (also referred to as HF-1) of *E. coli* required for replication initiation of the RNA phage Qβ (Franze de Fernandez et al, 1968).

Hfq belongs to the family of Sm and Sm-like (LSm) proteins which possess two characteristic Sm motifs and are involved in splicing as well as RNA decay in eukaryotes and archaea (Moller et al, 2002; Wilusz & Wilusz, 2005). Hfq differs from other members of the protein family by the formation of hexameric instead of heptameric complexes (Brennan & Link, 2007). The doughnut-shaped architecture of the Hfq hexamer exposes three principle interaction sites for nucleic acids: the proximal (exposing the N-terminus of the protein) and the distal surfaces of the ring, as well as the rim (Sauer et al, 2012). The proximal site preferentially interacts with uridine-rich sequences, while the distal site favours the binding of ARN or ARNN motifs (with R being a purine, and N any nucleotide) (Link et al, 2009; Sauer & Weichenrieder, 2011; Schumacher et al, 2002). These vague motifs can however not explain the observed selectivity of Hfq for mRNAs and sRNAs over other, more abundant RNA species like tRNAs or ribosomal RNA (Vogel & Luisi, 2011). The recognition of sRNAs has recently been suggested to occur via the Rho-independent terminator including its 3' poly(U) tail which, within an overall heterogeneous design, serves as a common structural denominator of sRNA species (Ishikawa et al, 2012; Otaka et al, 2011; Sauer & Weichenrieder, 2011). Hundreds of protein-coding transcripts certainly carry an equivalently structured terminator and indeed, mRNA 3' ends are found to be highly enriched in Hfq co-immunoprecipitations (Chao et al, 2012; Kingsford et al, 2007; Sittka et al, 2009; Zhang et al, 2003). Of interest, several sRNAs originally missed in computational predictions have recently been identified to originate from within mRNA loci and to overlap with 3' ends. These sRNA candidates may either result from mRNA processing or be transcribed from independent promoters with a terminator shared with the overlapping mRNA (Chao et al, 2012). Pull-downs of Hfq and subsequent analyses of bound cellular RNAs on microarrays or by high-throughput sequencing have in the past been a valuable tool to identify numerous novel sRNAs. Both SdsR and RydC, the two sRNAs the present study is focusing on, have been repeatedly recovered together with Hfq (Sittka et al, 2009; Zhang et al, 2003). Monitoring the sRNAs associated with Hfq over growth revealed that the profiles at individual time-points varied tremendously (Fig. 1.3; (Chao et al, 2012)). RydC occupies Hfq throughout growth at medium levels. ArcZ and ChiX, two well-known examples of growth-phase

independent sRNA expression (Argaman et al, 2001; Figueroa-Bossi et al, 2009; Rasmussen et al, 2009; Vogel et al, 2003), display a qualitatively similar pattern albeit both RNAs are recovered at higher abundancies. In contrast, SdsR only accumulates towards stationary phase but, together with RprA, dominates the late stages of growth.

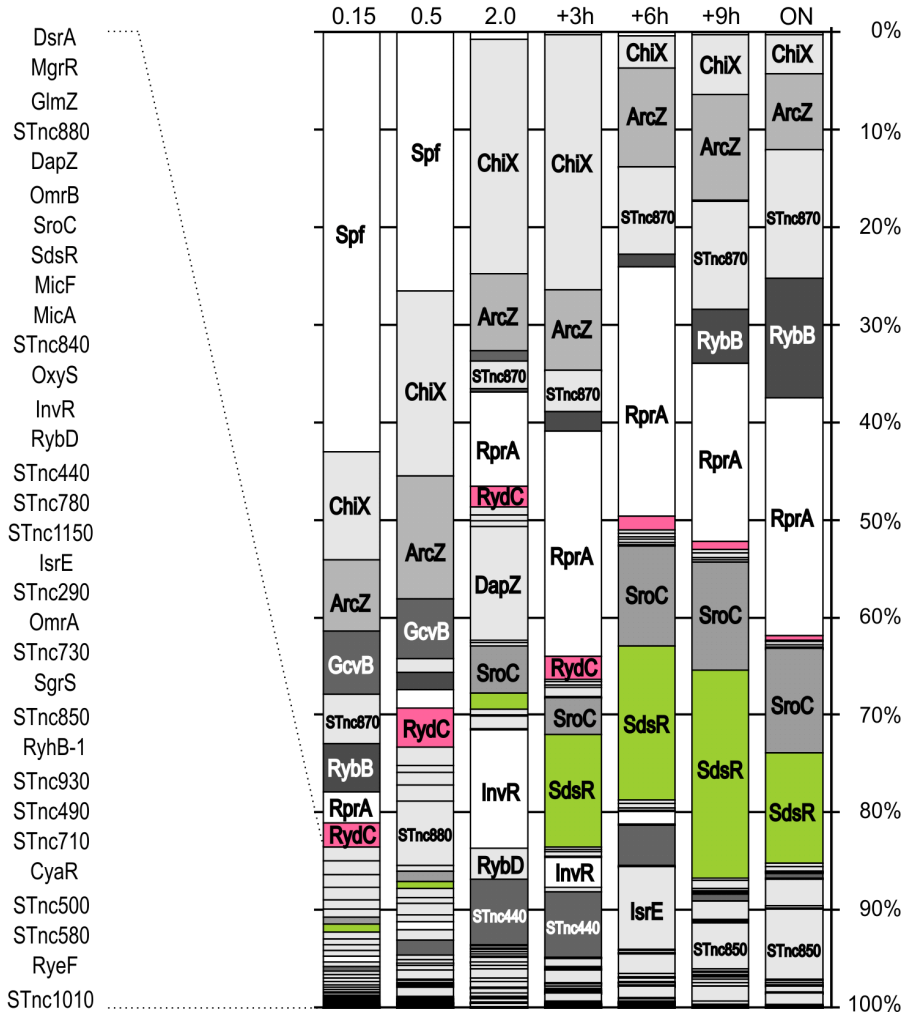

Figure 1.3 Profiles of Hfq-associated sRNAs over growth.

The proportion of individual sRNAs enriched by Hfq co-immunoprecipitation at various time-points over growth (OD_{600} of 0.15; 0.5; 2.0; 3, 6, and 9 hours after cells had reached an OD_{600} of 2.0; overnight) is plotted in respect to the total number of experimentally validated sRNAs. SdsR and RydC are highlighted in green and pink, respectively. Modified from (Chao et al, 2012).

In many cases, Hfq binding protects sRNAs from endonucleolytic decay in the absence of targets (Waters & Storz, 2009). The stabilization of sRNAs partially explains the requirement of the RNA chaperone for riboregulation. In the context of post-transcriptional control of gene expression Hfq was also found to inhibit translation (Vytvytska et al, 2000), to decrease transcript stability by triggering polyadenylation (Hajnsdorf & Regnier, 2000; Mohanty et al, 2004) and to impact tRNA modification (Lee & Feig, 2008; Scheibe et al, 2007). Most important however, Hfq displays chaperone activity: it helps cognate sRNA/mRNA targets to base-pair by remodeling potentially inhibitory structures (Maki et al, 2010), by increasing annealing rates (Fender et al, 2010; Hopkins et al, 2011; Hwang et al, 2011), and by stabilization of duplexes (Soper et al, 2010).

1.3.2 The major ribonuclease RNase E

In the course of riboregulation Hfq may recruit additional protein factors to exert its activity. A prime candidate for such interaction is RNase E as it is not only known to functionally co-operate but can also be co-purified together with Hfq and sRNAs in higher order complexes (Morita et al, 2005).

Besides helping mature stable RNAs, the essential endoribonuclease RNase E mediates the major pathway of mRNA decay in enterobacteria (Carpousis, 2007). RNase E exhibits strong preference for A/U-rich, single-stranded RNA substrates and initiates rapid decay either via internal entry or via the 5' end of a transcript (Baker & Mackie, 2003; McDowall et al, 1994). In the latter case, a hallmark of RNase E is its preference for 5'-monophosphorylated RNA species which are recognized by a 5' sensor located within the N-terminal catalytic core of the enzyme (Callaghan et al, 2005; Mackie, 1998).

RNase E not only interacts with RNA but also engages additional factors to form a multiprotein complex referred to as the degradosome (Carpousis, 2007). RNase E associates as a homotetramer, and the largely unstructured C-terminal domains within each monomer accommodate RNase helicase B (RhlB), a dimer of the glycolytic enzyme enolase and a trimer of polynucleotide phosphorylase (PNPase) (Fig. 1.4; (Marcaida et al, 2006)). One auxiliary interaction partner of RNase E is Hfq which can interact with the C-terminus in a region overlapping the RhlB binding domain (Ikeda et al, 2011; Marcaida et al, 2006; Morita et al, 2005). RNase E serves a vital role to increase the robustness of regulations by ensuring concomitant degradation of an sRNA with its target upon base pairing (Masse et al, 2003). While translational repression by sRNAs renders the targeted mRNA more vulnerable to RNase E-dependent degradation due to the loss of protecting ribosomes, recent studies also propose an active recruitment of RNase E to inactivate the target independent of translational repression (Pfeiffer et al, 2009; Prevost et al, 2011).

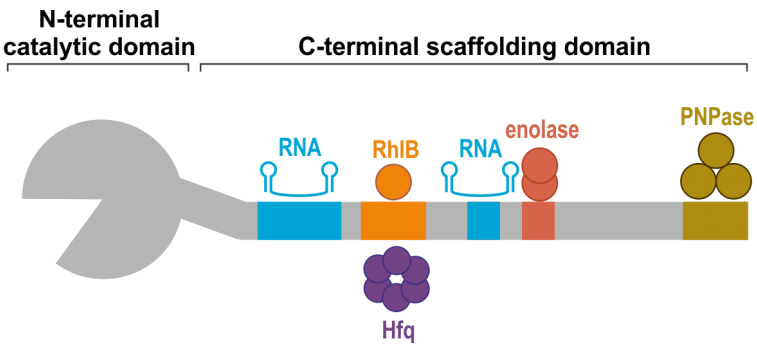

Figure 1.4 Schematic structure of RNase E and organization of the degradosome.

The compact N-terminal domain of RNase E harbours the catalytic core. The mostly unstructured C-terminal portion of the enzyme serves as a scaffold to accommodate RNA, RhlB, a dimer of enolase and a trimer of PNPase. Note that the potential binding of Hfq to RNase E occurs mutually exclusive with RhlB association (based on (Marcaida et al, 2006)).

1.4 The model pathogen *Salmonella* Typhimurium

Salmonellae are important Gram-negative bacterial pathogens infecting both humans and animals to cause a variety of diseases ranging from mild diarrhea to severe infections including typhoid fever (Hansen-Wester & Hensel, 2001). Of an estimated 21 million cases of the systemic typhoid fever occurring every year, approximately 244,000 infections are fatal (Crump et al, 2004). In addition, more than 90 million annual cases of acute human gastroenteritis are due to non-typhoid salmonellosis, resulting in ~ 155,000 deaths (Majowicz et al, 2010).

Thousands of different *Salmonella* serovars can be defined due to their distinct patterns of surface-exposed flaggelin and lipopolysaccharide molecules (Lan et al, 2009). One of the most important serotypes responsible for salmonellosis in humans is *Salmonella enterica* serovar Typhimurium (referred to as *S.* Typhimurium). Aside from its clinical importance, *S.* Typhimurium is an established model organism to study of host-pathogen interactions, bacterial genetics and gene expression regulation (Thiennimitr et al, 2012). *S.* Typhimurium SL1344 used as wild-type strain in this work is a histidine auxotroph generated from the ancestral strain ST4/74 which was originally isolated from an infected calf (Hoiseth & Stocker, 1981; Rankin & Taylor, 1966). The SL1344 genome contains a total of 4742 protein-coding genes on a circular chromosome and three plasmids, pSLT^{SL1344}, pCol1B9 ^{SL1344} and pRSF1010 ^{SL1344} (Kröger et al, 2012).

Salmonellosis is generally contracted by humans through the consumption of contaminated food. Due to their adaptive acid-stress response *Salmonella* can survive the low pH of the stomach and progress through the gastrointestinal tract to the small intestine (Foster & Spector, 1995). While non-typhoidal *Salmonella* induce only local inflammation within the

intestinal lumen, systemic infections are characterized by the active invasion of non-phagocytic enterocytes or preferentially M-cells (microfold cells) which enable passage of the bacteria to lymphoid cells in the underlying Peyer's patches (Haraga et al, 2008). Having crossed the epithelial barrier *Salmonella* can enter and proliferate within intestinal macrophages, thus evading clearance by the host immune system (Hansen-Wester & Hensel, 2001).

Like for many bacterial pathogens the virulence capacity of *Salmonella* is defined within horizontally acquired genetic regions termed pathogenicity islands (Dobrindt et al, 2004). Two common characteristics of these clusters - namely the rather AT-rich base composition when compared to the core genome as well as their frequent association with insertion sites at tRNAs – can be attributed to their foreign origin (Hensel, 2004). Several of the currently described 12 *Salmonella* pathogenicity islands (SPIs) are found specific to certain serovars while the hallmarks of *Salmonella* virulence, *i.e.* the invasion and intracellular survival of host cells, are mainly connected to the common SPI-1 and SPI-2, respectively (Hensel, 2004).

SPI-1 and SPI-2 encode for type III secretion systems (T3SS) which function as molecular syringes to inject so-called effector proteins into the host cell cytosol (Galan, 2009; Hansen-Wester & Hensel, 2001). Upon adherence to the surface of the host the SPI-1 system is expressed, and several secreted effectors orchestrate the reorganization of the host actin cytoskeleton to induce bacteria-mediated phagocytosis (Haraga et al, 2008). Inside the cell, the pathogen resides within the so-called *Salmonella*–containing vacuole. This phase of infection is characterized by the expression of the SPI-2-encoded T3SS and the secretion of a second set of effector proteins to mediate intracellular survival and replication (Haraga et al, 2008).

1.5 Identification and functional characterization of sRNAs in *Salmonella*

With regard to sRNA-mediated gene regulation *S.* Typhimurium can be considered the most extensively studied bacterial pathogen (Papenfort & Vogel, 2010). The central role of riboregulation in this bacterium is also reflected by the manifold and diverse phenotypes caused by a deletion of the major RNA chaperone, Hfq (Chao & Vogel, 2010; Vogel, 2009): among the more than 70 abundant proteins deregulated in the absence of Hfq are also the major OMPs, which results in chronic activation of the envelope stress response (Figueroa-Bossi et al, 2006; Sittka et al, 2007). In addition, Hfq is required in *Salmonella* for both motility and effector protein secretion. The loss of these virulence determinants at least partially accounts for the observed severe attenuation of the *hfq* mutant in invasion and replication in cultured cells in as well as in mouse infections (Figueroa-Bossi et al, 2006; Sittka et al, 2007). Despite the dramatic effect of *hfq* deletion only a few sRNAs have been identified to influence *Salmonella* virulence (Hebrard et al, 2012).

To gain more insight into the specific sRNA profile of an organism pull-down assays with RNA binding proteins and high-throughput sequencing have proven successful (Sharma & Vogel, 2009). In *Salmonella*, deep sequencing of the whole transcriptome and of RNAs bound by Hfq has revealed a plethora of previously unknown sRNA candidates (Kröger et al, 2012; Sittka et al, 2008; Sittka et al, 2009). The bulk of *Salmonella* sRNAs was however annotated based on conservation of candidate genes identified in genome-wide searches for sRNAs in *E. coli* (Argaman et al, 2001; Rivas et al, 2001; Wassarman et al, 2001). The close relatedness of both organisms, and the preserved arrangement of flanking regions enabled the identification of numerous RNA species in *Salmonella* (Hershberg et al, 2003). Likewise, SdsR and RydC, the two core sRNAs characterized in the current study are found encoded next to at least one conserved flanking gene in *E. coli* and *Salmonella* (Fig. 1.5). The *sdsR* gene is furthermore hyperconserved in numerous enterobacterial species, and in all cases located downstream of *yebY* (STM1873 in *S.* Typhimurium) on the same strand. RydC is transcribed from the opposite strand downstream of *cybB* in the majority of cases, however overall displays a lower degree of conservation.

In many cases, conservation of the sRNAs not only covers genomic location but - as demonstrated by several studies conducted in parallel in both *Salmonella* and *E. coli* - also the physiological function of an RNA regulator. The identifcation of overlapping target gene profiles and corresponding transcriptional regulators could for example verify the conserved role of RybB and CyaR in porin expression control in *Salmonella* and *E. coli* (De Lay & Gottesman, 2009; Johansen et al, 2008; Johansen et al, 2006; Papenfort et al, 2008; Papenfort et al, 2006).

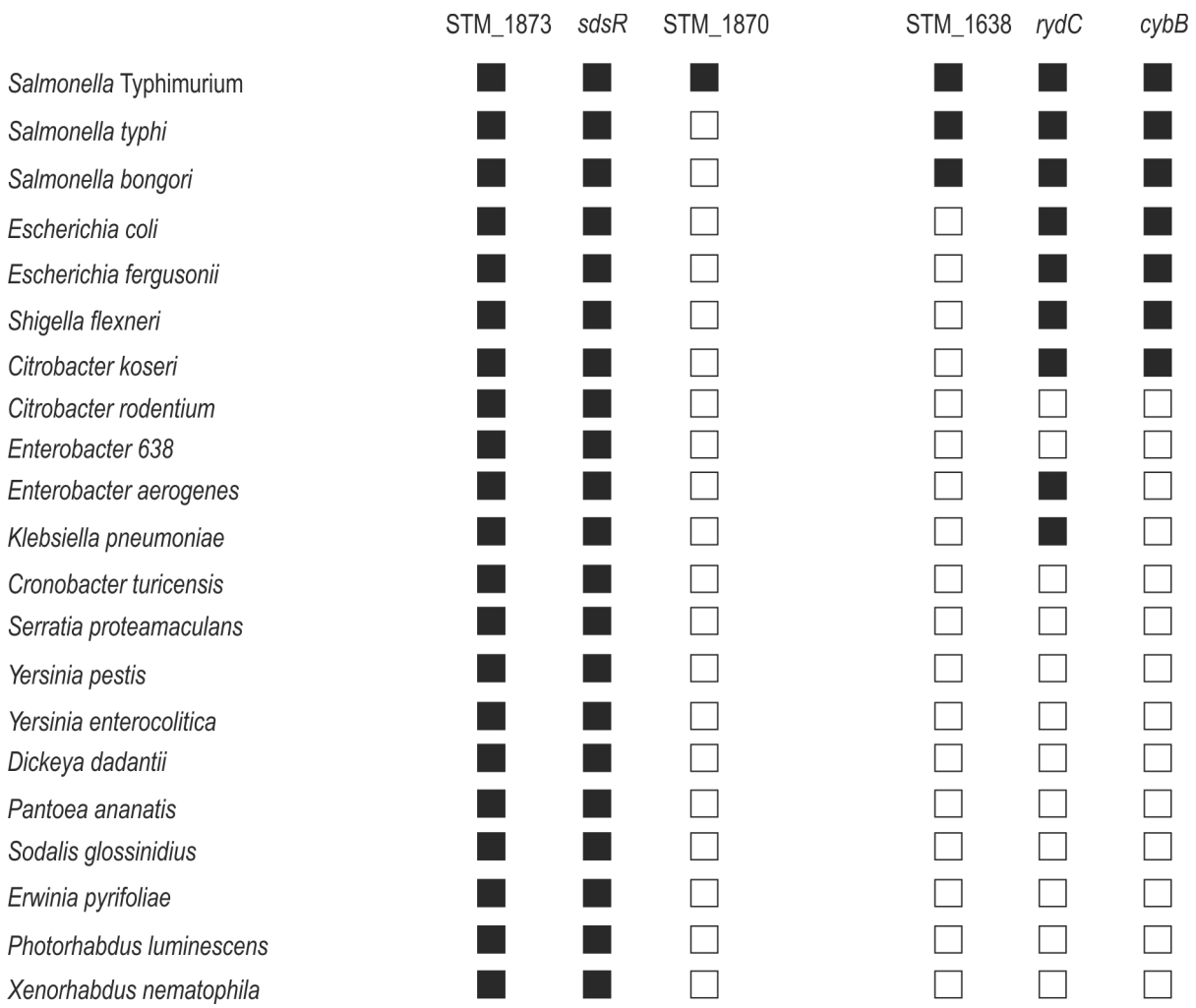

Figure 1.5 Conservation analysis of the two core sRNAs SdsR and RydC.

The middle box in each column represents the sRNA gene itself while the right and left boxes represent the upstream and downstream adjacent genes, respectively. A black box indicates conservation while a white box represents absence of the flanking gene.

1.6 Aim of the study

It is now accepted that non-coding RNAs play important regulatory roles in all kingdoms of life. In bacteria, Hfq-associated small regulatory RNAs (sRNAs) constitute the largest class of post-transcriptional regulators with remarkable diversity in both size and secondary structure. sRNAs typically modulate translation and stability of their cognate target mRNAs by forming short, often imperfect base-pairing interactions (Waters & Storz, 2009).

While serendipitous discoveries of individual sRNAs as regulators of single targets dominated the early research on riboregulation in bacteria, more recent investigations uncovered several sRNAs to govern large post-transcriptional networks similar to the regulatory

scope observed for transcription factors (Papenfort & Vogel, 2009). Genome-wide screens using both bioinformatics and wet-lab approaches have increased the number of sRNAs to more than 150 in *E. coli* and *Salmonella* (Chao et al, 2012; Kröger et al, 2012; Padalon-Brauch et al, 2008; Pfeiffer et al, 2007; Vogel et al, 2003; Wassarman et al, 2001; Zhang et al, 2003). While many sRNA genes display species-specific conservation patterns, some sRNAs appear to be widely conserved (Papenfort et al, 2012). The study of this "enterobacterial core set" of sRNAs is particularly interesting as it allows the identification of central cellular functions that extend beyond the individual bacterial species. However, only a minor fraction of these riboregulators has been characterized to date with regard to their target spectra and biological roles (Peer & Margalit, 2011). This paucity in sRNA functions has largely hampered the general understanding of sRNA-mediated gene control with implications on the physiological as well as mechanistic aspects underlying riboregulation in bacteria. This study aimed at the characterization of two highly conserved and Hfq-associated sRNAs, SdsR and RydC, in the model organism *Salmonella* Typhimurium.

Both RNAs had been previously identified in genome-wide screens for sRNAs in *E. coli*. SdsR, formerly known as RyeB, was anticipated to be one of the most abundant stationary phase-specific sRNAs (Vogel et al, 2003; Wassarman et al, 2001; Zhang et al, 2003), however, no biological function had been assigned to this sRNA, yet. The present work addresses the selective expression of SdsR and investigates the mechanism underlying target regulation of this sRNA. The systematic study of sRNA-target pairs in genetically tractable model organisms such as *E. coli* and *Salmonella* can be considered of major importance in order to expand the current knowledge on sRNA functions in bacteria or even riboregulation in general.

The second sRNAs investigated in this study is RydC, an sRNA repeatedly pulled-down with Hfq albeit being only weakly expressed at all stages of growth (Antal et al, 2005; Chao et al, 2012; Sittka et al, 2009; Zhang et al, 2003). A unique feature of RydC is the formation of a pseudoknotted secondary structure in the 3' end of the molecule (Antal et al, 2005), making it an interesting sRNA with potentially unusual regulatory functions. This study investigates the role of the secondary structure of RydC with regard to the sRNA function and aims to identify the relevant targets of the RydC in *Salmonella*.

2 Characterization of the conserved σ^S-dependent small RNA SdsR in *Salmonella*

2.1 SdsR is highly abundant in stationary phase cells

One of the sRNAs that is expressed in a highly growth rate-dependent manner is SdsR, which was originally described as RyeB in *E. coli* (Vogel et al, 2003; Wassarman et al, 2001). The *sdsR* gene is located downstream of the conserved *yobA-yebZY* operon (*yobA*-STM1874-STM1873 in *Salmonella*) in numerous eubacterial chromosomes (Fig. 2.1 A). In *E. coli* and several related species (including *Salmonella* and *Shigella*) expression from this locus yields a second non-coding transcript. The sense-oriented SraC sRNA (a.k.a. RyeA, Tpke79, IS091) contains an internal segment of full complementarity to SdsR (Argaman et al, 2001; Balbontin et al, 2008; Vogel et al, 2003; Wassarman et al, 2001).

Expression of SdsR in *Salmonella* was confirmed at different time-points over growth in LB (Fig. 2.1 B, lanes 1-7). SdsR was detected as two forms, a ~103 nt full-length transcript and a less abundant ~70 nt long processing product (Fig. 2.1 B). This pattern had been also observed for *E. coli* SdsR (Vogel et al, 2003; Wassarman et al, 2001) and the 5' end of the processed form in *Salmonella* was located to residue 31 using 5'RACE (Supplementary Fig. 4.6). The conservation of the transcriptional start site as well as the processing were furthermore confirmed by analyzing whole transcriptome data obtained by differential RNA sequencing (dRNA-seq) of samples of *S*. Typhimurium, *E. coli*, *S. flexneri* and *C. rodentium* (chapter 4.1). According to bioinformatic predictions of the SdsR secondary structure processing occurs in between two stem-loops in the 5' portion of the molecule; a third stem-loop is considered to function as a ρ-independent transcription terminator (Fig. 2.1 C).

Results from a previous shot-gun cloning screen for sRNAs in *E. coli* suggested that SdsR ranges among the most abundant sRNAs in stationary phase (Vogel et al, 2003). To quantify the cellular levels of SdsR over growth, sRNA expression was compared to defined amounts of *in vitro*-synthesized SdsR transcript on Northern blots (Fig. 2.1 B). This analysis indicated that SdsR expression is low during exponential growth and peaks in late stationary phase, accumulating to more than 300 copies per cell (6 hours after cells reached an OD_{600} of 2.0).

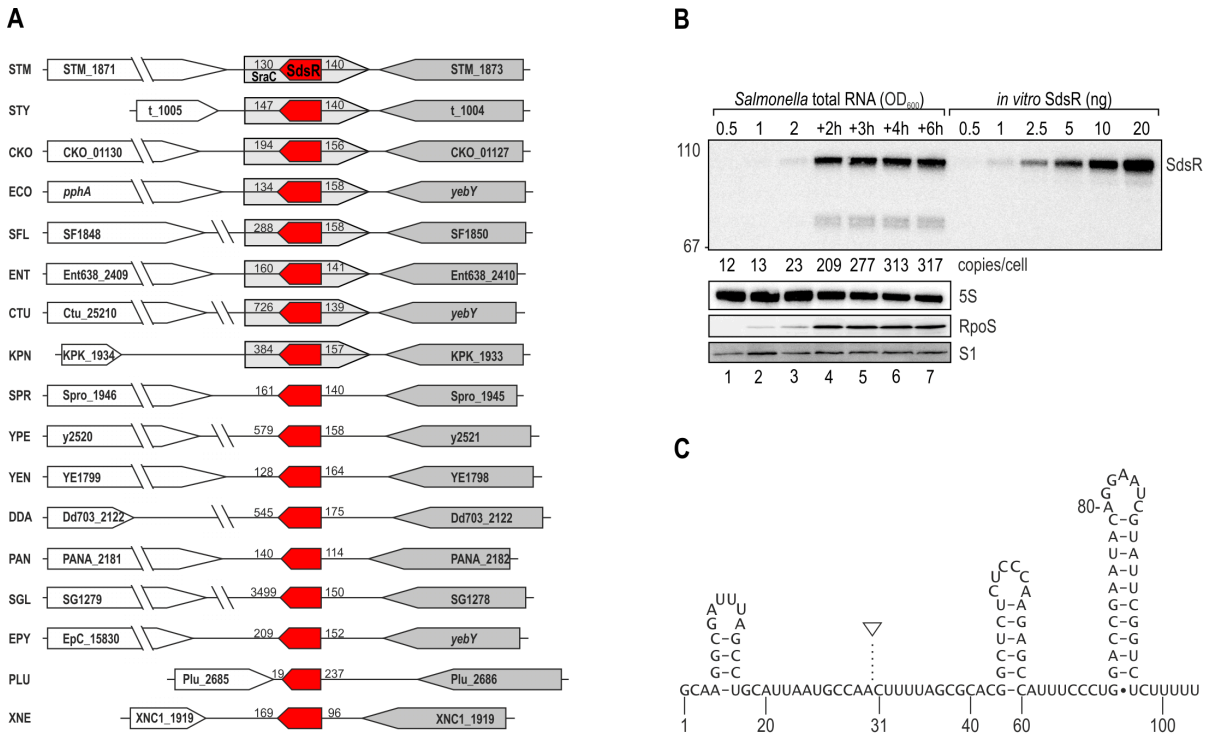

Figure 2.1 Genomic localization, expression and secondary structure of SdsR.

(A) Synteny analysis of the *sraC*/*sdsR* genes. In all cases, *sdsR* is located downstream of *yebY* or homologues thereof. In several species *sraC* is encoded opposite of *sdsR*. Distances to flanking genes are indicated in bp. STM: *Salmonella* Typhimurium; STY: *Salmonella typhi*; CKO: *Citrobacter koseri*; ECO: *Escherichia coli*; SFL: *Shigella flexneri*; ENT: *Enterobacter spp.*; CTU: *Cronobacter turicensis*; KPN: *Klebsiella pneumoniae*; SPR: *Serratia proteamaculans*; YPE: *Yersinia pestis*; YEN: *Yersinia enterocolitica*; DDA: *Dickeya dadantii*; PAN: *Pantoea ananatis*; SGL: *Sodalis glossinidius*; EPY: *Erwinia pyrifoliae*; Plu: *Photorhabdus luminescens*; XNE: *Xenorhabdus nematophila*. (B) SdsR copy number over growth. SdsR levels of wild-type *Salmonella* at various time-points of growth (OD_{600} of 0.5, 1.0, 2.0 and 2, 3, 4 or 6 hours after cells had reached an OD_{600} of 2.0) were compared by Northern blot analysis to signals of *in vitro* transcribed SdsR in indicated amounts. Probing for 5S RNA confirmed equal loading. Expression of RpoS at different growth stages was determined on Western blots. Detection of ribosomal protein S1 served as loading control. (C) Predicted secondary structure of SdsR. The full-length RNA is processed between the first and second stem-loop. The third stem-loop is predicted to promote ρ-independent termination.

2.2 SdsR expression depends on the alternative σ factor σ^S

The cause for the stationary-phase selectivity of *sdsR* expression was unknown. However, given the strong recovery of SdsR from stationary phase *E. coli* (Vogel et al, 2003), it was likely that the promoter was recognized by a transcription factor active in later stages of growth. A phylogenetic analysis of *sdsR* genes in diverse enterobacterial species suggested conservation of the -10 and -35 recognition elements which are required for transcriptional initiation at most bacterial promoters (Fig. 2.2). Moreover, the primary sequences of all *sdsR* promoters exhibited conservation of distinct elements recognized by the alternative σ factor σ^S. The RNAP core enzyme (consisting of five subunits $\beta\beta'\alpha_2\omega$) is performing transcription elongation and termination, but requires an additional subunit, the σ factor in order for initiation at a specific position (Browning & Busby, 2004). Due to a high degree of structural similarity, the RNAP holoenzymes in conjunction with σ^S ($E\sigma^S$) or σ^{70} ($E\sigma^{70}$), respectively, are able to recognize identical -10 and -35 consensus motifs *in vitro* (Gaal et al, 2001). *In vivo*, however, a number of σ^S-selective promoter features favour transcription only by the alternative σ factor (Typas et al, 2007). The conserved C at position -13 relative to the transcriptional start site is considered a hallmark of σ^S–dependent promoters and present in ~70% of all experimentally confirmed sites (Typas et al, 2007). The importance of this residue is defined by its direct contact with σ: two different amino acid residues, E458 and K173 in the respective sites of σ^{70} and σ^S, confer counter-selection of σ^{70} and promote interaction with σ^S (Becker & Hengge-Aronis, 2001; Lee & Gralla, 2001). Indeed, a cytosine at position -13 is present in all investigated *sdsR* promoter sequences (Fig. 2.2). Additionally, the *sdsR* promoter also meets several additional features of the proposed σ^S consensus sequence, including a 3 bp-long A/T-rich discriminator exactly downstream the -10 box, a preference for nucleotides -8C, -14G or T as well as a suboptimal spacer length in between -10 and -35 boxes (16 instead of 17 bp).

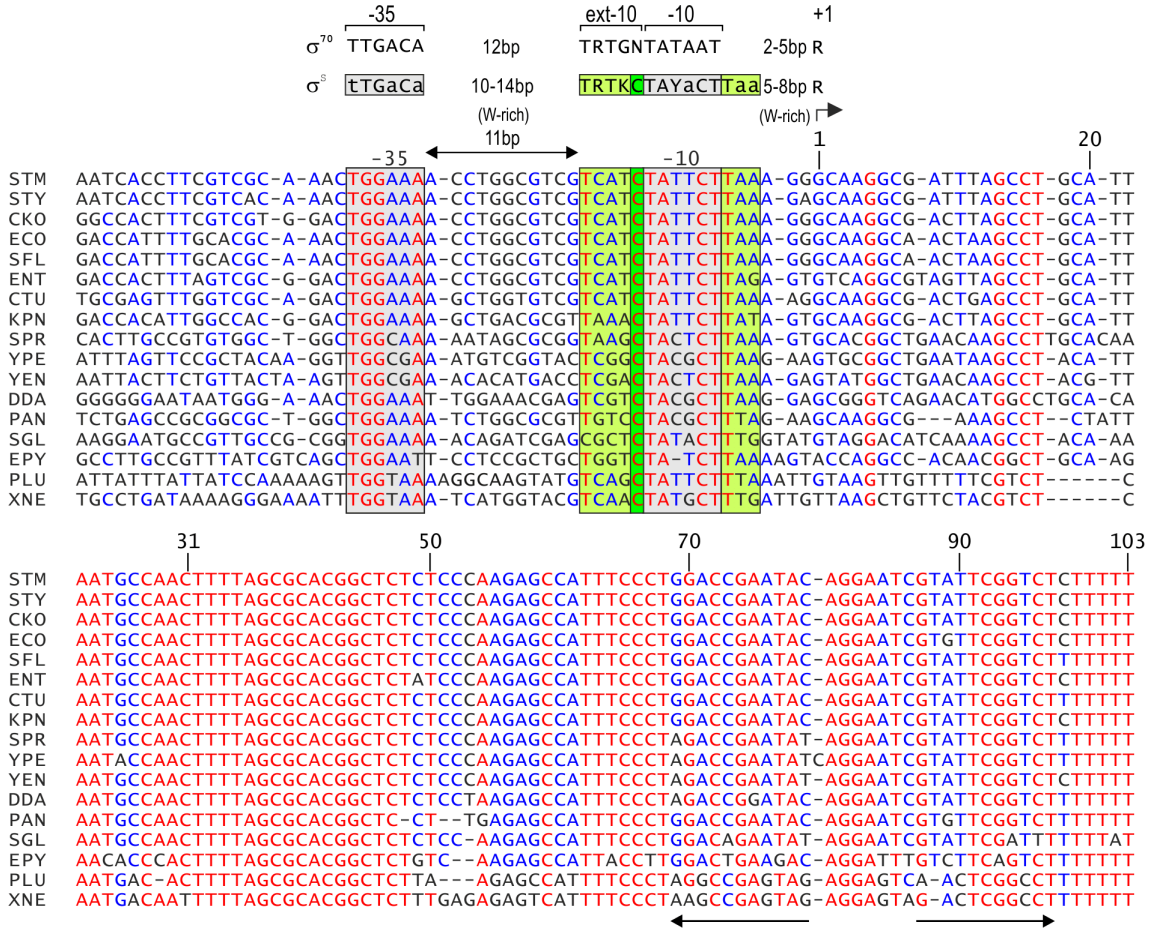

Figure 2.2 Non-redundant alignment of the *sdsR* gene and its upstream promoter region.

σ^{70} or σ^{S}-specific promoter consensus motifs (Typas et al, 2007) are indicated above the alignment (W=A/C; R=A/G; Y=C/T; K=T/G); the putative -10 and the -35 sites of the *sdsR* promoter are boxed in grey, σ^{S}-specific extensions of the -10 element are marked in light green and the conserved cytosine residue at position -13 is boxed in green. The transcriptional start site is marked by an arrow. Positioning of the ρ-independent terminator is indicated by inverted arrows. All nucleotides are coloured according to their degree of conservation (red: high conservation; blue: partial conservation; black: little or no conservation).

To experimentally validate σ^{S}-dependent transcription of *sdsR*, expression levels of the small RNA were compared in *Salmonella* wild-type and *rpoS* mutant cells grown to exponential or stationary phase. As expected, expression of SdsR increased in stationary phase, along with elevated levels of RpoS in wild-type cells (Fig. 2.3 A, lanes 1-3). In contrast, mutation of the *rpoS* gene abrogated SdsR expression in all phases of growth (lanes 4-6). Complementation of the Δ*rpoS* strain with a plasmid carrying *E. coli rpoS* under the control of the constitutive P_{tac} promoter resulted in comparable RpoS protein levels at all selected growth stages. In contrast, SdsR expression could only be fully restored in stationary phase cells (lanes 8-9), while slightly elevated SdsR levels were detected when compared to wild-type cells in late exponential phase

(compare lanes 1 and 7). Preservation of the stationary-phase specific expression of the sRNA in the presence of σ^S argued that activity rather than abundance of the σ factor is essential to drive transcription from the *sdsR* promoter. Transcription at many σ^S-dependent promoters depends on the alarmone guanosine tetraphosphate (ppGpp) (Kvint et al, 2000). The low-molecular weight effector molecule ppGpp accumulates to high levels during the so-called "stringent response" to amino acid starvation which results in rapid repression of ribosome production (Sands & Roberts, 1952; Stent & Brenner, 1961). In *E. coli* and *Salmonella*, ppGpp metabolism is primarily controlled by RelA and SpoT (Potrykus & Cashel, 2008). While *relA* mutants fail to accumulate wild-type levels of ppGpp upon starvation, the basal alarmone levels under normal growth conditions are mostly independent of RelA and rather rely on the activity of the bifunctional enzyme SpoT which can both synthesize and degrade ppGpp (Hernandez & Bremer, 1991; Xiao et al, 1991). To test a putative influence of ppGpp on SdsR expression, sRNA levels in *Salmonella* wild-type and a Δ*relA* Δ*spoT* mutant strain unable to produce ppGpp (Tedin & Norel, 2001) were compared at various growth points ranging from exponential to stationary phase. In clear contrast to *E. coli*, *rpoS* expression is only slightly decreased in a *Salmonella* Δ*relA* Δ*spoT* strain when compared to wild-type (Pizarro-Cerda & Tedin, 2004) and similar levels of RpoS protein were detected in both strains (Fig. 2.3 B, lower panel). SdsR was detected during late growth, and expression was reduced ~3-fold in the Δ*relA* Δ*spoT* strain when compared to wild-type *Salmonella* (Fig. 2.3 B, upper panel, compare lanes 3/4 and 7/8), arguing that ppGpp was required for σ^S–dependent transcription from the *sdsR* promoter.

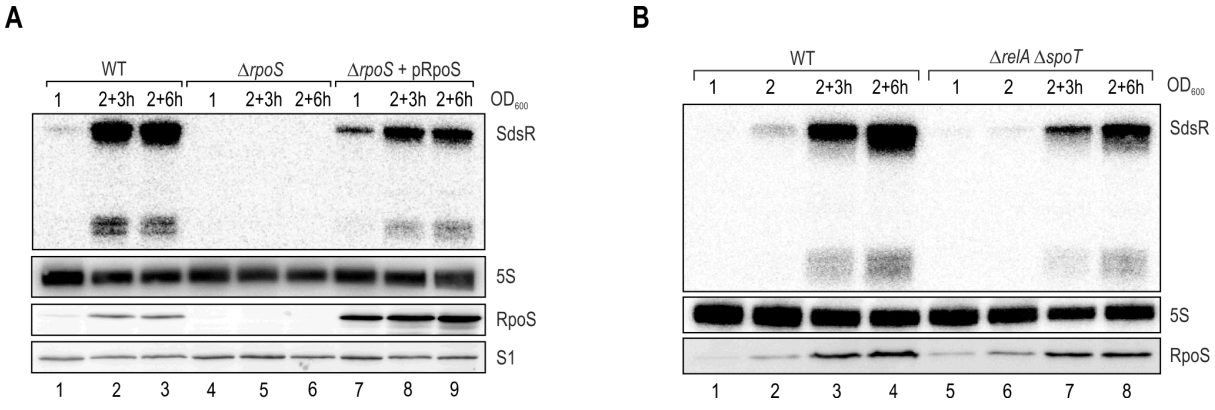

Figure 2.3 SdsR expression is dependent on σ^S and the alarmone ppGpp.

(A) SdsR sRNA is not detectable in the absence of RpoS. SdsR levels were determined by Northern blot analysis of RNA isolated at indicated time-points over growth from *Salmonella* wild-type and *rpoS* mutant cells carrying either a control vector or a plasmid constitutively expressing *E. coli* RpoS. RpoS expression was monitored on Western blots. (B) SdsR levels of *Salmonella* wild-type and a Δ*relA* Δ*spoT* mutant were determined on Northern blots at indicated time-points over growth. Expression of RpoS was monitored by Western blot analysis.

The consensus promoters for $E\sigma^S$ and $E\sigma^{70}$ are highly similar and numerous promoters are recognized by either of the two forms of RNAP (Typas et al, 2007). Since SdsR was not detectable in Δ*rpoS* (Fig. 2.3 A), the *sdsR* promoter appeared to be inaccessible for the housekeeping σ factor.

To test whether replacement of the highly conserved residue -13C by any other nucleotide would render the *sdsR* promoter more amenable to σ^{70}, the *sdsR* gene including its endogenous promoter was cloned on a low-copy plasmid and nucleotide -13C was permuted to either A, G or T. SdsR levels in Δ*sdsR* or Δ*sdsR* Δ*rpoS* mutant cells each complemented with either of the four plasmids were determined. SdsR originating from any of the four plasmids was neither detectable during exponential growth (OD_{600} of 1.0; Fig. 2.4 A) nor in the absence of RpoS (Fig. 2.4 A and B, lanes 5-8). In contrast, σ^S-dependent SdsR expression during stationary phase (3h after cells had reached an OD_{600} of 2.0) revealed differences in sRNA levels between the four promoter variants with maximal reduction (~3.5-fold) for -13T (Fig. 2.4 B, lanes 1-4).

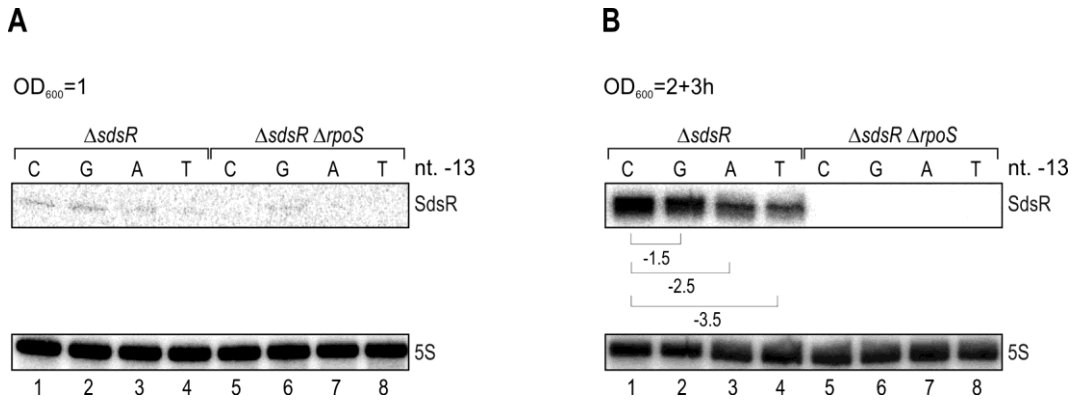

Figure 2.4 Permutation of cytosine at position -13 in the *sdsR* promoter.

Salmonella Δ*sdsR* and Δ*sdsR* Δ*rpoS* mutants were complemented with plasmid p*sdsR* or either of three derivatives differing in the nucleotide at position -13 of the *sdsR* promoter (p*sdsR* C-13G; p*sdsR* C-13A; p*sdsR* C-13T). SdsR expression during exponential (A) and stationary growth (B) was analyzed on Northern blots. Quantification of fold-changes in SdsR abundances is indicated below the panel.

The sensitivity of SdsR expression to the mutation of -13C was in accordance with the observed dependence on σ^S. However, since no shift in favour of σ^{70}-dependent transcription was observed for either *sdsR* promoter variant, additional determinants were likely to contribute to σ^S-specific recognition. Besides the consensus sequence, promoter selectivity can also be generated by additional, co-regulating transcription factors or DNA supercoiling (Kusano et al, 1996). One of the protein factors determining the organization of the bacterial chromosome is the abundant DNA-binding protein H-NS. Preferentially interacting with curved, AT-rich DNA regions, H-NS can promote bridging DNA-protein-DNA complexes to compact, and

thus silence the genetic material (Stoebel et al, 2008). The two regulons governed by RpoS and H-NS considerably overlap as numerous σ^S-dependent genes appear de-repressed in *hns* mutants (Barth et al, 1995). In addition, *rpoS* expression itself is negatively controlled by H-NS through inhibition of *iraD* and *iraM*, the genes encoding two anti-adaptor proteins which prevent σ^S degradation via the ClpXP protease (Battesti et al, 2012). A potential interference of H-NS with *sdsR* expression was examined in Δ*sdsR*, Δ*sdsR hns_trunc*, or Δ*sdsR* Δ*rpoS hns_trunc* mutants complemented with *sdsR* on plasmids carrying one of the four possible variants at position -13 in the promoter. In *Salmonella*, *hns* deletion mutants are only viable in the presence of compensatory mutations in other regulatory loci (Navarre et al, 2006). In contrast, truncation of the C-terminal DNA binding domain de-represses the majority of H-NS-silenced genes, and can be combined with additional mutants (Dillon et al, 2010; Falconi et al, 1991). Independent of the tested growth phases, expression of SdsR remained strictly dependent on the presence of σ^S also when H-NS was truncated (Fig. 2.5). Cells grown into stationary phase displayed the previously observed changes in expression from different promoter versions but no additional effect of *hns* truncation (Fig. 2.5 B, lanes 1-8). In contrast, mutation of H-NS resulted in expression of SdsR during exponential growth, probably due to an increase in RpoS (Fig. 2.5 A, lanes 5-8).

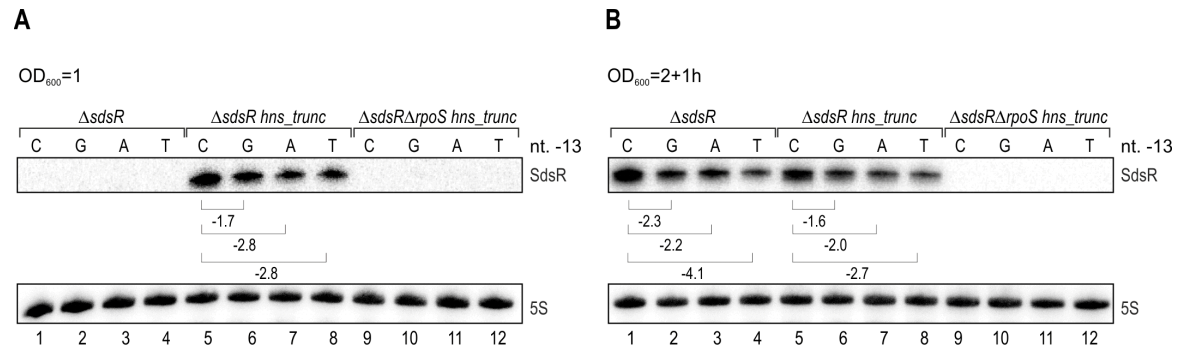

Figure 2.5 σ^S-dependency of the *sdsR* promoter is independent of H-NS.

Salmonella Δ*sdsR*, Δ*sdsR hns_trunc*, or Δ*sdsR* Δ*rpoS hns_trunc* mutants were complemented with plasmid p*sdsR* or either of three derivatives differing in the nucleotide at position -13 of the *sdsR* promoter (p*sdsR*; p*sdsR* C-13G; p*sdsR* C-13A; p*sdsR* C-13T). SdsR expression during exponential (A) and stationary growth (B) was analyzed by Northern blot analysis; quantification of fold-changes in SdsR abundances is indicated below the panel.

2.3 SdsR exhibits σ^S-dependent regulation under stress

The expression of SdsR was dependent on increasing σ^S activity upon entry into stationary growth phase. More globally, RpoS is also responsible for rewiring the cellular transcriptome under various stress conditions including heat or osmotic shock (Hengge-Aronis, 1996).

To test whether SdsR was co-induced with known members of the σ^S-regulon at elevated temperatures, wild-type as well as *rpoS* and *sdsR* mutant *Salmonella* were grown at 30°C to mid-exponential phase (OD_{600} of 0.3) when the culture was split and either continuously grown at 30°C or subjected to heat-shock at 44°C. RpoS was strongly induced within 15 minutes in both wild-type and *sdsR*-mutant strains, and levels declined again as cells became adapted to growth at higher temperature (Fig. 2.6, lower panel). In parallel, SdsR levels were induced in an σ^S-dependent manner and decreased in expression with time following the pattern observed for RpoS at the protein level (Fig. 2.6, upper panel). The *osmY* mRNA, a well-known target of $E\sigma^S$, served as a control (Lange & Hengge-Aronis, 1991; Muffler et al, 1997). As expected, expression of *osmY* increased as a consequence of the σ^S-mediated heat shock response, displaying the same expression pattern as observed for SdsR sRNA. The parallel induction of both *osmY* and *sdsR* promoters as a consequence of RpoS induction under heat-shock supported the hypothesis that SdsR expression was directly controlled by this alternative σ factor.

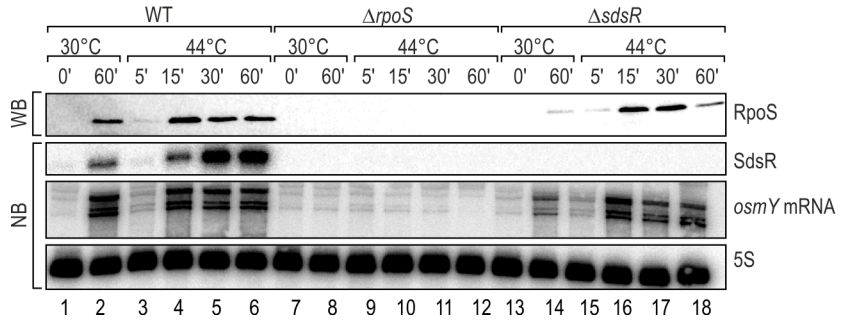

Figure 2.6 Rapid induction of SdsR sRNA and *osmY* mRNA during heat stress.

Salmonella wild-type, Δ*rpoS* and Δ*sdsR* mutants were grown at 30°C or subjected to heat-shock at 44°C. Total RNA samples withdrawn prior to and at selected time-points after temperature up-shift were analyzed by Northern blot analysis. Expression of RpoS was monitored on Western blots.

Another condition known to trigger the σ^S-mediated stress response is osmotic shock. To monitor expression from both *osmY* and *sdsR* promoters under high salt conditions, wild-type as well as *rpoS*- or *sdsR*-mutant *Salmonella* were grown in M9 minimal medium supplemented with 0.4% glycerol and 0.2% casamino acids to mid-exponential phase (OD_{600} of 0.3). Next, cultures were split and osmotic shock was induced in one aliquot by the addition of NaCl (final concentration of 0.3 M). Western blot analysis of protein samples withdrawn prior to and at selected time-points after NaCl addition confirmed that salt treatment promoted rapid accumulation of RpoS in wild-type and *sdsR*-mutant strains (Fig. 2.7, first panel). In addition, and similar to the observations upon heat shock, a qualitative correlation between SdsR and *osmY* mRNA expression levels was detected (Fig. 2.7, second and third panel).

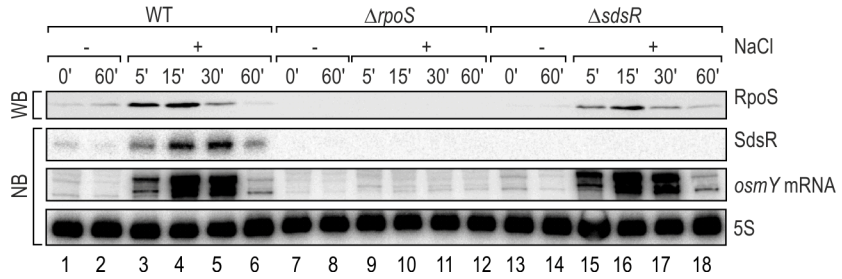

Figure 2.7 σ^S-dependent induction of SdsR during osmotic stress.

Determination of SdsR and *osmY* mRNA levels on Northern blots of total RNA prepared from wild-type, Δ*rpoS* and Δ*sdsR* mutant cells. Samples were withdrawn prior to or at indicated time-points after addition of NaCl (final concentration: 0.3 M). Expression of RpoS was controlled by Western blot analysis.

Determination of RNA levels on Northern blots is useful to determine transcript levels, however, does not necessarily allow the comparison of the induction dynamics at different promoters. Transcriptional *lacZ*$^+$ reporter fusions were employed to measure the activity of the *sdsR* and *osmY* promoters upon heat and osmotic shock induced as described above. Determination of relative β-galactosidase levels at different time-points after stress onset revealed the *sdsR* and *osmY* promoters to respond almost identically to the respective conditions (Fig. 2.8 A and B). In agreement with the Northern blot analyses (Fig. 2.6 and 2.7), activation appeared delayed under heat shock when compared to osmotic stress.

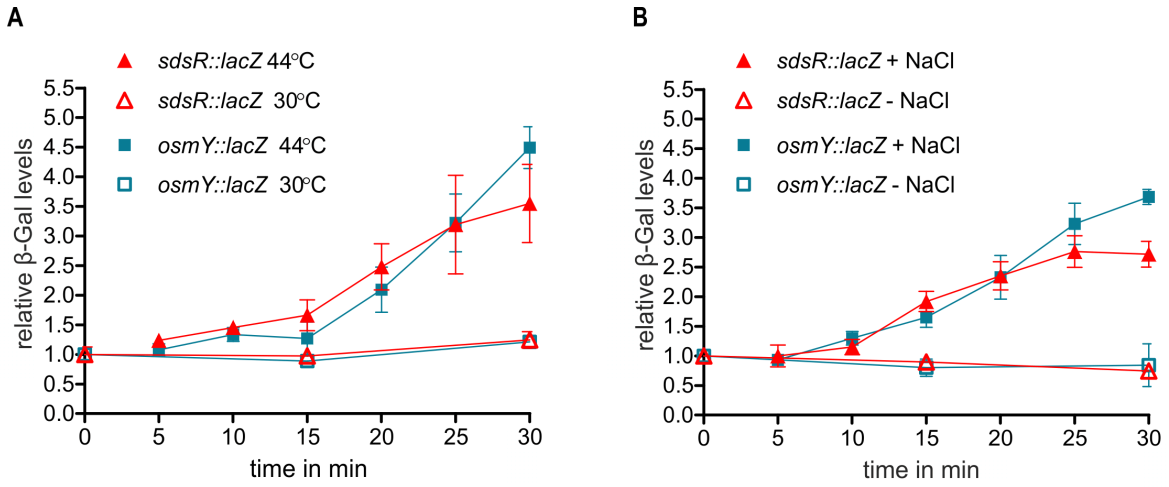

Figure 2.8 Activity of *sdsR* and *osmY* promoters during heat and osmotic shock.

Promoter activities of *Salmonella sdsR::lacZ* (red triangles) and *osmY::lacZ* (blue squares) fusions were determined by measuring relative ß-galactosidase activities over 30 min in culture samples upon (A) heat-shock induced by a temperature shift from 30°C (open symbols) to 44°C (filled symbols) or (B) in the presence (filled symbols) or absence (open symbols) of 0.3 M NaCl. Error bars represent the standard deviation calculated from three biological replicates.

2.4 The influence of SraC on SdsR expression

The *sdsR* gene is transcribed from a locus positioned internal to a second sRNA gene, the oppositely located *sraC* (Argaman et al, 2001; Balbontin et al, 2008; Vogel et al, 2003; Wassarman et al, 2001). While sequence and promoter elements of *sdsR* are highly conserved in numerous enterobacterial genomes (Fig. 2.2), similar analysis of the *sraC* gene revealed poor maintenance and the sRNA could only be predicted in approximately half of the evaluated species (Fig. 2.1 A). Sequence conservation of *sraC* is mostly restricted to the region overlapping with *sdsR* and strikingly, also location and nucleotide composition of putative *sraC* promoter elements are highly variable among different organisms (Fig. 2.9). In detail, the -10 promoter element determined for *E. coli* (Argaman et al, 2001) is not conserved in other enterobacteria. Instead, *Salmonella* and *Shigella* sequences feature a potential -10 box ~35 bp further upstream (Fig. 2.9). The exact 5' ends of SraC were determined by analyzing dRNA-seq data of *S*. Typhimurium, *E. coli*, *S. flexneri* and *C. rodentium* transcriptomes (chapter 4.1; Table 4.2). The specific enrichment of SraC primary transcripts enabled the mapping of the transcriptional start sites with a spacing of six bp downstream the predicted -10 boxes in *S*. Typhimurium, *E. coli* and *S. flexneri* (Fig. 2.9).

SdsR and SraC expression in *E. coli, Salmonella,* and *Shigella* species was analyzed at different stages of growth. In accordance with its overall high degree of sequence conservation, the expression pattern of SdsR was comparable between the three species, and the sRNA accumulated with entry into stationary phase (Fig. 2.10, top panel). Likewise, the strict dependence on σ^S was apparent in all three species and almost constitutive expression of the alternative σ factor seemed to account for the low levels of SdsR detected during exponential growth in *Shigella* (Fig. 2. 10, first panel and second panel from the bottom). In contrast to SdsR expression, probing of SraC gave a mosaic picture (Fig. 2.10, second panel): In accordance with the predicted promoter elements and the transcriptome data, *Shigella* and *Salmonella* SraC RNAs were observed to be ~35 nt longer than the *E. coli* counterpart, and detected primarily in exponential phase (lanes 1-4 and 9-12). SraC levels in *E. coli* were slightly higher than in the other two species (lanes 5-8) and commonly, SraC and SdsR appeared to accumulate inversely. In addition, both full-length and several processed versions of SraC were detected in all three organisms.

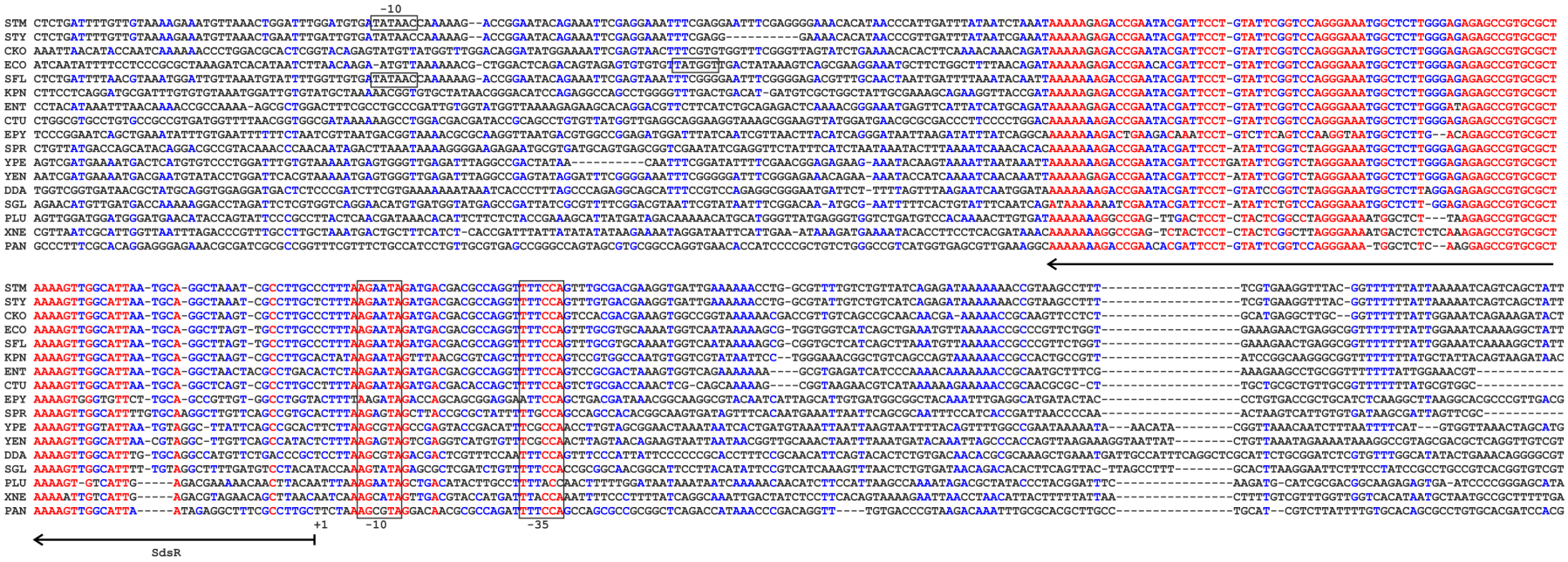

Figure 2.9 Non-redundant alignment of the *sraC* promoter region.

The putative -10 sites of the *sraC* promoter in *Salmonella* (STM), *E. coli* (ECO) and *Shigella* (SFL) are boxed. Location of *sdsR* is indicated by an arrow, and *sdsR* -10 and -35 sequences are boxed. All nucleotides are coloured regarding their degree of conservation (red: high conservation; blue: partial conservation; black: little or no conservation).

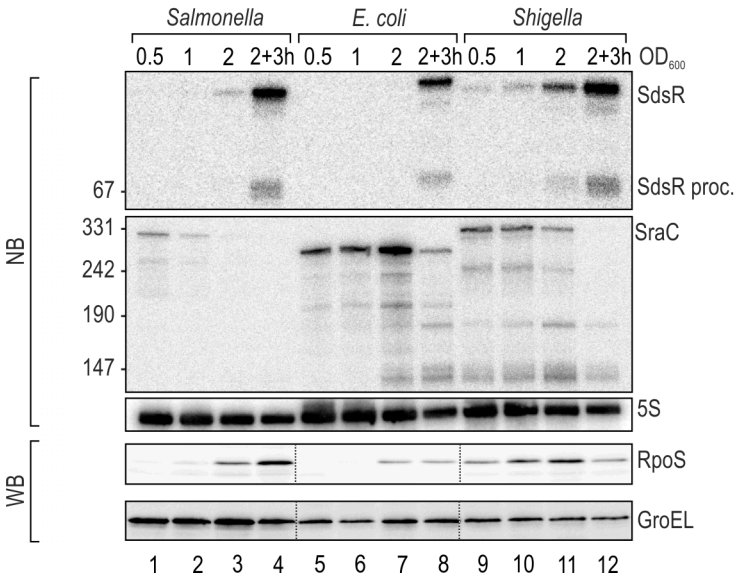

Figure 2.10 Expression patterns of SdsR and SraC in *Salmonella*, *E. coli* and *Shigella*.

Northern blot analysis of total RNA isolated from wild-type *Salmonella*, *E. coli* and *Shigella* cells grown to OD_{600} of 0.5, 1.0, 2.0 and 3 h after cells had reached an OD_{600} of 2.0. SdsR and SraC sRNAs were detected by radio-labelled oligo probes recognizing conserved sRNA sequences. Expression of RpoS and GroEL was monitored by Western blot analysis.

A previous study in *E. coli* demonstrated processing of SraC to be dependent on the double-strand specific nuclease RNase III and suggested cleavage to result from base-pairing to SdsR (Vogel et al, 2003). Thus, both RNAs could in principal influence the expression of the oppositely encoded gene. To determine the effect of SdsR on SraC accumulation and *vice versa*, the expression profiles of both sRNAs were investigated in individual mutants of *Salmonella* and *E. coli*. Expression of SraC was abolished by deleting its promoter sequence (encompassing bp -30 to +12 relative to the transcriptional start site) from the chromosome. Since deletion of *sdsR* or its promoter would concomitantly result in SraC truncation, an *rpoS* mutant strain served as an indirect knock-out for SdsR. In *Salmonella* and *E. coli sraC* promoter mutants SdsR levels were only mildly increased (~1.5-fold) at early time-points (Fig. 2.11 A and B, top panels, lanes 3/4 vs. 7/8). Thus, given its low degree of conservation and the slight changes in SdsR levels in its absence, SraC appeared to only play a minor role in modulation of SdsR expression. In contrast, deletion of *rpoS* – *i.e.* absence of SdsR – abrogated the growth-phase-dependent detection of SraC observed in wild-type strains and resulted in constitutive levels of the sRNA (Fig. 2.11 A and B, middle panels, lanes 1-4 vs. 9-12). Thus SdsR appeared to be responsible for the restricted expression of SraC during early phases of growth. Interestingly, as observed from the *E. coli* samples, SraC is also processed in the absence of SdsR (Fig. 2.11 B, lane 12) but the cleavage pattern differs clearly compared to the wild-type strain (Fig. 2.11 B, lanes 4 vs. 12).

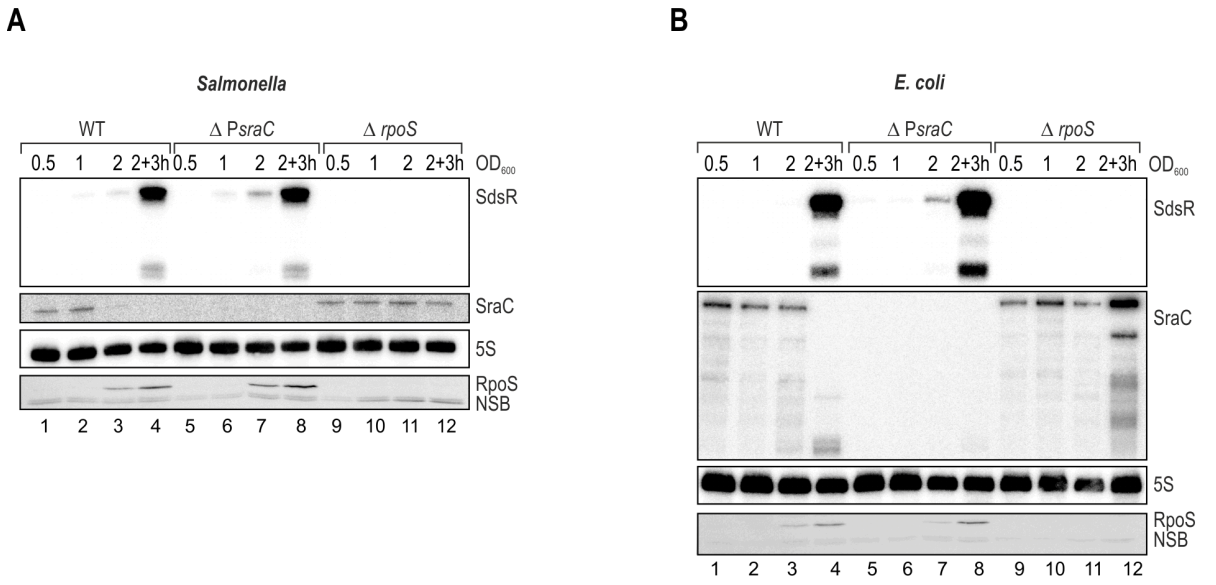

Figure 2.11 Interdependence of SdsR and SraC expression in *Salmonella* and *E. coli*.

Expression of SdsR and SraC sRNAs were compared on Northern blots between (A) *Salmonella* and (B) *E. coli* wild-type, *sraC* promoter mutants and *rpoS* mutants grown in LB to an OD_{600} of 0.5, 1.0, 2.0 and 3 hours after cells had reached an OD_{600} of 2.0. RpoS levels were determined by Western blot analysis of total protein samples; a non-specific band (NSB) served as loading control.

2.5 SdsR represses synthesis of the major porin OmpD

Of the more than 100 Hfq-associated sRNAs identified to date in well-studied Gram-negative bacteria like *E. coli* or *Salmonella*, cellular functions have only been assigned to a minority of riboregulators (Peer & Margalit, 2011). The characterization of the biological role of an sRNA requires the definition of its cellular target molecules.

One possibility to identify potential targets is to compare protein expression patterns by SDS-PAGE in the presence and absence of a given regulatory RNA. Although this approach covers only abundant proteins and does *a priori* not allow to distinguish primary from secondary targets it has been proven successful in the discovery of interaction partners of numerous Hfq-bound sRNAs (Vogel & Wagner, 2007). The *sdsR* gene was cloned on a plasmid under the control of the constitutive P_L-promoter (synthetic P_{LlacO} derivative; (Lutz & Bujard, 1997)). *Salmonella* wild-type and *sdsR* mutants carrying either a control vector or the pP_L-SdsR expression plasmid were grown in LB and global protein profiles of various time-points were analyzed. Whereas comparison of wild-type and Δ*sdsR Salmonella* did not reveal differences (Fig. 2.12 A, lanes 1-8), constitutive, P_L-driven SdsR expression specifically depleted an abundant, ~40 kDa protein in all phases of growth (Fig. 2.12 A, lanes 9-12). The band resembled the migration pattern of the major *Salmonella* outer membrane protein D (Lee & Schnaitman, 1980). To verify this prediction, expression of *ompD* was monitored both at the mRNA and at the protein level in

Salmonella wild-type, Δ*sdsR* (carrying either a control plasmid or pP_L-SdsR) and Δ*ompD* cells grown into early stationary phase. OmpD abundance was strongly reduced in the presence of SdsR while the levels of the other major OMPs, namely OmpC, OmpF and OmpA, remained largely unchanged (Fig. 2.12 B, second panel from the top). Concomitantly, the changes observed at the protein level were also reflected by lower abundance of the *ompD* transcript (Fig. 2.12 B, third panel from the top), arguing that the observed regulation was due to specific restriction of *ompD* expression by SdsR.

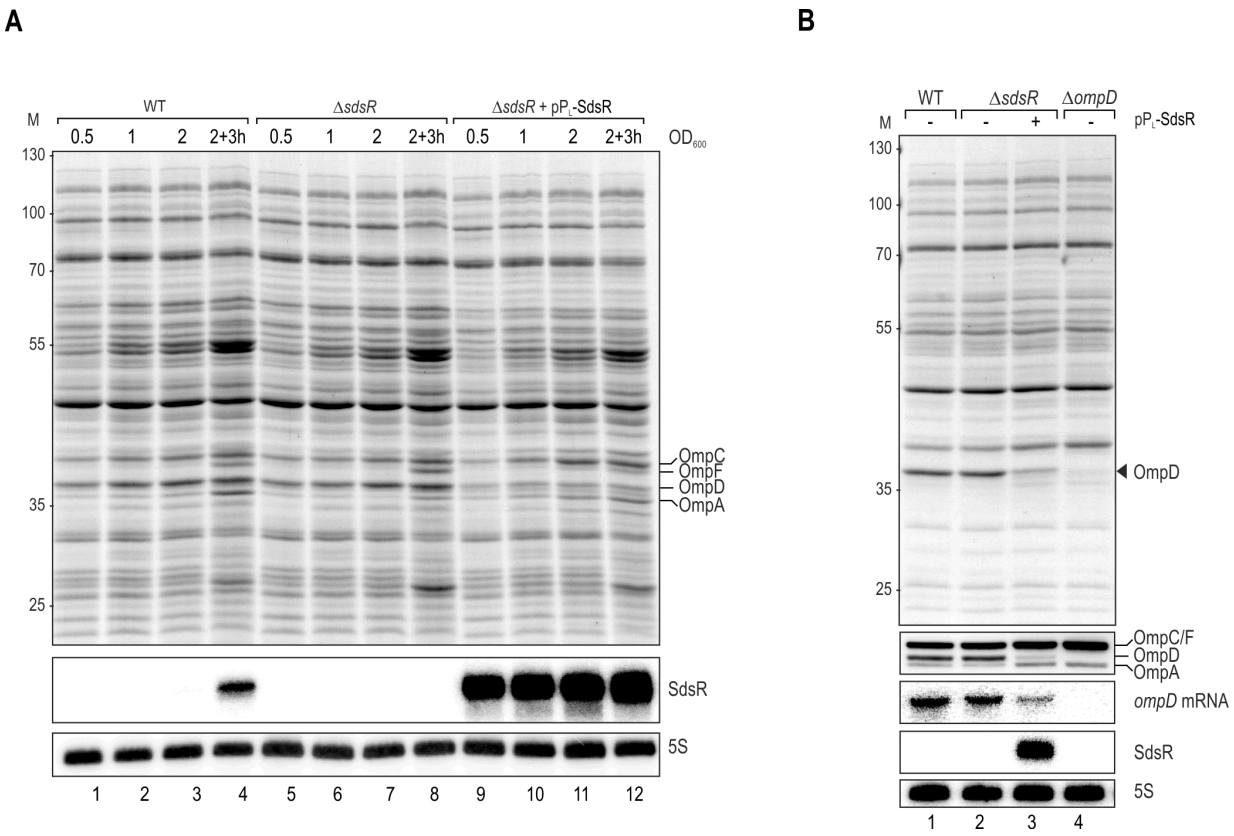

Figure 2.12 SdsR down-regulates the *Salmonella* OmpD protein.

(A) Whole-cell protein patterns of wild-type and Δ*sdsR Salmonella* carrying either a control vector or the constitutive SdsR-expression plasmid pP_L-SdsR grown in LB were compared by separation of total cell lysates from several conditions (OD_{600} of 0.5 (lanes 1, 5, 9); 1.0 (lanes 2, 6, 10); 2.0 (lanes 3, 6, 11); 3 h after cells had reached an OD_{600} of 2.0 (lanes 4, 9, 14)) by 11% SDS-PAGE; the gel was stained for abundant proteins with Coomassie Blue. Sizes of co-migrating marker proteins are indicated at the left (in kDa). Positions of the major porins OmpC, OmpF, OmpD and OmpA are marked. SdsR expression was determined by Northern blot analysis of RNA isolated from the same cultures. (B) Wild-type, Δ*sdsR* and Δ*ompD Salmonella* transformed with either the control vector or pP_L-SdsR were grown to an OD_{600} of 2.0, and OmpD protein levels were analyzed on SDS-PAGE gels and Western blots (the antiserum detected all major *Salmonella* porins as indicated). Northern blot analysis of the same strains revealed reduced *ompD* mRNA steady state levels in cells over-expressing SdsR.

2.6 Requirement of the SdsR 5' end for *ompD* regulation

Recently, the two regulatory sRNAs MicC and RybB have been described to target the *ompD* transcript via their conserved 5' ends and to accelerate mRNA decay (Papenfort et al, 2010; Papenfort et al, 2006; Pfeiffer et al, 2009). In contrast, the 5' end of full-size SdsR displayed overall less conservation when compared to the central part of the molecule constituting the processed fragment of SdsR (Fig. 2.2). To determine the minimal SdsR sequence required for OmpD repression, different truncated sRNA versions were expressed under the control of the constitutive P_L-promoter (Fig. 2.13 A). *Salmonella* Δ*sdsR* cells were transformed with either a control plasmid or the different SdsR constructs and expression of all tested variants of SdsR was confirmed (Fig. 2.13 B). Regulation of *ompD* was monitored at both the transcript (Fig. 2.13 B) as well as the protein level (Fig. 2.13 C). In contrast to the full-length sRNA, the processed form of SdsR (SdsR proc.) failed to repress OmpD (Fig. 2.13 C, lanes 1-3). Additional truncated versions were lacking the first 6 or 18 nucleotides, respectively, and thus constituted intermediates between the processed form and the full-length sRNA. While SdsR+19 had no regulatory effect on OmpD (Fig. 2.13 C, lane 5), SdsR+7 was as efficient in depleting the porin as the full-length sRNA (Fig. 2.13 C, lane 4). In addition, a chimeric RNA in which SdsR nt 14-32 were fused to the 3' portion of the unrelated sRNA MicA (truncated MicA, TMA) was constructed (SdsR-TMA; see Supplementary Fig. 4.7 for an alignment). When investigating the effect on *ompD* expression, the TMA scaffold alone did not exhibit an effect while SdsR-TMA was as efficient as wild-type SdsR in decreasing OmpD levels (Fig. 2.13 C, lanes 6/7).

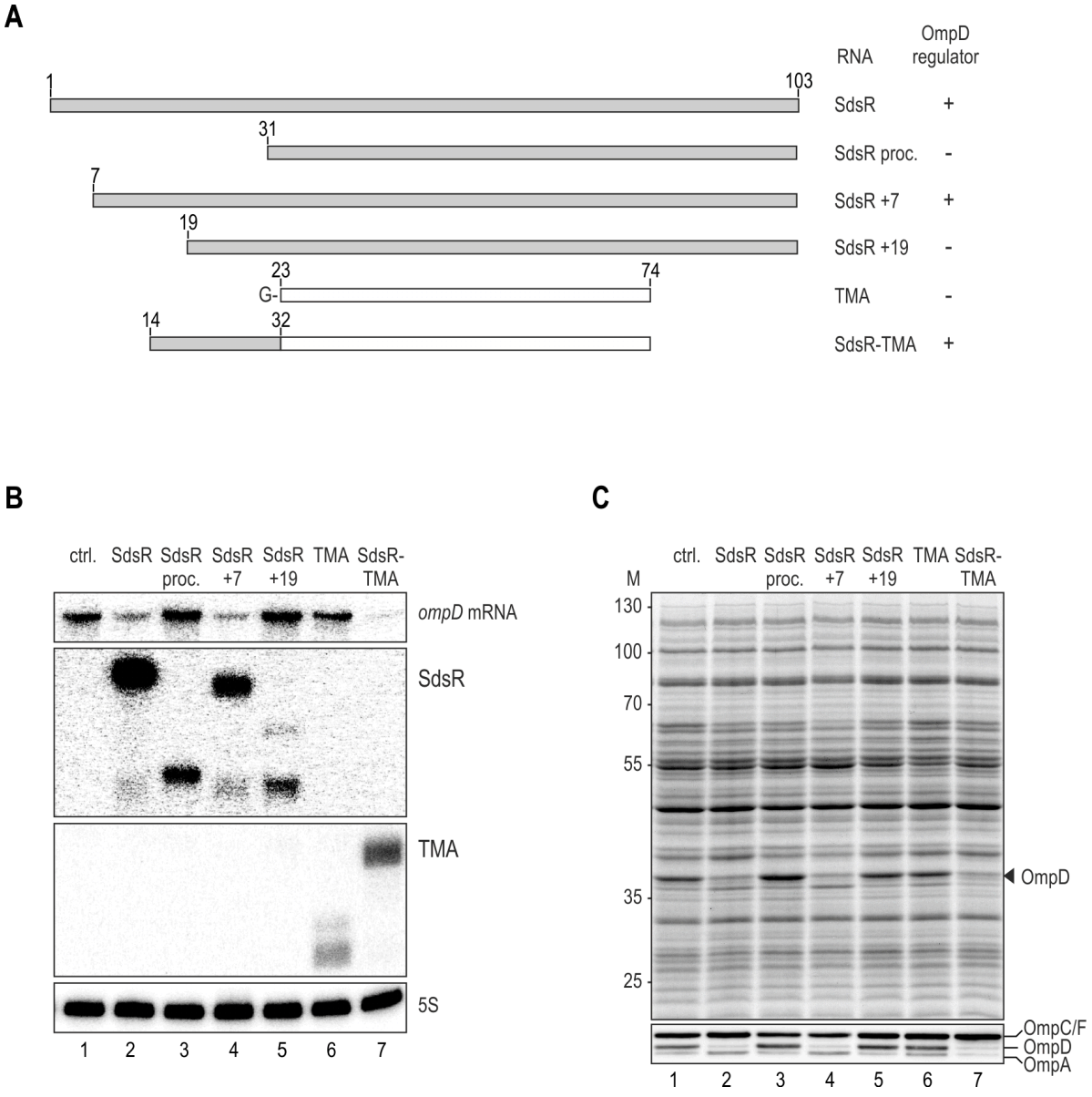

Figure 2.13 The SdsR 5' end is required for *ompD* regulation

(A) Schematic representation indicating size and composition of SdsR variants or chimeras tested for OmpD regulation (see Supplementary Fig. 4.7 for an alignment of all sRNA variants). TMA designates a 5' shortened variant of the unrelated MicA sRNA (Truncated MicA). (B) *Salmonella* Δ*sdsR* transformed with a control vector or plasmids constitutively expressing different versions of SdsR (as depicted in A; pP_L-SdsR; pP_L-SdsR proc.; pP_L-SdsR +7; pP_L-SdsR +19; pP_L-SdsR-TMA; pP_L-TMA) were grown to an OD_{600} of 2.0. Expression of *ompD* mRNA in the presence of control RNAs or the various SdsR constructs was determined on Northern blots. (C) Total protein samples in the presence of the control or the different SdsR expression constructs were analyzed by SDS-PAGE (upper panel), and specific deregulation of OmpD was confirmed by Western blot analysis (lower panel).

2.7 SdsR regulates *ompD* mRNA post-transcriptionally

Although SdsR clearly repressed *ompD* mRNA, the chosen experimental approach (constitutive overexpression of the sRNA) was insufficient to classify *ompD* as a primary target. In contrast, pulse expression of sRNA regulators has proven successful in the identification of directly interacting mRNAs (Masse et al, 2005; Papenfort et al, 2006). Short induction of the sRNA is considered to restrict the observed changes in mRNA levels to result from base-pairing rather than from secondary effects.

To assess whether *ompD* regulation resulted from a direct sRNA/mRNA interaction, SdsR was cloned on a plasmid under the control of an arabinose-inducible P_{BAD} promoter. *Salmonella* Δ*sdsR* or Δ*sdsR* Δ*ompD* were transformed with either pBAD-SdsR or a pBAD control vector and expression of the small RNA was induced by addition of L-arabinose. Pulse-expression of SdsR was accompanied by a ~10-fold drop of *ompD* mRNA levels within 10 minutes (Fig. 2.14, lanes 3-6). By contrast, *ompD* mRNA abundance was unaffected in the strain carrying the control plasmid (Fig. 2.14, lanes 1-2). This finding indicated that *ompD* mRNA was directly repressed by SdsR sRNA.

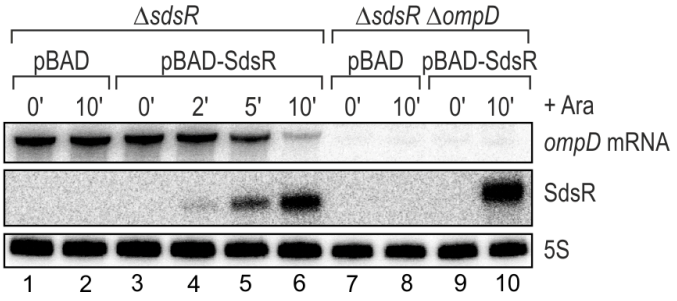

Figure 2.14 Pulse expression of SdsR sRNA results in a rapid decrease of *ompD* mRNA levels.

Salmonella Δ*sdsR* and Δ*sdsR* Δ*ompD* cells carrying either the pBAD control vector or plasmid pBAD-SdsR were grown to an OD_{600} of 1.5. Total RNA samples were collected prior to and at indicated time-points after L-arabinose addition (0.2% final concentration), and expression of SdsR and *ompD* mRNA was assessed by Northern blot analysis.

2.8 Coding-sequence targeting of *ompD* mRNA by SdsR

The default mechanism employed by sRNAs to downregulate bacterial gene expression is through sterical hindrance of ribosome assembly on the RNA by base-pairing around the translation initiation region (Shine-Dalgarno (SD) sequence and the start codon). In bacteria, translationally silenced mRNAs are usually subject to rapid degradation by ribonucleases and consequently, sRNA activity often results in drastically accelerated target decay (Waters & Storz,

2009). Regarding the spatial requirements for sRNA interference with translation initiation, a recent study has defined a "5-codon window". The riboregulator can achieve efficient exclusion of the ribosome from a target mRNA as it associates within the first five codons downstream the translational start site (Bouvier et al, 2008).

To address whether SdsR would target *ompD* mRNA within the 5-codon window, an established reporter system based on the constitutive co-expression of an sRNA and an amino-terminal translational fusion of the target gene to GFP was employed (Urban & Vogel, 2007). *Salmonella* Δ*sdsR* Δ*ompD* mutants were transformed with a combination of both P_L-SdsR and *ompD::gfp* comprising the 5' UTR plus increasing parts of the coding sequence (CDS) or the respective control plasmids (Fig. 2.15 A). SdsR slightly increased GFP expression of the control plasmid (~1.3-fold induction), but did not alter the levels of fusions to the first or the fifth codon, respectively, of OmpD when compared to the control strain (Fig. 2.15 B, C). In contrast, protein levels from GFP fusions reaching down to the 26th or further to the 33rd codon of OmpD were specifically reduced in the presence of SdsR. Consequently, regulation of *ompD* mRNA was demonstrated to depend on binding of SdsR downstream the fifth codon.

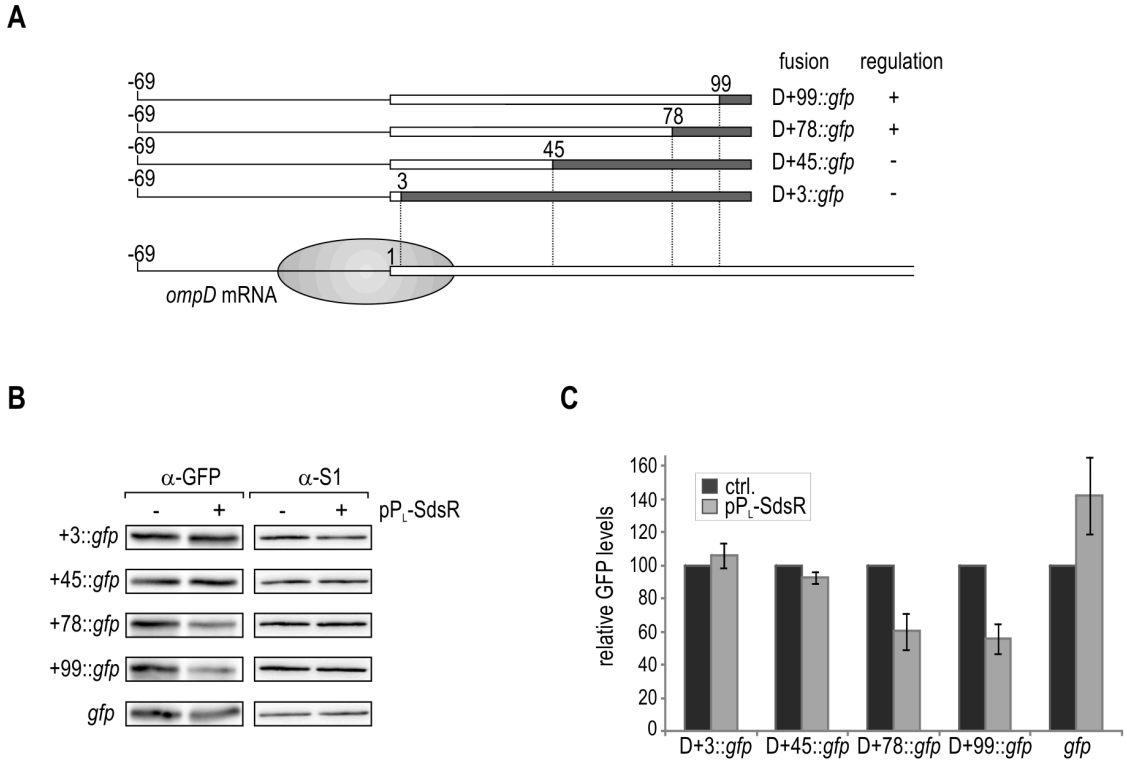

Figure 2.15 Regulation of *ompD::gfp* reporter fusions by SdsR.

(A) Schematic representation of a series of translational *ompD::gfp* fusions spanning the complete 5' UTR plus an increasing number of nucleotides of the *ompD* CDS (D+3::*gfp*; D+45::*gfp*; D+78::*gfp*; D+99::*gfp*). The filled circle indicates the approximate coverage of *ompD* mRNA by the 30S ribosomal subunit binding

to the RBS. (B) *Salmonella* Δ*sdsR* Δ*ompD* cells carrying the control vector or pP_L-SdsR were co-transformed with low-copy plasmids expressing *gfp* alone or translational *ompD::gfp* fusions as depicted in (A). Whole-protein samples were collected from cells grown to an OD_{600} of 2.0 and regulation of reporter fusions was determined on Western blots. (C) Relative GFP levels in the presence of the control plasmid (black bars; set to 100) or the constitutive pP_L-SdsR (grey bars); error bars indicate the standard deviation of three biological replicates.

2.9 SdsR requires RNase E for *ompD* mRNA decay

Three additional sRNAs regulate *ompD* expression at the post-transcriptional level in *Salmonella*. Notably, the binding sites for RybB, InvR and MicC are located within the *ompD* CDS. While the interaction sites of RybB and InvR are – at least partially – overlapping the translation initiation region, MicC base-pairs with *ompD* mRNA as far downstream as codons 23-26 and cannot interfere with ribosome association (Balbontin et al, 2010; Bouvier et al, 2008; Papenfort et al, 2010; Pfeiffer et al, 2009; Pfeiffer et al, 2007). Instead, MicC is considered to recruit the major endoribonuclease, RNase E, to the duplex and thus promotes rapid cleavage of the *ompD* mRNA (Pfeiffer et al, 2009). Like MicC, also SdsR only regulated reporter fusions including sequences downstream the 15th codon of *ompD* mRNA. To determine whether RNase E was an essential factor for the observed regulation by SdsR, a temperature-sensitive *Salmonella* strain mutant (*rne*-TS) for the otherwise essential enzyme was employed (Apirion, 1978; Figueroa-Bossi et al, 2009). When *rne*-TS cells are grown at 30°C, RNase E retains its activity but it is rapidly inactivated due to a conformational rearrangement when the culture is shifted to a non-permissive temperature of 44°C (Apirion, 1978; Figueroa-Bossi et al, 2009). To exclude any influence of the residual sRNA regulators, both the *rne*-TS as well as an isogenic wild-type strain were deleted for all four riboregulators known to target *ompD* mRNA (Δ*sdsR* Δ*micC* Δ*rybB* Δ*invR*) and transformed with pBAD-SdsR. Cells were grown at 30°C to early stationary phase when the culture was split. Upon continued growth at either 30°C or at 44°C for 30 minutes to inactivate RNase E in the temperature-sensitive strain, SdsR expression was induced. At 30°C, SdsR facilitated *ompD* mRNA downregulation in both *rne*-TS and the control strain (2.16, lanes 1-4). At 44°C, SdsR accumulated to even higher levels within the monitored time of induction, however *ompD* mRNA was no longer destabilized in the absence of functional RNase E (2.16, lanes 5-14) arguing that activity of the ribonuclease was essential for SdsR-mediated repression. Of note, inactivation of RNase E abrogated the accumulation of the less abundant, 70 nt species SdsR proc. (2.16, lanes 7/8 and 13/14).

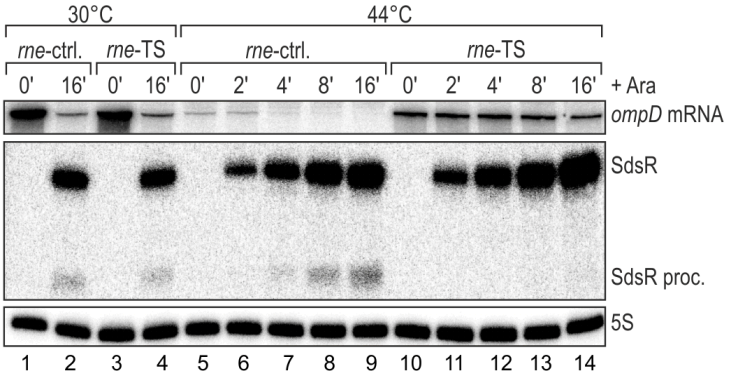

Figure 2.16 RNase E is essential for post-transcriptional repression of *ompD* mRNA by SdsR.

Salmonella rne-ctrl. deleted for *rybB*, *micC*, *invR* and *sdsR* sRNA genes and its isogenic *rne*-TS strain were transformed with pBAD-SdsR and grown at 30°C to an OD_{600} of 1.5 when cultures were split. Growth was continued for 30 min at 30°C or, to inactivate RNase E in *rne*-TS, at 44°C prior to arabinose-induced expression of SdsR for 10 minutes. Levels of *ompD* mRNA, SdsR RNA were determined by Northern blot analysis of total RNA.

Remarkably, the shift in temperature from 30°C to 44°C resulted in a reduction of basal *ompD* mRNA levels, which was more pronounced in the presence of functional RNase E (Fig. 2.16, lanes 1, 3, 5 and 10). The experiment had been performed in a strain deleted for *sdsR, micC, rybB* and *invR*. To test whether yet another sRNA was potentially involved in OmpD repression during heat-shock, mRNA decay was compared between wild-type cells and two strains either lacking all of the four relevant sRNAs (Δ*sdsR* Δ*micC* Δ*rybB* Δ*invR*) or carrying a mutation in *hfq*. As described above, cells were grown at 30°C to late exponential phase, and then shifted to 44°C in order to induce heat stress. Decay of *ompD* mRNA was monitored prior to and at different time-points after temperature shift. Strikingly, the absence of Hfq resulted in increased stability of the *ompD* transcript when compared to the sRNA deletion strain (Fig. 2.17; 6.6-fold (lanes 5/7) vs. 1.5-fold reduction (lanes 9/11) within 15 minutes). This observation indicated that *ompD* is – even in the absence of SdsR, MicC, RybB as well as InvR - potentially subject to additional, Hfq-dependent repression under heat shock.

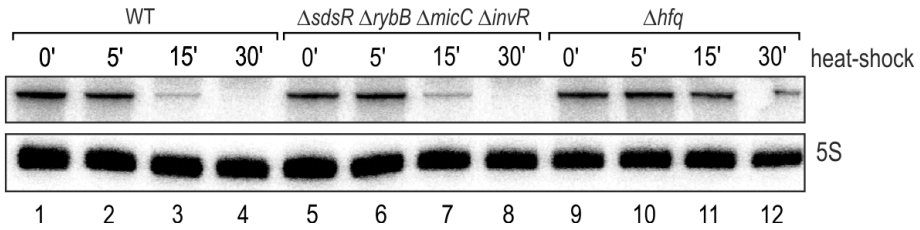

Figure 2.17 Hfq-dependent regulation of *ompD* under heat-shock.

Salmonella wild-type and strains deleted for either the four sRNAs *rybB*, *micC*, *invR* and *sdsR* or the *hfq* gene were grown at 30°C to an OD_{600} of 1.5 and subjected to heat shock at 44°C. Decay of *ompD* mRNA was determined by Northern blot analysis of total RNA samples taken at indicated time-points post temperature-shift.

2.10 A 3'RACE-based approach to target site identification

The strict requirement of RNase E for the SdsR-mediated repression of *ompD* was reminiscent of the mechanism by which MicC destabilizes the transcript. As MicC base-pairs within the *ompD* CDS, it recruits RNase E to the duplex and thus provokes cleavage of the transcript by the ribonuclease. This endonucleolytic cut was identified to occur 4-5 nt downstream the interaction site, and generated a stable intermediate of the *ompD* transcript. Consequently, mapping of the 3' end of the fragment accumulating upon sRNA activity approximated the position of the interaction site (Pfeiffer et al, 2009). Assuming that SdsR may similarly direct RNase E to process *ompD* mRNA in close proximity of the sRNA pairing region, fragments of the *ompD* transcript emerging after decay initiation by SdsR were investigated. In order to identify a potential region of interaction with the sRNA, 3'RACE was employed to define termini of accumulating *ompD* mRNA intermediates. To this end, DNA-free RNA was prepared from *Salmonella* Δ*sdsR* or Δ*sdsR* Δ*ompD* transformed with either pBAD-SdsR or a pBAD control vector prior to and at various time-points after induction with arabinose. Upon ligation of an RNA linker to the dephosphorylated RNA, cDNA was reverse transcribed and amplified using gene- and adapter-specific oligos (Fig. 2.18 A). When separating the products on an agarose gel, several *ompD*-specific bands could be observed. One ~150 bp fragment accumulated with increasing SdsR levels (Fig. 2.18 B, lane 6). This band was purified from the gel, subcloned and analyzed by sequencing. All obtained fragments ranged from the 5' end at the translational start site further than the fifth codon and accumulated at a region around amino acid 20 (Fig. 2.18 C). This result was in agreement with the regulation observed for the different translational *ompD::gfp* fusions (Fig. 2.15 B/C).

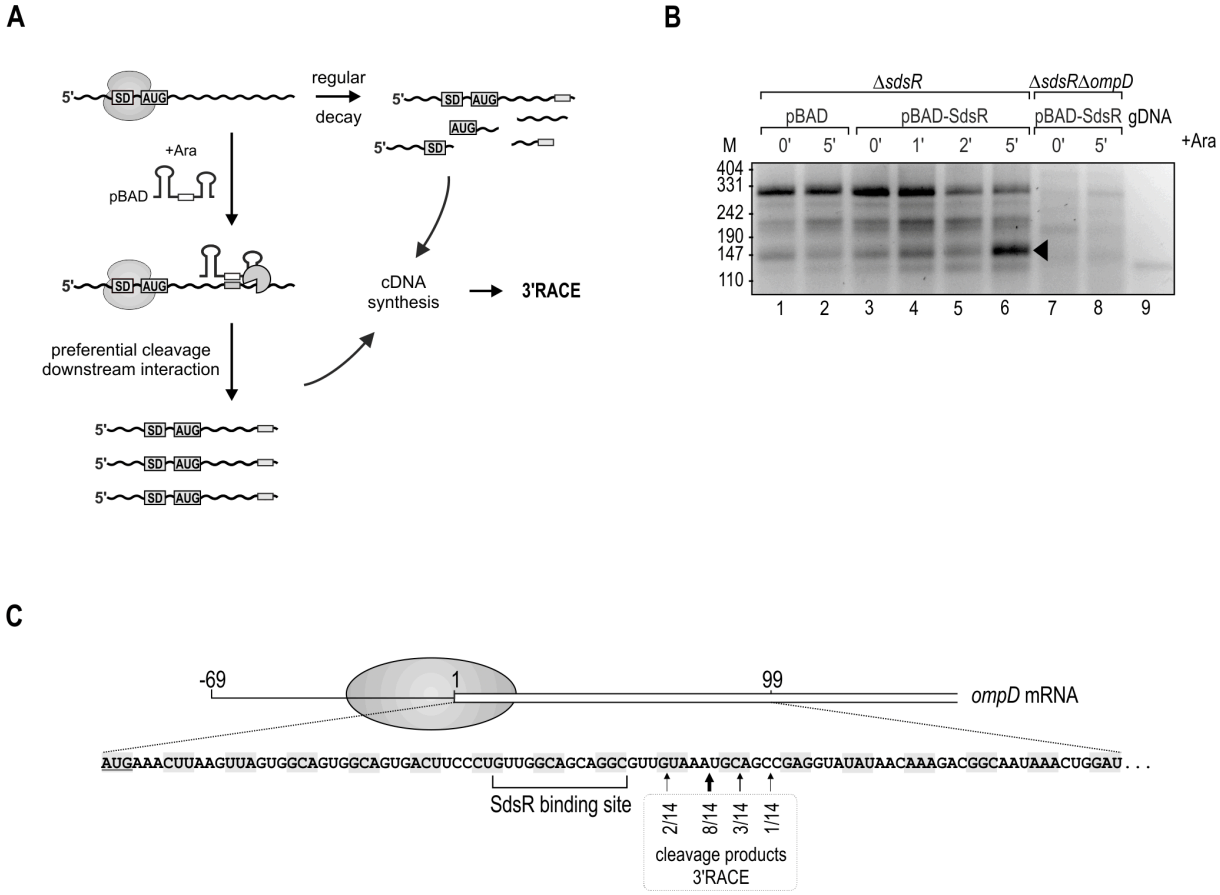

Figure 2.18 3'RACE analysis of *ompD* mRNA fragments enriched upon SdsR expression.

(A) Schematic illustration of the 3'RACE approach employed for target site determination. Pulse expression of SdsR resulted in an enrichment of mRNA fragments generated by processing downstream the sRNA binding site. (B) cDNA was prepared from total RNA of Δ*sdsR* cells as well as the Δ*sdsR* Δ*ompD* control strain prior to and at indicated time-points after SdsR induction from the inducible pBAD promoter. Cells transformed with the pBAD control plasmid and *Salmonella* genomic DNA (gDNA) served as controls. DNA fragments were recovered from the indicated band of ~150 bp (lane 6) and *ompD* 3' ends were determined by sequencing of subcloned fragments. (C) Mapping of *ompD* 3' ends obtained by 3'RACE analysis. Position as well as frequency of enriched break-down products determined by 3'RACE are shown below the sequence of the *ompD* CDS. The SdsR binding site (as determined in chapter 2.11) is indicated.

2.11 Validation of the SdsR binding site on *ompD* mRNA

The SdsR sequence essential for *ompD* repression had been narrowed down before by testing the regulatory potential of different truncation mutants (Fig. 2.13), and this result facilitated the biocomputational prediction of the sRNA/mRNA duplex. A potential interaction upstream of the 20th codon on the *ompD* messenger was determined using the RNA*hybrid* program (Rehmsmeier et al, 2004). The pairing of SdsR and the *ompD* CDS was predicted to consist of an imperfect duplex of two short helices interrupted by a 5-nt bulge in the sRNA (Fig. 2.19 A). Thus,

combining the data obtained for the SdsR truncation mutants, the results of the 3'RACE experiment (Fig. 2.18) and the bioinformatic predictions indicated that nt 14-31 of SdsR were involved in base-pairing with nt 39-51 of the *ompD* CDS.

The putative interaction was validated by a compensatory base-pair exchange. Mutation of a single guanosine at position 26 to a C in plasmid pP_L-SdsR (giving rise to P_L-SdsR*) was considered to disrupt the potential hybrid (Fig. 2.19 A). Indeed, in contrast to wild-type SdsR, SdsR* was no longer able to down-regulate *ompD* expression on both the mRNA and the protein level (Fig. 2.19 B and C, lanes 1-3). In accordance, a compensatory exchange of nucleotide C44 to G (*ompD**) of *ompD* in the chromosome established a mutant fully resistant to SdsR while regulation was restored in the presence of SdsR* (Fig. 2.19 B and C, lanes 4-6). This experiment confirmed the SdsR target site on *ompD* mRNA within the coding region, and emphasized the potency of the chosen 3'RACE-based approach in target site identification.

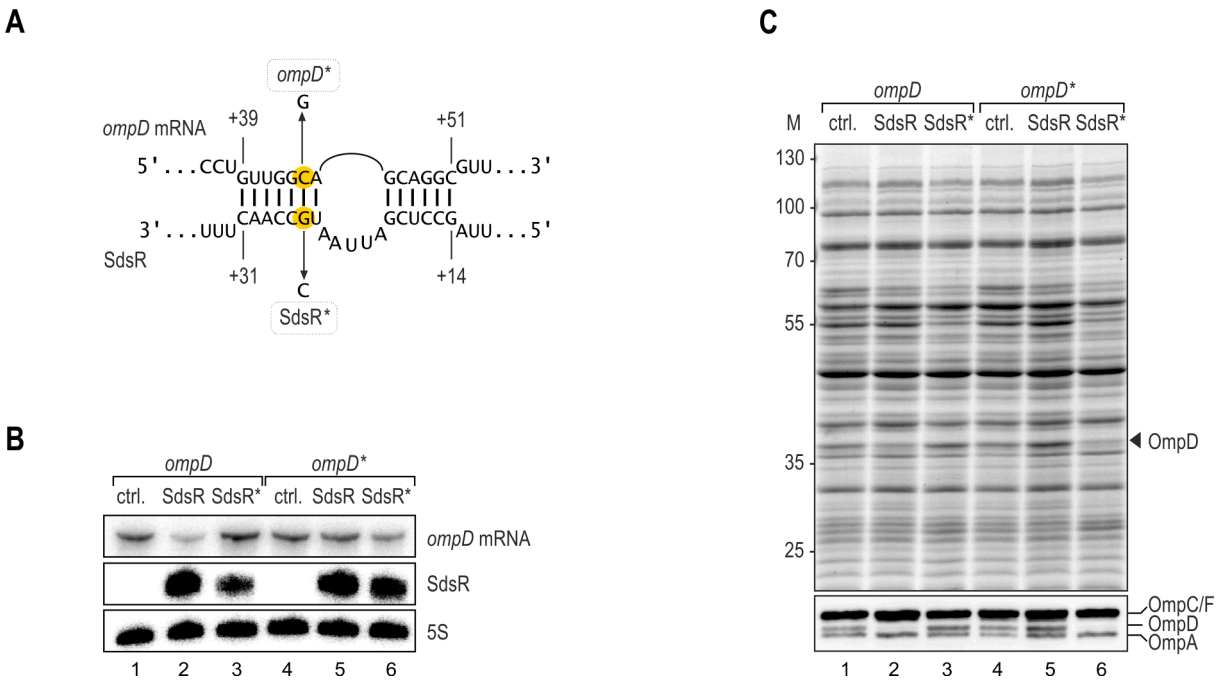

Figure 2.19 Compensatory base-pair exchanges validate the SdsR-*ompD* mRNA interaction.

(A) Predicted RNA duplex forming between SdsR sRNA and *ompD* mRNA. Point mutations to generate the compensatory *ompD** and SdsR* are indicated. (B) *Salmonella* Δ*sdsR ompD** mutant or isogenic Δ*sdsR ompD* cells carrying plasmids for the constitutive overexpression of either SdsR or SdsR*, respectively, were grown to an OD_{600} of 2.0. Expression levels of *ompD*/*ompD** mRNAs and SdsR/SdsR* sRNAs were determined by Northern blot analysis. (C) OmpD levels with respect to SdsR or SdsR* expression were analyzed on a stained SDS-PAGE gel (upper panel) and Western blot (lower panel) using total protein samples prepared in parallel to the RNA samples in (B).

2.12 The *ompD* translation initiation site is not refractory to sRNA targeting

With the validation of SdsR as a repressor of *ompD*, the total number of riboregulators post-transcriptionally controlling this major porin was increased to four. The binding sites of MicC and SdsR are located far downstream the start codon and both sRNAs probably function through the induction of RNase E-mediated cleavage of the mRNA (Pfeiffer et al, 2009; and this study). RybB and InvR are considered to impair translation initiation (Balbontin et al, 2010; Bouvier et al, 2008; Papenfort et al, 2010; Pfeiffer et al, 2009; Pfeiffer et al, 2007). Each of the sRNAs base-paired to an individual site within the coding region, however the reasons for the restricted positioning of targeting sites within the *ompD* mRNA were undetermined. Potentially, secondary structures within the translation initiation region, or the absence of a proximal binding site for the major RNA chaperone, Hfq, may prevent sRNA pairing.

To investigate whether the 5' UTR close to the translational start site was accessible for sRNA binding and could function as a targeting region, chimeric sRNAs containing an artificial seed sequence were constructed (Fig. 2.20 A/B). TMA (see chapter 2.6) served as an unrelated scaffold and was fused to either the 5' end of MicC (MicC-TMAl, carrying a longer version of TMA comprising nt 15-74 of MicA), or a sequence predicted to bind the 5' UTR of *ompD* mRNA (antiD-TMA). The latter sequence was designed in analogy to the interaction site of MicC on *ompC* mRNA (Fig. 2.20 A). Wild-type *Salmonella* were transformed with the respective plasmids (Fig. 2.20 B) and expression of the sRNAs was confirmed (Fig. 2.20 C). TMA alone had no effect on porin expression when compared to the control strain. In contrast, MicC-TMA was a potent repressor of both OmpC and OmpD. In addition, also OmpA levels were affected mildly (Fig. 2.21 D, lanes 1-3) and antiD-TMA specifically decreased OmpD protein levels (Fig. 2.20 D, lane 4). This result indicated that - although the known interactions with the four regulators InvR, RybB, SdsR and MicC occured within the coding region - the 5' UTR of *ompD* was in principle accessible for sRNAs.

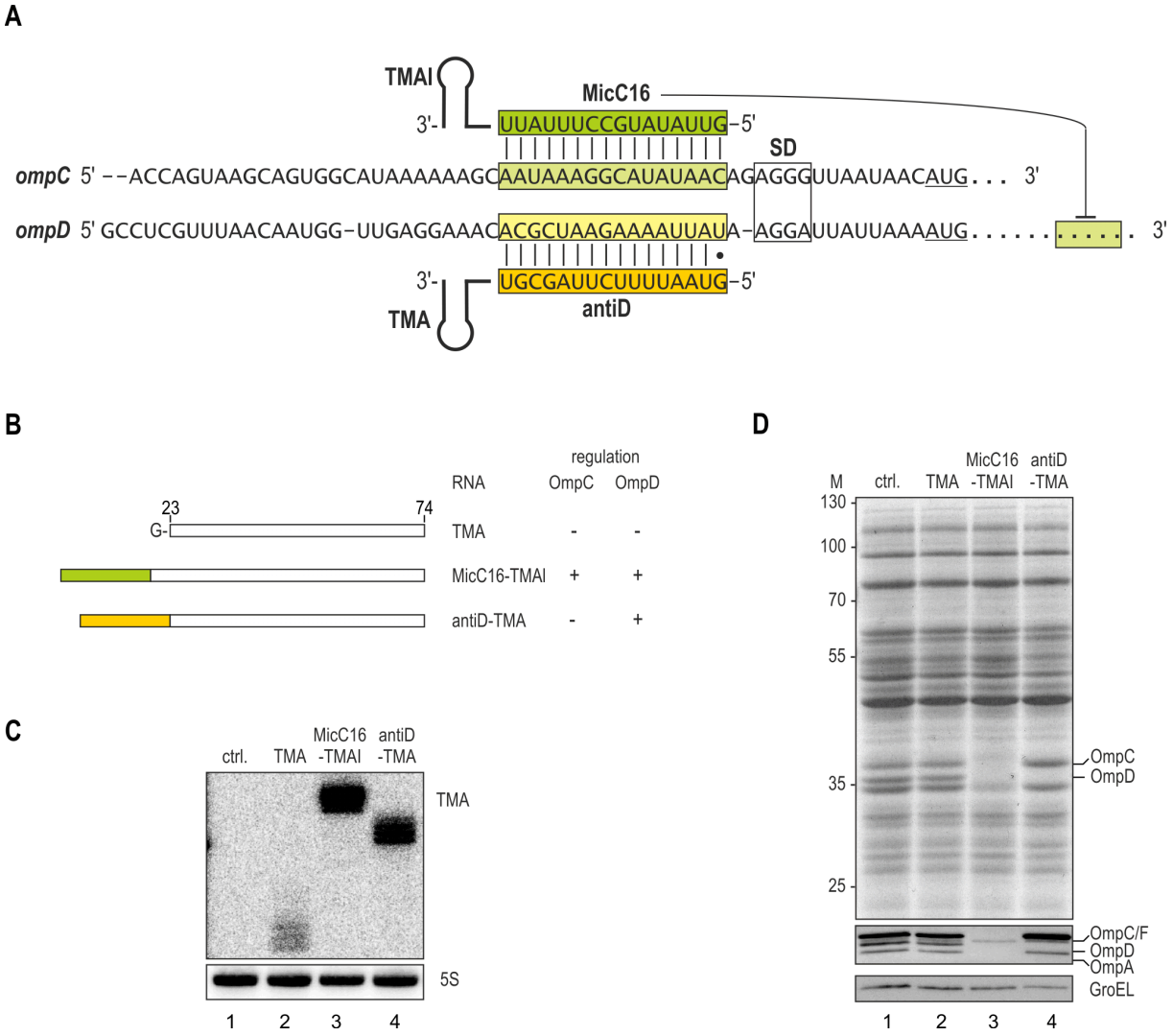

Figure 2.20 Repression of OmpD by an sRNA targeting the 5' UTR.

(A) Graphical representation of the *ompC* and *ompD* transcripts including the sequences from the TSS to the start codon. The target sites of MicC on both mRNAs and the potential interaction site of the synthetic "antiD" regulator on *ompD* are indicated. (B) Size and composition of chimeric sRNAs tested for their impact on OmpC and OmpD expression. TMAI designates a longer version of TMA and comprises residues 15-74 of MicA. (C) *Salmonella* wild-type cells carrying either a control plasmid or constructs for the constitutive expression of TMA, MicC16-TMAI and antiD-TMA were grown to an OD_{600} of 2.0. Expression of sRNAs was determined by Northern blot analysis. (D) OmpC and OmpD levels were analyzed by SDS-PAGE (upper panel) and Western blot (lower panel) using total protein samples prepared in parallel to the RNA samples in (C).

2.13 Overlapping and specific regulation of *ompD* expression by SdsR and RybB sRNAs

Generally, OMP expression is tightly regulated at the transcriptional and the post-transcriptional level (De la Cruz & Calva, 2010). However, the simultaneous presence of more than one riboregulator under certain growth conditions (Fig. 2.21 A) raised the question whether these sRNAs functioned redundantly. At least SdsR and RybB, whose expression depend on the alternative σ factors σ^S and σ^E, respectively, both accumulate during stationary growth and during multiple stresses like heat or high osmolarity (Muller et al, 2009; Raina et al, 1995; Rouviere et al, 1995).

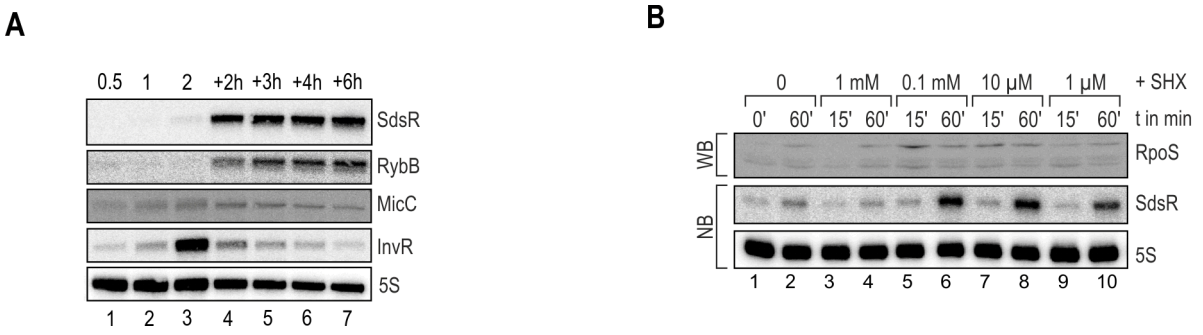

Figure 2.21 Expression of sRNAs regulating *ompD*.

(A) Expression of SdsR, RybB, MicC and InvR in wild-type *Salmonella* at various time-points of growth in LB (OD_{600} of 0.5, 1.0, 2.0 and 2, 3, 4 or 6 hours after cells had reached an OD_{600} of 2.0). (B) Induction of the stringent response in wild-type *Salmonella* by different concentrations of serine hydroxamate (SHX) was monitored by determining RpoS expression on Western blots and SdsR expression on Northern blots.

In contrast, certain other stresses are known to specifically trigger either of the alternative sigma factors: the stringent response to amino acid starvation is mediated by σ^S (Durfee et al, 2008; Traxler et al, 2011), while only σ^E orchestrates the envelope stress program (Humphreys et al, 1999). *Salmonella* strains transcribing *ompD* from a constitutive P_{tet} promoter, and derivative strains deleted for three of the four relevant sRNAs, were employed to determine the individual contribution for the RybB and SdsR sRNAs in post-transcriptional control of *ompD* under these conditions. The stringent response was elicited in cells grown to exponential phase by addition of serine hydroxamate (SHX). This serine analogue acts as a competitive inhibitor of aminoacylation of serine tRNAs (Tosa & Pizer, 1971), and the optimal concentration (0.1 mM) to study SHX-induced starvation, *i.e.* maximal induction of RpoS protein and consequently SdsR sRNA, was determined for *Salmonella* in a preliminary experiment (Fig. 2.21 B, lanes 5,6). SdsR but not RybB accumulated within 30 min of growth in the presence of SHX (Fig. 2.22, lanes 3/6).

Concomitantly, *ompD* mRNA levels dropped approximately 2-fold while remaining largely unchanged in an *sdsR* mutant strain.

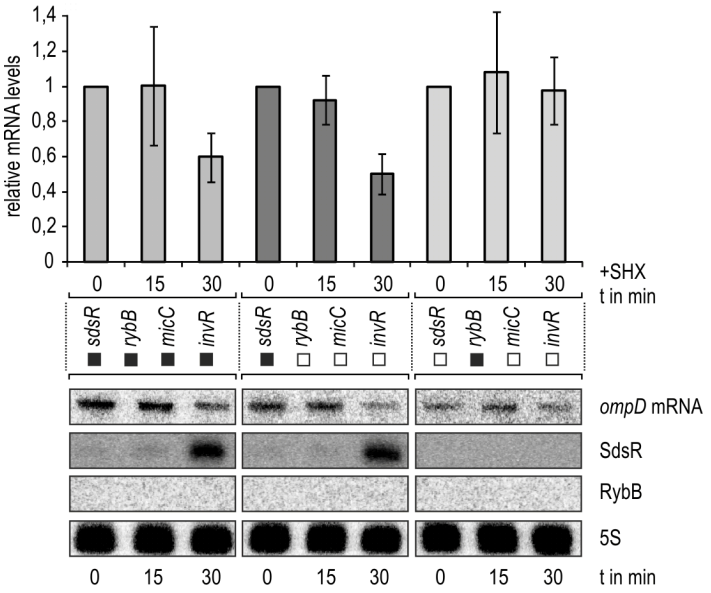

Figure 2.22 The stringent response triggers SdsR-specific *ompD* mRNA decay.

Salmonella expressing *ompD* from a constitutive $P_{LtetO-1}$ promoter and derivative strains carrying either only *sdsR* or *rybB* of the four relevant sRNA genes were grown in Nutrient broth (supplemented with 0.75 mM L-serine) to an OD_{600} of 0.15 and treated with 100 µM SHX. Total RNA samples withdrawn from cultures prior to and 15 or 30 minutes after SHX addition were analyzed on Northern blots. Bars represent relative *ompD* mRNA levels as determined from the quantification of Northern blots normalized by probing for 5S RNA; error bars indicate the standard deviation from three independent biological replicates. Black or white boxes mark the presence or absence of the indicated sRNA genes in the strains used.

The membrane-perturbing polymyxin B (PMB) rapidly activates the σ^E–mediated response which in turn leads to the transcription of two small RNAs, RybB and MicA (Papenfort et al, 2006). *Salmonella* constitutively expressing *ompD* in the presence of all four relevant sRNAs, or only SdsR and RybB were treated with PMB. SdsR was barely detectable under this growth condition, and its expression was unaffected by PMB (Fig. 2.23, left and middle panels). In contrast, RybB was rapidly induced within five minutes, and sRNA levels declined again already after ten minutes post treatment as a result of adaptation to the stress (Fig. 2.23, left and right panels). Rapid decay of *ompD* mRNA (around 5-fold within the first five min post treatment) was observed both in the wild-type strain and for *Salmonella* expressing only RybB (Fig. 2.23, lanes 2 vs. 8). In contrast, stability of the *ompD* transcript was ~ 3-fold higher in a *rybB* mutant (Fig. 2.23, lane 5).

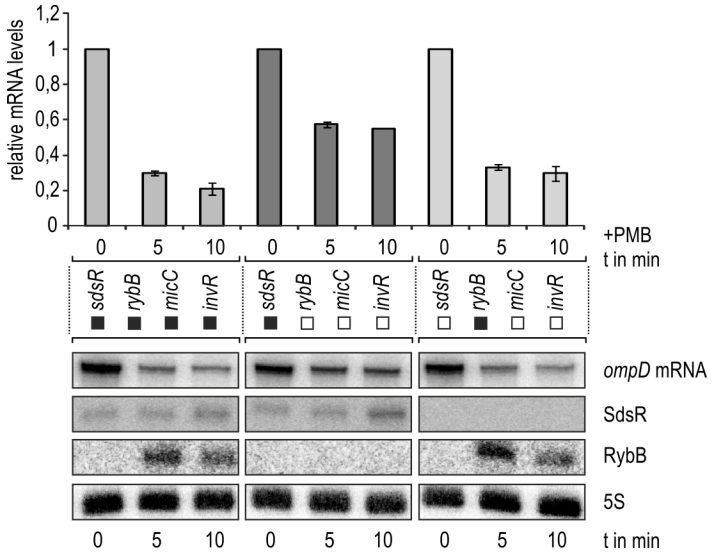

Figure 2.23 RybB facilitates *ompD* mRNA repression during membrane stress.

The envelope stress response was induced by addition polymyxin B (PMB; final concentration 5 µg/ml) to *Salmonella* (at an OD_{600} of 1.5) expressing *ompD* from a constitutive $P_{LtetO-1}$ promoter in the presence of all four sRNAs known to regulate *ompD* as well as to cells harbouring only either *sdsR* or *rybB*, respectively. Black or white boxes mark the presence or absence, respectively, of the indicated sRNA genes in the strains used. Northern blot analysis of total RNA samples prepared from cells collected prior to and 5 or 10 minutes after PMB addition revealed strong induction of RybB but not SdsR. Bars represent relative *ompD* mRNA levels as determined from the quantification of Northern blots normalized by probing 5S RNA; error bars indicate the standard deviation from three independent biological replicates.

2.14 Concluding remarks

The highly conserved and Hfq-dependent core sRNA SdsR was known as one of the most abundant sRNAs during stationary growth phase in *E. coli*. As determined in this study, conservation patterns in the *sdsR* promoter region and genetic analyses strongly suggest that the synthesis of SdsR is directly controlled by the alternative σ factor σ^S. In *Salmonella*, overexpression of SdsR RNA down-regulates the synthesis of the porin OmpD through direct base-pairing. SdsR constitutes the fourth sRNA regulator of this major OMP, and could be shown to play a specific role in porin regulation during the stringent response. Similar to the InvR, MicC, and RybB sRNAs, SdsR recognizes the *ompD* mRNA downstream of the start codon. The SdsR target site in *ompD* was mapped using a 3'RACE approach that might be generally useful for the experimental identification of sRNA-target interactions.

3 The conserved 5' end of RydC sRNA activates one of two isoforms of *cfa* mRNA

3.1 RydC sRNA is constitutively expressed in *Salmonella*

RydC was originally identified as an sRNA co-precipitating with the Hfq chaperone in *E. coli* (Zhang et al, 2003). The ~65 nt sRNA is conserved in several related enterobacterial species (Fig. 3.1 A). In *Salmonella*, the *rydC* gene is located on the plus strand in the intergenic region (IGR) between STM1638, encoding for a putative SAM-dependent methyltransferase, and *cybB* encoding cytochrome B561 (Fig. 3.1 B).

The transcriptional start site of *rydC* in *E. coli* had previously been mapped by primer extension to two sites either five or six nucleotides downstream of the potential -10 box (Antal et al, 2005). To determine the sRNA's 5' end in *Salmonella*, a 5'RACE protocol involving tobacco acid pyrophosphatase (TAP) treatment was employed (Bensing et al, 1996; Vogel et al, 2003). Cleavage of the 5' triphosphate group which is characteristic of primary transcripts by TAP renders the RNA a preferred substrate in the adjacent step of RNA linker ligation. The transcriptional start site of *rydC* in *Salmonella* was mapped to a single, TAP-dependent site, a conserved T (hereafter referred to as +1 site; Fig 3.1 C) located in perfect 6 bp spacing from the potential -10 box matching the σ^{70} consensus sequence (Fig. 3.1 A). Transcription of RydC was predicted to terminate at a ρ-independent terminator at nucleotide +64 relative to the start site. The transcriptional start and termination sites were also validated by the RNA sequencing data obtained for the total transcriptomes of *S*. Typhimurium, *E. coli*, *S. flexneri* and *C. rodentium* (chapter 4.1). The dRNA-seq approach chosen for the transcriptome analysis specifically enriches for primary transcripts, and could be employed to precisely localize the TSS to a single nucleotide. This method confirmed that the RydC TSS determined by 5'RACE in *Salmonella* was conserved in *E. coli* and *S. flexneri*, whereas *rydC* was absent from the *C. rodentium* genome.

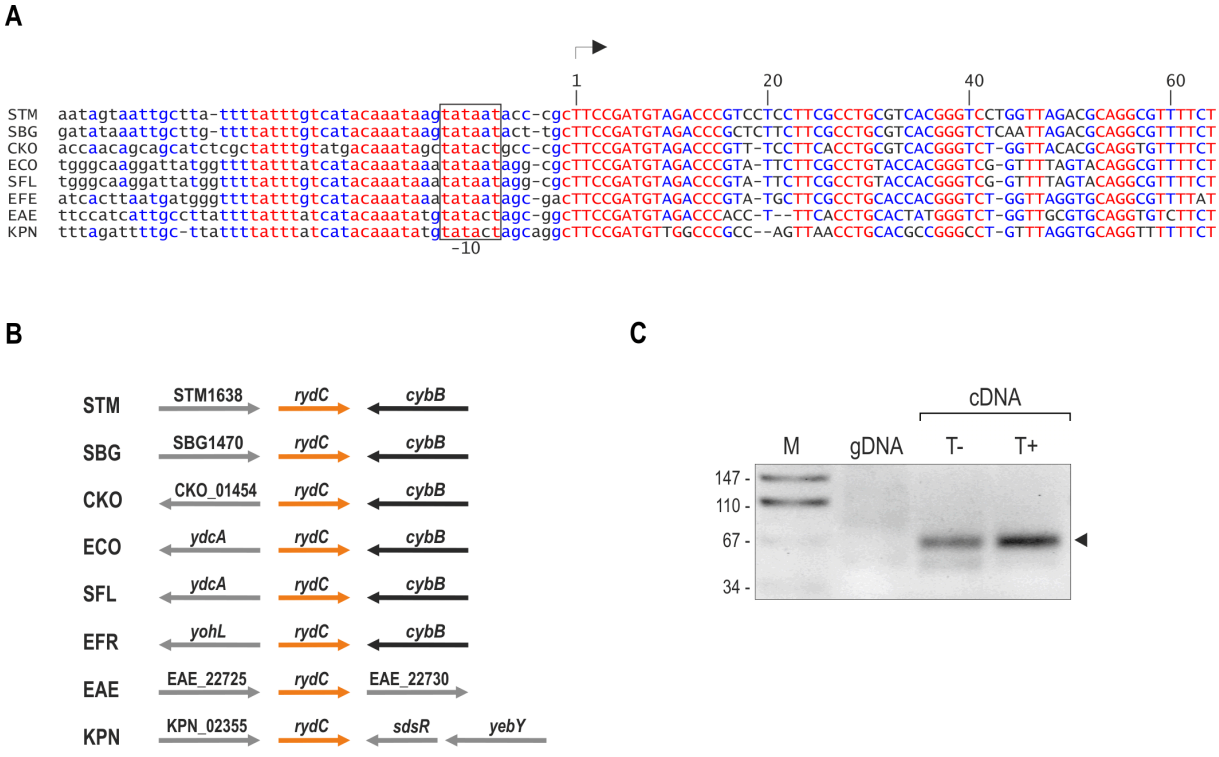

Figure 3.1 Conservation and 5' end mapping of RydC.

(A) Non-redundant alignment of the *rydC* gene including the upstream promoter region. STM: *Salmonella* Typhimurium; SBG: *Salmonella bongori*; CKO: *Citrobacter koseri*; ECO: *Escherichia coli*; SFL: *Shigella flexneri*; EFE: *Escherichia fergusoni*; EAE: *Enterobacter aerogenes*; KPN: *Klebsiella pneumoniae.* The transcriptional start site is marked by an arrow. All nucleotides are coloured with regard to their degree of conservation (red: high conservation; blue: partial conservation; black: little or no conservation). (B) Synteny analysis of the *rydC* gene. In *Salmonella*, *rydC* is located in the IGR between STM1638 and *cybB*. (C) 5'RACE analysis to determine the transcriptional start site of *rydC* in *Salmonella*. RNA was extracted from exponentially growing (OD_{600}=0.5) *rydC* mutant cells complemented with *rydC* expressed under control of its own promoter on a multi-copy plasmid (p*rydC*). cDNA was prepared from TAP-treated (T+) or mock-treated (T-) RNA samples. *Salmonella* gDNA served as negative control. A TAP-dependent PCR product was extracted, cloned and sequenced. The transcriptional start of *rydC* was assigned to a conserved T residue 6 bp downstream of the predicted -10 box (Fig. 3.1 A).

To examine the regulation of *rydC* in *Salmonella,* its expression was monitored over growth in LB and in media mimicking virulence-relevant conditions of *Salmonella* invasion (SPI-1 condition) or intracellular replication (SPI-2 condition). RydC was expressed under all examined conditions. An estimation of its intracellular concentration by comparing signal intensities relative to *in vitro* transcribed RNA on Northern blots revealed RydC to be present at low quantities (~3-11 copies/cell) peaking under growth in minimal medium (Fig. 3.2 A).

Similar to many Hfq-associated sRNAs, RydC exhibited a strong dependence on the RNA chaperone as it could not be detected in *Salmonella hfq* mutant cells (Fig. 3.2 B).

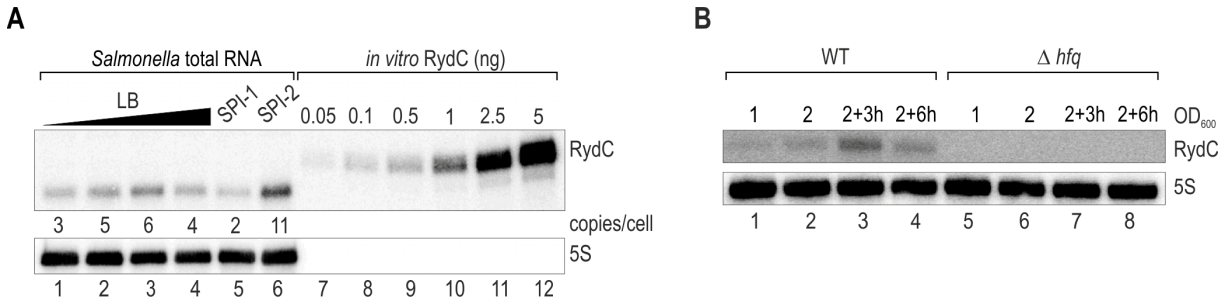

Figure 3.2 Expression of *rydC* over growth.

(A) RydC levels in RNA samples of wild-type *Salmonella* at various time-points of growth (OD_{600} of 0.5, 1.0, 2.0, and 3 hours after cells had reached an OD_{600} of 2.0; SPI-1: 12h growth in LB containing 0.3 M NaCl under oxygen limitation; SPI-2: PCN 1 minimal medium, OD_{600} of 0.5) were compared on Northern blots to signals of *in vitro* transcribed RydC in indicated amounts. (B) RydC is an Hfq-dependent sRNA. Expression profiles of RydC were compared between wild-type and *hfq* mutant cells at indicated stages of growth.

3.2 The molecular architecture of RydC sRNA determines its stability

Except for the very 5' end of the sRNA, RydC is only partially conserved at the sequence level (Fig. 3.1 A). Structure probing experiments and bioinformatic predictions suggested that RydC forms a pseudoknot *in vitro* (Antal et al, 2005): while both the 5' and 3' end of the RNA molecule remain single stranded, the central part of RydC forms two internal duplexes. This peculiar structure seemed to be highly conserved. The comparative analysis of single-nucleotide exchanges in different species revealed that mutations that were present in sequence stretches involved in duplex formation were in all cases neutralized by compensatory mutations. Consequently, similar secondary structures were predicted for all different RydC species (Fig. 3.3).

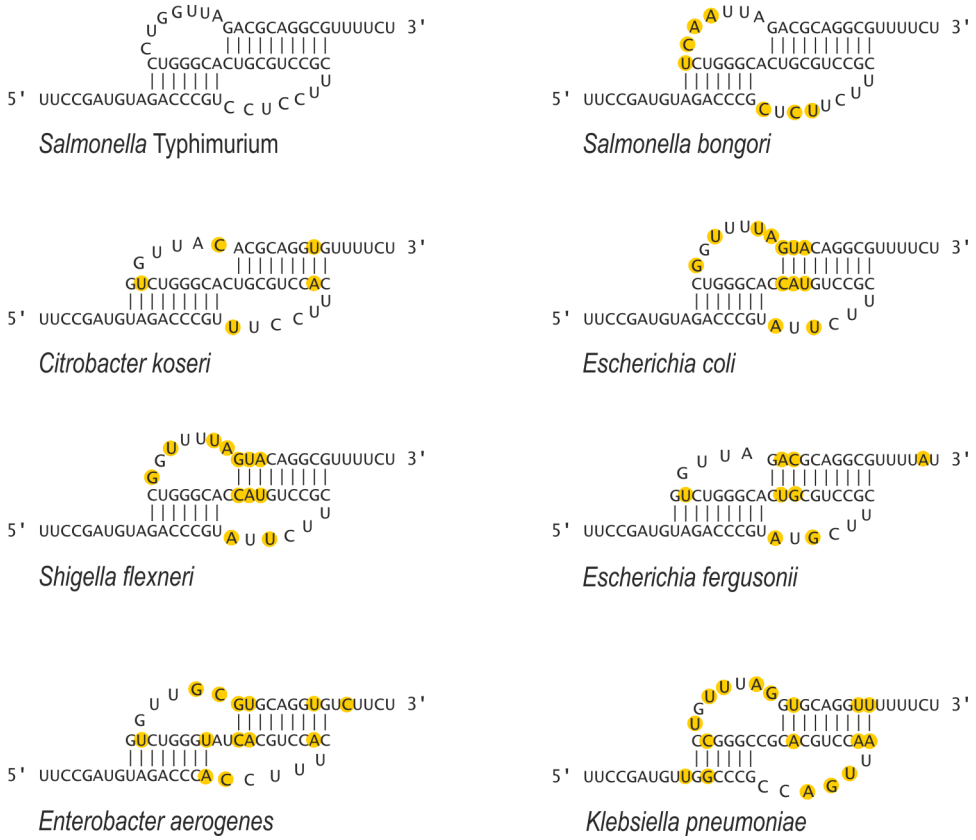

Figure 3.3 Predicted secondary structures of RydC in different enterobacteria.

Pseudoknot formation was predicted for RydC sRNA orthologues of different enterobacteria. Single-nucleotide exchanges in comparison to *Salmonella* Typhimurium RydC are marked in yellow.

Albeit RydC is only weakly expressed under standard growth conditions, this sRNA has been observed to be among the most highly enriched transcripts recovered from co-immunoprecipitations with the RNA chaperone, Hfq (Chao et al, 2012; Sittka et al, 2008). In addition, endogenous RydC cannot be detected in *hfq* mutant cells (Fig.1.3 B; (Antal et al, 2005)). These findings suggested that RydC bound Hfq with very high affinity and that the interaction stablilized the sRNA. To determine the putative role of the pseudoknotted secondary structure in sRNA stability, different RydC variants were cloned under the control of a constitutive P_L promoter (synthetic P_{Llac01} variant; (Lutz & Bujard, 1997)). Compared to the wild-type RNA (Fig. 3.4 A), two nucleotides were exchanged in a region critical for the base-pairing of the pseudoknot to obtain a "knot-mutant", referred to as RydC-K1 (Fig. 3.5 B). To control for the influence of the nucleotide sequence on stability, two additional mutants were constructed in which either the base-pairing in RydC-K1 was restored by compensatory exchanges (RydC-K1/2; Fig. 3.4 C), or in which two nucleotide exchanges disrupted the pseudoknot at a position further upstream (RydC-K2; Fig. 3.4 D).

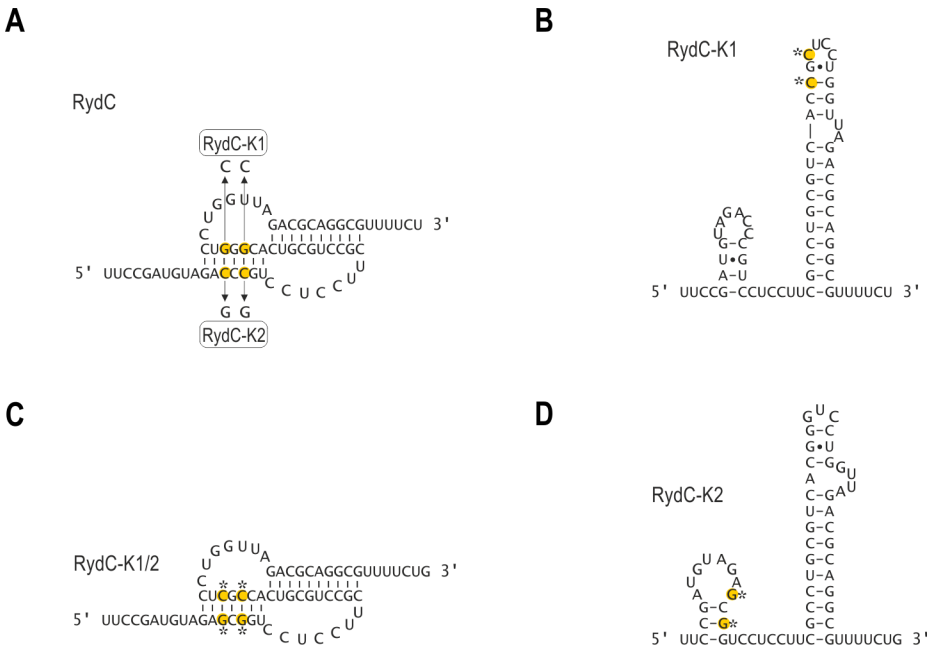

Figure 3.4 Predicted secondary structure of RydC and RydC mutants.

(A) To disrupt pseudoknot formation two sets of point mutations were introduced in the *rydC* sequence. (B) Predicted structure of mutant RydC-K1 (G37C; G39C). (C) Predicted structure of mutant RydC-K1/2. Pseudoknot formation is restored by compensatory mutations (C13G; C15G; G37C; G39C) (D) Predicted structure of mutant RydC-K2 (C13G; C15G).

To test for the individual sRNAs' stabilities, *Salmonella* Δ*rydC* mutant cells carrying either of the RydC variant expressing plasmids were grown to late exponential phase, when transcription was abrogated by adding the RNA polymerase-inhibitor rifampicin. RNA samples were withdrawn from the culture prior to and at various time-points after rifampicin treatment and sRNA stabilities were monitored on Northern blots using an oligo probe recognizing the very 3' end of all RydC variants. Wild-type RydC displayed a relatively high *in vivo* stability ($t_{1/2}$ > 32 min; Fig. 3.5 A/D). In contrast, interference with nucleotides required for intra-molecular base-pairing in RydC-K1 rendered the sRNA mutant highly instable as revealed by the comparably lower levels at t=0 min and its rapid degradation upon rifampicin treatment ($t_{1/2}$ ~ 3 min; Fig. 3.5 A/D). Similarly, RydC-K2 displayed a faster decay rate than wild-type RydC, albeit being more stable than RydC-K1 ($t_{1/2}$ = 10 min; Fig 3.5 B/D). Reconstitution of the internal duplex restored sRNA stability to wild-type levels in RydC-K1/2 ($t_{1/2}$ > 32 min; Fig 3.5 B/D).

Since RydC expression had been observed to depend on Hfq (Fig. 3.2 B), the intrinsic stabilities of both RydC as well as RydC-K1 were investigated in the absence of the RNA chaperone. As expected, RydC was less stable in an *hfq* mutant background ($t_{1/2}$ ~ 4 min; Fig 3.5 C/D). In contrast, decay of RydC-K1 was unchanged in a Δ*hfq* strain compared to wild-type cells

(Fig. 3.5 C/D). This observation indicated that, in contrast to RydC, RydC-K1 was not stabilized in the presence of Hfq.

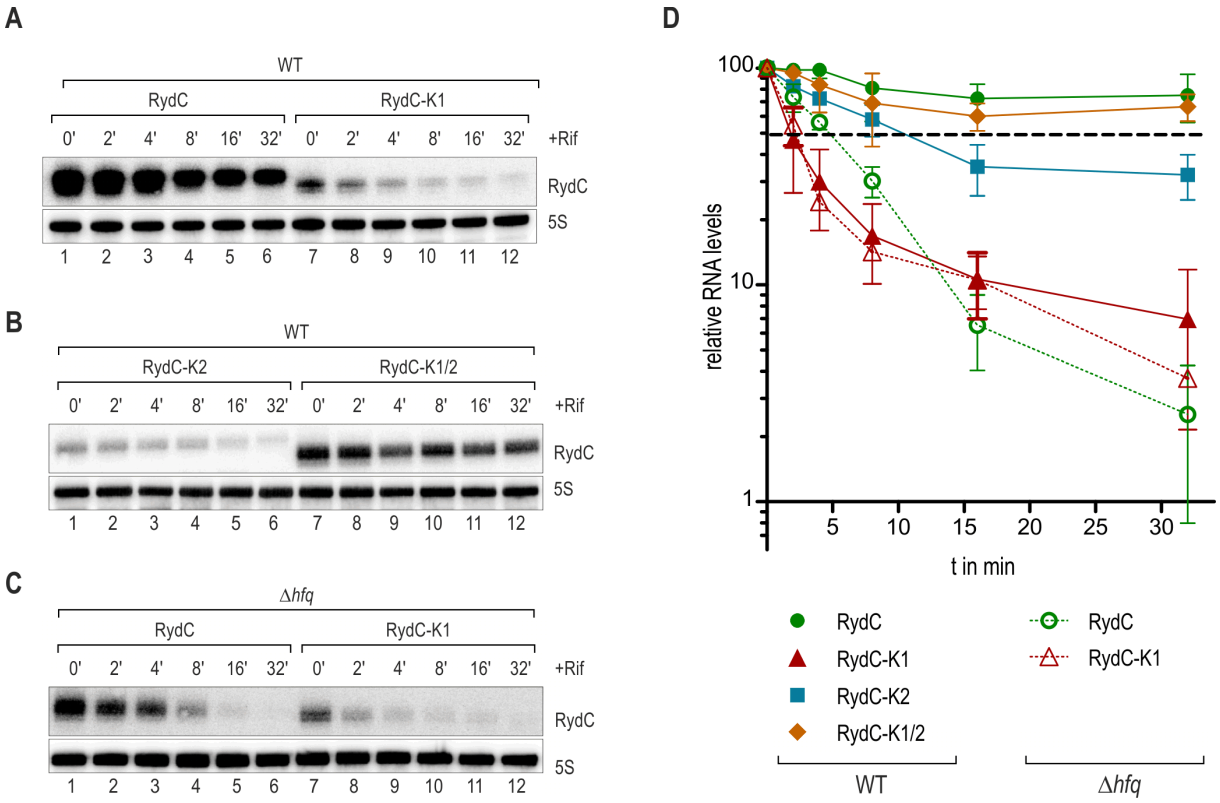

Figure 3.5 Stability of RydC and RydC variants.

(A) Stability of RydC and RydC-K1 was determined in Δ*rydC Salmonella* by Northern blot analysis of total RNA samples withdrawn prior to and at indicated time-points after inhibition of transcription by rifampicin (OD_{600} of 1). (B) Determination of *in vivo* stabilities of RydC-K2 and RydC-K1/2 as described in (A). (C) Stability of RydC and RydC-K1 was probed in Δ*hfq Salmonella* as described in (A). (D) Quantification of *in vivo* stabilities of RydC sRNA variants. The signal obtained at 0 min was set to 100, and the amount of mRNA remaining at each time-point was plotted on the y-axis versus time on the x-axis. The time-point at which 50% of RydC had been decayed (dashed line) was calculated to determine the half-life ($t_{1/2}$). Error bars represent the standard deviation calculated from three independent biological replicates.

To determine whether the variation of *in vivo* stabilities of RydC and RydC-K1 was due to different affinities for Hfq, the association of the two RNA variants with the chaperone was tested *in vitro* in gel-mobility shifts. In accordance with Hfq pulldown experiments (Sittka et al, 2008), RydC displayed a very high affinity for Hfq (K_D~4 nM; Fig. 3.6 A, lanes 1-7). Also RydC-K1 was able to bind Hfq and was part of several complexes forming in the presence of higher concentrations of the RNA chaperone. However, when compared to RydC, RydC-K1 displayed considerably lower affinity for Hfq (K_D~30 nM; Fig. 3.6 A, lanes 8-14).

The abundance of Hfq is a limiting factor for sRNA activity *in vivo* (Fender et al, 2010; Hussein & Lim, 2011) and individual RNAs compete for binding to the chaperone. To assay the performance of RydC and RydC-K1 in competition for Hfq binding, the stability of preformed RNA/Hfq complexes in the presence of increasing amounts of unlabelled competitor RNA was determined by gel-mobility shifts. RydC formed a stable complex with Hfq and could be only partially outcompeted in the presence of a 500-fold excess of cold RydC-K1 (Fig. 3.6 B, lanes 1-7). In contrast, RydC-K1/Hfq complexes appeared more susceptible to competition and were already destabilized in the presence of 10-fold excess of unlabelled RydC RNA (Fig. 3.6 B, lanes 8-14). Thus, the low *in vivo* stability of RydC-K1 was probably due to its lower affinity for Hfq and its relatively weak performance in competition for chaperone binding.

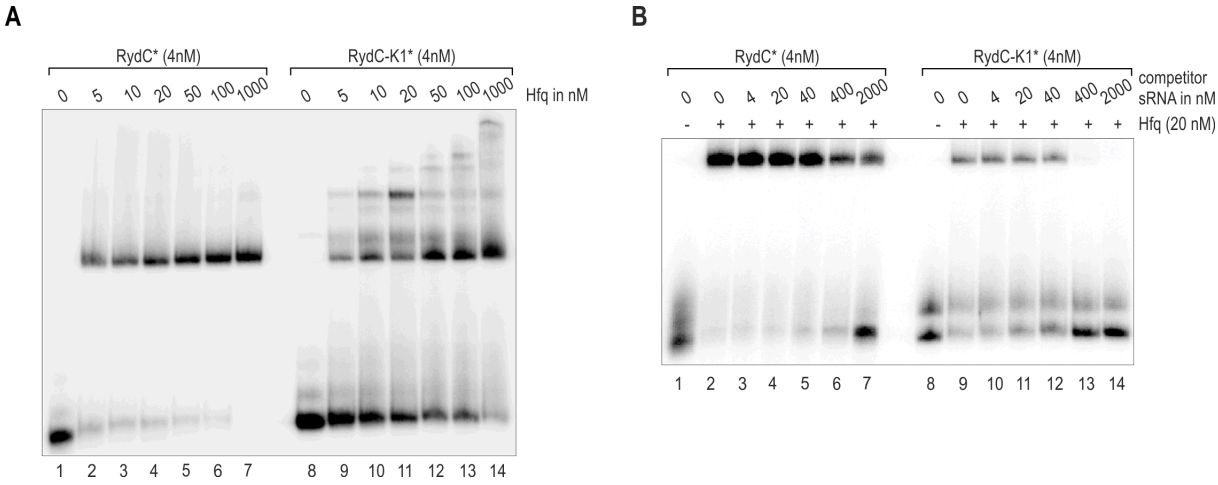

Figure 3.6 RydC and RydC-K1 association with Hfq *in vitro*.

(A) Electrophoretic mobility shift assay (EMSA) with *in vitro* synthesized, 5' end-labelled RydC and RydC-K1 RNAs (RydC* and RydC-K1*, 4 nM) in the presence of increasing concentrations of Hfq protein as indicated. (B) EMSA with *in vitro* synthesized, 5' end-labelled RydC and RydC-K1 RNAs (RydC* and RydC-K1*). Preformed RNA*/Hfq complexes were incubated with increasing concentrations of cold competitor RNA (RydC-K1 for RydC*; RydC for RydC-K1) in the indicated concentrations.

3.3 Transcriptome-based identification of RydC targets

Prior to the present study, RydC was reported to influence the expression of the putative ABC transporter system, *yejABEF*, in *E. coli* (Antal et al, 2005). When inspecting whole cell protein profiles on an SDS PAGE gel to identify potential targets of the sRNA, no differences were observed between WT and Δ*rydC Salmonella* carrying either a control or a RydC overexpression plasmid (Fig. 3.7).

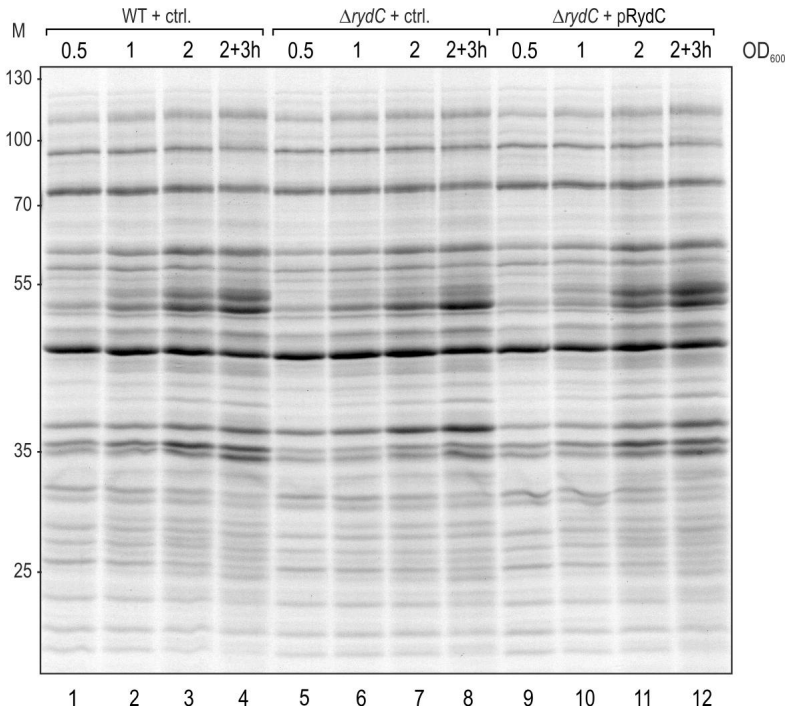

Figure 3.7 Whole cell protein patterns of wild-type and *rydC* mutant *Salmonella*.

Whole cell protein samples of WT and *rydC* mutant cells carrying either a control plasmid or a complementation plasmid to over-express RydC from the constitutive P_L-promoter were separated by SDS PAGE, and abundant proteins were stained with Coomassie Blue.

The identification of direct targets of RydC - *i.e.* mRNAs whose expression change as a consequence of sRNA base-pairing - was addressed employing an approach which combines sRNA pulse expression and subsequent whole transcriptome profiling. In more detail, the *rydC* gene was cloned on a high copy plasmid under the control of the arabinose-responsive pBAD promoter (pBAD-RydC), and its expression was induced for 15 minutes in *rydC* mutant cells grown to early stationary phase (OD_{600} of 1.5; Fig. 3.8 A). The short induction time was sufficient to accumulate high levels of RydC in the cell (Fig. 3.8 B), but is considered to allow post-transcriptional regulation and to minimize secondary effects (Masse et al, 2005; Papenfort et al, 2006). By comparing relative mRNA abundances on *Salmonella*-specific microarrays to a sample taken in parallel from cells harbouring a pBAD control plasmid (Fig. 3.8 A), four transcripts were detected to be deregulated at least 3-fold (Table 3.1). The sole target of RydC proposed by a study in *E. coli*, *yejABEF* mRNA (Antal et al, 2005), was not among the differentially regulated transcripts.

The custom-designed microrarray included probes for sRNA computationally-predicted candidates, like for example STnc200. This RNA had not been validated experimentally, and no transcript expressed from the STnc200 locus was detected when inspecting the RNA sequencing data set described in chapter 4.1. Consequently, this putative target was not analyzed further.

The only transcript repressed upon RydC pulse-expression was STM3820 mRNA, encoding for a cytochrome C peroxidase. Regulation of this candidate was addressed using a translational GFP-reporter fusion, however could not be validated (Supplementary Fig. 4.8).

The strongest effect (6.5-fold upregulation) of RydC overexpression was observed for a putative small RNA, STnc730, which was previously annotated as a fragment of the 5' UTR of *cfa* mRNA (Sittka et al, 2009). Intriguingly, also *cfa* mRNA itself was found upregulated (~5-fold). Probing for *cfa* mRNA on a Northern blot revealed a *cfa*-specific transcript to increase concomitant with RydC induction, while the inducer arabinose itself did not affect *cfa* levels (Fig. 3.8 B). A smaller fragment corresponding to STnc730 was not detected, arguing that its differential expression monitored in the microarray experiment may have been due to cross-hybridization of the full-length transcript.

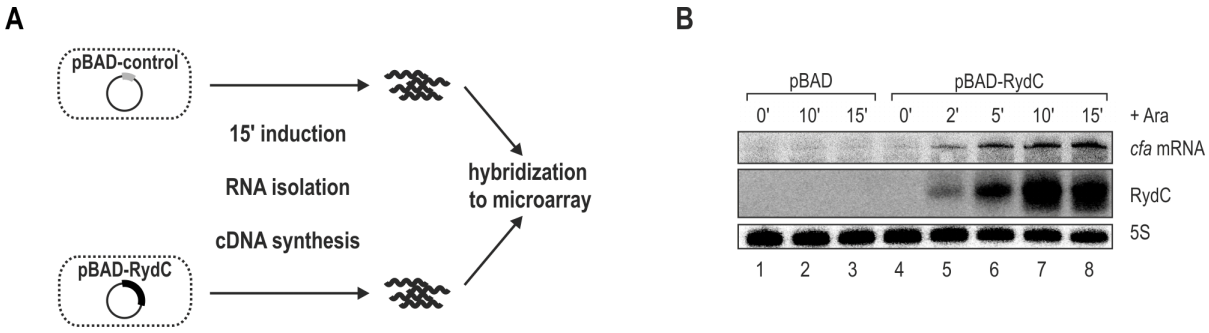

Figure 3.8 Transcriptomic experiments identify *cfa* mRNA as a putative target of RydC.

(A) Graphical representation of the experimental approach. sRNA pulse-expression from an inducible pBAD promoter was combined with whole transcriptome analysis on *Salmonella*-specific microarrays. (B) RydC expression was induced by addition of arabinose to *rydC* mutant cells carrying pBAD-RydC. Cells carrying plasmid pBAD served as control. RydC and *cfa* mRNA levels were determined on Northern blots.

Table 3.1 Transcripts deregulated 3-fold or more upon RydC pulse-expression.

gene	ID	fold regulation	description
STnc730	STnc730	+6,53	Processed 5' UTR of *cfa* mRNA (Sittka et al., 2009)
STnc200	STnc200	+5,27	sRNA candidate; not validated (Pfeiffer et al., 2007)
cfa	SL1359	+4,97	cyclopropane fatty acid synthase
STM3820	SL3786	-3,02	putative cytochrome c peroxidase

It is worth mentioning that an initial pulse-expression experiment of similar design was performed employing a plasmid expressing a version of RydC with two additional nucleotides at its 5' end. The results of this experiment are described and discussed in chapter 4.2.

3.4 The *cfa* mRNA is positively regulated by RydC

The *cfa* gene encodes for the membrane-modifying cyclopropane fatty-acid synthase. This enzyme catalyzes the transfer of a methyl group from *S*-adenosylmethionine (SAM) to the double bond of an unsaturated fatty-acid of phospholipids in the bacterial membrane to form a *cis*-cyclopropane ring (Grogan & Cronan, 1997). To verify the positive influence of RydC on *cfa* expression, a 3xFLAG epitope was fused to the 3' end of the gene. Cfa::3xFLAG levels were increased at all phases of growth in a strain overexpressing RydC from the constitutive P_L promoter. There was however no significant change in Cfa::3xFLAG levels in *rydC* mutants carrying a control plasmid relative to wild-type *Salmonella* (Fig. 3.9 A). Determination of RydC levels in the examined strains revealed sRNA levels in the constitutive mutant to be ~500-fold higher than in the wild-type. Thus, basal levels of RydC did not influence *cfa* expression under normal growth conditions.

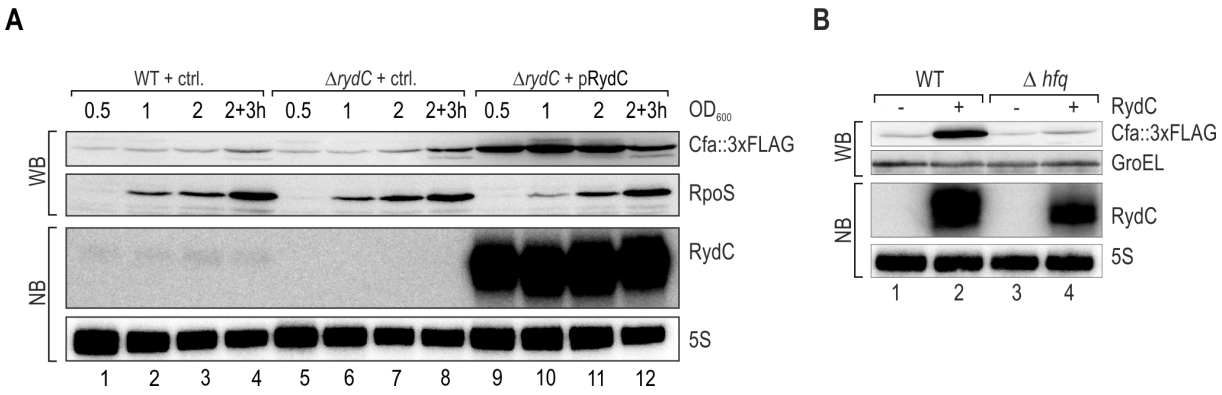

Figure 3.9 Cfa::3xFLAG expression is activated by RydC.

(A) Expression of Cfa::3xFLAG in wild-type and Δ*rydC* mutant *Salmonella* either carrying a control plasmid or a RydC overexpression plasmid was monitored over growth on Western blots. (B) Expression of Cfa::3xFLAG in Δ*rydC* Δ*rpoS Salmonella* and isogenic Δ*hfq* mutant cells transformed with a control plasmid or a RydC overexpression plasmid was determined by Western blot analysis.

Given that RydC is tightly associated with and dependent on Hfq ((Antal et al, 2005; Sittka et al, 2009); Fig. 1.3; Fig. 3.2 B) the requirement of the RNA chaperone for the activation of *cfa* expression was assayed. To this end, Cfa::3xFLAG levels were determined in wild-type and *hfq* mutant cells transformed with either a control or a plasmid constitutively overexpressing RydC, respectively. Albeit RydC levels in the *hfq* mutant strain were slightly reduced (~ 1.8-fold) when compared to wild-type cells, lack of Cfa::3xFLAG induction in the absence of Hfq argued for the strict requirement of the RNA chaperone for the RydC-activated *cfa* expression (Fig. 3.9 B).

3.5 RydC selectively activates the longer of two *cfa* mRNA isoforms

Expression of *cfa* is tightly controlled at multiple levels. Post-translationally, Cfa is degraded by a so-far unknown RpoH-dependent protease (Chang et al, 2000; Wang & Cronan, 1994). In addition, transcription of *cfa* in *E. coli*, *Salmonella* and several related enterobacteria is governed by two independent promoters (Fig. 3.10 A; (Kim et al, 2005; Wang & Cronan, 1994)). The conservation of the upstream promoter site was also confirmed in the dRNA-seq data of *S.* Typhimurium, *E. coli*, *S. flexneri* and *C. rodentium* (chapter 4.1; Fig. 4.4). While the distal site (TSS1) exhibits the consensus sequence of a σ^{70}-dependent promoter resulting in a transcript comprising a comparably long 5' UTR of 210 nt, the proximal promoter (TSS2) is growth-phase dependent and recognized by σ^{S}. Expression from the proximal transcription start site accounts for the increase in Cfa levels at the transition to stationary phase (Cronan, 2002). Since RydC was expressed in all phases of growth, the sRNA was co-existent in the cell with both of the two mRNA versions.

To unravel the fate of the individual *cfa* mRNAs with regard to the presence and absence of RydC sRNA, the relative levels of both transcripts were determined by primer extension analysis. In addition, Cfa::3xFLAG protein levels were monitored. Wild-type and Δ*rpoS* mutant *Salmonella* were transformed with either the pBAD control plasmid or pBAD-RydC. Induction of RydC increased levels of both the Cfa::3xFLAG protein as well as the longer *cfa* mRNA version while the abundance of the shorter transcript remained largely unchanged (Fig. 3.10 B, lanes 1-4). As expected, deletion of *rpoS* abrogated detection of the shorter *cfa* transcript originating from TSS2 (Fig. 3.10 B, lanes 5-8). In contrast, transcription from the distal start site TSS1, as well as the positive effect of RydC on Cfa::3xFLAG expression were unaffected in the *rpoS* mutant.

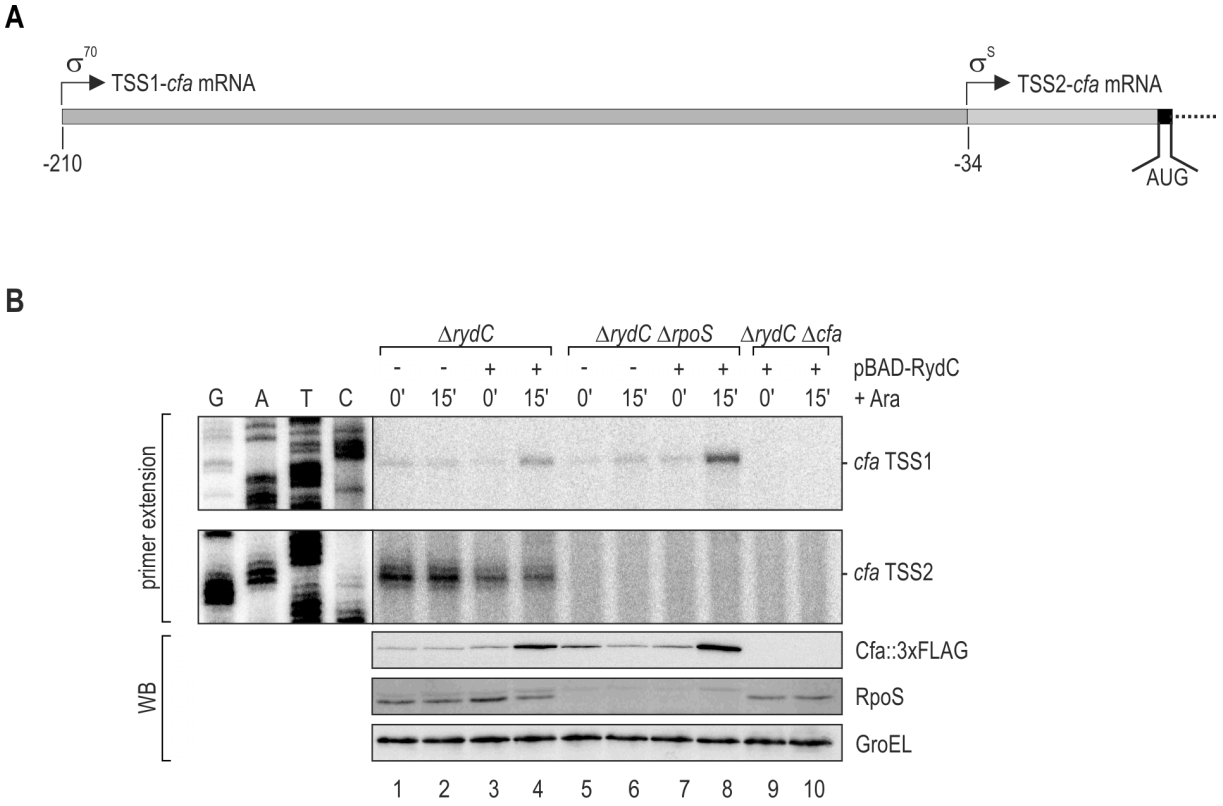

Figure 3.10 Cfa is expressed from two independent promoters.

(A) Schematic representation of the *cfa* gene including the upstream promoter region. Transcription can initiate from two start sites at -210 bp (distal start site TSS1; σ^{70}-dependent) or -34 bp (proximal start site TSS2; σ^{S}-dependent) relative to the translational start site, respectively. (B) *Salmonella cfa*::3xFLAG Δ*rydC* cells or an isogenic Δ*rpoS* mutant were transformed with the pBAD control plasmid (-) or the pBAD-RydC overexpression plasmid (+); *Salmonella* Δ*cfa* Δ*rydC* served as a negative control. All strains were grown to an OD_{600} of 2, and total RNA samples withdrawn prior to and 15' after arabinose addition were used as templates in primer extension with oligo JVO-7022. A gene-specific sequencing ladder is shown at the left. Expression of Cfa::3xFLAG, RpoS and GroEL was monitored on Western blots.

To uncouple RydC function from transcriptional regulation of *cfa*, an established system based on the constitutive co-expression of an sRNA with an amino-terminal translational fusion of the target gene to GFP was employed (Urban & Vogel, 2007; Urban & Vogel, 2009). Two fusions harbouring either the long or the short 5' UTR of *cfa* and additional 45 nt of the CDS (TSS1-*cfa::gfp* and TSS2-*cfa::gfp*, respectively; Fig. 3.11 A) were constructed. These plasmids were co-transformed into *Salmonella rydC* mutants carrying either a control plasmid or expressing RydC from the constitutive P_L promoter. Analysis of GFP levels indicated two results consistent with the observations in the primer extension experiment (Fig. 3.10 B): First, the expression of RydC sRNA did not affect GFP levels of the short *cfa* reporter fusion (Fig. 3.11 B,

lanes 1 and 2), but in contrast resulted in a ~10-fold increase of the reporter harbouring the long *cfa* 5' UTR (Fig. 3.11 B, lanes 3 and 4). Second, when comparing basal levels of GFP expression between both *cfa*-fusions, *i.e.* in the presence of the control plasmid, a significantly weaker signal (~10-fold) was observed for the fusion starting from the distal TSS1 (Fig. 3.11 B, lanes 1 and 3). Since both fusions are driven by the same, constitutive promoter, the long *cfa* fusion seemed to be expressed less efficiently and could be activated in the presence of RydC.

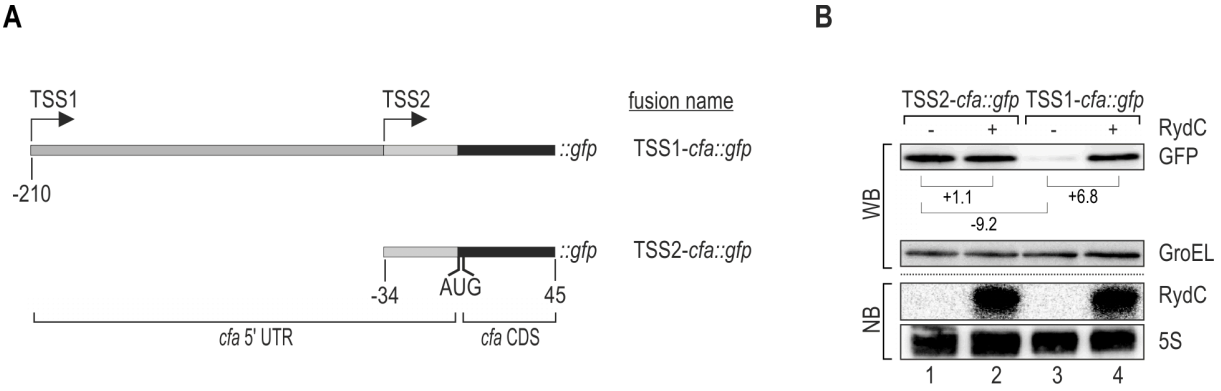

Figure 3.11 Regulation of *cfa::gfp* reporter gene fusions by RydC.

(A) Schematic representation of translational *cfa::gfp* fusions comprising the 5' upstream region from the distal or the proximal start site and the first 45 nucleotides of the CDS. (B) Regulation of reporter fusions was monitored by Western blot analysis. At an OD_{600} of 1, total protein samples were prepared from *Salmonella* Δ*rydC* Δ*rpoS* mutants carrying plasmids for expression of TSS2-*cfa::gfp* or TSS1-*cfa::gfp* in combination with a control plasmid (-) or pP_L-RydC (+). Fold-regulation as quantified from the blot is indicated. Expression of RydC was validated on a Northern blot.

3.6 RydC and *cfa* promoter architectures are conserved

In line with the finding that RydC was required to selectively activate the longer of two *cfa* mRNA isoforms, the architecture of the *cfa* dual promoter was conserved among all species encoding RydC sRNA. An alignment of the *cfa* upstream region is provided in Fig. 3.12. Interestingly, *cfa* expression is also driven from two promoters in *Enterobacter sp. 638*, a species from which RydC is absent. In contrast, more distantly related species like *Yersinia* or *Vibrio* neither harbour RydC sRNA nor seem to have the upstream promoter site in *cfa*.

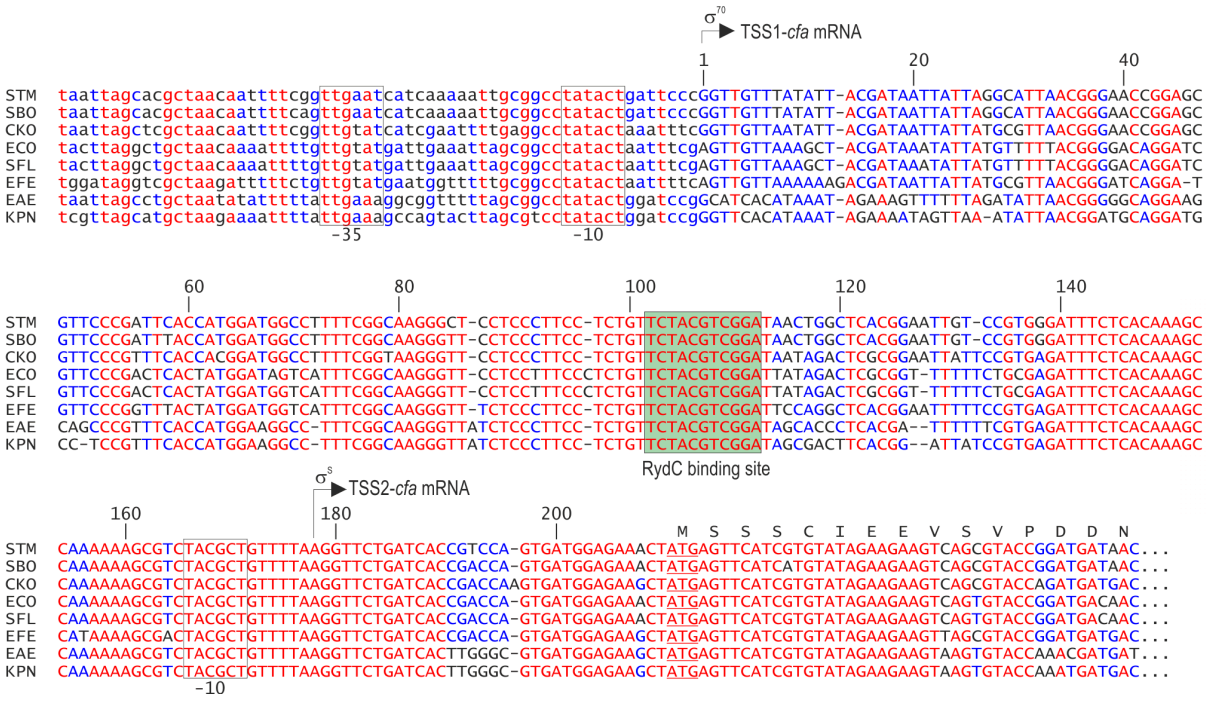

Figure 3.12 Conservation of the *cfa* gene in enterobacteria.

Non-redundant alignment of the *cfa* gene including the upstream promoter sequence. STM: *Salmonella* Typhimurium; SBO: *Salmonella* bongori; CKO: *Citrobacter koseri*; ECO: *Escherichia coli*; SFL: *Shigella flexneri*; EFE: *Escherichia fergusoni*; ENT: *Enterobacter aerogenes*; KPN: *Klebsiella pneumoniae*. The transcriptional start sites are marked by arrows. The amino acid sequence of the first 15 codons in *Salmonella* is indicated above the alignment. All nucleotides are coloured with regard to their degree of conservation (red: high conservation; blue: partial conservation; black: little or no conservation). The binding site of RydC sRNA is boxed in green.

Two additional reporter fusions comprising the long or the short 5' UTR, respectively, and the first 15 codons of *Enterobacter sp. 638 cfa* (TSS1-*cfa(Ent)::gfp* and TSS2-*cfa(Ent)::gfp*) were constructed. GFP levels of the *Enterobacter* fusions were lower than the *Salmonella* constructs (Fig. 3.13). Expression of RydC had no effect on GFP levels from the constructs harbouring the shorter UTR (Fig. 3.13, lanes 1/2 and 5/6), but was required to activate the reporter with the long *cfa* 5' UTR (Fig. 3.13, lanes 3/4 and 7/8). In contrast to the *Salmonella* construct, RydC expression increased Cfa-GFP expression from the *Enterobacter 638* fusion only mildly (~ 3-fold compared to ~ 8-fold). Considering the conservation of the *cfa* promoter as well as the RydC interaction site in *Enterobacter 638* it seemed likely that *rydC* was lost from the genome only recently.

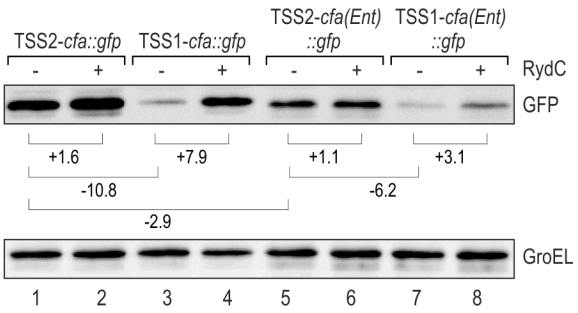

Figure 3.13 Regulation of *Salmonella* and *Enterobacter cfa::gfp* fusions.

Regulation of reporter fusions was monitored by probing for GFP on Western blots. Total protein samples were prepared from *Salmonella* Δ*rydC* Δ*rpoS* mutants in exponential growth (OD_{600} of 1) carrying either plasmids to express *Salmonella* or *Enterobacter 638 cfa::gfp* fusion plasmids (*Salmonella*: TSS1-*cfa::gfp* and TSS2-*cfa::gfp*; *Enterobacter 638*: TSS1-*cfa(Ent)::gfp* and TSS2-*cfa(Ent)::gfp*) in combination with a control plasmid (-) or pP_L-RydC (+). Fold-regulations as quantified from the blot are indicated.

3.7 Identification of the RydC binding site on *cfa* mRNA

The 5' UTR region of *cfa* upstream of the RpoS-dependent transcriptional start site was scanned for a RydC binding site using the *RNAhybrid* algorithm (Rehmsmeier et al, 2004). An 11 bp duplex was predicted to form between the single-stranded 5' end of RydC starting from position +2 and a conserved sequence stretch ~100 nt upstream of the *cfa* translational start site (Fig. 3.14 A).

To validate the potential interaction site, a single-nucleotide exchange was introduced in the TSS1-*cfa::gfp* fusion. Replacement of C-102 (relative to the translational start; Fig. 3.14 B) by a G residue rendered the resulting construct TSS1-*cfa*::gfp* irresponsive to RydC without affecting the basal expression levels in absence of the sRNA (Fig. 3.14 B, lanes 1 and 2 vs. 4 and 5). An sRNA variant carrying a compensatory mutation (G5C; RydC*) restored the activation of TSS1-*cfa*::gfp* while having no effect on TSS1-*cfa::gfp* (Fig. 3.14 B; upper two panels, lanes 3 and 6), and was expressed to the same level as wild-type RydC (Fig. 3.14 B; lower two panels).

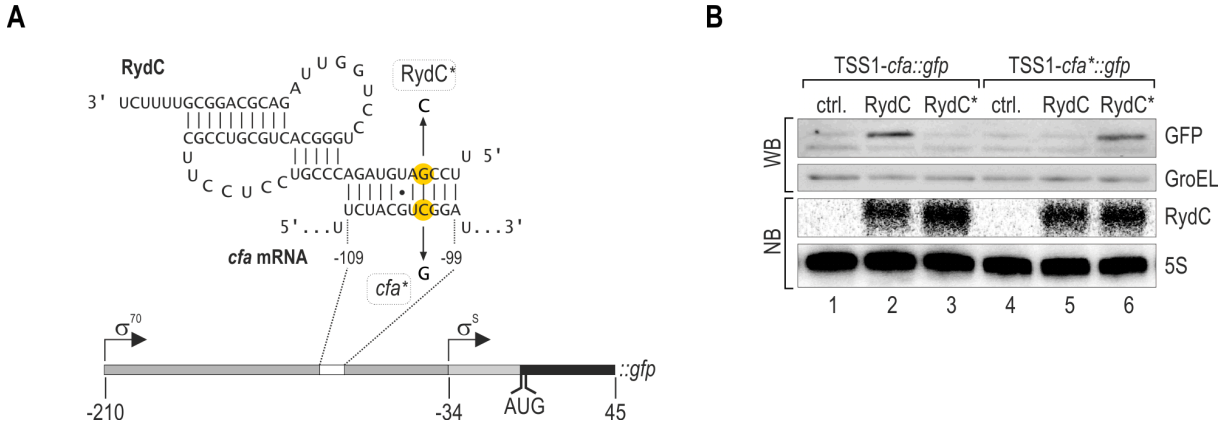

Figure 3.14 Analysis of the RydC-*cfa* mRNA interaction *in vivo*.

(A) Predicted duplex forming between RydC (nt 2 to 11) and *cfa* mRNA (nt -109 to -99 relative to the translational start site). Single-nucleotide exchanges to generate the compensatory RydC* and *cfa** mRNA are indicated. (B) Validation of the RydC-*cfa* mRNA interaction. *Salmonella* Δ*rydC* Δ*rpoS* mutants carrying plasmids for TSS1-*cfa::gfp* and TSS1-*cfa*::gfp* in combination with a control plasmid or RydC overexpression plasmids pP_L-RydC and pP_L-RydC*. Expression of GFP-fusion proteins was monitored on Western blots of total protein samples prepared from cells in exponential growth (OD_{600} of 1). Equal expression of RydC and RydC* was controlled by Northern blot analysis.

To test whether the identified binding site within the *cfa* 5' UTR was the only region recognized by RydC, *in vitro* synthesized 5' end-labelled mRNA (TSS1 to nt 70 in the CDS) was subjected to structure probing with lead(II) acetate (specifically recognizing single stranded regions) and RNase T1 (cleaving after single-stranded guanosine residues) in the presence and absence of Hfq and RydC. A comparison of the cleavage patterns revealed an Hfq and RydC-dependent "footprint", *i.e.* a site protected from cleavage, at the expected region between nt -99 to -109 relative to the translational start site of the mRNA (Fig. 3.15 A, lanes 7/11). A structural rearrangement in the presence of Hfq, but independent of RydC, was observed at the beginning of the coding sequence (Fig. 3.15 A, lanes 9/11).

Similarly, a shorter 5' fragment of *cfa* mRNA (TSS1 to nt -72 relative to the translational start site) was analyzed by structure probing. Labelled *cfa* mRNA was incubated with Hfq and RydC or RydC*, and subjected to lead(II) or RNase T1 cleavage. The footprint between nt -99 and -109 relative to the translational start site on the mRNA was dependent on the presence of Hfq and RydC (Fig. 3.15 B, lanes 8/14) whereas RydC* did not protect the mRNA from cleavage (Fig. 3.15 B, lanes 9/15).

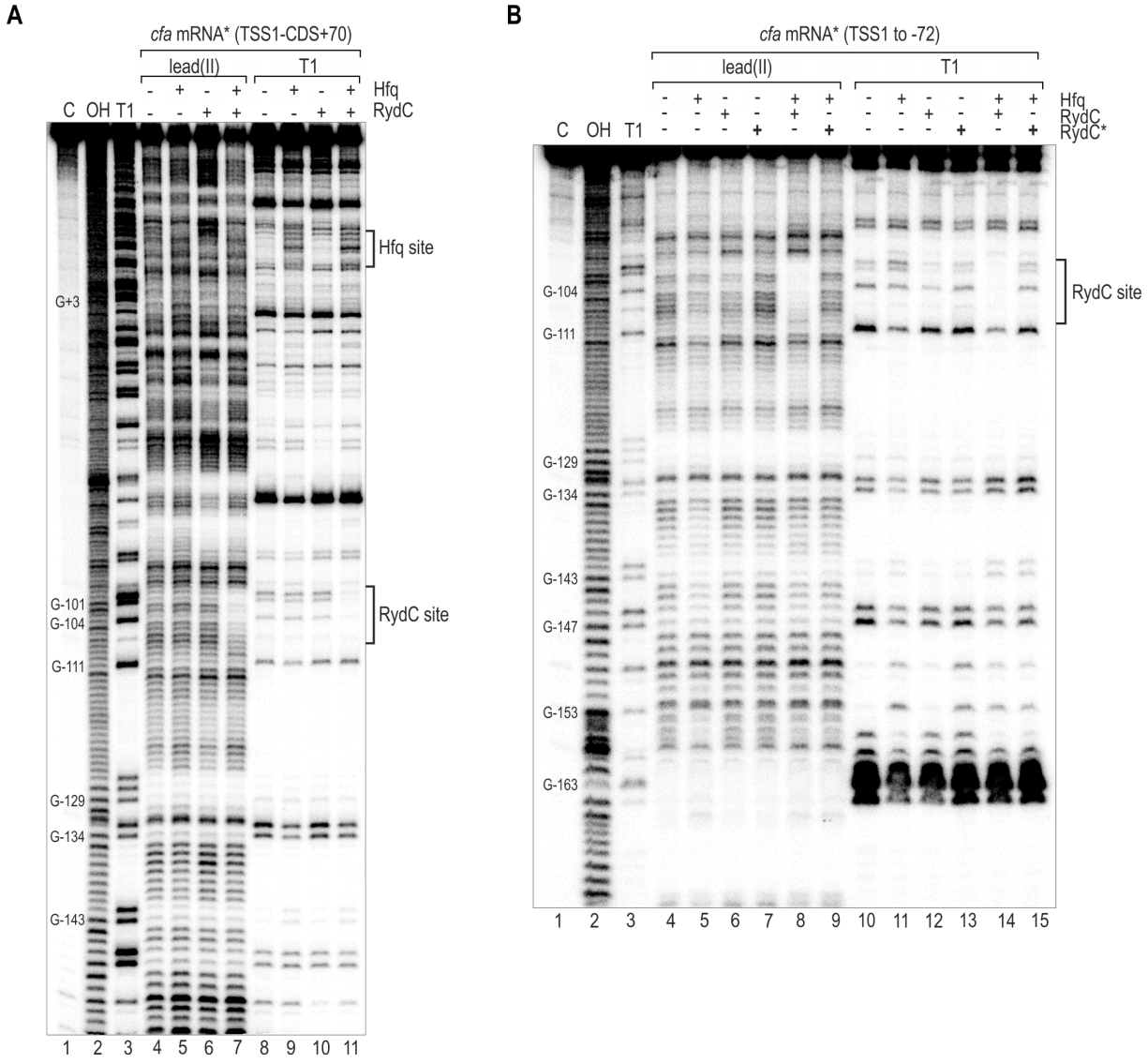

Figure 3.15 ***In vitro*** **structure probing confirms RydC interaction site on** ***cfa*** **mRNA.**

(A) *In vitro* structure probing using 0.2 pmol 5' end-labelled *cfa* mRNA (TSS1 to nt 70 of the CDS) with lead(II) acetate (lanes 1-3) and RNase T1 (lanes 4-6) in the presence and absence of Hfq (20 nM) and RydC (200 nM). The RydC binding site is indicated. A sequence stretch within the CDS rearranged in the presence of Hfq is marked. RNase T1 and alkaline ladders of *cfa* mRNA were employed to map cleaved fragments. Positions of G-residues are indicated. (B) Structure probing as in (A) using 0.2 pmol of a 5' end labelled *cfa* mRNA fragment (TSS 1 to nt -72 relative to the translational start site) in the presence or absence of Hfq (20 nM), RydC (200 nM) and RydC* (200 nM).

3.8 The 5' end of RydC is sufficient to activate *cfa* expression

The interaction site between RydC sRNA and *cfa* mRNA was mapped to an 11 bp duplex using compensatory base-pair exchanges in GFP reporter fusions and structure probing (Fig. 3.14 B and Fig. 3.15, respectively). To confirm that the 5' end of the RNA was sufficient to activate the

reporter, an sRNA-chimera was constructed by fusing the first 12 nt of RydC to a truncated form of the unrelated sRNA MicA (residues +23 to 74) termed TMA (see Fig. 3.16 A for a schematic representation of the chimera, and Supplementary Fig. 4.10 for an alignment of the RNAs). Co-expression of the TSS1-*cfa::gfp* construct with TMA alone did not affect fusion protein levels when compared to the control (Fig. 3.16 B, lanes 1 and 2). In contrast, RydC-TMA activated expression of the GFP reporter similar to wild-type RydC (Fig. 3.16 B, lanes 3 and 4). This identified RydC as the first sRNA to activate expression of a target mRNA by base-pairing via its 5' end.

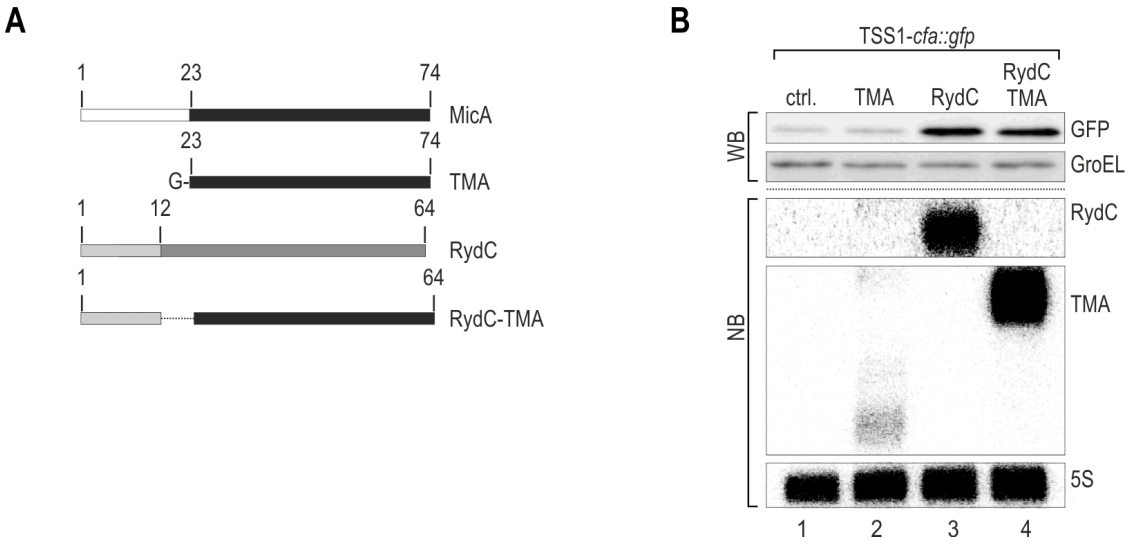

Figure 3.16 A chimera carrying the RydC 5' end as a *cfa* mRNA regulator.

(A) Schematic representation of wild-type MicA and RydC as well as the derivative constructs. The first 12 nt of RydC were fused to the 3' part (nt 23-74; TMA) of MicA to construct RydC-TMA. (B) GFP levels were determined on Western blots of total protein samples isolated from *Salmonella* Δ*rydC* Δ*rpoS* mutants carrying plasmids for TSS1-*cfa::gfp* and either a control or plasmids for P_L-driven overexpression of TMA, RydC or RydC-TMA. Expression of sRNAs was monitored by Northern blot analysis.

3.9 A 5' inhibitory element within the long *cfa* mRNA

Activation of gene expression by sRNAs is often based on a so-called anti-antisense mechanism (Fröhlich & Vogel, 2009). Herein, the translational start site of an mRNA is sequestered in a stable secondary structure which blocks ribosome association and thus translation. The activating sRNA interacts with the upstream leader of its target, and successfully competes with formation of the inhibitory structure. As a consequence, the translation initiation site is no longer sequestered and translation is stimulated.

When inspecting the *cfa* 5' untranslated leader initiating from the distal transcriptional start site for sequences capable of base-pairing with the SD site and/or start codon, no obvious self-inhibitory structure could be identified (see Fig. 3.12 for an alignment). Thus, a series of truncations of the *cfa* 5' UTR in the GFP fusion plasmid starting from TSS1 to the RydC binding site were constructed (Fig. 3.16 A) and tested for their potential to be activated in the presence of the small RNA. When shortening the 5' end for the first 27 or 36 nt (fusions -183*cfa::gfp* and -174*cfa::gfp*, respectively), no difference in basal Cfa::GFP levels or RydC-mediated activation was observed when compared to TSS1-*cfa::gfp* (see Fig. 3.16 B, top three panels). In contrast, deletion of the first 53 nt of the *cfa* 5' leader (-157*cfa::gfp*) increased Cfa::GFP levels similar to TSS2-*cfa::gfp*, and expression occured independent of RydC (see Fig. 3.16 B, lower two panels).

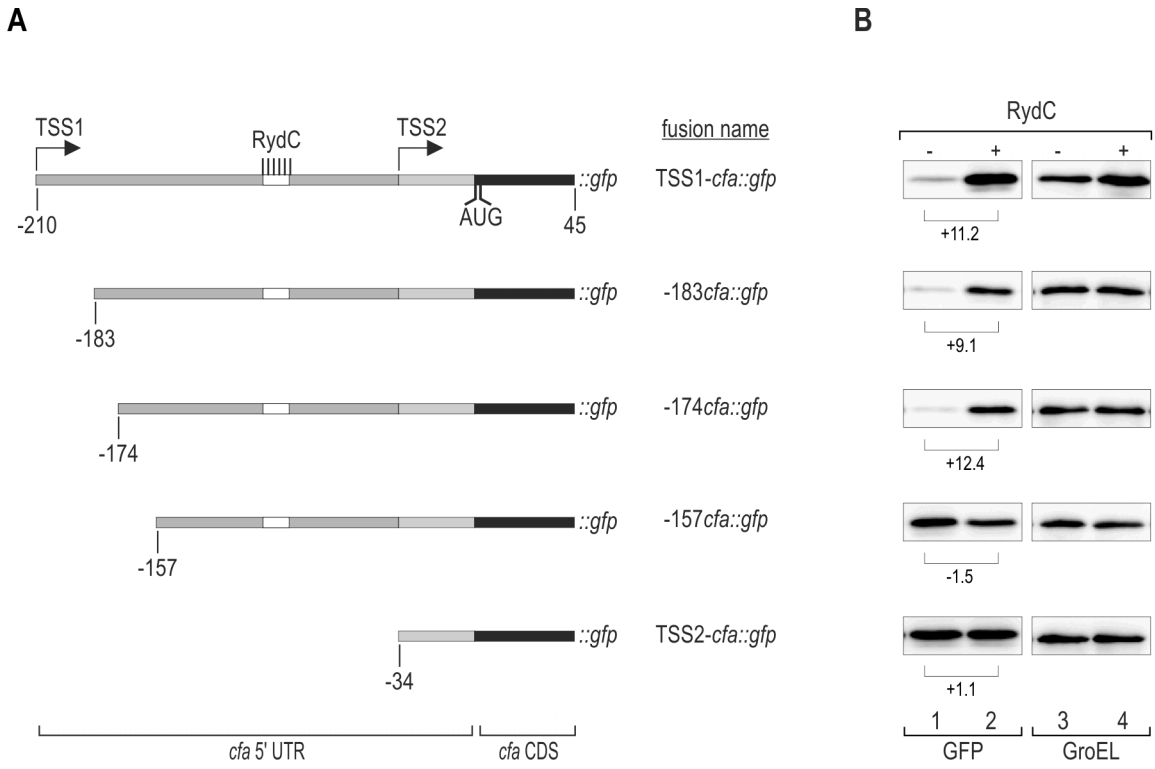

Figure 3.17 Regulation of mutant *cfa::gfp* reporter fusions in the presence of RydC.

(A) Schematic representation of a series of *gfp* fusion plasmids encompassing indicated fragments of the *Salmonella cfa* 5' upstream region and the first 15 amino acids of the CDS fused to the second codon of *gfp*. (B) Regulation of reporter fusions was monitored by Western blot analysis. Total protein samples were prepared from *Salmonella* Δ*rydC* Δ*rpoS* mutants carrying a series of *Salmonella cfa::gfp* fusion plasmids as depicted in (A) in combination with a control plasmid (-) or pP_L-RydC (+).

The 5’ end of *cfa* was relevant for the RydC-dependent activation of *cfa* expression. To investigate whether this site directly inhibited translation initiation, *i.e.* base-paired to the region around the SD site and the start codon, two versions of the 5' end of *cfa* UTR were inserted upstream of the unrelated *ompX::gfp* fusion (comprising the 5’ UTR and the first 10 aa of *ompX*) to establish fusions TSS1-*cfa-X::gfp* and -183*cfa-X::gfp* (Fig. 3.18 A). Regarding the nucleotide sequence, the *ompX* leader and the replaced stretch of the *cfa* 5' UTR including the translation initiation site displayed only very minor similarity (Supplementary Fig. 4.9). Efficient binding of RydC to the relevant fragment of the *cfa* 5’ UTR (TSS1 to nt -72 relative to the translational start site) was confirmed by *in vitro* structure probing (Fig. 3.15 B). When comparing the levels of GFP-fusion protein expressed from the different constructs, the same pattern of regulation as for the native *cfa::gfp* fusions tested before was observed. Both TSS1-*cfa-X::gfp* and -183*cfa-X::gfp* were weakly expressed in the absence of RydC and induced in cells constitutively overexpressing the sRNA. In contrast, expression from a control plasmid carrying *ompX::gfp* only was not altered by the presence of RydC (see Fig. 3.18 B). Thus, the 5’ UTR of *cfa* appeared to contain a repressory element which could be transplanted to an unrelated *gfp* fusion.

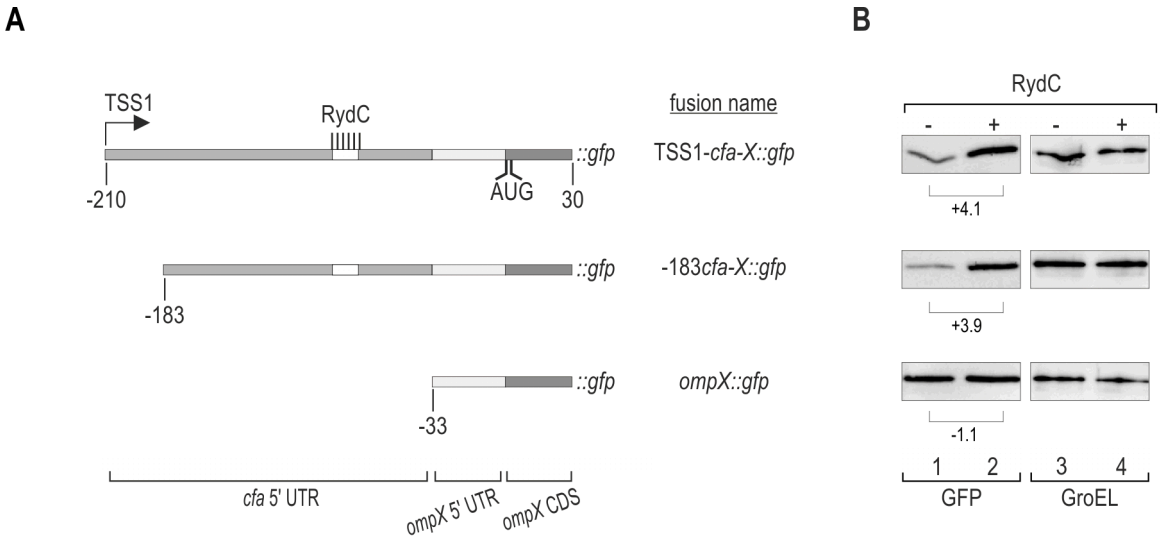

Figure 3.18 Regulation of translational *cfa::ompX::gfp* fusion variants by RydC.

(A) Schematic representation of *gfp* fusion plasmids encompassing indicated fragments of the proximal *cfa* 5’ UTR (TSS1 to nt -63 and nt -183 to nt -63, respectively, relative to the translational start site) inserted upstream of the 33 nt long 5’ UTR and the first 10 amino acids of *ompX* fused to the second codon of *gfp*. (B) Regulation of reporter fusions as described in (A) was monitored by Western blot analysis of total protein samples prepared from *Salmonella* Δ*rydC* Δ*rpoS* mutants in the absence (-) and presence (+) of RydC.

To investigate whether the observed effect of RydC in activation of *cfa-X::gfp* fusions was independent of translation initiation, toeprint experiments were performed. In this assay, formation of ternary initiation complexes at translation start sites is monitored *in vitro*. Primer extension of an mRNA is prematurely interrupted if the template is bound by a 30S ribosomal subunit and the characteristic termination product ~15 nt downstream of the start codon is referred to as "toeprint" (Hartz et al, 1988).

Two *in vitro* transcribed mRNAs, TSS1-*cfa-X::gfp* and *ompX::gfp*, were annealed to an end-labelled primer (complementary to *gfp*) and incubated - either in the presence or absence of uncharged initiator $tRNA^{fMET}$ - with 30S ribosomal subunits. Subsequently, Hfq and *in vitro* transcribed sRNA were added to the reaction mix and cDNA synthesis was carried out. The molar ratios of mRNA, sRNA and Hfq were chosen in correspondence to the structure probing experiments to facilitate efficient complex formation. Analysis of the extension products obtained in the presence of 30S ribosomal subunits identified the expected $tRNA^{fMET}$-dependent termination site at position +15 relative to the translational start site in both TSS1-*cfa-X::gfp* and *ompX::gfp* (Fig. 3.19). The presence of Hfq (in equimolar concentration) mildly reduced the toeprint intensities for both transcripts (Fig. 3.19, lanes 4, 12). The addition of a 10-fold excess of RydC, as well as RydC and Hfq, did only modestly strengthen toeprint formation. An influence of the sRNA in translation initiation on TSS1-*cfa-X::gfp in vitro* was thus considered unlikely (Fig. 3.19, lanes 5, 6). Toeprint formation on control mRNA *ompX::gfp* did not change in the presence of RydC or RydC and Hfq (Fig. 3.19, lanes 13, 14). Another sRNA, the CRP-controlled CyaR, is known to target the translation initiation site of *ompX* (Johansen et al, 2008; Papenfort et al, 2008) and served as a positive control in the experiment. As expected, 30S binding to *ompX::gfp* was strongly reduced when CyaR and Hfq were added (Fig. 3.19, lanes 15, 16). Albeit less pronounced, the same effect was observed for TSS1-*cfa-X::gfp* mRNA (Fig. 3.19, lanes 7, 8).

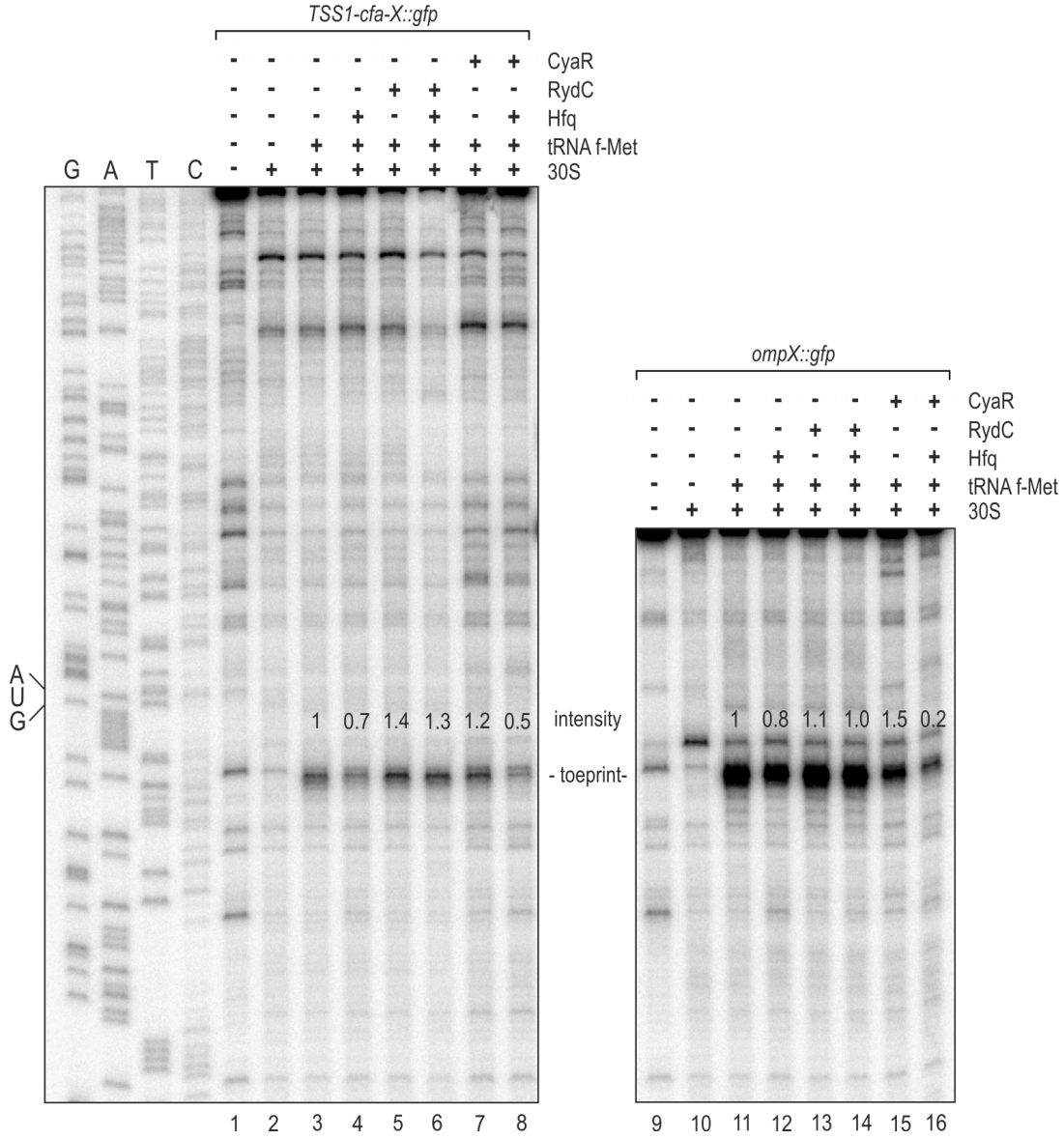

Figure 3.19 Toeprint formation on TSS1-*cfa-X::gfp* and *ompX* mRNAs.

30S toeprint formation on 20 nM *TSS1-cfa-X::gfp* (lanes 1-8) and *ompX::gfp* mRNAs (lanes 9-16) was analyzed by reverse transcription using a 5' end labelled, *gfp*-specific oligo. The presence of 30S ribosomal subunits (20 nM), uncharged initiator $tRNA^{fMET}$ (100 nM), Hfq (20 nM) and the sRNAs RydC or CyaR (200 nM) is indicated by "-" and "+" above the lanes. The position of the AUG start codon was mapped using a co-migrating sequencing ladder. The 30S toeprint signal is marked, and quantifications of relative toeprint intensities are indicated.

3.10 Processing of the *cfa* mRNA in the presence of RydC

The 5' UTR of *cfa* had been shown to exert a negative effect on the expression of both the native *cfa* as well as the *cfa-X::gfp* reporter fusions which was relieved in the presence of RydC (Fig.

3.11 and Fig. 3.18). The integrity of the *cfa* leader region in the absence or presence of the sRNA was determined by primer extension.

Analysis of the *cfa::gfp* mRNA elongation products revealed that RydC expression increased the levels of the full-length transcript which coincided with the appearance of several shorter products (Fig. 3.20, lanes 3-8, black arrowheads). However, one band was absent when the sRNA was expressed (Fig. 3.20, lanes 3-8, white arrowhead). The 5' end of this shorter fragment mapped exactly to the site in the *cfa* mRNA which was recognized by RydC (Fig. 3.14).

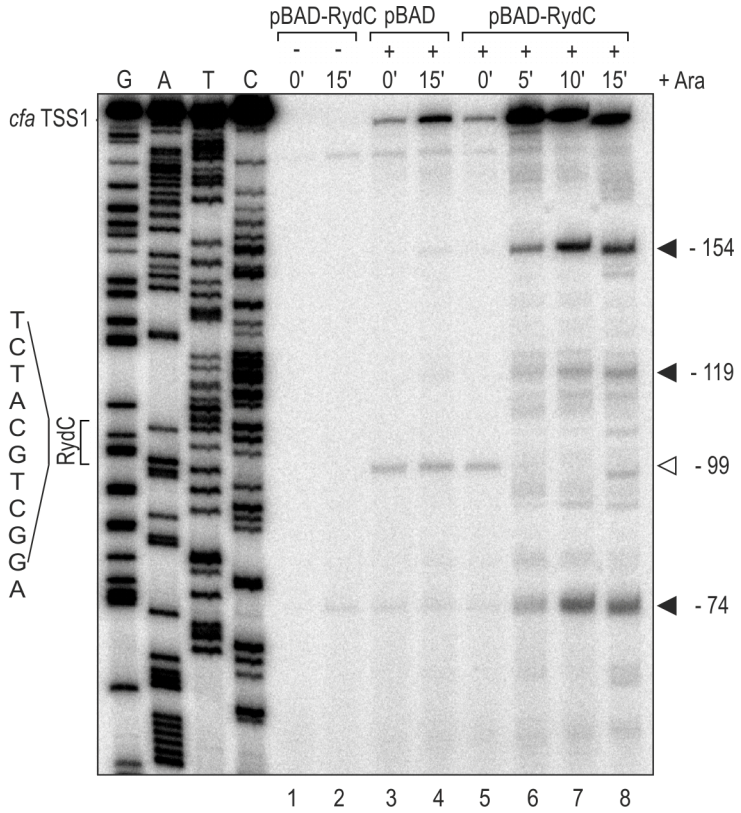

Figure 3.20 Primer extension analysis of *cfa::gfp* mRNA in the presence of RydC.

Salmonella Δ*rydC* Δ*cfa* Δ*rpoS* carrying either TSS1-*cfa::gfp* (+) or the control plasmid pXG-0 (-) in combination with plasmids pBAD-RydC or pBAD were grown to early stationary phase (OD_{600} of 1.5). 5' ends of the *cfa::gfp* mRNA were determined by primer extension of RNA prepared from cells prior to and at indicated time-points after arabinose-addition using a 5' labelled *cfa*-specific oligo (JVO-4364). Arrowheads indicate *cfa* mRNA intermediates, and positions relative to the *cfa* translational start site are indicated.

To determine whether the increased levels of full-length *cfa* mRNA upon sRNA pulse-expression resulted from increased stability, the decay of the *cfa* transcript was monitored in the presence and absence of RydC. To this end, a *Salmonella* Δ*rydC* Δ*rpoS* strain carrying either the

pBAD control plasmid or pBAD-RydC was grown to late exponential phase upon which sRNA expression was induced. After 15 min of growth in the presence of arabinose, transcription was inhibited by rifampicin treatment (Fig. 3.21 A). Decay of *cfa* mRNA was monitored by quantitative real-time PCR (qRT-PCR; Fig. 3.21 B). The expression of RydC resulted in a prolonged *cfa* mRNA half-life when compared to the control strain ($t_{1/2}$ of ~11 min vs. ~4 min).

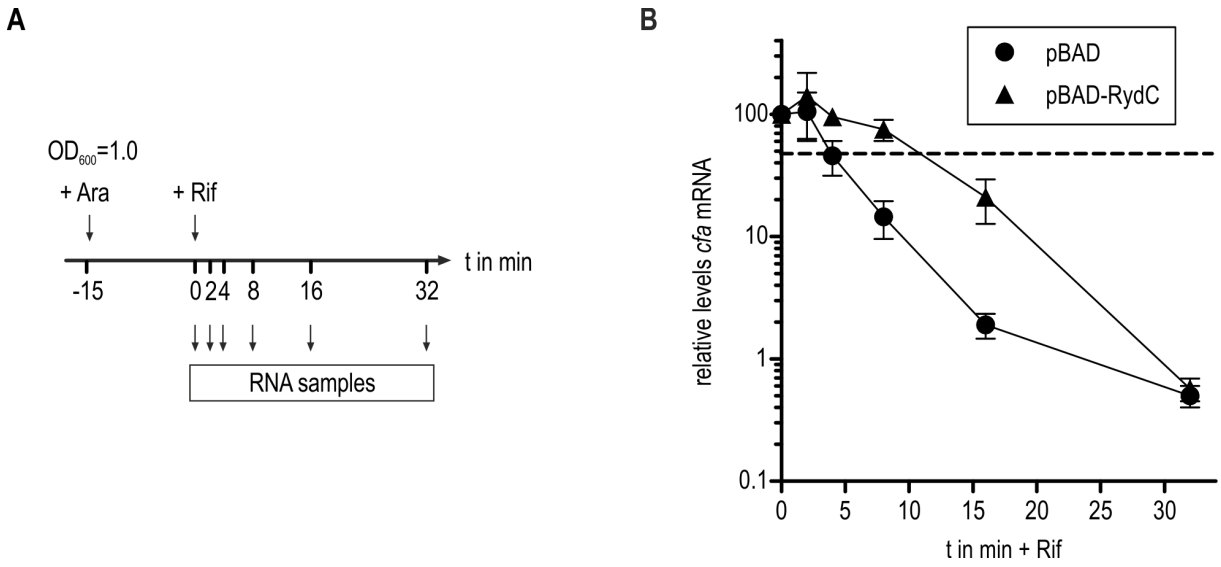

Figure 3.21 Stability of *cfa* mRNA in the presence of RydC.

(A) *Salmonella* Δ*rydC* Δ*rpoS* cells carrying either plasmids pBAD or pBAD-RydC were grown to OD_{600} of 1.0 when L-arabinose was added to induce RydC expression. After 15 min of induction, cultures were treated with rifampicin, and RNA samples were prepared from cells prior to (0 min) and at 2, 4, 8, 16 and 32 min post rifampicin treatment. (B) Abundance of *cfa* mRNA was determined by qRT-PCR analysis. The signal obtained at 0 min was set to 100%, and the percentage of mRNA remaining at each time-point was plotted on the y-axis versus time on the x-axis. The time-point at which 50% of *cfa* mRNA had been decayed (dashed line) was calculated to determine the half-life ($t_{1/2}$). Error bars represent the standard deviation calculated from three independent biological replicates.

3.11 Involvement of ribonucleases in RydC-mediated regulation of *cfa*

Regulation of target gene expression by sRNAs frequently involves the activity of ribonucleases which function in the processing and turnover of the cellular RNA pool. The differential pattern of *cfa* mRNA fragments observed in the primer extension experiment hinted at the activity of RNases in the RydC-mediated activation of *cfa* expression. The major ribonuclease in mRNA decay is the single-strand specific RNase E which can associate with additional proteins via its unstructured C-terminus to form an RNA degrading complex referred to as the degradosome

(Carpousis, 2007). The catalytic domain of RNase E is located in the N-terminus of the enzyme, and exerts essential functions in processing of stable RNAs (Kushner, 2002). RNase E-deficient strains are not viable, while C-terminal truncations impaired for degradosome formation can be obtained (Carpousis, 2007). Additional major ribonucleases are the RNase E-paralogue RNase G and the double-strand specific RNase III. Albeit one main function of the latter is rRNA processing (Babitzke et al, 1993; Burgin et al, 1990), RNase III mutant strains are viable in both *Salmonella* and *E. coli*; RNase G is not essential either (Li et al, 1999; Nicholson, 1999).

To test whether any of the major ribonucleases played a role in activation of *cfa* expression by RydC, expression of the translational TSS1-*cfa::gfp* in the presence or absence of RydC was compared between wild-type and single deletions of RNase G, RNase III and an RNase E truncation mutant incapable of degradosome assembly (*rne701*). In all three mutant strains Cfa-GFP fusion proteins were expressed similarly, and no differences in activation by RydC could be observed (Fig. 3.22).

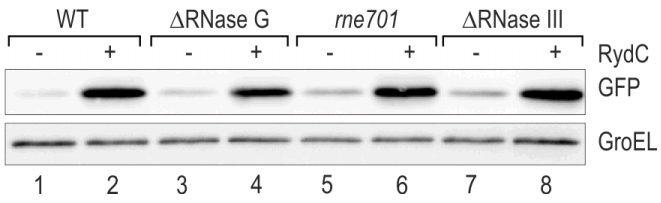

Figure 3.22 Effect of RNases on *cfa::gfp* expression in the presence of RydC.

Salmonella wild-type or derivative mutants of RNase G, RNase III as well as a RNase E truncation mutant defective for degradosome formation (*rne701*) were transformed with TSS1-*cfa::gfp* in combination with a control construct (-) or a plasmid constitutively overexpressing RydC (+). GFP levels were determined by Western blot analysis of total protein samples collected at exponential growth (OD_{600} of 0.5).

An additional experimental approach was chosen to determine a potential involvement RNase E. The catalytic activity of the essential enzyme can be abrogated in a conditional mutant. In the temperature-sensitive RNase E *Salmonella* strain (*rne-ts*), RNase E retains its normal capacity when grown at the permissive temperature of 28°C. As cells are shifted to 44°C, RNase E undergoes a conformational rearrangement rendering it catalytically inactive (Apirion, 1978; Figueroa-Bossi et al, 2009). The use of *gfp* fusion plasmids as read-out of RydC-mediated regulation of *cfa* expression was not compatible with the temperature-sensitive RNase E mutant, as both constructs are marked with the same resistance cassette. Instead, a constitutive P_{tet} promoter was integrated upstream of TSS1 of the chromosomal *cfa* gene carrying a 3xFLAG tag. In addition, the strains carried further mutations in *rpoS* (to avoid expression of *cfa* from the σ^S-

dependent proximal promoter upon temperature upshift) and in *rydC* (to exclude basal levels of sRNA expression). RydC was induced from a pBAD construct, and *cfa* expression was analyzed by primer extension and by Western blot analysis. As expected, *cfa* regulation was similar in control (WT) and *rne*-TS cells at 28°C, *i.e.* overexpression of RydC resulted in increased levels of *cfa* full-length transcript, as well as Cfa::3xFLAG protein (Fig. 3.23, lanes 1-8). In addition, the same pattern of shorter *cfa* mRNA fragments as before was observed, including one band within the RydC targeting region to disappear in the presence of the sRNA (Fig. 3.23, indicated by a white arrowhead). In contrast, differences in *cfa* expression both at the mRNA and the protein level were observed upon growth at 44°C, and concomitant inactivation of RNase E in the *rne*-TS strain. Full length *cfa* mRNA levels were again increased upon induction of RydC in both strains. In addition, a mild up-regulation was also observed in the absence of RydC 30 min post arabinose addition (Fig. 3.23, lanes 9-16). Interestingly, inactivation of RNase E also specifically abrogated detection of the *cfa* mRNA intermediate whose 5' end was located within the RydC binding site (Fig. 3.23, indicated by a white arrowhead). All other shorter fragments remained present (Fig. 3.23, black arrowheads). At 44°C, the Cfa::3xFLAG protein level did not fully correlate with the observed mRNA regulation. Generally, basal protein levels were increased in the control strain when compared to growth at 28°C, but RydC expression could significantly boost protein expression (Fig. 3.23, lanes 1-8 vs. 9-12). In contrast, Cfa::3xFLAG was only slightly induced in the presence of RydC in the *rne*-TS strain Fig. 3.23, lanes 13-16).

All but one *cfa* mRNA fragment were still present in RNA samples prepared in the absence of functional RNase E. The observed bands could be cleavage products of another RNase, specific degradation intermediates, or result from premature termination of primer extension due to strong secondary structures within the *cfa* transcript. To analyze the quality of *cfa* mRNA fragments, 5'RACE experiments were performed on RNA samples isolated from control and *rne*-TS strains grown at 44°C prior to and 30 min post-induction of RydC from an arabinose-responsive promoter (as used in primer extension; Fig. 3.23, lanes 11/12 and 15/16). Two specific PCR products of ~ 300 and ~ 190 bp were detected (Fig. 3.24 A). The longer, TAP-dependent fragment corresponded to the transcriptional start site of *cfa* (Fig. 3.24 A; indicated by a black arrowhead), whereas the shorter fragment was insensitive to TAP treatment and was mapped to the previously identified RNase E-dependent cleavage site within the RydC binding region (Fig. 3.23 and Fig. 3.24 A/B; indicated by white arrowhead). The second band was only observed in the absence of RydC, and when RNase E was functional (Fig. 3.24 A, lanes 1/2). As no further fragments were detectable in the 5'RACE experiment, the additional *cfa* mRNA fragments observed in primer extension assays (Fig. 3.20 and Fig. 3.23; indicated by black arrowheads) may constitute premature termination products.

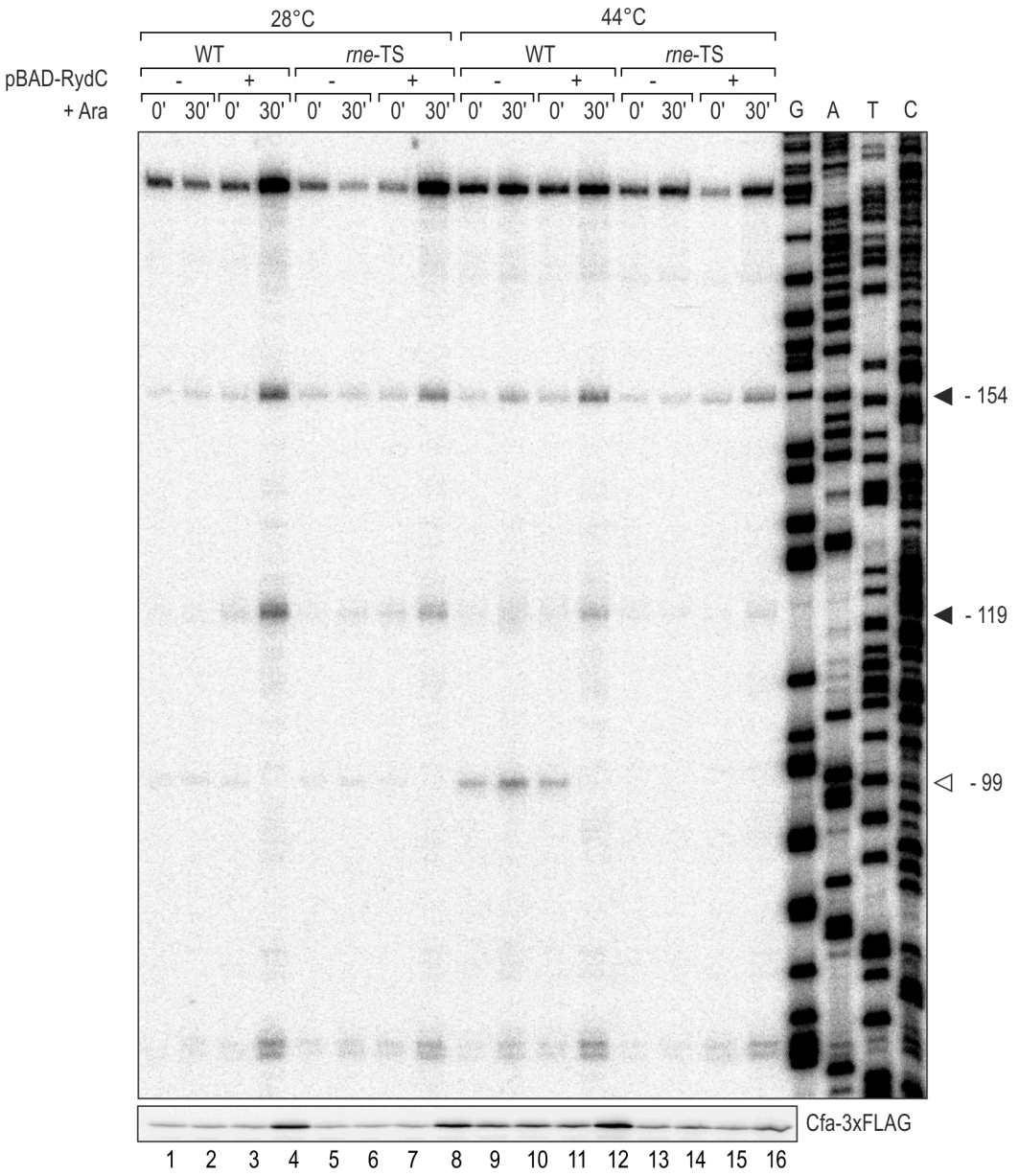

Figure 3.23 Effect of RNase E on *cfa::gfp* expression in the presence of RydC.

Salmonella Δ*rydC* Δ*cfa* Δ*rpoS* P_{tet}-*cfa::3xFLAG rne-ctrl* (WT) and its isogenic *rne-ts* strain (*rne*-TS) carrying either plasmids pBAD (-) or pBAD-RydC (+) were grown at 28°C to an OD_{600} of 1.0, upon which cultures were split and growth was continued for 30 min at 28°C, or at 44°C to inactivate RNase E in *rne-ts* strains. Subsequently, expression from the pBAD promoter was induced by addition of arabinose, and RNA as well as protein samples were collected prior to and 30 min after induction. 5' ends of the *cfa* mRNA were monitored by primer extension of RNA using a 5' labelled *cfa*-specific oligo (JVO-5769). Arrowheads indicate *cfa* mRNA intermediates. Cfa-3xFLAG levels were determined on Western blots.

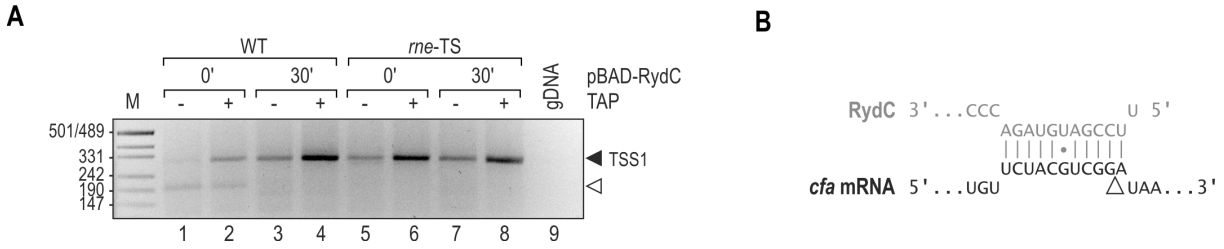

Figure 3.24 5'RACE analysis of *cfa* mRNA fragments in the presence and absence of RydC.

(A) 5'RACE experiments were performed to determine the 5' ends of *cfa* mRNA fragments in the absence and presence of RydC. *Salmonella* Δ*rydC* Δ*cfa* Δ*rpoS* P_{tet}-*cfa::3xFLAG rne-ctrl* (WT) and its isogenic *rne-ts* strain (*rne*-TS) carrying plasmid pBAD-RydC were grown at 44°C for 30 min. RNA isolated from culture samples withdrawn prior to and 30 min after induction of RydC was TAP-treated (+) or mock-treated (-) and used to prepare cDNA. A TAP-dependent elongation product (black arrowhead) and a second, TAP-independent PCR fragment (white arrowhead) were extracted, cloned and sequenced. *Salmonella* genomic DNA (gDNA) served as negative control. (B) Mapping of the TAP-independent PCR product isolated in (A). The 5' end of the *cfa* fragment (white arrowhead) corresponded to the RNase E-dependent site observed by primer extension (Fig. 3.23).

3.12 Reconstitution of RNase E-mediated cleavage of *cfa* mRNA *in vitro*

A cleavage site on *cfa* mRNA overlapping the RydC binding region was shown to depend on RNase E (Fig. 3.23). To assess the role of the RNase E and RydC sRNA in *cfa* mRNA processing in more detail, the RNase E cleavage reaction was reconstituted *in vitro*. To this end, an *in vitro* synthesized *cfa* mRNA fragment was incubated for up to 30 min with purified RNase E N-terminal domain (NTD) in the absence or presence of RydC and Hfq, respectively (Fig. 3.25). Under these conditions, *cfa* mRNA was decayed by RNase E NTD within 30 min (Fig. 3.25, lanes 2-4). However, addition of Hfq to the reaction mix mostly protected *cfa* mRNA from degradation (Fig. 3.25, lanes 5-7). In contrast, addition of RydC could not prevent *cfa* mRNA cleavage (Fig. 3.25, lanes 8-10) unless Hfq was provided simultaneously (Fig. 3.25, lanes 11-13). Thus, Hfq appeared to promote *cfa* mRNA stability. Interestingly, in both the presence and absence of Hfq, one characteristic cleavage intermediate could be observed which was absent if RydC was included in the reaction (Fig. 3.25, indicated by a white arrowhead).

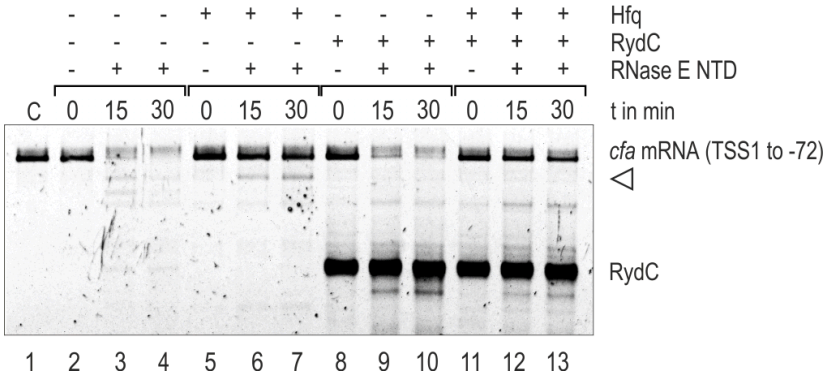

Figure 3.25 *In vitro* cleavage of *cfa* mRNA by RNase E.

Time-course experiment monitoring RNase E-mediated decay of an *in vitro* transcribed *cfa* mRNA fragment (TSS1 to nt -72 relative to the translational start site). 200 nM of mRNA were incubated with 300 nM purified RNase E N-terminal domain (RNase E NTD) in the absence or presence of Hfq (200 nM) or RydC sRNA (2 µM) as indicated. Reactions were stopped prior to and 15 or 30 min post RNase E NTD addition, separated on denaturing PAA gels and stained with SYRB Gold to visualize RNA. A cleavage intermediate of *cfa* mRNA is indicated by a white arrowhead.

To verify whether the RNase E-dependent formation of the *cfa* mRNA intermediate fragment was specifically inhibited by RydC, an additional *in vitro* RNase E cleavage assay was performed. Herein, a RydC variant carrying a point mutation (RydC*) which prevented association with *cfa* mRNA *in vivo* (Fig. 3.14 B) and *in vitro* (Fig. 3.15 B) was included. As expected, the presence of RydC, but not of RydC*, abrogated detection of the *cfa* mRNA fragment (Fig. 3.26, lanes 8-19, indicated by white arrowhead). Consequently, the presence of this *cfa* mRNA intermediate was specifically inhibited by RydC sRNA. Where present, Hfq repressed RNase E-mediated decay (Fig. 3.26, lanes 5-7 and 14-19).

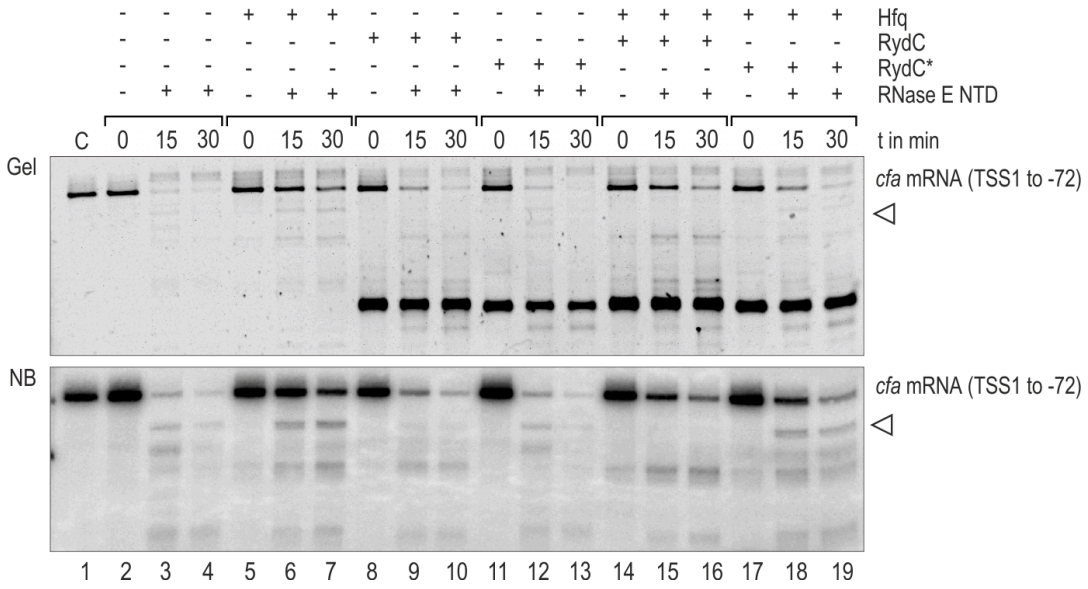

Figure 3.26 Specific inhibiton of *in vitro* cleavage of *cfa* mRNA by RydC.

Time-course experiment monitoring RNase E-mediated decay of an *in vitro* transcribed *cfa* mRNA fragment (TSS1 to nt -72 relative to the translational start site). 200 nM of mRNA were incubated with 300 nM purified RNase E NTD in the absence or presence of Hfq (200 nM), and RydC or RydC* sRNAs (2 µM) as indicated. Reactions were stopped prior to, and 15 or 30 min post RNase E NTD addition. Samples were either separated on denaturing PAA gels and stained with SYBR gold to visualize RNA (top panel), or analyzed on a Northern blot (bottom panel). An intermediate *cfa* mRNA fragment is indicated by a white arrowhead.

The *cfa* mRNA fragment observed in the *in vitro* RNase E cleavage assay (Fig. 3.24 and 3.25) was reminiscent of the intermediate observed in primer extension and 5'RACE experiments of *in vivo* RNA samples (Fig. 3.20, 3.23 and 3.24). To map the *in vitro* cleavage site, an RNase E assay was performed monitoring the decay of 5' labelled *cfa* mRNA in the presence of Hfq, RydC or RydC as before. The obtained fragments were separated in the presence of sequencing ladders. The result (Fig. 3.27) backed the observations made in the previous experiments, and confirmed that RydC was able to prevent cleavage of RNase E at a specific site (at position -99 relative to the translational start site) located within the region complementary to the sRNA (Fig. 3.27, indicated by a white arrowhead). In addition, Hfq reduced *cfa* mRNA degradation by RNase E (Fig. 3.27, lanes 4-6 and 13-18). The overall increased decay of *cfa* transcript when compared to experiments using unlabelled mRNA might be due to the differences in RNA 5' ends in the two assays: RNase E displays a preference for mono-phosphorylated (as present in the 5' labelled *cfa* mRNA fragment) over tri-phosphorylated (as present in cold assays) or hydroxylated 5' ends (Mackie, 1998). In addition, a moderately higher excess of RNase E NTD was used in this experiment when compared to previous assays (2.5-fold excess vs. 1.5-fold excess).

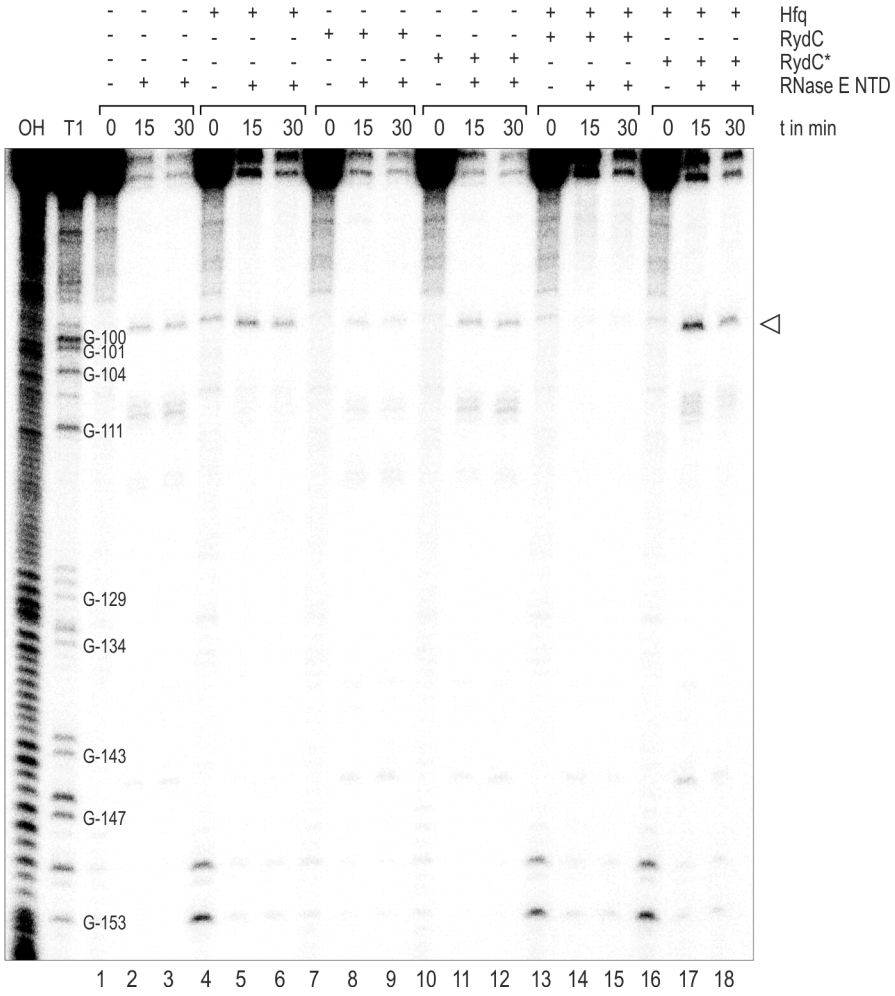

Figure 3.27 Mapping of *cfa* mRNA cleavage sites *in vitro*.

Time-course experiment monitoring RNase E-mediated decay of 5' labelled *in vitro* transcribed *cfa* mRNA fragment (TSS1 to nt -72 relative to the translational start site). 20 nM of mRNA were incubated with 50 nM purified RNase E NTD in the absence or presence of Hfq (20 nM), and RydC or RydC* sRNAs (200 nM) as indicated. Reactions were stopped prior to and 15 or 30 min post addition of RNase E NTD. RNase T1 and alkaline ladders of *cfa* mRNA were employed to map cleavage products. Positions of G-residues are indicated. The cleavage intermediate of *cfa* mRNA is indicated by a white arrowhead and could be mapped to position -99 relative to the *cfa* translational start site.

3.13 The role of RydC in induction of *cfa* under different stress conditions

Whereas overexpression of RydC strongly increased *cfa* expression, RydC levels in a wild-type strain under standard growth conditions were not sufficient to influence Cfa abundance when compared to a *rydC* mutant (Fig. 3.9). The Cfa-catalyzed modification of phospholipid bilayers – the conversion of unsaturated fatty acids to their cyclopropane derivatives – has been proposed to reduce membrane permeability (Chang & Cronan, 1999; Taylor & Cronan, 1979). Expression

of *cfa* is induced during several cellular stress responses which require increased membrane stability including growth under low pH, in the presence of acetate as well as osmotic and heat shock (Chang & Cronan, 1999; Rosenthal et al, 2008; Weber et al, 2005). All these conditions also trigger σ^S-activity. Since the alternative σ factor controls the proximal promoter in *cfa*, a potential contribution of RydC to further increase Cfa via regulation of the transcript originating from the distal start site was investigated.

To this end, Cfa::3xFLAG levels were determined in wild-type as well as Δ*rydC* and Δ*rpoS* mutant cells subjected to different stresses. In accordance with the literature, Cfa::3xFLAG expression was induced in the presence of acetate and heat shock. However, the observed increase in Cfa::3xFLAG levels was in both cases completely dependent on σ^S as it was absent in Δ*rpoS* mutant cells (Fig. 3.28 A lanes 3/4 and 7/8; Fig. 3.28 B lanes 4-6 and 16-18). The presence or absence of a functional *rydC* copy in the genome significantly increase expression of Cfa::3xFLAG under the stress conditions tested (Fig. 3.28 A lanes 3/4 and 11/12; Fig. 3.28 B lanes 4-6 and 10-12), and consequently could not reconstitute Cfa::3xFLAG levels in Δ*rpoS Salmonella*. Thus, a role for RydC in the regulation of Cfa under conditions known to induce the expression of the membrane-modification enzyme was not observed.

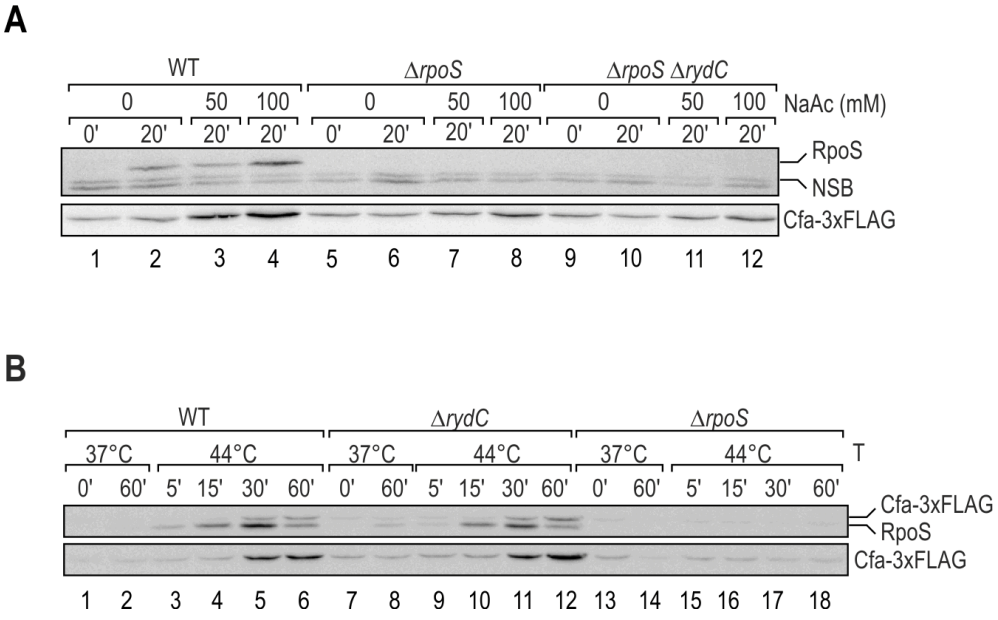

Figure 3.28 Regulation of Cfa::3xFLAG under stress.

(A) Expression of Cfa::3xFLAG and RpoS was determined by Western blot analysis of whole-cell protein samples prepared from wild-type, Δ*rpoS* and Δ*rpoS* Δ*rydC* grown in LB to exponential phase (OD_{600} of 0.4) prior to and 20 min after addition of neutral sodium acetate (NaAc) in indicated concentrations. (B) Heat-shock was induced in wild-type, Δ*rydC* and Δ*rpoS Salmonella* grown at 37°C in LB to exponential phase (OD_{600} of 0.5) by shifting the cultures to 44°C. Expression of Cfa::3xFLAG and RpoS was monitored on Western blots.

3.14 Transcriptional regulation of *rydC*

In order to identify a condition under which RydC expression was induced, and thus could potentially contribute to *cfa* induction, the regulation of *rydC* at the transcriptional level was analyzed. RydC expression was almost constitutive at low copy numbers during all phases of growth (Fig. 3.2). Inspection of the *rydC* promoter revealed the presence of a -10 element, while no -35 box could be predicted. Instead, a conserved, inverted repeat was present upstream of the -10 box enclosing bp -15 to -31 relative to the transcriptional start site (Fig. 3.1). When querying both *Salmonella* and *E. coli* genomes for the detected pattern in proximity to transcriptional start sites, the sequence stretch appeared uniquely present in the promoter of *rydC*. Thus, wet-lab based attempts to identify a potential regulator of *rydC* employing different transcriptional reporters were made.

To establish a single-copy *Salmonella rydC'::lacZ*$^{+}$ fusion (Fig. 3.29 A), the *lacZY* genes were integrated downstream the fifth nucleotide of *rydC* in its native genomic locus based on λRED-mediated recombination as previously described (Ellermeier et al, 2002). To restore the native *rydC* gene, this fusion was also moved to the unrelated STM4242 locus.

In addition, the *Salmonella rydC* promoter region and a 5' end fragment of the sRNA were fused to *gfp* on a high-copy plasmid (pP$_{rydC}$*::gfp*; Fig. 3.28 B). A chromosomal *gfp*-reporter fusion (*E. coli rydC'::gfp*) was obtained by λRED-mediated integration of pP$_{rydC}$*::gfp* in the silent pseudogene *yjhC* located in the *yjhD-insN* intergenic region of *E. coli* (Fig. 3.28 C).

A chromosomal *E. coli rydC'::lacZ*$^{+}$ fusion was constructed by inserting the *E. coli rydC* promoter region (comprising the *ydcA-rydC* intergenic region and the first five nucleotides of *rydC*) upstream of the native *lacZ* gene in a strain lacking *mhpR* and *lacI* (Fig. 3.28 D). The native *rydC* gene remained intact in both *E. coli rydC'::gfp* and *E. coli rydC'::lacZ*$^{+}$ reporter fusions. Both reporters were combined in one strain by P1 transduction. The native *rydC* locus remained intact for reporter constructs described in Fig. 3.28 B/C/D.

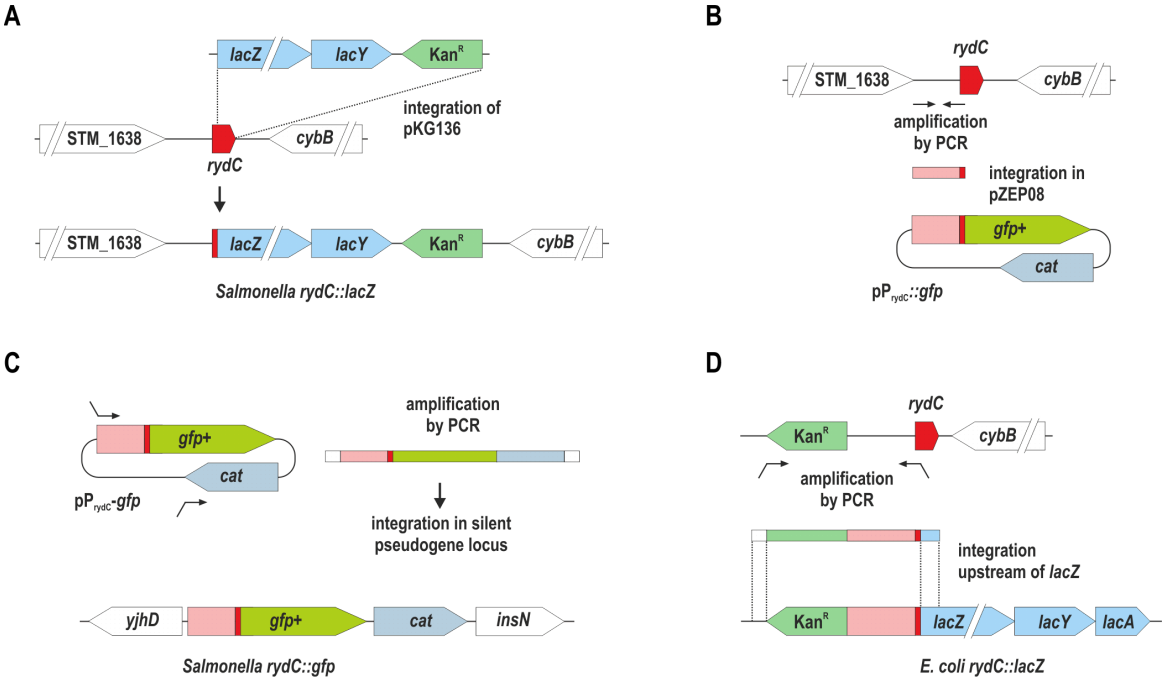

Figure 3.29 Transcriptional *rydC* reporter fusions.

(A) The *Salmonella rydC'::lacZ*$^+$ was constructed by insertion of *lacZY*, and a kanamycin resistance cassette (Kan^R) as marker gene in the native *rydC* locus downstream of the fifth nucleotide of *rydC*. To this end a λRED-derived *rydC* mutant (deletion of the DNA sequence downstream of nt +5 including the terminator of the *rydC* gene) was cured of the resistance cassette, and helper plasmid pKG136 was integrated via the FRT scar sites. In an additional version of this reporter, the fusion was moved to the unrelated STM4242 locus. (B) A plasmid-borne, transcriptional fusion pP$_{rydC}$*::gfp* fusion was established by PCR amplification of the *rydC* promoter region (encompassing bp -212 to +6 relative to the transcriptional start site) and insertion of the fragment into plasmid pZEP08 (Hautefort et al. 2008). (C) Plasmid pP$_{rydC}$*::gfp* fusion was used as template for PCR amplification of a sequence stretch comprising the transcriptional *rydC::gfp* fusion and the chloramphenicol resistance cassette (*cat*). The linear PCR product was inserted into the silent *yjhD-insN* intergenic region of the *E. coli* recipient strain using the λRED system. (D) To construct the *E. coli rydC'::lacZ*$^+$ fusion, a fragment comprising the *rydC* promoter region as well as a kanamycin resistance cassette (Kan^R) was amplified by PCR using the *ydcA* mutant of the KEIO collection (5' flanking gene of *rydC*, *ydcA*, is replaced by Kan^R) as template. The resulting PCR product was integrated into the *E. coli lacZYA* locus of a recipient strain deficient for *mphR* and *lacI.*

All three different chromosomal *rydC* reporter fusions were subjected to different screening assays involving both transposon as well as overexpression plasmid libraries. Mutants selected in either screen were isolated, and transferred by phage transduction to a control strain harbouring a chromosomal *arcZ'::lacZ*$^+$ transcriptional fusion. Only mutants which did specifically alter the expression of the *rydC* reporter were analyzed further. Table 3.2 summarizes the different experiments performed.

Table 3.2 Screening experiments to identify a transcriptional regulator of *rydC*.

reporter fusion	screening approach	obtained clones	hits
Salmonella rydC'::lacZ⁺	transposon insertion Tn10 (Tet^R) by transduction; P22 stocks provided by J. Casadesus	~ 10,500	-
Salmonella rydC'::lacZ⁺	transposon insertion Ez-Tn5 kit (Epicentre)	~ 25,000	*slyA, leuO*
Salmonella rydC'::lacZ⁺ in STM4242 locus	overexpression plasmid library (pBR322 based; 9-11 kB *Salmonella* genome fragments); provided by J. Casadesus	~ 25,000	-
E. coli rydC'::lacZ⁺	transposon insertion Tn7 (Kan^R) by conjugation; donor strain provided by A. Böhm	~ 20,000	*ptsI*
E. coli rydC'::lacZ⁺ rydC'::gfp	overexpression plasmid library (pBR322 based; 9-11 kB fragments of the *E. coli* genome); provided by A. Böhm	~ 8,000	-

Few mutants derived from two different transposon screens using *Salmonella rydC'::lacZ⁺* and *E. coli rydC'::lacZ⁺* reporter fusions were isolated due to their phenotype on X-Gal indicator plates. The colour-less lactose analogue X-Gal can be hydrolyzed by β-galactosidase, which results in the accumulation of an insoluble, blue product. Therefore, accumulation of the blue dye can be used as a read-out of *lacZ* activity in the reporter constructs.

Generally, the *rydC'::lacZ⁺* fusions appeared to be not very strong regarding galactosidase activity as judged from their light blue colour on X-Gal indicator plates. Two individual transposon insertions were mapped to the regulatory genes *slyA* and *leuO* in *Salmonella*. The disruption of *slyA* resulted in a white phenotype of the colony while mutation of *leuO* increased *lacZ* activity, and produced darker colonies. The effect was specific to the *rydC'::lacZ⁺* fusion and the same mutations did not change the expression of the unrelated *arcZ'::lacZ⁺* reporter. However, no effect of the mutations was observed as the reporter fusion was moved to the unrelated STM4242 locus. In addition, introduction of Δ*slyA* and Δ*leuO* mutations, as well as overexpression of SlyA and LeuO in *Salmonella* wild-type cells did not alter RydC RNA levels as determined by Northern blot analysis (not shown). It was thus possible that SlyA and LeuO had an effect on the upstream gene of *rydC*, STM1638, and that readthrough had activated the promoter fusion.

Five transposon insertions selected from an experiment using the *E. coli rydC'::lacZ⁺* reporter were mapped to *ptsI*. All mutants were of lighter colour than the WT when grown in the presence of X-Gal and importantly, three different insertion sites in both possible orientations

were isolated. PtsI (EnzymeI; EI) and PtsH (histidine protein; HPr) are the two sugar non-specific components of the phosphoenolpyruvate (PEP):carbohydrate phosphotransferase system (PTS). EI and HPr in combination with many different, carbohydrate specific enzyme II variants (EII) mediate the coupled phosphorylation and import of sugars across the bacterial membrane (Deutscher et al, 2006). The effect of a *ptsI* mutation on the transcriptional fusion was determined by a GFP reporter assay. Different mutations of the PTS were introduced by P1 transduction into the *E. coli rydC'::lacZ*$^{+}$ reporter strain. To this end, phage lysates were prepared from an isolated *ptsI* transposon insertion clone as well as knockout mutants of *ptsI*, and the glucose specific PTS permease components, *ptsG* and *crr* (Keio collection; (Baba et al, 2006)). All resulting strains were transformed with the pP_{rydC}*::gfp* reporter plasmid. GFP levels were measured in lysates of cells grown overnight in M9 minimal medium supplemented with glucose, maltose or fructose as carbon source. Both the *ptsI* transposon mutant and the *ptsI* knock-out displayed a severe growth defect. In addition, both mutants were characterized by strongly reduced GFP levels independent of the available carbon source (Fig. 3.30 A). In contrast, neither deletion of *ptsG* nor *crr* decreased GFP accumulation (Fig. 3.30 A). RydC expression levels were determined in *E. coli* wild-type as well as *ptsI*, *ptsG* and *crr* mutants. The absence of *ptsI* and *crr* had a mild effect on RydC expression while *ptsG* deletion did not affect sRNA levels (Fig. 3.30 B). The effect of a *ptsI* mutation on the activity of the *E. coli rydC'::lacZ*$^{+}$ might thus be indirect. Two possibilities for an involvement of *ptsI* in the regulation of *rydC* expression are possible: First, a metabolite whose import into the cell is PTS-dependent is required for transcription from the *rydC* promoter. Second, the activity of a potential transcription factor is regulated by PTS-catalyzed phosphorylation, as observed for numerous DNA binding proteins possessing PTS regulation domains (Deutscher et al, 2006). Both possibilities require further experimental evidence to elucidate the transcriptional regulation of *rydC*.

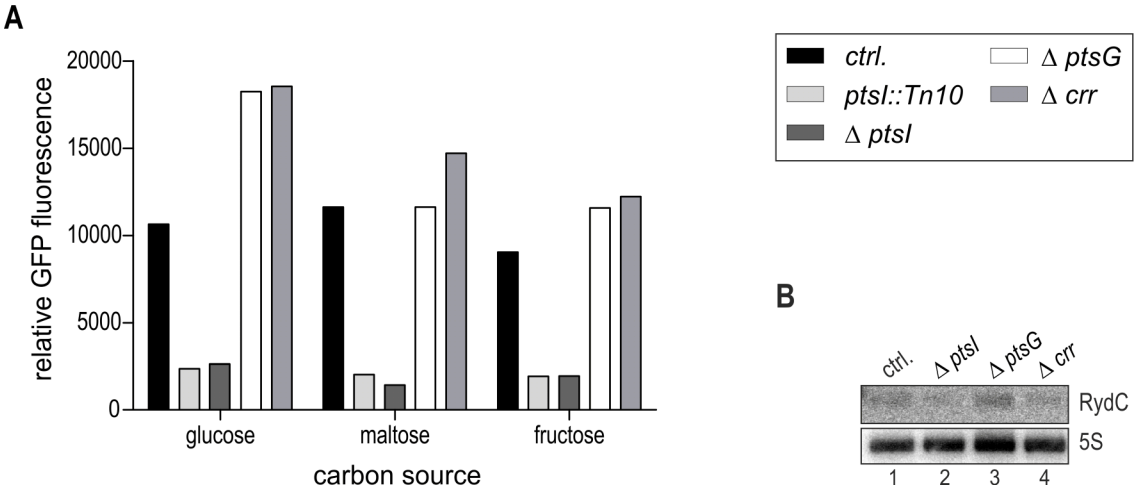

Figure 3.30 Activity of *rydC::gfp* reporter fusions in different mutants of the PTS.

(A) GFP activity was measured in lysates of *E. coli* strains carrying a chromosomal *rydC'::lacZ*$^{+}$ fusion and the pP$_{rydC}$*::gfp* reporter plasmid in a wild-type (*ctrl.*), a Δ*ptsI* mutant isolated from the transposon screen (*ptsI::Tn10*), Δ*ptsI*, Δ*ptsG* or Δ*crr* mutant background. Cells were grown o/n in M9 minimal medium supplemented with cas-amino acids and 0.2% of glucose, maltose or fructose, respectively, as carbon source. (B) Expression of RydC was probed on Northern blots of total RNA samples prepared from *E. coli* wild-type (*ctrl.*) and Δ*ptsI*, Δ*ptsG* or Δ*crr* mutant cells grown in LB to OD_{600} of 1.0.

3.15 Concluding remarks

RydC is one of the sRNAs showing the highest enrichment in co-immunoprecipitations with the RNA chaperone, Hfq (Chao et al, 2012; Sittka et al, 2008). RydC was initially discovered in *E. coli* (Zhang et al, 2003) but appears to be conserved in many related γ-proteobacteria, and thus, can be assigned to the group of enterobacterial core sRNAs. Under standard growth conditions, RydC is expressed constitutively at low levels and the main transcriptional regulator of the sRNA has not been identified yet. An interesting aspect of RydC is that it folds into a compact structure involving a pseudo-knot configuration, while the 5' end remains single-stranded. This study identified RydC as an activator of the *cfa* gene, encoding a cyclopropane fatty acid synthase. In *Salmonella* and several related enterobacteria, transcription of *cfa* is driven by two independent promoters (Wang & Cronan, 1994). RydC employs its conserved, unstructured 5' end to selectively activate the longer isoform of *cfa* mRNA by short seed pairing within its 5' UTR. Analysis of mRNA decay intermediates suggested that RydC masks a recognition site of the major endoribonuclease, RNase E, in the *cfa* leader region. Reconstitution of *cfa* mRNA decay by *in vitro* RNase E assays argued that RydC was able to abolish cleavage within a site located in the sRNA recognition region, and that the association with Hfq slowed decay of *cfa* mRNA. The exact mechanism employed by RydC to promote *cfa* expression remains to understood.

4 Appendices

4.1 Global transcriptome analysis of five enterobacterial species

Differential RNA sequencing (dRNA-seq) was employed to determine transcriptional start sites in two strains of *Salmonella* Typhimurium and the closely related enterobacteria *E. coli*, *Shigella flexneri* and *Citrobacter rodentium*. The dRNA-seq method is based on the discrimination of primary transcripts carrying a 5' tri-phosphate group from 5' mono-phosphorylated transcripts which originate from processing of primary transcripts (Sharma et al, 2010). The RNA pools prepared from cultures of the five different species grown in LB to early stationary phase (OD_{600} of 2.0) were used for the preparation of two libraries each, either covering all transcripts or being specifically enriched for primary transcripts by treatment with terminator exonuclease (TEX). This enzyme exclusively depletes 5' mono-phosphorylated RNAs but does not affect 5' tri-phosphorylated transcripts.

Following sequencing on an Illumina-Solexa platform the sequencing reads were mapped onto the reference genomes; statistics regarding the mapping of reads obtained from TEX-treated (T+) and mock-treated (T-) libraries to the individual species' genomes are summarized in Table 4.1. The distribution of reads mapping to each nucleotide in the genome was visualized using the Integrated Genome Browser (IGB), and sequence read plots of the five chromosomes revealed full, unbiased coverage of the individual chromosomes (Fig. 4.1 A-D).

Transcriptional start sites were determined based on the characteristic enrichment of cDNAs towards the 5' end of primary transcripts when comparing TEX-treated to untreated libraries (Sharma et al, 2010).

Exemplary, the three sRNA genes *sdsR*, *sraC* and *rydC* as well as the *cfa* gene, which is under post-transcriptional control of RydC, were analyzed in more detail (Fig. 4.2, 4.3, 4.4). The TEX-dependent enrichment at transcriptional start sites was observed for the majority of the inspected promoters, and allowed the annotation of the 5' ends. In some cases, reads originating from untreated libraries displayed higher abundancies than the TEX-treated samples (*sdsR* in *S*. Typhimurium SL1344, Fig. 4.2 A; *sraC* in *S*. Typhimurium 14028S, Fig. 4.2 B; *cfa* TSS1 in *S. flexneri*, Fig. 4.4 D). In addition, the proximal start site of *cfa* could only be determined unambiguously in *S*. Typhimurium SL1344 as the number of reads for the transcript was too low in other organisms (Fig. 4.4). In these cases, positions of 5' ends were extracted from untreated libraries. For SdsR, 5' ends of the processed fragment were deduced from a distinct step-like profile in un-treated libraries. The transcriptional start sites, SdsR processing sites and 3' ends as determined by manual inspection of the transcriptomic data are summarized in Table 4.2.

Table 4.1 Mapping of sequencing reads to the reference genomes.

species	total number of reads	total number of mapped reads	in %
***S*. Typhimurium SL1344**	T+ 1.738.867 T - 2.123.066	T+ 1,723,916 T - 2,123,243	T+ 99.1% T - 98.8%
chromosome NC_016810		T+ 1,544,178 T - 2,067,894	
pCol1B9_SL1344 NC_017718		T+ 82,710 T - 39,591	
pRSF1010_SL1344 NC_017719		T+ 4,031 T - 3,822	
pSLT_SL1344 NC_017720		T+ 92,997 T - 11,936	
***S*. Typhimurium 14028S**	T+ 1,553,171 T - 1,360,668	T+ 1,539,133 T - 1,331,900	T+ 99.1% T - 97.9%
chromosome NC_016856		T+ 1,527,573 T - 1,317,613	
plasmid NC_016855		T+ 11,588 T - 14,332	
E. coli BW2952 NC_012759	T+ 2,828,029 T - 2,284,035	T+ 2,806,238 T - 2,264,459	T+ 99.2% T - 99.1%
***S. flexneri* 8401 (serotype 5b)**	T+ 1,064,843 T - 867,044	T+ 1,018,240 T - 816,627	T+ 95.6% T - 94.2%
chromosome NC_008258		T+ 939,602 T - 699,680	
plasmid pWR501 NC_002698		T+ 87,271 T - 124,767	
***C. rodentium* ICC168**	T+ 1,443,309 T - 1,863,020	T+ 1,373,019 T - 1,832,518	T+ 95.1% T - 98.4%
chromosome NC_013716		T+ 1,246,268 T - 1,773,654	
plasmid pCROD1 NC_013717		T+ 113,954 T - 39,665	
plasmid pCROD2 NC_013718		T+ 6,530 T - 11,786	
plasmid pCROD3 NC_013719		T+ 7,676 T - 9,185	

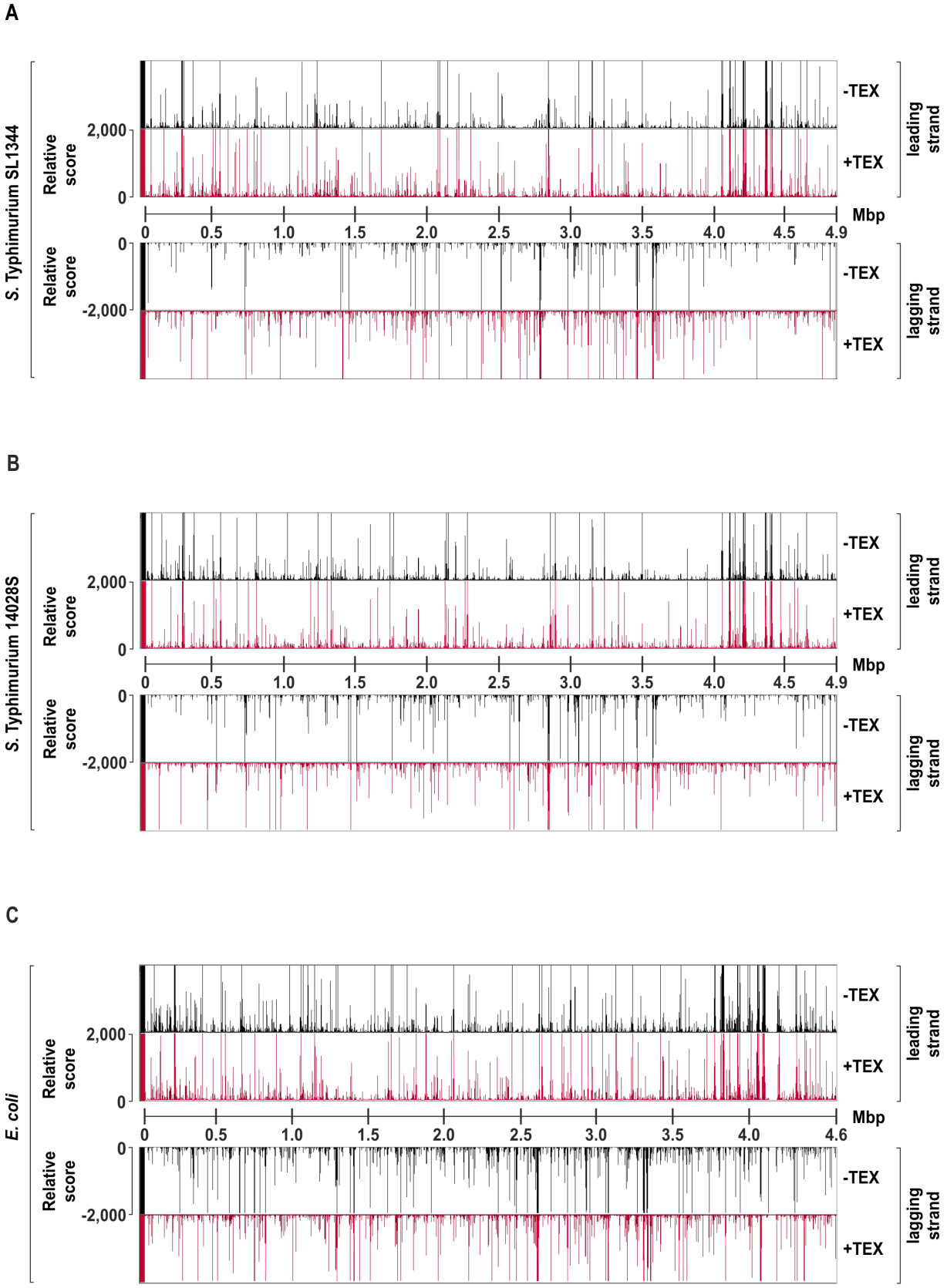
A
S. Typhimurium SL1344
Relative score
2,000
0
-2,000
-TEX
+TEX
leading strand
lagging strand
Mbp
0 0.5 1.0 1.5 2.0 2.5 3.0 3.5 4.0 4.5 4.9
B
S. Typhimurium 14028S
C
E. coli
0 0.5 1.0 1.5 2.0 2.5 3.0 3.5 4.0 4.6

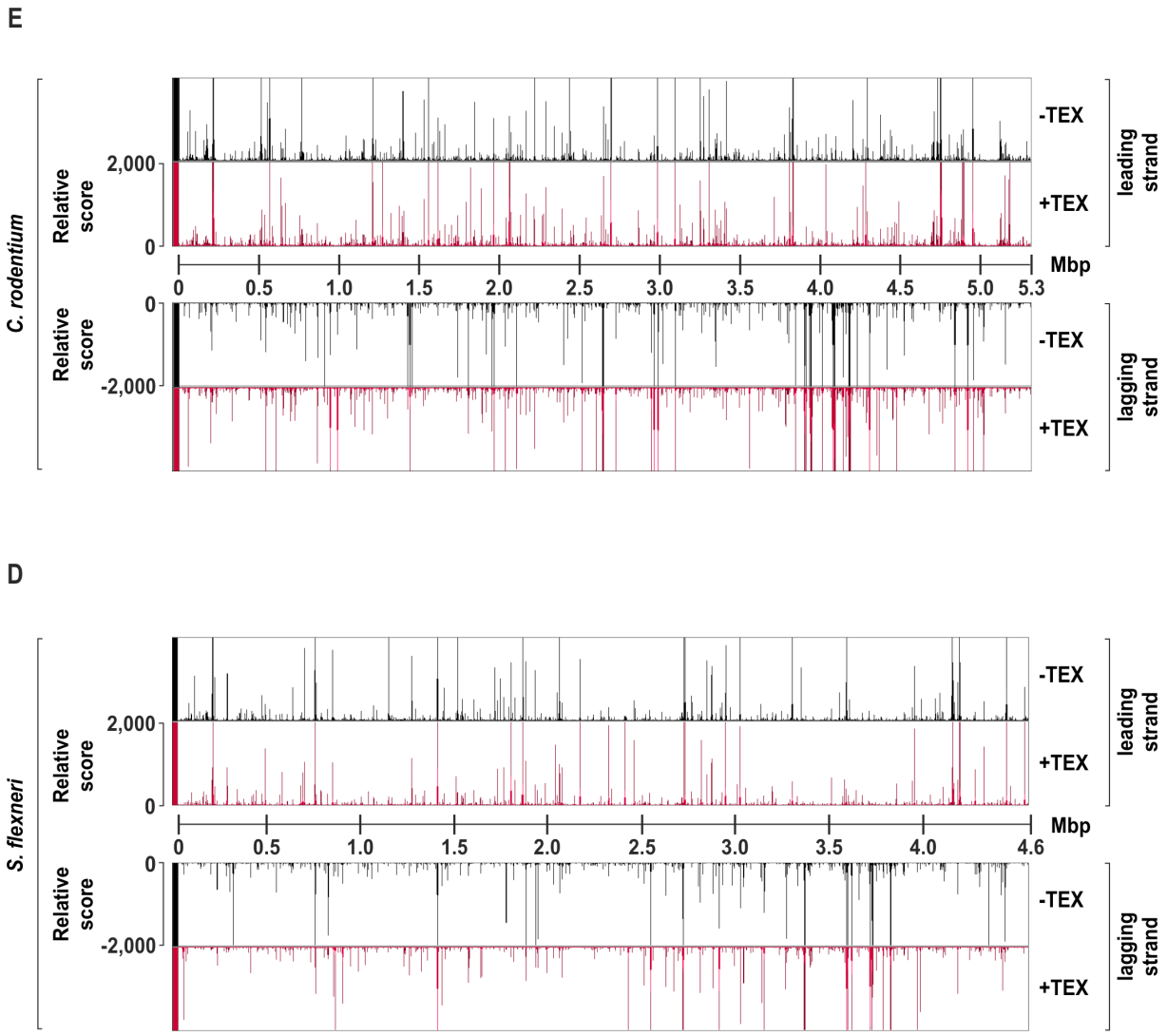

Figure 4.1 Read coverage across the reference genomes.

Combined cDNA reads without (black, -TEX) or with (red, +TEX) terminator exonuclease treatment mapped to the chromosomes of (A) *S.* Typhimurium SL1344, (B) *S.* Typhimurium 14028S, (C) *E. coli BW2952*, (D) *S. flexneri* 8401 and (E) *C. rodentium* ICC168. All libraries were adjusted to the same scale and the Y-axis in each graph represents 0-2,000 mapped reads per genome position. The genome coordinates are indicated in the centre.

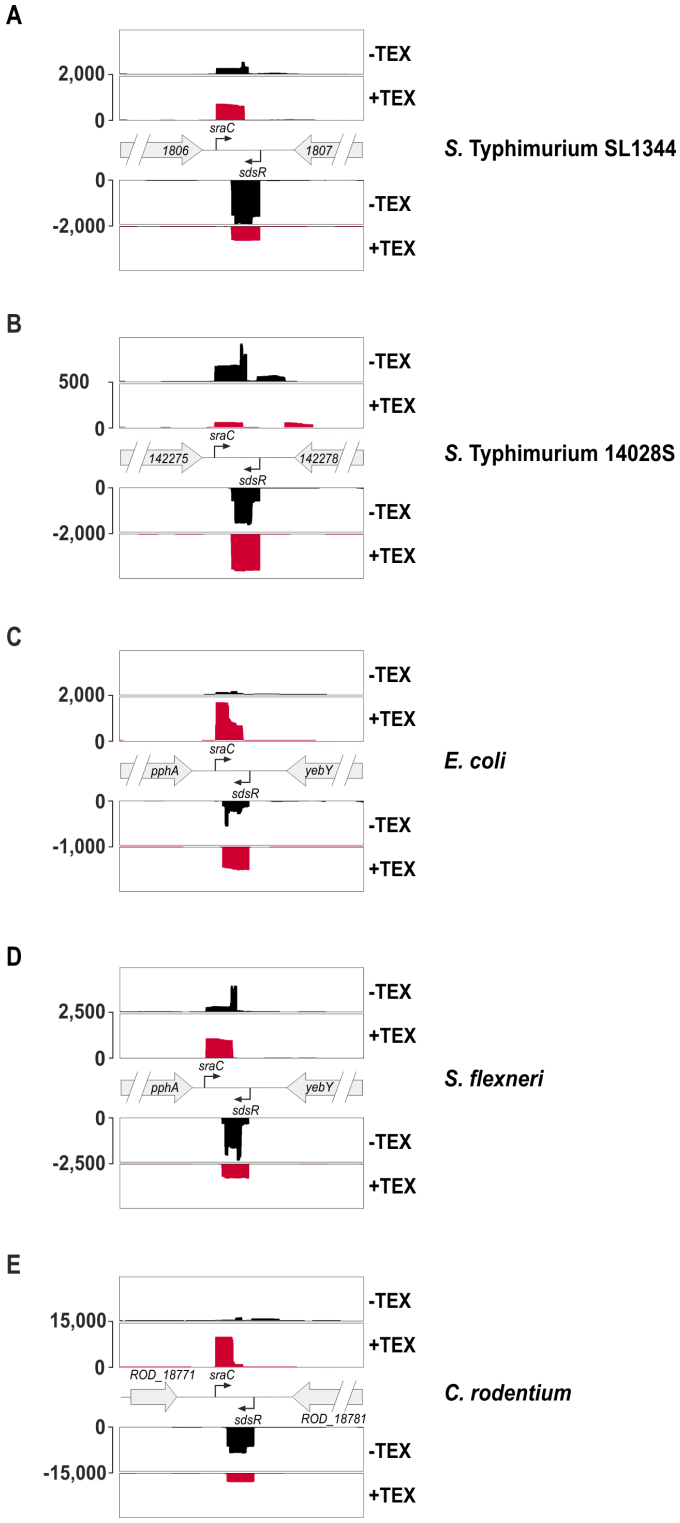

Figure 4.2 cDNAs mapped onto the *sraC/sdsR* locus.

Non-enriched (-TEX, black) and enriched (+TEX, red) cDNAs mapped onto the *sraC/sdsR* locus in (A) *S.* Typhimurium SL1344, (B) *S.* Typhimurium 14028S, (C) *E. coli* BW2952, (D) *S. flexneri* 8401 and (E) *C. rodentium* ICC168. The Y-axis in each plot indicates a scale the number of mapped reads per genome position. The flanking genes are indicated as grey arrows.

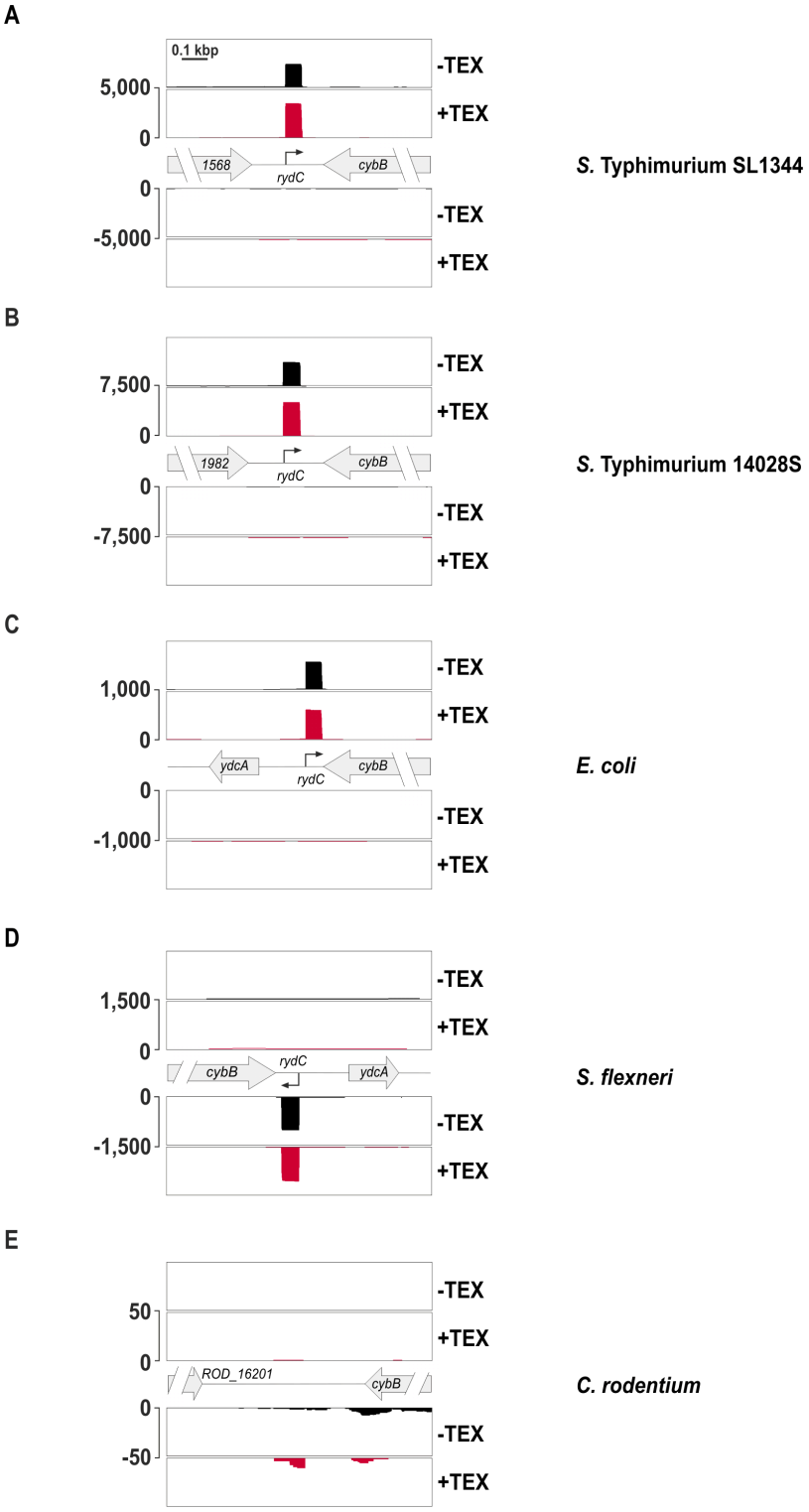

Figure 4.3 cDNAs mapped onto the *rydC* locus.

Non-enriched (-TEX, black) and enriched (+TEX, red) cDNAs mapped onto the *rydC* locus in (A) *S.* Typhimurium SL1344, (B) *S.* Typhimurium 14028S, (C) *E. coli* BW2952, (D) *S. flexneri* 8401 and (E) *C. rodentium* ICC168. The Y-axis in each plot indicates a scale the number of mapped reads per genome position. The flanking genes are indicated as grey arrows.

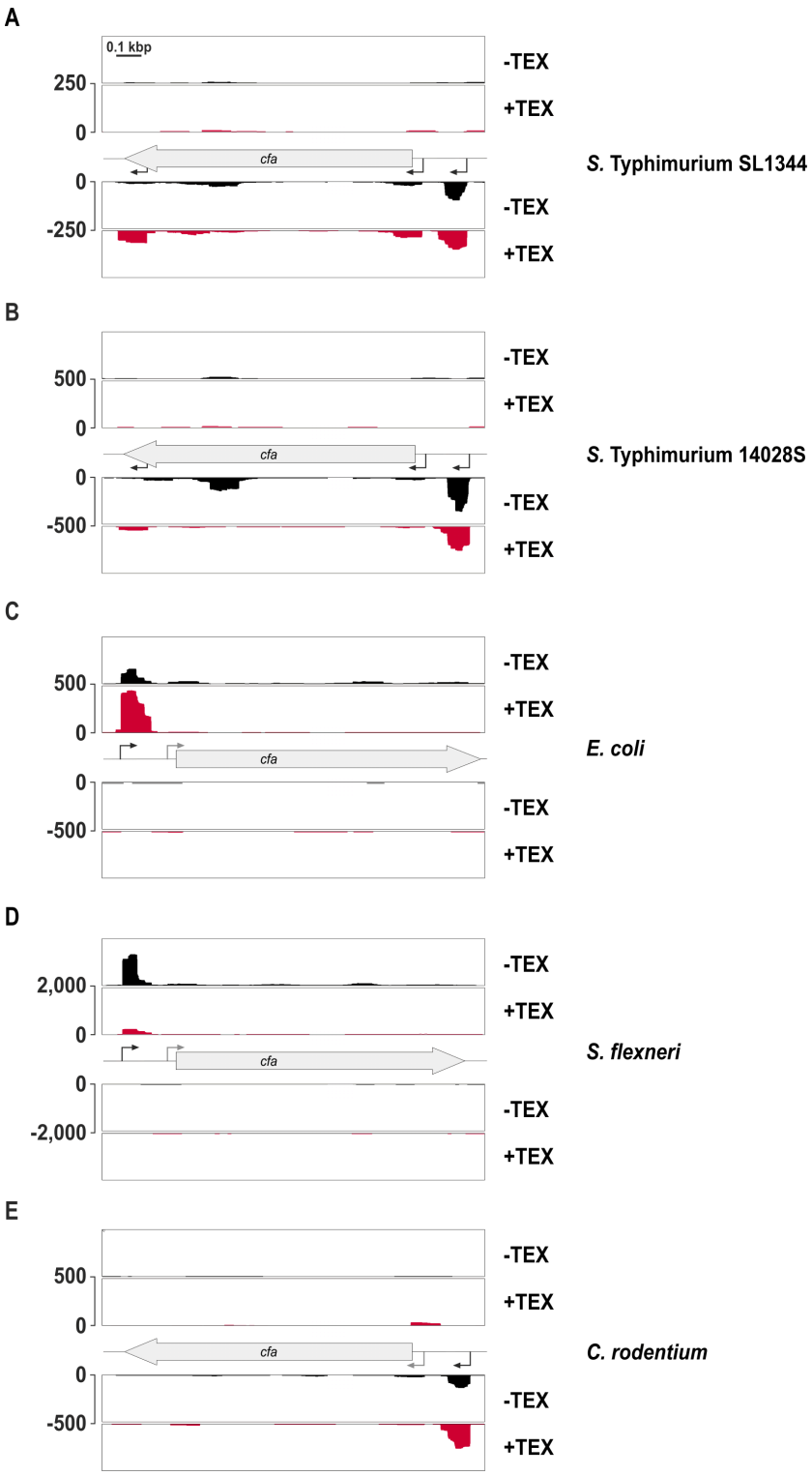

Figure 4.4 cDNAs mapped onto the *cfa* locus.

Non-enriched (-TEX, black) and enriched (+TEX, red) cDNAs mapped onto the *cfa* locus in (A) *S.* Typhimurium SL1344, (B) *S.* Typhimurium 14028S, (C) *E. coli* BW2952, (D) *S. flexneri* 8401 and (E) *C. rodentium* ICC168. The Y-axis in each plot indicates a scale the number of mapped reads per genome position.

Table 4.2 Annotation of 5' and 3' ends of SdsR, SraC, RydC and *cfa* mRNA.

	SdsR	**SdsR proc.**	**SraC**	**RydC**	***cfa* TSS1**	***cfa* TSS2**
***S*. Typhimurium SL1344**						
5' end	1,925,723	1,925,693	1,925,253	1,686,527	1,462,445	1,462,268
3' end	1,925,610	1,925,610	n.d.	1,686,592	1,461,065	1,461,065
***S*. Typhimurium 14028S**						
5' end	1,979,560	1,979,530	1,978,953	1,739,651	1,515,569	1,515,392
3' end	1,979,446	1,979,446	1,979,710	1,739,714	1,514,189	1,514,189
E. coli						
5' end	1,813,289	1,813,259	1,813,148	1,381,588	1,631,285	1,631,463
3' end	1,813,177	1,813,177	1,813,422	1,381,526	1,632,680	1,632,680
S. flexneri						
5' end	1,887,699	1,887,669	1,887,519	1,829,761	1,720,335	1,720,513
3' end	1,887,586	1,887,586	1,887,829	1,829,823	1,721,729	1,721,729
C. rodentium						
5' end	1,998,965	1,998,935	1,998,806	-	1,509,218	1,509,041
3' end	1,998,854	1,998,854	1,999,069	-	1,507,838	1,507,838

The established dRNA-seq datasets and the transcriptomic analysis have proven useful in verifying transcriptional start sites, especially if promoter sequences are not conserved between different species, as observed for the *sraC* gene (Fig. 4.1 and Table 4.2). In addition, transcriptome data can be employed to detect previously unidentified transcripts including sRNAs. Manual inspection of the *cfa* locus in *Salmonella* revealed for example an additional start site within the CDS which gives rise to a transcript overlapping the 3' end of the gene (Fig. 4.4 A/B). The possibility of double function output from an mRNA locus by producing both a protein as well as an sRNA has recently been described (Chao et al, 2012). Whether the transcript observed in the sequencing data constituted an independent sRNA remains to be verified, i.e. by Northern blot analysis.

4.2 On the necessity of 5' end determination

Prior to this study, RydC was cloned both under the control of the constitutive P_L promoter as well as the arabinose-inducible P_{BAD} promoter to establish a series of *Salmonella* sRNA expression plasmids (J. Vogel (unpublished data) and (Papenfort et al, 2008)). The RydC sequence expressed from these constructs was based on the determination of the 5' end in *E. coli* (Antal et al, 2005). An additional, conserved guanosine was added at the 5' end to enhance transcription initiation. For *E. coli*, two different 5' ends of RydC had been observed in primer extension experiments and transcription of *rydC* was predicted to start in a distance of five or six nucleotides downstream the potential -10 box (Fig. 3.1 A; (Antal et al, 2005)). Primer extension is based on reverse transcription of cellular RNAs and visualization of the cDNA product by using a labelled oligonucleotide to prime the synthesis. Although this method is a valuable and fast tool to monitor the integrity and length of a transcript, mapping of RNA 5' ends can be inaccurate due to the ability of reverse transcriptase to add non-templated nucleotides to the 3' end of the synthesized DNA (Chen & Patton, 2001). Consequently, 5' termini may be spuriously annotated to positions upstream of *in vivo* transcriptional start sites. In contrast, 5'RACE involving a linker ligated to the 5' end of cellular transcripts prior to cDNA conversion preserves the original start site. The latter method was used to determine the transcriptional start site of *rydC* in *Salmonella*, and resulted in the identification of a conserved T in 6 nt spacing from the -10 box as the single 5' end (Fig. 3.1 C). Thus, the earlier established plasmids pBAD-RydC-2 and pP_L-RydC-2 expressed versions of the sRNA which carried two additional nucleotides at the 5' end when compared to the riboregulator produced from its endogenous locus. In order to identify putative targets of the sRNA, a transcriptomic approach combining pulse-expression of RydC and global scoring of changes in mRNA abundancies on microarrays had been performed similar to the experiment described in chapter 3.3. *Salmonella* carrying either the control plasmid pBAD or the sRNA expression plasmid pBAD-RydC-2 were grown in LB to early stationary phase (OD_{600} of 1.5) when arabinose was added. RNA was prepared from culture samples withdrawn prior to and 10 min post induction of the P_{BAD} promoter and subjected to microarray analysis.

When compared to the control, only two transcripts were deregulated more than 3-fold upon pulse overexpression of RydC-2. The levels of *cfa* mRNA were found 3.6-fold increased while *luxS* mRNA showed a ~ 3-fold reduction in transcript abundance (see Table 4.3).

Table 4.3 Transcripts deregulated 3-fold or more upon RydC-2 pulse-expression.

gene	ID	fold regulation	description
cfa	SL1359	+3,61	cyclopropane fatty acid synthase
luxS	SL2802	-3,01	*S*-ribosylhomocysteine lyase

LuxS is the synthase of the hormon-like signaling molecule AI-2 mediating cell-to-cell communication during quorum sensing (Surette et al, 1999). Recently, *luxS* expression was shown to be post-transcriptionally controlled by CyaR sRNA which inhibits translation initiation by pairing to the *luxS* SD sequence (De Lay & Gottesman, 2009). To validate the regulatory effect of RydC-2 on *luxS* expression, a translational fusion of the 5' UTR plus the first 61 codons of the target mRNA to *gfp* was established. GFP levels were determined in cells co-transformed with the reporter construct and either a control plasmid or constructs constitutively expressing RydC-2, RydC, or CyaR, respectively. As determined by plate imaging and on Western blots, the presence of CyaR resulted in the expected repressory effect on *luxS::gfp* and lowered the GFP levels ~2-fold (Fig. 4.5 B/C). Consistent with the results obtained by microarray analysis, co-expression of RydC-2 also reduced GFP levels ~2-fold (Fig. 4.5 B/C). In contrast, RydC did not alter *luxS::gfp* expression when compared to the control (Fig. 4.5 B/C). Since both sRNA versions RydC and RydC-2 only differed by two nucleotides at the 5' end, a potential pairing involving this region was bioinformatically predicted with *luxS* mRNA as the target. Indeed, RNA*hybrid* analysis (Rehmsmeier et al, 2004) revealed a putative interaction between the RydC 5' end up to residue 7 (based on the transcriptional start site as determined for *Salmonella*) and the *luxS* SD site. The determined pairing region was partially overlapping the validated CyaR interaction site (Fig. 4.5 A). More important, the predicted duplexes between *luxS* mRNA and RydC or RydC-2, respectively, differed as to RydC-2 was capable of forming two additional base-pairs with its extra nucleotides at the 5' end (Fig. 4.5 D). Although sRNA/mRNA interactions can be as short as six consecutive base-pairs (Kawamoto et al, 2006) the 7 bp duplex predicted for RydC and *luxS* mRNA did not appear sufficient for target regulation *in vivo* (Fig. 4.5 B/C). The extension of the interaction resulted in an increase of the minimum free energy (MFE) calculated for both hybrids from -12.6 (*luxS* mRNA/RydC) to -16.8 kcal/mol (*luxS* mRNA/RydC-2). The predicted duplex between *luxS* mRNA and CyaR was likewise determined to -16.8 kcal/mol. Given that typical MFE values range between -24.2 to -18.8 kcal/mol (Papenfort et al, 2010), the duplex between *luxS* mRNA and RydC-2 was considered rather weak, and the predicted interaction with RydC was likely not strong enough to form *in vivo*. These results corroborated the observed differences in *luxS::gfp* regulation in the presence of the two sRNA versions.

RydC is one of several sRNAs which interact with their target via conserved sequence stretches at the 5' end. Given the observed variation in target gene selection by modifying the 5' end by two additional nucleotides, exact determination of sRNA transcriptional start sites is crucial for the correct characterization of potential interactions of the riboregulator.

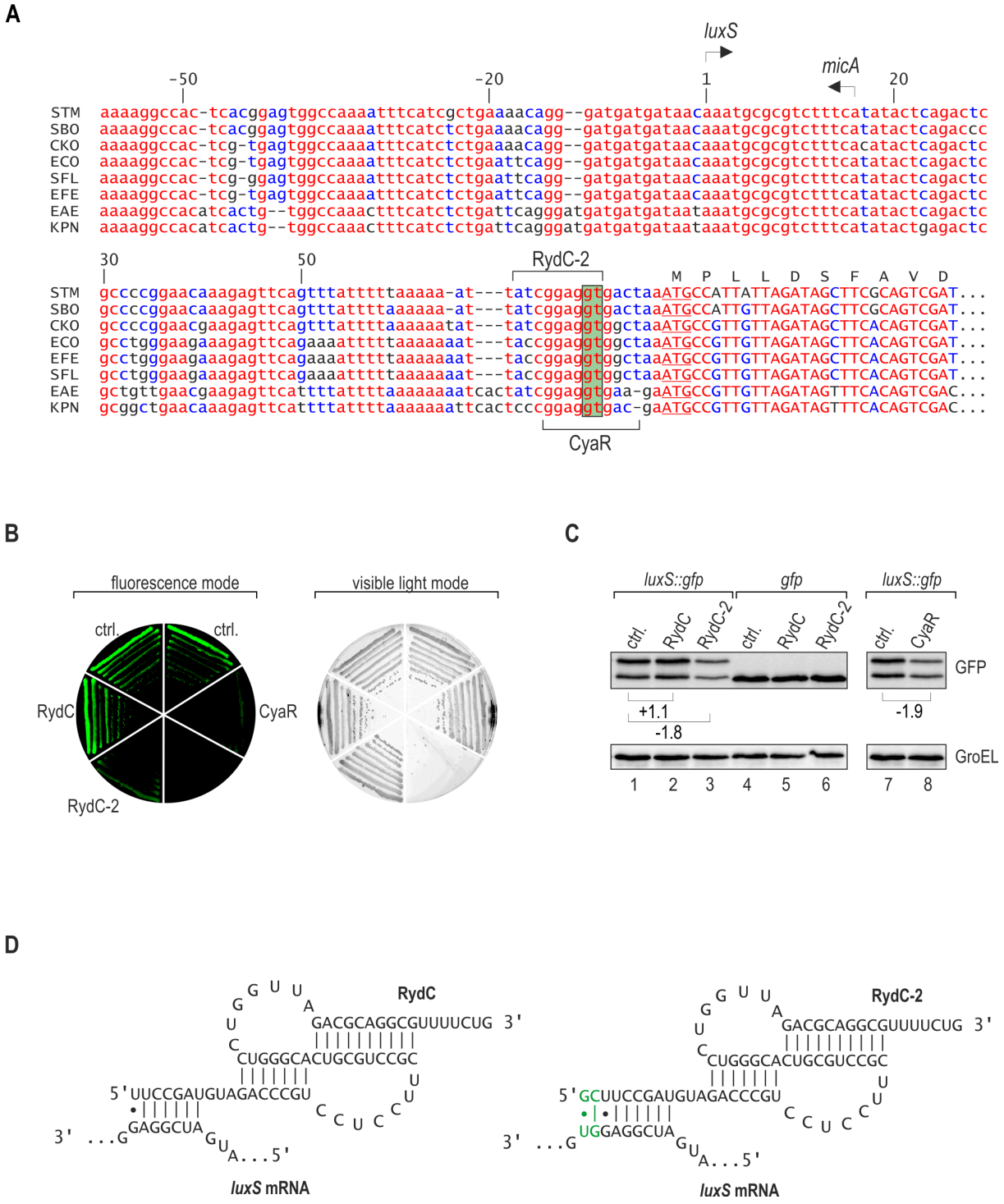

Figure 4.5 Regulation of translational *luxS::gfp* fusions by RydC-2.

(A) Non-redundant alignment of the *luxS* gene including the upstream promoter region. STM: *Salmonella* Typhimurium; SBO: *Salmonella bongori*; CKO: *Citrobacter koseri*; ECO: *Escherichia coli*; SFL: *Shigella flexneri*; EFE: *Escherichia fergusoni*; ENT: *Enterobacter aerogenes*; KPN: *Klebsiella pneumonia.* The transcriptional start site as determined previously (De Lay & Gottesman, 2009) is marked by an arrow. The 5' UTR of *luxS* partially overlaps with the *micA* gene transcribed from the opposite strand (transcriptional start site indicated). Amino acids encoded by the first ten codons in *Salmonella* are indicated above the alignment. The predicted interaction regions with CyaR and RydC-2 sRNAs are

marked above the alignment. The two nucleotides specifically pairing RydC-2 but not RydC are boxed in green. All nucleotides are coloured regarding their degree of conservation (red: full conservation; blue: partial conservation; black: little or no conservation). (B) Comparison of GFP fluorescence by plate imaging. *Salmonella rydC* mutants carrying a plasmid to express a translational *luxS::gfp* fusion in combination with a control plasmid, pP_L-RydC or pP_L-RydC-2, and *Salmonella cyaR* mutants transformed with *luxS::gfp* and either the control plasmid or pP_L-CyaR were grown on LB agar plates. Pictures of the plate were taken in the fluorescence (left image) or the visible light mode (right image), respectively. (C) Regulation of reporter fusions was quantified by Western blot analysis of total protein samples prepared from *Salmonella* strains described in (B) grown to OD_{600} of 1.0. Fold-regulations as quantified from the blot are indicated. (D) Predicted duplex forming between RydC (nt 1 to 7) or RydC-2 sRNA (nt -2 to 7 relative to the experimentally validated transcriptional start site) and *luxS* mRNA (nt -9 to -15 or nt -7 to -15, respectively, relative to the translational start site). The two additional base-pairs formed with RydC-2 are indicated in green.

4.3 Supplementary figures

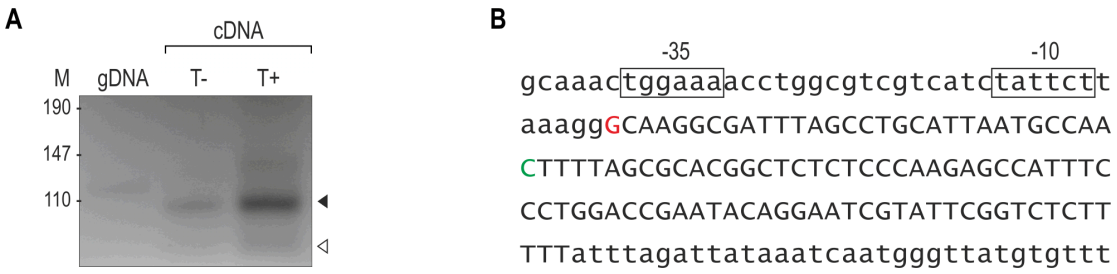

Figure 4.6 Determination of SdsR 5' ends.

(A) 5'RACE experiment to determine the transcriptional start site and the processing site of SdsR. RT-PCR products of mock-treated (T-) or tobacco acid pyrophosphatase (TAP)-treated samples (T+) were separated on a 3.5% agarose gel. *Salmonella* gDNA was used as template in a control PCR reaction. The black arrowhead denotes a TAP-enriched product which corresponds to the full-length SdsR transcript. The white arrowhead marks a non-enriched band which corresponds to the processed form of SdsR. DNA marker sizes are indicated at the left. (B) Sequence of the *Salmonella sdsR* gene. The -35 box and -10 box of the sdsR promoter are indicated. The sequence of SdsR is marked by capital letters. The transcriptional start site and 5' end of the processed version are highlighted in red and green, respectively.

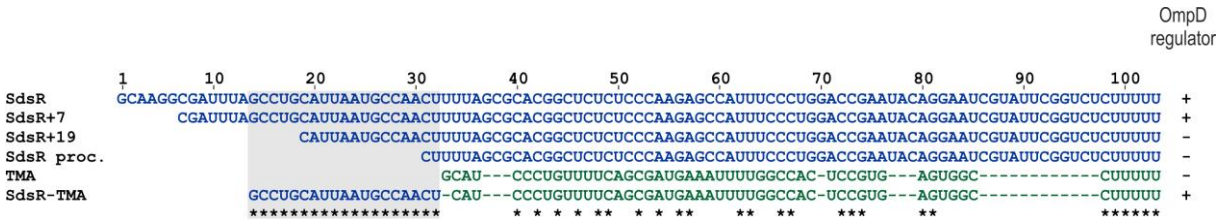

Figure 4.7 Alignment of SdsR, truncated SdsR variants and SdsR chimera.

SdsR-derived sequences are shown in blue, fragments of MicA are in green. Matching nucleotides are marked by asterisks at the bottom of the alignment. A potential regulatory effect on OmpD is indicated (+/-), and the region of SdsR involved in *ompD* mRNA-pairing is boxed in light grey.

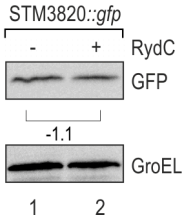

Figure 4.8 Regulation of STM3820*::gfp*

Regulation of the STM3820*::gfp* reporter fusion (nucleotides -84 to +105 relative to the translational start site of STM3820 fused to the second codon of *gfp*) was monitored by Western blot analysis. Total protein samples were prepared from *Salmonella* Δ*rydC* mutants carrying the reporter plasmid in combination with a control plasmid (-) or pP_L-RydC (+).

```
                1         10        20        30        40        50        60        70
cfa mRNA        AAAGCCAAAAAAGCGUCUACGCUGUUUUAAGGUUCUGAUCACCGUCCAGUGAUGGAGAAACUAUGAGUUCAUCGUGU
ompX mRNA                                 UUAGGACUUACUUGAAGCACAUUUGAGGUGGU--UAUGAAAAAAAUUGCA
                                          * ***   *  *    *  ** *   ** *    *****    *
```

Figure 4.9 Alignment of *cfa* and *ompX* mRNAs.

Sequence alignment of *cfa* (comprising the region replaced in *cfa-ompX* chimera; starting at nt +152 relative to the distal start site TSS1) and *ompX* mRNAs including the first five codons. The start codon is underlined. Matching nucleotides are marked by asterisks at the bottom of the alignment.

```
               1         10        20        30        40        50        60
RydC           UUCCGAUGUAGA-CCCGUCCUCCUUCGCCUGCGUCACGG-GUCCUGGUUAGACGCAGGCGUUUUCU
TMA                        GCAUCCCUGUUUUCAGCGAUGAAAUUUUGGCCACUCCGUGAGUGGCC-UUUU-U
RydC-TMA       UUCCGAUGUAGA-CAUCCCUGUUUUCAGCGAUGAAAUUUUGGCCACUCCGUGAGUGGCC-UUUU-U
               ************ *    *    ***  *   *  *    * **         *    * **** *
```

Figure 4.10 Alignment of RydC, TMA and RydC-TMA.

RydC-derived sequences are shown in blue, fragments of MicA are in green. Matching nucleotides are marked by asterisks at the bottom of the alignment. The region of RydC involved in *cfa* mRNA-pairing is boxed in light grey.

5 Discussion

5.1 Post-transcriptional control by small RNAs

Bacteria are characterized by their competence to thrive in almost every possible niche, and to react and adapt rapidly to changing environmental conditions. For this purpose, bacteria require the ability to trigger distinct response programs, *i.e.* to coordinate the expression of a specific set of genes (Battesti et al, 2011; Wood, 2011). Gene expression control is a stringent and multilayered process involving the interplay of proteins, acting for example as transcription factors, and regulatory RNAs operating at the post-transcriptional level. While several sRNAs modify protein activity, the majority of regulatory RNAs exert their function through the formation of base-pair interactions with mRNA targets (Storz et al, 2011). Trans-encoded small RNAs (sRNAs) are the most abundant class of regulatory RNAs known. As they are transcribed from genetic loci unrelated to the targeted mRNA, sRNAs may display only limited complementarity with their interaction partners (Waters & Storz, 2009).

Prototypic enterobacterial sRNAs are encoded by free-standing genes and of heterogeneous sizes ranging from ~50-400 nt (Storz et al, 2004). In addition, their secondary structures are highly diverse and characterized by only a few commonalities. In fact, most of the sRNAs which have been investigated today can be grouped by three main features. First, most sRNAs associate with the RNA-chaperone, Hfq. This interaction protects the sRNA from turn-over by cellular ribonucleases and facilitates base-pairing with target mRNAs (Vogel & Luisi, 2011). The strict requirement for Hfq-binding has been crucial for the identification of many well-studied sRNA regulators, including RydC and SdsR. Both sRNAs, as well as their major target mRNAs *ompD* and *cfa,* have been co-immunoprecipitated with Hfq from cellular lysates of *E. coli* and *Salmonella* (Chao et al, 2012; Sittka et al, 2008; Zhang et al, 2003).

The second common denominator of sRNA design is the mode of transcription termination. While many mRNA transcripts require the termination factor Rho for efficient dissociation of RNA-polymerase (Nudler & Gottesman, 2002), transcription of sRNAs usually terminates through an intrinsic structure composed of a GC-rich hairpin element followed by a poly(U)-stretch at the 3' end of the molecule. This mechanism is referred to as ρ-independent termination (Platt, 1986), and is common to Hfq-binding sRNAs (Vogel & Luisi, 2011). The principle underlying this strong bias has not been fully explored yet, however, two not mutually exclusive explanations seem plausible. First, the stem-loop at the 3' end antagonizes the 3' to 5'-directed sRNA decay by ubiquitous exonucleases, such as PNPase, and therefore enhances sRNA stability (Andrade et al, 2012). Second, the ρ-independent terminator has been recently discovered as an important loading site for Hfq (Ishikawa et al, 2012; Otaka et al, 2011; Sauer & Weichenrieder, 2011). These observations further underpin the broad biological relevance of

this ubiquitous structural element. One interesting aspect is the potential implication for sRNA evolution and the role of Hfq binding in this process. Since many mRNA transcripts also contain ρ-independent terminators, these may well function as a general Hfq loading site and constitute the origin for novel sRNAs (Chao et al, 2012). However, most of the sRNA-mediated control on *trans*-encoded targets operates at the proximal end of the transcript, and it seems likely that multiple, autonomous Hfq-binding sites exist within mRNAs, which might act independently or by loading through an sRNA regulator (Desnoyers & Masse, 2012).

The third component of most sRNAs is the base-pairing domain. This region is often marked by strong sequence conservation among various species which typically exceeds the degree of conservation observed for structural elements like the ρ-independent terminator. In loose analogy to the field of eukaryotic miRNAs, this domain of the sRNA is frequently referred to as the "seed" domain which engages base-pairing with often multiple target mRNAs. Importantly, the composition of the seed region seems to implement a decisive function for target mRNA selection to the sRNA (Papenfort et al, 2012), and is likely to define the number of target transcripts as well as their amplitude of regulation. Of note, several sRNAs (e.g. GcvB and Spot42) have been reported to regulate various mRNAs via more than one targeting domain (Beisel et al, 2012; Sharma et al, 2011), suggesting a complex interplay of Hfq-binding, target-site selection and subsequent mRNA decay. This setup might be further extended by defined processing events, such as those observed for SdsR (see below) directly impacting on all of these parameters. Given that *cfa* is the only firmly validated target of RydC, it is yet unclear if similar considerations might apply for this sRNA as well, however, the unusual pseudoknot structure in the 3'end of the molecule (Fig. 3.3) poses an interesting question as to its function in base-pairing with target mRNAs.

5.2 Identification of bacterial sRNAs

Despite the multitude of computational and experimental screens performed, the exact number of sRNAs expressed in a single bacterium is unknown. Besides rather obvious sRNA candidates expressed from orphan promoter/terminator pairs located in intergenic regions of the bacterial chromosome, hundreds of antisense RNAs mapping to the opposite strand of protein coding genes have been detected in studies employing deep sequencing or tiling arrays. Few of these transcripts have been confirmed by independent experiments and it remains to be verified how many candidates can be assigned to a specific physiological function or whether some represent technical artefacts (Thomason & Storz, 2010). In addition, genuine bacterial sRNAs might have been missed in previous screens either because they are only transcribed under very specific conditions or because they were misannotated as parts of mRNAs. A recent study has described numerous Hfq-associated sRNAs in *Salmonella* to be derived from 3’ UTRs and previous pull-

down experiments have suggested stable 5' UTR fragments as putative sRNA candidates (Chao et al, 2012; Sittka et al, 2008).

Conservation analysis of related bacterial genomes has been the method of choice for initial screens for sRNAs in *E. coli* and other bacteria (Altuvia, 2007). Based on the close relatedness of both organisms and the preserved arrangement of flanking regions, the majority of *E. coli* RNA species could also be annoted in *Salmonella* (Hershberg et al, 2003). This distinct group of conserved regulators including also SdsR and RydC are referred to as "core sRNAs", and are considered to serve central functions in bacterial regulatory networks. The recent advent of the high-throughput sequencing technology has revolutionized the identification of sRNAs in many species (van Vliet, 2011) and increased the number of sRNA regulators, for example in *Salmonella* to ~ 150 (Chao et al, 2012; Kröger et al, 2012). This relatively high number of sRNA regulators is contrasted by only very limited knowledge on the cellular functions these regulators fulfill. In total, only ~70 sRNA-mRNA target pairs involving 23 sRNAs have been reliably verified in *Salmonella* and *E. coli* (Peer & Margalit, 2011). Specifically, the study of individual sRNA-target pairs has proven most powerful to decipher new regulatory sRNA functions, and has unraveled the mechanisms underlying post-transcriptional gene regulation in bacteria. Importantly, understanding the basic principles of sRNA-mediated expression control will foster the design of synthetic regulators operating at the post-transcriptional level.

5.2.1 SdsR is highly conserved among Enterobacteria

An intriguing feature of many *Salmonella* and *E. coli* sRNAs is their highly growth-rate-dependent expression even under normal laboratory conditions. Several studies that included expression profiling observed a large fraction of the sRNAs to accumulate specifically towards stationary phase (Argaman et al, 2001; Vogel et al, 2003; Wassarman et al, 2001). Entry of bacterial growth into stationary phase is marked by drastic morphological and global gene expression changes, and includes the partial up-regulation of numerous stress responses with crucial roles for long-term survival in the absence of growth (Navarro Llorens et al, 2010; Nystrom, 2004). It was hypothesized that the observed stationary phase-specific up-regulation of the newly identified sRNA genes actually reflected control by stress-related transcription and alternative sigma factors active under stationary growth (Argaman et al, 2001).

SdsR (a.k.a. RyeB) was originally discovered in systematic searches for non-coding RNAs in *E. coli* as an abundant, stationary-phase specific sRNA (Argaman et al, 2001; Vogel et al, 2003; Wassarman et al, 2001). In this study, the preserved location downstream the *yobA-yebZY* operon and the strong sequence conservation of the ~ 100 nt sRNA were employed to predict SdsR orthologues in a plethora of γ-proteobacteria (Fig. 2.1 A). Northern blot analysis of SdsR revealed two different species of the sRNA corresponding to the full-length molecule and a

processed, ~ 70 nt species representing the 3' end of the RNA (Fig. 2.1 B). By analogy to two other highly conserved sRNAs, ArcZ and RprA, which are also detected as two distinct sRNA species each (Argaman et al, 2001), the observed processing of SdsR depends on the activity of the major ribonuclease RNase E (Fig. 2.16; (Papenfort et al, 2009) and K. Papenfort and J. Vogel, unpublished results). However, different from the aforementioned ArcZ and RprA, full-length SdsR is by far the more abundant species compared to the processed version (Fig. 2.1 B and Fig. 5.1). In all three sRNAs, the region downstream the processing site displays the highest degree of sequence conservation within the molecule (Fig. 2.2 and Fig. 5.1; (Papenfort et al, 2009) and K. Papenfort and J. Vogel, unpublished results). ArcZ employs this conserved stretch to base-pair with its target transcripts *sdaC* mRNA, *tpx* mRNA, STM3216 mRNA and *rpoS* mRNA (Mandin & Gottesman, 2010; Papenfort et al, 2009). RprA interacts with its two confirmed targets, *rpoS* and *csgD* mRNAs, via distinct sites located both upstream and downstream of the cleavage site (Fig. 5.1 C; (Majdalani et al, 2002; Mika et al, 2012)). SdsR uses an internal sequence element which only comprises the first nucleotide of the processed form of the sRNA to repress the porin OmpD (Fig. 2.19 A and Fig. 5.1 A). Since *ompD* is not highly conserved but SdsR can be predicted in a multitude of enterobacterial species, a much wider putative target repertoire of the sRNA is conceivable. Considering the regulation of further target mRNAs via interaction sites located within the sRNA's 5' end or overlapping the processing site, cleavage of the full-length SdsR could constitute an additional layer of controlling its regulatory capacity. As to whether cleavage of the RNA is regulated and whether the processed species can by itself function as a regulator remains to be elucidated.

Intriguingly, SdsR displays full complementarity to an internal region of a second non-coding transcript, SraC. Both sRNAs are encoded within the same intergenic region and expressed from opposite strands (Argaman et al, 2001; Balbontin et al, 2008; Vogel et al, 2003; Wassarman et al, 2001). In contrast to SdsR, SraC can only be identified in about half of the investigated species (Fig. 2.1 A) and with regard to the nucleotide sequence, exclusively the stretches of SraC overlapping SdsR display a high degree of conservation (Fig. 2.9). Also the *sraC* promoter elements display significant variation between species, and probing of the sRNA on Northern blots revealed differences in size and expression levels between *Salmonella*, *E. coli* and *Shigella* (Fig. 2.10). Whole transcriptome analyses of *Salmonella*, *E. coli*, *Shigella*, and *Citrobacter* strains using differential RNA sequencing confirmed the predicted differences in transcriptional start sites and allowed the identification of the SraC 5' end for all these species (Table 4.2). According to their antisense orientation, the expression patterns of the two sRNAs appear inversely correlated, *i.e.* SraC disappears as SdsR accumulates at the onset of stationary phase (Fig. 2.10). Indeed, SraC expression is almost constitutive in strains unable to express SdsR due to a mutation in *rpoS* (Fig. 2.11 A/B, lanes 9-12). In contrast, SdsR levels remain mostly unchanged if SraC transcription is abrogated (Fig. 2.11 A/B, lanes 5-8). Thus, SdsR seems to play

a significant role in the control of SraC expression, however, SraC does not decisively influence SdsR expression, especially when cells enter stationary phase. While the biological function of SraC is yet to be determined, one may speculate on the general role of antisense regulation via two non-coding RNAs. Inferring from concepts that have largely been shaped by work from toxin-antitoxin systems (Gerdes & Maisonneuve, 2012), antisense arrangements often serve as the genetic framework to establish heterogeneity among bacterial populations allowing the differentiation into more dedicated "cell types". In this respect, the variation in SraC expression patterns observed in *E. coli*, *Shigella* and *Salmonella* may indicate distinct requirements for differentiation among these related species, e.g. in the transition from exponential to stationary phase growth, a process which involves the activation of σ^S, and therefore of SdsR.

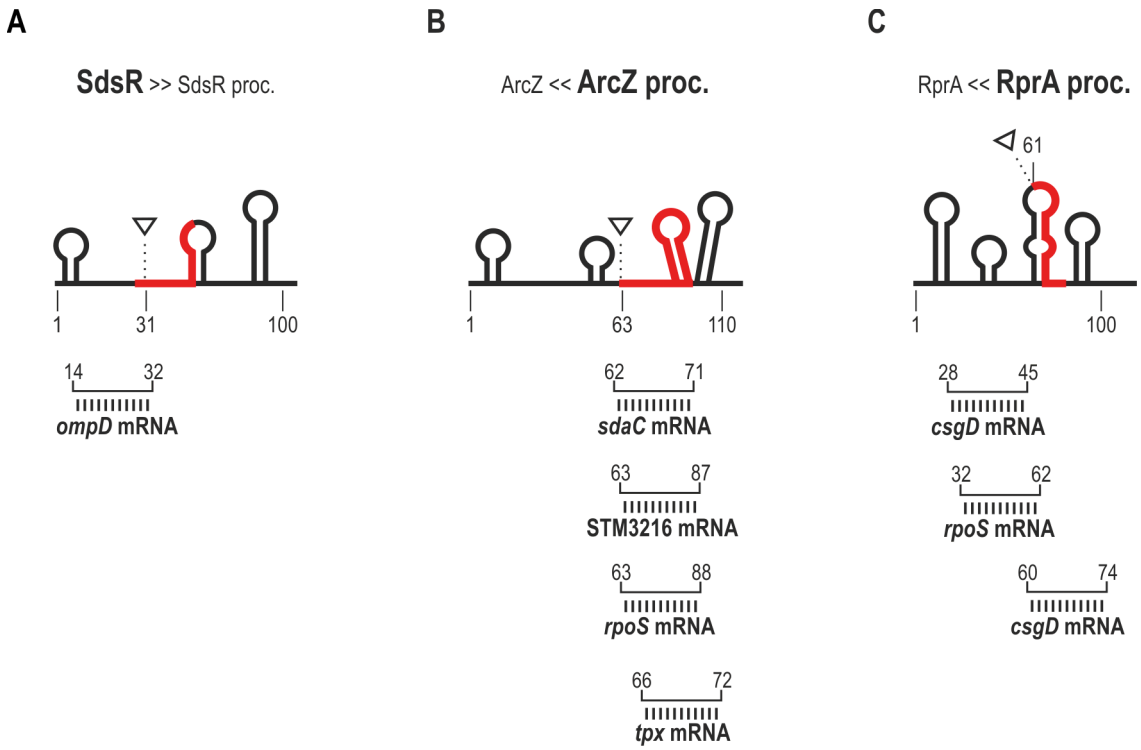

Figure 5.1 Distribution of targeting sites in the processed sRNAs SdsR, ArcZ and RprA.

Schematic representation of the three core sRNAs SdsR (A), ArcZ (B) and RprA (C). The stretches with the highest degree of sequence conservation are marked in red. The processing sites are indicated by dashed lines. Location of binding sites with confirmed target mRNAs are represented below the structure.

5.2.2 The RydC pseudoknot: form follows function

RydC is a ~ 65 nt sRNA originally identified by Hfq pulldown experiments in *E. coli* (Zhang et al, 2003). A peculiarity of RydC is its conserved secondary structure which involves the formation of an H-type RNA pseudoknot (Antal et al, 2005). RNA pseudoknots constitute one of the simplest RNA folding motifs and contain at least two helical segments connected via two single-stranded loops (Giedroc et al, 2000). The structurally diverse group of RNA pseudoknots is present in various types of cellular RNAs including ribosomal RNAs, mRNAs, ribozymes and riboswitches (Giedroc et al, 2000), RydC was however the first bacterial sRNA which was proven to contain a pseudoknot (Antal et al, 2005). In an H-type fold, the nucleotides within a hairpin loop form intramolecular base-pairs with residues outside the stem. This leads to the formation of a pseudoknotted structure comprising two stems and two loops. As the two stems are able to stack on top of each other, a quasi-continuous helix with one continuous and one discontinuous strand is formed. Thus, the rather simple H-fold pseudoknot can yield a highly stable and compact secondary structure (Staple & Butcher, 2005).

The RydC pseudoknot was first described in *E. coli* (Antal et al, 2005). When comparing orthologues of RydC in different enterobacteria with regard to their capability of forming a pseudoknot, this structure was found conserved in all species (Fig. 3.3). Similar conservation at the structural but not the sequence level was observed for other classes of RNAs, including tRNAs, miRNA precursors in eukaryotes and also prokaryotic sRNAs. For example, 6S RNA is a highly conserved sRNA mimicking the structure of an DNA open promoter complex and altering the activity of RNAP (Wassarman, 2007). In the ε-proteobacterium *Helicobacter pylori*, no orthologue of 6S RNA could be predicted based on sequence conservation. However, the characteristic structure involving a long hairpin structure with a central asymmetric bulge matches the well-studied *E. coli* 6S RNA and thus enabled the identification of the RNA (Sharma et al, 2010). Thus, the secondary structure of RNA molecules happens to be more conserved than the sequence in order to maintain a distinct function also in sRNAs. In RydC variants of different species, single nucleotide exchanges within regions involved in intramolecular base-pairing are always compensated by respective mutations within the interacting sequence (Fig. 3.3). This observation argues in favour of a strong evolutionary pressure to maintain the sRNA secondary structure. One reason could be the experimentally verified high stability of RydC which was reduced when the pseudoknot structure was disturbed (Fig. 3.5 A). *In vitro*, RydC exhibited a higher affinity for Hfq than the pseudoknot mutant (Fig. 3.6 A). Thus, the structure appears to confer stability to the molecule by facilitating tight binding to Hfq. This assumption is in clear accordance with the observation that RydC is among the top-ranked sRNAs pulled-down with Hfq although its intracellular expression under standard conditions is relatively low (Fig. 3.2; (Chao et al, 2012; Sittka et al, 2008)).

Besides the pseudoknot, RydC harbours a second hyperconserved domain. The nucleotide sequence of the unstructured stretch at the 5' end of the RNA is maintained among all species expressing RydC. As confirmed by chemical probing and genetic analyses, RydC employs residues 2 to 13 of its single-stranded 5' end to base-pair with its target *cfa* mRNA to promote its expression (Fig. 3.14 A). The 5' end of sRNAs has recently been observed as a hotspot for target interactions, and approximately one third of all sRNAs characterized to date in *Salmonella* and *E. coli* act by 5' terminal pairing to their respective targets (Papenfort et al, 2010). Similar to RydC, the 5' ends of MicC, MicF and RybB also function as autonomous target binding domains: chimeric sRNAs in which the 5' ends of the respective sRNAs are grafted onto an unrelated scaffold RNA display the same activity as the native regulators (Fig. 3.16 B; (Corcoran et al, 2012; Papenfort et al, 2010; Pfeiffer et al, 2009)). While all the aforementioned sRNAs act to repress their mRNA targets, RydC is the first sRNA to activate target gene expression using its conserved 5' end.

5.3 Integration of core sRNAs into cellular networks

Intriguingly, conservation of sRNAs in different species is not restricted to nucleotide composition, structure and genomic location but can also cover the physiological function of an RNA regulator. Several in-depth analyses of individual core sRNAs, for example, the σ^E-controlled RybB or the CRP/cAMP-dependent CyaR in *Salmonella* and *E. coli* have uncovered that the orthologous sRNAs are involved in parallel regulatory pathways in both organisms (De Lay & Gottesman, 2009; Johansen et al, 2008; Johansen et al, 2006; Papenfort et al, 2008; Papenfort et al, 2006). Bacteria use sRNAs typically as modulators to adapt their gene expression profiles in global stress responses to overcome environmental pressures such as starvation, osmotic stress, oxidative stress or low iron concentrations (Waters & Storz, 2009).

The observation that various central physiological responses in bacterial involve the regulatory activity of an sRNA has prompted the assumption that every major regulon contains at least one conserved sRNA (Gottesman, 2005). Thus, one of the goals of the present study was to assign the two core sRNAs SdsR and RydC to one of the conserved transcriptional networks in bacteria.

5.3.1 SdsR is directly controlled by the alternative σ factor σ^S

The RNAP holoenzyme is composed of a multi-subunit core associated with a specific σ factor subunit. Besides the housekeeping σ^{70}, enterobacterial species such as *E. coli* or *Salmonella* encode six alternative σ factors σ^E, σ^S, σ^N, σ^F, σ^H and σ^{FecI} (Fig. 5.2). Each of these σ factors orchestrates a distinct regulon, allowing optimal adaptation to changing environmental conditions (Ishihama, 2000).

The present study provides evidence that the sRNA SdsR is under direct transcriptional control of the general stress σ factor σ^S. Alternative σ factors that control the expression of sRNA genes have been reported before (Fig. 5.2), and those activated under nitrogen limitation (under control of σ^N) or membrane damaging conditions (under control of σ^E) have been studied in more detail. Two direct sRNA targets of the σ^E-associated RNA-polymerase in *E. coli* and *Salmonella* - MicA and RybB - act to regulate expression of multiple porin-encoding genes (Johansen et al, 2006; Papenfort et al, 2006; Udekwu & Wagner, 2007), while VrrA sRNA underlies σ^E-control in *Vibrio cholerae* (Song et al, 2008). Similarly, σ^N, the alternative σ factor relevant for survival under nitrogen limiting conditions (Reitzer, 2003) has documented functions in the expression of the enterobacterial sRNAs GlmY and GlmZ (Göpel et al, 2011; Reichenbach et al, 2009; Urban et al, 2007), as well as CrcZ and Qrr1-5 of *Pseudomonas* and *Vibrio* species, respectively (Lenz et al, 2004; Sonnleitner et al, 2009; Tu & Bassler, 2007). Although expression of the *Salmonella*-specific IsrE (a homologue of RyhB sRNA) as well as the *cis*-regulatory sRNA GadY in *E. coli* are reduced in the absence of a functional *rpoS* allele (Opdyke et al, 2004; Padalon-Brauch et al, 2008), no conserved sRNA had been assigned to the regulon of σ^S. Being the major stress σ factor, σ^S orchestrates the expression of ~10% of genes in *E. coli* (Maciag et al, 2011; Weber et al, 2005). Its activity sharply increases under a variety of stress conditions including heat and osmotic shock but also as cells enter stationary growth phase (Hengge-Aronis, 1996).

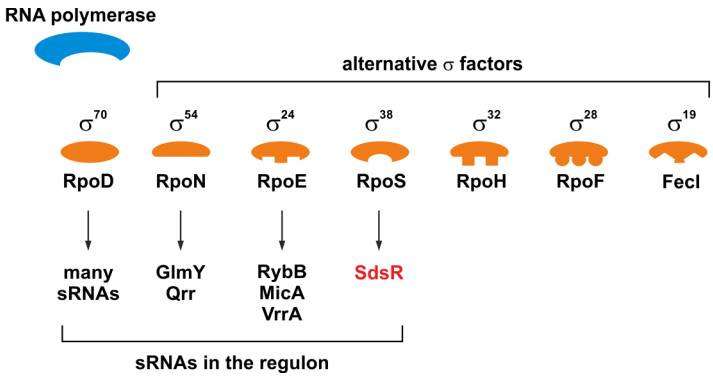

Figure 5.2 sRNAs under the control of alternative σ factors.

In *E. coli* and *Salmonella*, the RNAP core enzyme (blue) can either associate with the housekeeping σ^{70} subunit or one of six alternative σ factors (orange). RpoN (activated under nitrogen starvation) controls the expression of the sRNAs GlmY in *E. coli* and Qrr1-4 in *Vibrio* species and RpoE (activated by envelope stress) is required for the transcription of RybB and MicA in *E. coli* and *Salmonella* as well as VrrA in *V. cholerae*. SdsR was identified in the present study as the first sRNA under direct control of the general stress σ factor RpoS.

In the case of SdsR, mutation of *rpoS* completely abolished sRNA expression and plasmid-borne σ^S not only complemented stationary phase activation but also increased SdsR levels during exponential growth (Fig. 2.3 A). Likewise, *rpoS* deficiency fully abrogated stress-mediated SdsR activation, in a similar manner to the known σ^S-controlled gene *osmY* (Fig. 2.8).

At the sequence level, the *sdsR* promoter almost exactly matches the previously defined σ^S-recognition motif (Weber et al, 2005) with no mismatches in the -10 element and only two diverging residues at the -35 constituent (Fig. 2.2). Interestingly, this arrangement resembles those of the *micA* and *rybB* sRNA promoters both of which contain the σ^E-consensus sequence (Johansen et al, 2006; Papenfort et al, 2006; Thompson et al, 2007), and which have recently been ranked among the strongest σ^E-dependent promoters in *E. coli* and *Salmonella* (Mutalik et al, 2009). Albeit no global cross-comparisons with other σ^S-controlled promoters have been conducted yet, its close-to consensus sequence and the strong conservation in other enterobacteria suggest that the *sdsR* promoter might well show one of the strongest responses to σ^S.

An intriguing feature of sRNAs acting within σ factor-controlled networks is their ability to provide an immediate repressor function to the regulon. For MicA and RybB sRNAs, rapid accumulation of both sRNAs upon σ^E-activation and subsequent *omp* mRNA decay that operates within a time-frame of a few minutes has been proposed (Papenfort et al, 2010; Papenfort et al, 2006). The envelope stress response is dependent on the division of labour between the σ factor and the sRNAs to ensure full control of gene expression. As an activator of transcription, σ^E exploits the post-transcriptional repressors RybB and MicA to indirectly function as a negative regulator (Gogol et al, 2011). In fact, SdsR could take up a similar position in the σ^S-regulon. Like σ^E, σ^S can intrinsically only promote target gene expression, and could employ SdsR to facilitate decay of certain transcripts. Upon specific triggering of the σ^S-response SdsR may thus adjust the levels of OmpD and other putative target genes.

5.3.2 SdsR regulates expression of the major porin OmpD

The outer membrane constitutes the interface between the bacterial cell and its environment, and thus, integrity and functionality of the outer membrane play decisive roles for bacterial survival and growth (Bos et al, 2007). This generally impermeable barrier is equipped with a number of channel-forming porins to selectively allow the uptake of nutrients and to at the same time prevent unrestrained influx of molecules. *Salmonella* expresses four abundant porins - OmpC, OmpF, OmpD and OmpA - of which OmpD is the most abundant one (Santiviago et al, 2003). Conditions perturbing the proper folding and assembly of OMPs trigger the σ^E-controlled envelope stress response. However, not only external stimuli but also the overexpression of porins can activate the σ^E due to a saturation of the folding capacity of periplasmic chaperones

(Alba & Gross, 2004). Thus, the abundance of OMPs is subject to multiple layers of control, including post-transcriptional regulation by several sRNAs (Fig. 5.3).

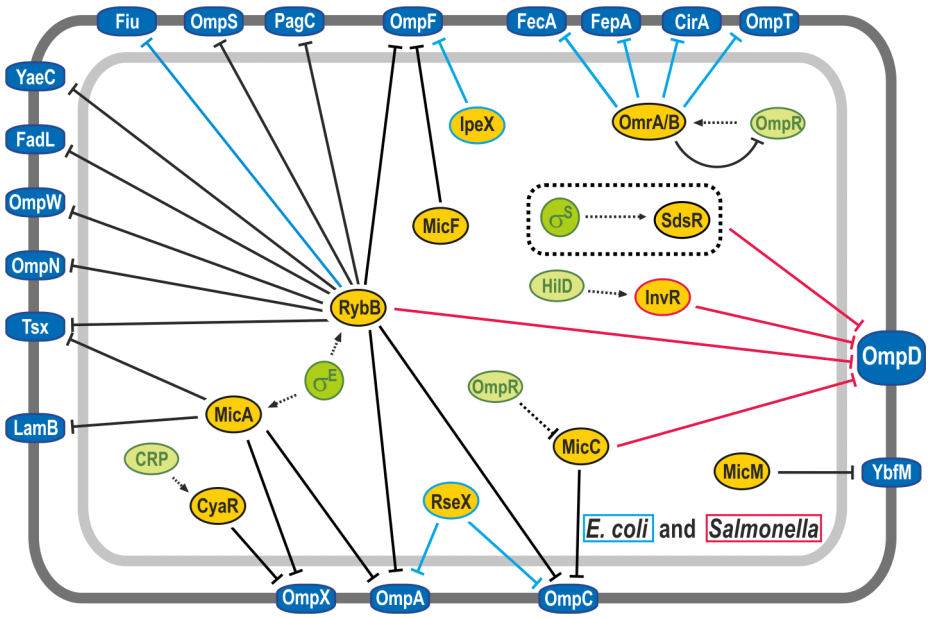

Figure 5.3 Network of Hfq-dependent sRNA regulating outer membrane protein synthesis.

Transcriptional regulators are represented as green, sRNAs as yellow and OMPs as dark blue circles, respectively. Black lines mark sRNAs and regulatory functions common to both species while light blue or red lines denote sRNAs or regulation specific to *E. coli* or *Salmonella*, respectively. Note that a gene similar to *ompD* is generally present in *E. coli* and referred to as *nmpC*. However, in many *E. coli* strains including strain K12—serving as reference here—the NmpC/OmpD porin is not expressed due to an insertion element; consequently the sRNA-mediated regulation of OmpD is marked as specific to *Salmonella*, although the *nmpC* mRNA was also shown to be a RybB target in *E. coli*.

MicF, the first of many examples of enterobacterial sRNAs repressing the translation of OMP-encoding transcripts (Vogel & Papenfort, 2006), was identified more than twenty years ago as a potent repressor of the *ompF* mRNA (Mizuno et al, 1984). Recent studies have identified additional conserved sRNAs targeting both single porins, *i.e.* InvR and CyaR (De Lay & Gottesman, 2009; Johansen et al, 2008; Papenfort et al, 2008; Pfeiffer et al, 2007) or multiple members of the class of OMPs, e.g RybB and OmrA/B (Fig. 5.2; (Papenfort & Vogel, 2009)). Conversely, not only a single riboregulator may control multiple porins, some messengers are also targeted by various sRNAs. Following the discovery of InvR (Pfeiffer et al, 2007), RybB (Papenfort et al, 2006) and MicC (Pfeiffer et al, 2009), SdsR constitutes the fourth sRNA to inhibit translation of the *ompD* mRNA. All four sRNAs accumulate under stationary phase

conditions and overlapping expression profiles might argue for redundancy in sRNA function and target mRNA control (Fig. 2.21 A). However, since RybB is induced in a σ^E-dependent manner upon envelope damage (Johansen et al, 2006; Papenfort et al, 2006; Thompson et al, 2007), and InvR is controlled by the dedicated virulence transcription factor, HilD (Pfeiffer et al, 2007), already two of these regulators have been assigned to distinct regulatory networks. The current study identified SdsR expression to be strictly governed by σ^S (Fig. 2.3 A), not only upon entry into late growth stages but also during heat and osmotic stress responses (Fig. 2.7). Moreover, non-redundant activity in the post-transcriptional regulation of *ompD* by both SdsR and RybB could be monitored during the stringent response or polymyxin-induced envelope stress, respectively (Fig. 2.22 and 2.23). Thus, it is likely that although redundancy of the four sRNAs during stationary phase might occur, each single regulator is required for *ompD* regulation under additional, distinct conditions.

It is currently not understood why certain mRNAs have acquired regulation through multiple sRNAs, while others display more confined restrictions to a single sRNA. The recent discovery of *csgD* mRNA being regulated by five individual sRNAs, i.e. GcvB, RprA, McaS and OmrA/B, provides another example of target regulation by multiple sRNAs (Holmqvist et al, 2010; Jorgensen et al, 2012; Mika et al, 2012; Thomason et al). Analogous to the regulation of *ompD* by SdsR, RybB, InvR and MicC, expression of all these sRNAs relies on specific input signals providing transcriptional activation. In this context, it remains to be investigated if the occurence of an initial sRNA-target mRNA pair promotes the evolution of multiple sRNA regulators targeting the same transcript and how Hfq-binding may facilitate this process.

5.3.3 Transcriptional control of RydC

While *cis*-encoded sRNAs often display almost constitutive expression (Waters & Storz, 2009), the majority of *trans*-encoded sRNAs in *E. coli* and *Salmonella* are subject to tight transcriptional regulation which restricts sRNA synthesis to distinct growth conditions. In line with the hypothesis that every transcriptional network contains at least one sRNA (Gottesman, 2005), numerous examples have been identified in the past including, for example, RyhB under direct control of the iron-responsive repressor Fur (Masse et al, 2005), MgrR as a member of the PhoP/Q regulon (Moon & Gottesman, 2009), and ArcZ and FnrS, which are regulated dependent on oxygen availability by the ArcA/B or Fnr systems, respectively (Boysen et al, 2010; Durand & Storz, 2010; Mandin & Gottesman, 2010).

RydC does not display differential expression under standard growth (Fig. 3.2), and was not induced under any of the stress conditions known to trigger expression of *cfa*, the target gene of RydC (Fig. 3.28). With regard to its cellular copy number of <10 copies on average, RydC can be considered as weakly expressed. In comparison, SdsR accumulates to more than 300

copies/cell during stationary phase, and oxidative stress was shown to induce expression of OxyS to ~3,000 molecules/cell (Fig, 2.1; (Altuvia et al, 1997)).

While the *rydC* promoter harboured a conserved -10 box, a conserved palindromic repeat reminiscent of a transcription factor recognition element seemed to replace the -35 element (Fig. 3.1). The motif at positions -31 to -15 relative to the transcriptional start site did not resemble any known transcription factor consensus sequence, and computational analyses suggested it to be exclusively present within the *rydC* promoter but not upstream of any other gene in *Salmonella* or *E. coli*.

Several factors might contribute to the weak expression of RydC under standard growth conditions. First, the *rydC* promoter may be transcriptionally repressed by a protein factor. Repressors are frequently employed by bacteria to shut down gene expression and only allow synthesis of their target genes in response to a certain environmental trigger. One example of an sRNA controlled by a transcriptional repressor is RyhB. Only when iron is scarce, the Fur repressor dissociates from the *ryhB* promoter. In turn, the sRNA is induced and reduces iron consumption by repressing transcripts which encode for iron-containing proteins (Masse & Gottesman, 2002; Masse et al, 2005).

Alternatively, detected RydC levels may represent the "basal level" of transcription from this promoter in the absence of a distinct transcriptional activator. Bacteria possess the genetic repertoire to adapt to a variety of environmental conditions. In *E. coli*, ~ 30 two-component systems and more than a hundred transcription factors have been identified (Clarke & Voigt, 2011; Madan Babu et al, 2006). Distinct regulons are selectively activated in the presence of the respective stimuli, and consequently numerous transcriptional regulators are not expressed under standard laboratory growth conditions. In *E. coli*, for example, expression of FnrS sRNA strictly depends on FNR, a transcriptional regulator which is exclusively present under anaerobic conditions (Boysen et al, 2010; Durand & Storz, 2010).

To identify a putative regulator of RydC, transcriptional fusions to the *lacZ* reporter were employed in screening both transposon insertion and plasmid overexpression libraries. Transcriptional *lacZ* fusions monitor only the synthesis rate from the upstream promoter, and this method had been successfully applied to identify the transcriptional regulation of sRNAs, e.g. CRP-mediated regulation of CyaR sRNA (Papenfort et al, 2008). Clones were selected in the presence of the chromogenic substance X-Gal, which is converted by the *lacZ* gene product to the insoluble dye indigo and acts as an indicator of *lacZ* levels and thus of promoter activity (Shuman & Silhavy, 2003). The wild-type *rydC'-lacZ*$^{+}$ fusion appeared pale blue on X-Gal plates, and thus the system was principally suitable to screen for both up- and down-regulation of fusion activity. Albeit different approaches aiming in both directions (*i.e.* to identify positive or negative regulation of the reporter fusion) have been pursued, no *bona-fide* transcriptional regulator of the *rydC* promoter has been identified, yet. Mild repression of RydC was detected in

the absence of PtsI, a sugar-unspecific factor of the PTS. The PTS is a bacterial transport system which facilitates concomitant transport and phosphorylation of carbohydrates, essentially sugars. In the cytosol, phosphoryl groups are relayed over the two general factors, EI and HPr, to a membrane-embedded EII complex which constitutes the sugar-specific transport component (Deutscher et al, 2006). Differential expression of RydC in the absence of PtsI might therefore hint at the requirement of a certain carbohydrate imported via the PTS to trigger transcription. In addition to their function in sugar transport, several components of the PTS have been shown to play a role in intracellular signal transduction. For example, unphosphorylated PtsI was reported to inhibit activation of the sensor kinase CheA of the bacterial chemotaxis machinery (Lux et al, 1995). Likewise, PtsI may function in an additional, yet unlinked signaling pathway involving the regulation RydC sRNA.

Failure to identify a transcriptional regulator by means of a reporter fusion might be due to various reasons. First, using transposon or plasmid overexpression libraries selects only cells which are viable under the given conditions, *i.e.* both disruption of essential genes as well as transformation of plasmids carrying genes which are toxic when overexpressed will not yield viable clones (Shuman & Silhavy, 2003). Second, both mentioned types of screens - transposon insertions and plasmid over-expression libraries - are only capable of monitoring the effect of single genes on the transcriptional output from the reporter fusion. In more detail, if the activity of a promoter is governed by redundant or cooperative factors, no phenotypic change will be observed in the screen. This intrinsic problem of the screen is not restricted to potential regulatory proteins. Likewise, an environmental co-factor, such as a metabolite, absent under the given conditions may be required for regulation. Also in this case, deregulation of a putative regulator would not result in an observable phenotype. An additional, rather technical explanation for the failure of the screen could be the design of the transcriptional fusion itself. The reporter gene *lacZ* was inserted downstream the *rydC* promoter, keeping the first five nucleotides of the sRNA intact. Potentially, a transcriptional regulator might require a broader stretch reaching further into the sRNA sequence for recognition and thus would not regulate the reporter fusion. To exclude this limitation, a future approach to identify a transcriptional regulator should be based on a redesigned, extended reporter fusion.

5.3.4 Physiological consequences of RydC-mediated *cfa* activation

The present study identified the sRNA RydC as a post-transcriptional regulator of *cfa* which encodes a cyclopropane fatty acid synthase. This enzyme functions in the post-synthetic modification of the bacterial phospholipid bilayer (Grogan & Cronan, 1984). Bacteria can adjust their membrane characteristics in order to adapt to environmental changes including differences in temperature, pH, and osmolarity as well as the presence of organic solvents or antimicrobial peptides. The composition of glycerolipids determines the viscosity of the

membrane and thus influences crucial functions including protein-protein interactions, passive permeability and active solute transport. For example, linear, straight-chain fatty acids can be tightly packed to form a bilayer with very low permeability, whereas *cis*-unsaturated fatty acids introduce central kinks that disrupt the order of the bilayer and thereby increase membrane fluidity (Zhang & Rock, 2008). In many bacteria, the double-bond of *cis*-unsaturated fatty acid side chains can be converted to a cyclopropane. The required methylation reaction is carried out by Cfa, which uses *S*-adenosylmethionine as a methyl donor (Grogan & Cronan, 1997). Intriguingly, albeit the biophysical properties of the resulting phospholipids are highly similar to those carrying unsaturated fatty acid side-chains, the biochemical properties readily change (Zhang & Rock, 2008). In comparison, cyclopropane fatty acids were found to be more stable, to show higher resistance towards acid stress and to decrease the influence of temperature on membrane fluidity (Chang & Cronan, 1999; Dufourc et al, 1984).

The cyclopropanation of fatty acids is irreversible, and their content within the various glycerolipids can only be diluted during cell division (Zhang & Rock, 2008). Thus, *cfa* expression is tightly regulated both at the transcriptional and at the post-transcriptional level. In *E. coli*, *Salmonella* and several related enterobacteria, transcription of the *cfa* mRNA is driven from two independent promoters (Kim et al, 2005; Wang & Cronan, 1994). A proximal site displays a consensus typical for σ^S. The alternative σ factors responsible for *cfa* expression during stationary phase and under various stress conditions including heat shock, osmotic stress, acidic pH and the stringent response upon amino acid starvation (Grogan & Cronan, 1997). The distal promoter elements located more than 200 bp upstream of the translational start site are recognized by RNAP in conjunction with the housekeeping σ factor σ^{70}, and active transcription occurs at all phases of growth (Cronan, 2002). The present study identified the sRNA RydC as an activator of the long version of the *cfa* transcript. A transcriptomic analysis employing *Salmonella*-specific microarrays revealed an increase of *cfa* mRNA in response to RydC pulse expression (Fig. 3.8 and Table 3.1). The specific effect of RydC on the longer of the two *cfa* transcripts was detected by primer extension experiments which allowed the detection of both mRNA fragments in the presence and absence of the sRNA. RydC specifically increased the levels of the long transcript, while having no effect on the mRNA transcribed from the proximal, RpoS-dependent promoter (Fig. 3.10). To verify that RydC operates at the post-transcriptional level, both mRNA versions were cloned as translational *cfa*::*gfp* fusions under the control of constitutive promoters. Again, RydC did not show any effect on expression of the shorter mRNA *cfaTSS2*::*gfp* fusion but increased GFP levels were expressed from *cfaTSS1*::*gfp* (Fig. 3.11 B). Intriguingly, basal expression differed ~ 10-fold between the two fusions, indicating that the long *cfa* 5' UTR harbours a repressor element which can be neutralized by RydC.

It is yet not clear under which conditions RydC facilitates Cfa expression, and how that relates to the physiological context of the cell. However, since no transcriptional regulator of

RydC expression could be identified yet (see chapter 5.3.3), it seems plausible that discovery of this factor will also provide information of the physiological requirement of RydC. In fact, sRNA-mediated regulation has been observed to require highly specific conditions as recently reported for interaction of MicM sRNA with the *chb* operon mRNA. Expression of *chb* is strictly limited to the uptake of chitosugars, and only under these conditions the interaction of *chb* with MicM will induce decay of the sRNA regulator (Figueroa-Bossi et al, 2009). Similarly, RydC expression could be limited to defined conditions which do not require or allow σ^S-mediated activation of the proximal *cfa* promoter.

The functional coupling between the sRNA and the *cfa* transcript as a target was confirmed when analyzing the conservation pattern of both RNAs in different species. In all enterobacteria carrying the *rydC* allele, the *cfa* gene was equipped with the described dual promoter arrangement (Fig. 3.12). Two of the investigated species, *Citrobacter rodentium* and *Enterobacter sp.* 638, show an equivalent organization of the *cfa* upstream region albeit *rydC* is absent from these organisms. For *C. rodentium*, the function of both promoter elements was observed in total transcriptome analyses employing a RNA sequencing approach which specifically enriches primary transcripts (Supplementary Fig. 4.4 E), and it can be anticipated that a copy of *rydC* may have recently been lost in the evolution of this organism. When compared to the closely related *C. koseri* strain which harbours a *rydC* allele, the region downstream of *cybB* - the gene flanking the sRNA at the 3' end – has been replaced in *C. rodentium*. The two versions of *Enterobacter sp.* 638 *cfa* were compared to the *Salmonella* orthologue using GFP reporter fusions; although expression was reduced ~ 3-fold when compared to the *Salmonella* constructs, RydC activated expression of the TSS1-*cfa(Ent)::gfp* fusion, but had no effect on the GFP levels expressed from the TSS1-*cfa(Ent)::gfp* construct (Fig. 3.12). The regulation of the *cfa* transcript from the upstream promoter site thus appeared conserved. By activating the *cfa* mRNA, the RydC sRNA might actively modify the glycerolipid composition of the bacterial membrane in various enterobacterial species. As the trigger for RydC expression has not been identified yet the exact environmental condition under which the sRNA induces *cfa* expression remains enigmatic.

5.4 The mechanisms employed by Hfq-dependent sRNAs

In the majority of cases post-transcriptional regulation by sRNAs is dependent on Hfq, a bacterial member of the Sm family of RNA binding proteins. Albeit no precise target sequence has been identified, the hexameric Hfq is considered to preferentially interact with unstructured A/U-rich sequence stretches in close proximity to hairpins (Valentin-Hansen et al, 2004). Hfq is conserved in ~50% of all bacterial species (Chao & Vogel, 2010), and numerous sRNAs in *E. coli*, *Salmonella* and other bacteria were identified by co-purification with the RNA chaperone

(Berghoff et al, 2011; Chao et al, 2012; Sittka et al, 2008; Sittka et al, 2009; Zhang et al, 2003). Also the two core sRNAs, SdsR and RydC, characterized in this study are among the most abundant RNAs recovered in Hfq pull-down experiments. The tight association with Hfq was found to stabilize sRNAs by preventing ribonucleolytic decay; consequently, the half-life of many sRNAs is markedly reduced in the absence of Hfq. In line with this observation, the stability of RydC was shown to depend on Hfq. While the half-life of the sRNA exceeded 32 min in wild-type cells, half of the cellular RydC pool was decayed within four minutes in an isogenic *hfq* mutant strain (Fig. 3.5 A/C).

Hfq not only stabilizes regulatory RNAs, it may also contribute as an important co-factor to the sRNA-mediated post-transcriptional control of gene expression. The chaperone activity of Hfq is considered to promote annealing between cognate sRNA-mRNA binding partners and to furthermore melt inhibitory secondary structures which occlude RNA pairing sites (Fender et al, 2010; Hopkins et al, 2011; Hwang et al, 2011; Maki et al, 2010). The requirement for Hfq in riboregulation was first reported in a study analyzing the role of OxyS RNA in the cellular response to oxidative stress (Zhang et al, 1998). Hfq is also obligatory for the repression of *ompD* by SdsR and the activation of *cfa* expression by RydC, the two sRNA/mRNA pairs identified in the present study. Apart from serving as a platform for base-pairing of sRNAs with their cognate target transcripts, Hfq can also actively be involved in the regulation of mRNAs. As an example, Spot42 binds upstream the translation initiation site in the 5' UTR of *sdhC*. Hfq, which is associated with the sRNA, is redirected to a binding site overlapping the SD and thus blocking 30S association (Desnoyers & Masse, 2012).

5.4.1 SdsR represses *ompD* by binding within the deep coding sequence

Most sRNAs repress their target genes. An effective way to inhibit gene expression is to prevent translation initiation and numerous sRNAs act by base-pairing to the RBS or proximal regions and thus block association of 30S ribosome subunits. In the absence of translating ribosomes, the mRNA is no longer protected from endoribonucleolytic attack and therefore rapidly degraded (Waters & Storz, 2009). In addition, sRNAs can also accelerate mRNA turnover by recruiting the RNA degradation machinery to the RNA duplex and thereby promote mRNA cleavage (Masse et al, 2003). Repression of translation initiation is restricted to the region of the mRNA which is commonly covered by initiating 30S ribosome subunits, *i.e.* a sequence stretch comprising approximately residues -35 to +19 relative to the translational start site (Bouvier et al, 2008; Hüttenhofer & Noller, 1994). Additionally, in *E. coli* and *Salmonella*, a number of sRNAs have been described which repress translation initiation by binding far upstream of the start codon and act by interfering with ribosome standby-sites, enhancer elements or the translation of a leader peptide (Darfeuille et al, 2007; Sharma et al, 2007; Vecerek et al, 2007). Contrary, the CDS in bacterial messengers was regarded refractory to efficient sRNA-targeting as the strong

helicase activity of the processing ribosome was considered to unwind sRNA-mRNA duplexes (Takyar et al, 2005). This view has recently been challenged by the discovery of MicC sRNA binding deep in the CDS of *ompD* downstream of positions relevant for translation initiation (Pfeiffer et al, 2009). In the current model, MicC-*ompD* duplex formation guides RNase E to a position downstream the interaction site and that this process is influenced by the nature of the MicC 5' end, *i.e.* stimulated in the presence of a 5' mono-phosphate (Bandyra et al, 2012). Regarding the SdsR-mediated repression, both the strict requirement of RNase E for regulation (Fig. 2.16) and the accumulation of *ompD* mRNA cleavage intermediates exhibiting 3' ends downstream the identified SdsR binding site (Fig. 2.18) support a mechanism analogous to MicC. In fact, the observation that MicC and SdsR both regulate *ompD* by a mechanism employing CDS targeting might argue that some mRNAs are more prone to alternative regulatory pathways than others. Intriguingly, all four sRNAs known to repress OmpD target the transcript within its CDS. Interestingly, an artificial sRNA targeting the *ompD* SD sequence was able to repress OmpD (Fig. 2.20 D). Thus, the previously assumed inaccessibility of the *ompD* translation initiation site could be excluded (Fröhlich et al, 2012). The observation that the decay of *ompD* mRNA upon heat-shock was higher in the absence of the four known post-transcriptional regulators SdsR, MicC, RybB and InvR sRNAs than in an *hfq* mutant strongly argues for the involvement of an additional sRNA in *ompD* expression (Fig. 2.17). The identity and putative interaction site of this regulator remain to be determined. Generally, CDS targeting might be more common than previously considered as other sRNA-target pairs such as ArcZ-*tpx* (Papenfort et al, 2009), RybB-*fadL* (Papenfort et al, 2010), SgrS-*manX* (Rice & Vanderpool, 2011) and MicF-*lpxR* (Corcoran et al, 2012) pair at positions predicting a regulatory mechanism independent of translation initiation as well. The mode of target repression, *i.e.* inhibition of 30S ribosome association *vs.* codon sequence targeting, is dictated by the binding site within the mRNA rather than the sRNA. Indeed, most known CDS-targeting sRNAs regulate additional targets by interference with 30S association (Chen et al, 2004; Papenfort et al, 2010; Papenfort & Vogel, 2009; Pfeiffer et al, 2009). In addition, the recent discovery of RyhB inhibiting *sodB* translation initiation, followed by distal CDS cleavage might account for a mixed mode of regulation implying translational control followed by ribonuclease recruitment (Prevost et al, 2011). Future studies will be required to determine the denominators of CDS targeting. Hfq, RNase E (and the degradosome) as well as intrinsic elements such as codon composition of the mRNA are likely to constitute key factors of this process.

5.4.2 RydC activates *cfa* mRNA

In *Salmonella* and numerous other enterobacterial species, the *cfa* gene is under the control of two distinct promoters (Fig. 3.10 A). Expression of *cfa* from the distal promoter site only results in basal levels of the Cfa protein unless activated by RydC. In contrast, expression of the shorter, RpoS-transcribed messenger is not altered in the presence or absence of the sRNA (Fig. 3.11 B).

Several examples of sRNA-mediated activation of a transcript have been described in bacteria, and probably the most intensively studied case is the *rpoS* gene itself which is under extensive post-transcriptional control. The 5' UTR of *rpoS* mRNA is sequestered in a stable hair-pin structure which covers the RBS and thereby prevents translation initiation. Base-pairing within the upstream leader to the 'anti-Shine Dalgarno sequence', by any of the three sRNAs DsrA, RprA and ArcZ can alleviate the self-inhibitory structure of the *rpoS* mRNA and stimulate translation (Majdalani et al, 2001; Majdalani et al, 1998; Mandin & Gottesman, 2010). This interference with the *cis*-regulatory 5' UTR element is commonly referred to as the anti-antisense mechanism for target gene activation and was repeatedly observed for various examples including the activation of *hla* mRNA by RNAIII in *S. aureus* or of *glmS* mRNA by GlmZ sRNA in *E. coli* (Kalamorz et al, 2007; Morfeldt et al, 1995; Urban & Vogel, 2008).

To determine if regulation of *cfa* expression by RydC occured via the anti-antisense mechanism, the mRNA's 5' UTR was inspected with regard to a potential secondary structure covering the translation initiation site, but no such element could be predicted. Moreover, the *cfa* leader appeared to harbour a repressory sequence element which functioned independent of the sequence of the translation initiation region. A chimeric mRNA in which the 5' end of the *cfa* transcript including the sRNA binding site fused to the unrelated *ompX* mRNA displayed similar dependence on RydC for efficient expression as did the native construct (Fig. 3.17 B and 3.18 B). Since both *cfa* as well as *ompX* mRNAs revealed no significant sequence similarities within their ribosome binding sites (Supplementary Fig. 4.9), the observed regulation appeared to be independent of an inhibitory fold involving the translation initiation region. Thus, the classical anti-antisense mechanism does not seem to apply for the regulation of *cfa* by RydC.

Several alternative mechanisms, namely the interference of RydC with a transcriptional attenuator within the *cfa* 5' UTR, the expression of a leader peptide, an upstream ribosome binding site as well as the RNase E-mediated decay of *cfa* mRNA will be discussed below.

The activating effect of RydC on *cfa* expression was monitored when both RNA interaction partners were under the control of constitutive promoters, and thus the regulation occurred downstream of transcription initiation. However, the *cfa* 5' UTR might still harbour a transcriptional attenuator similar to *cis*-regulatory sequence elements commonly observed in certain types of riboswitches. Attenuator sequences are able to fold into two alternative secondary structures which either facilitate or hamper transcription elongation. Within riboswitches, association of a small molecule to the aptamer domain promotes the formation of

one of the two RNA structures (Grundy & Henkin, 2004). Similarly, interaction with a regulatory RNA could lock the mRNA in a conformation which favours or blocks transcription elongation. An sRNA-sensing aptamer has not been reported yet, however, in many Gram-positive bacteria, regulation of aminoacyl-tRNA synthetases is under the control of so-called T-box riboswitches. In this system the leader region directly binds uncharged t-RNAs which induce a structural rearrangement that disintegrates a transcriptional terminator and allows synthesis of the mRNA (Green et al, 2010). Thus, an RNA-controlled attenuator is in principle to be taken into consideration for the regulation of *cfa* expression by RydC sRNA. Such regulation would however implicate significant reorganization of the secondary structure within the *cfa* leader region upon sRNA base-pairing. Although specific binding of RydC to the *cfa* transcript was observed in chemical probing (Fig. 3.14), this interaction did not cause major differences in the folding of the mRNA. Thus, also not to be completely excluded, a mechanism of *cfa* regulation by RydC is unlikely based on the control of a transcriptional attenuator. Nevertheless, one experimental set-up to test the potential influence of RydC sRNA on *cfa* would be *in vitro* transcription assays which have successfully been employed to identify attenuation sites (Yakhnin & Babitzke, 2002; Zhang & Switzer, 2003).

Instead of promoting transcription, RydC could also influence *cfa* translation. In general, translation is initiated by sequence-specific anchoring of 30S ribosomes at the RBS. If bacterial genes are organized in polycistronic transcriptional units, translation of the consecutive genes within the operon can be coupled to promote expression of downstream cistrons (Oppenheim & Yanofsky, 1980; Schümperli et al, 1982). On the one hand, this coupling increases the local concentration of ribosomes upstream the translational start site and in addition, the helicase activity of translating ribosomes may relieve a potential sequestration of translational start sites (Jacques & Dreyfus, 1990; Unoson & Wagner, 2007). Similar to upstream genes within a polycistronic message, also leader peptides which denote short, upstream ORFs within 5' UTRs can stimulate translation initiation. Interference with the translation of the upstream ORF marks another mechanistic principle by which sRNAs can govern target gene expression. Both RyhB and GcvB repress the synthesis of two leader peptides encoded upstream of *fur* and *thrABC*, respectively, and a recent study suggested activation of leader peptide translation by a regulatory RNA in *Pseudomonas*. PhrS sRNA induces a structural rearrangement within the upstream ORF of *pqsR* encoding one of the major quorum sensing regulators in *P. aeruginosa*. As a consequence, synthesis of both the leader peptide as well as translationally-coupled PqsR is induced. Although the *cfa* 5' UTR harbours several highly conserved sequence stretches, and alternative translation initiation codons (TTG, GTG) were taken into account, no conserved ORF could be predicted within these elements. Thus, the involvement of a *cfa* leader peptide was not considered as a potential regulation mechanism.

Apart from leader peptides, additional elements within the 5' UTR could contribute to the observed regulation of *cfa* expression by RydC. Interestingly, although masking of the translation initiation site in *cfa-X::gfp* fusions was excluded, toeprint formation for the native *ompX* fusion was much more prominent than for the chimeric version carrying the *cfa* 5' UTR (Fig. 3.18). Although these two RNAs may have very different biochemical properties, the reduction in 30S association at the RBS could be due to scavenging of the ribosomal subunits by the 5' UTR. In *E. coli*, the sRNA IstR-1 has been shown to interfere with translation of *tisB* mRNA by blocking a ribosome standby site within the 5' UTR of the transcript (Darfeuille et al, 2007). Ribosome standby sites are regulatory elements which serve to increase the local pool of 30S subunits in proximity to translational start sites and thus to promote initiation of protein synthesis (Unoson & Wagner, 2007). By contrast, a sequence stretch within the *cfa* 5' UTR might exhibit high affinity for ribosomes and snatch them away from the translation initiation site. In this scenario, RydC in conjunction with Hfq could mask such 'alternative ribosome binding site' and thus promote association of 30S subunits at the *cfa* start codon. This mechanism is highly speculative: For example, how would such scavenging site prevent dislocation of ribosomes to the translational start site? Future experiments using footprinting assays might help localize a putative binding site for ribosomes within the 5' UTR and thus provide evidence arguing either in favour or against the mechanism.

A recent publication has suggested yet another mechanism of gene expression activation. In *S. pyogenes*, FasX interferes with nucleolytic decay of *ska* mRNA to stabilize the transcript. Similarly, RydC could be shown to increase the stability of *cfa* mRNA (Fig. 3.20), and to mask an internal RNase E cleavage site (Fig. 3.22). In bacteria, mRNA degradation is initiated by endoribonucleases to produce fragments which are then degraded by 3' to 5' exonucleases (Carpousis, 2007). The major endoribonuclease, RNase E, can initiate cleavage of a transcript either via the 5' end or by internal entry (Baker & Mackie, 2003; McDowall et al, 1994). Following an initial cut, RNase E is considered to elicit a 5' to 3' wave of cleavages and thus to rapidly fragment the transcript (Goodrich & Steege, 1999; Mackie, 1998). Inhibition of such processive degradation by masking a consecutive cleavage site can impede RNA decay and contribute to stability of the transcript. The cleavage within the *cfa* 5' UTR by RNase E can be reconstituted *in vitro*, and while pairing of RydC prevents the specific cut within a *cfa* site dedicated to bind the sRNA, stabilization of the mRNA is mediated by Hfq (Fig. 3.24 and 3.25). Thus, a plausible explanation for the mechanism employed by RydC is that the sRNA prevents rapid decay of the transcript by masking an RNase E site, and that the concomitant recruitment of the RNA binding protein Hfq accounts for the stabilization of the mRNA, and thus increases its expression.

5.5 Identification of sRNA binding sites

The identification of mRNA targets is the critical bottleneck in establishing a functional role for base-pairing sRNAs. Within sRNAs, highly conserved seed regions have repeatedly been found located in well-accessible regions including single-stranded stretches or hairpin loops (Beisel et al, 2012; Peer & Margalit, 2011) and in many cases - including RydC - seed sequences are positioned at the very 5' end of sRNAs. Other sRNAs such as GcvB, FnrS and also SdsR appear to contain several, internal base-pairing regions (Fig. 2.19; (Boysen et al, 2010; Durand & Storz, 2010; Sharma et al, 2011).

A variety of computational tools have been developed on the basis of known characteristics of sRNA/mRNA interactions to predict potential target sites (Backofen & Hess, 2010). Although these algorithms are in principle capable of sRNA target identification, the high number of false-positive predictions requires experimental validations. Different wet-lab approaches were chosen to validate the binding sites of the two sRNAs RydC and SdsR in this study.

5.5.1 RydC interacts with a conserved sequence stretch within the *cfa* 5' UTR

The activating effect of RydC was restricted to the mRNA version of *cfa* originating from the distal promoter site (Fig. 3.11). To identify a potential base-pairing interaction with the sRNA, *in vitro* synthesized and 5' end-labelled *cfa* mRNA was subjected to chemical probing in the presence or absence of RydC and Hfq, respectively. Structure probing has been proven a powerful tool to map sRNA-mRNA interaction sites like for example MicF/*ompF* mRNA or GcvB-*oppA* mRNA (Andersen & Delihas, 1990; Sharma et al, 2007). In addition, the method is advantageous if the region of potential pairing is long (as is the case for *cfa* mRNA), and thus less amenable to computational predictions. In addition, probing the structure of the mRNA prior to and after being bound by the regulatory RNA may reveal putative structural rearrangements.

A single, highly conserved stretch within nt -99 to -109 relative to the translational start site in *cfa* was protected from cleavage in the presence of Hfq and RydC (Fig. 3.15). This site displayed perfect complementarity to the very 5' end of the sRNA, and direct basepairing was further validated *in vivo* by compensatory nucleotide-exchanges in RydC and *cfa* mRNA (Fig. 3.13). Since no additional changes in the mRNA cleavage pattern were observed upon RydC binding, the sRNA did not induce restructuring of the *cfa* 5' UTR.

5.5.2 A 3'RACE approach to identify the SdsR binding site on *ompD* mRNA

In contrast to sRNA seed regions, much less information is available on characteristics associated with binding sites on mRNAs. As sRNAs recognize their targets typically via short stretches of Watson-Crick interactions which happen to be interspersed with non-Watson-Crick

base-pairs or mismatches, reliable predictions of binding sites are rare. The quality of these computational approaches can however be strongly increased by narrowing down the putative regions involved in the interaction. Experimental approaches to approximate target sites include the employment of truncation mutants and, as in the present study, a novel 3'RACE-based strategy.

The current work identified SdsR as the fourth sRNA to post-transcriptionally control the expression of the major *Salmonella* porin OmpD. Studying the regulation of a series of translational *gfp* fusions comprising the 5' UTR and an increasing number of nucleotides of the *ompD* CDS in the presence of SdsR revealed that the sRNA recognizes the *ompD* mRNA downstream of the 15th codon (Fig. 2.15). A recent study uncovered that MicC facilitates *ompD* mRNA degradation by recruitment of RNase E which results in cleavage of the transcript 4-5 nucleotides downstream of the interaction site (Pfeiffer et al, 2009). Also SdsR requires RNase E to down-regulate *ompD* expression (Fig. 2.16) and was thus proposed to function by a mechanism analogous to MicC. Break-down products of *ompD* mRNA accumulating upon SdsR pulse-induction were mapped by 3'RACE (Fig. 2.18 B). Sequence analyses of enriched fragments revealed *ompD* 3' ends mapping to various nucleotides between +55 to +65 of the CDS (Fig. 2.18 B). Querying the region upstream the observed cleavage site for a potential binding site of SdsR involving the sRNA regions identified by genetic analysis to be essential for regulation (Fig. 2.13), resulted in the prediction of the *bona-fide* SdsR-*ompD* interaction site (Fig. 2.19 A). The anticipated duplex forming between residues 14 to 31 of SdsR and nucleotides +39 to +51 within the *ompD* CDS was verified by compensatory base-pair exchanges (Fig. 2.19 B). In contrast to the four nucleotides distance observed between the MicC-*ompD* interaction sequence and 3' ends of enriched break-down products (Pfeiffer et al, 2009), positions of *ompD* 3' ends enriched upon SdsR pulse-expression mapped mostly to a site eight nucleotides downstream SdsR interaction site (Fig. 2.18 B). Albeit these observed differences in spacing between sRNA binding region and RNase E cleavage site, the employed 3'RACE-based method has proven useful to narrow down sRNA-mRNA interaction sites located in the deep CDS. Importantly, the approach has been also been applied for the prediction of additional sRNA binding regions including the RybB interaction site on *fadL* mRNA (V. Pfeiffer, unpublished results) and the MicF binding site on *lpxR* mRNA (Corcoran et al, 2012). Thus, the experimental approach promises to be useful for the identification of further sRNA-mRNA interactions in bacteria.

5.6 Conclusions and perspective

The present study aimed to characterize the two Hfq-associated sRNAs SdsR and RydC in *Salmonella*. Due to their high degree of conservation in various additional enterobacterial species both regulators are considered to be integrated in central cellular pathways.

SdsR was shown to be under direct transcriptional control of the alternative σ factor σ^S. In *Salmonella*, overexpression of SdsR down-regulates the abundant porin OmpD, however this target displays by far less conservation in other species than its cognate regulatory RNA. It is thus likely that SdsR governs a much larger post-transcriptional regulon of additional target genes. Two other sRNAs, RybB and MicA, have recently been shown to constitute the repressor arm of the σ^E-dependent envelope stress response. Likewise, σ^S - which is intrinsically restricted to activate gene expression - could employ SdsR to rapidly shut down expression of transcripts under distinct conditions. The engagement of regulatory RNAs in networks to control gene expression is accompanied by various advantages: First, the synthesis of sRNAs is produces less metabolic costs than a protein factor. By the same token, the faster synthesis and the fact that sRNAs act on existing mRNA pools contribute to a potentially accelerated impact on target gene expression. One central question remaining is thus how SdsR might be integrated in one or several regulatory circuits within the σ^S stress response.

SdsR regulates OmpD expression by a mechanism deviating from the canonical pathway employed by repressor sRNAs. In the majority of cases regulatory RNAs inhibit initiation of translation by blocking ribosome entry. In contrast, SdsR pairs *ompD* mRNA far downstream the translational start site and most likely recruits the endoribonuclease, RNase E, to induce target decay. As the coding sequence of target mRNAs has mostly been neglected in searches for sRNA binding sites it remains to be established whether this alternative mechanism proves to be more common.

RydC, the second sRNA characterized in this study was identified as a highly stable molecule due to a compact, pseudoknotted structure and the association with Hfq. To promote expression of the membrane-modifying enzyme, Cfa, RydC employs a conserved, single-stranded stretch at the 5' end and binds the longer of two distinct *cfa* transcripts. The exact way of target gene activation is still to be investigated but the present data suggests that RydC uses a novel mechanism which involves masking of an internal cleavage site for the endoribonuclease RNase E, and the recruitment of the RNA chaperone Hfq as a stabilizing factor to the mRNA.

In summary, both analyzed sRNAs, SdsR and RydC, act as post-transcriptional regulators employing two distinct, uncommon mechanisms. Future studies will have to prove to what extent the observed types of regulation are employed also in additional sRNA-mRNA pairs, or whether they mark a rare observation.

6 Material and Methods

6.1 General equipment

Table 6.1 Equipment and instruments.

Equipment and Instruments	Manufacturer
centrifuge Eppendorf 5415R	Eppendorf
centrifuge Eppendorf 5424	Eppendorf
centrifuge Eppendorf 5810R	Eppendorf
CFX96 RealTime System	Bio-Rad
electroporator MicroPulser	Bio-Rad
eraser for imaging plates FLA	GE Healthcare
gel documentation system Gel iX Imager	Intas
gel dryer Bio-Rad Model 583	Bio-Rad
heating block Eppendorf comfort	Eppendorf
horizontal electrophoresis systems PerfectBlue Mini S, M, L	Peqlab
hybridization oven UVP HB-1000	Thermo Fisher Scientific
imaging plates BAS-IP MS 2325, 2340	Fujifilm
imaging plates cassettes BAS 2325, 2340	Fujifilm
imaging System Image Quant LAS 4000	GE Healthcare
incubator Innovens 55 EB1	Thermo Fisher Scientific
phosphorimager Typhoon FLA 7000	GE Healthcare
photometer Ultrospec 10 Cell Density Meter	GE Healthcare
Pipetman P10, P20, P200, P1000, P5000	Gilson
power supplies peqPOWER E250, E300	Peqlab
qRT PCR machine 7900HT	Applied Biosystems
semi-dry electroblotter PerfectBlue SEDEC M	Peqlab
shaking incubator Innova 40	New Brunswick Scientific
shaking incubator Innova 40R	New Brunswick Scientific
shaking incubator Innova 44	New Brunswick Scientific
shaking water-bath incubator GFL 1092	GFL
spectrophotometer NanoDrop 2000	Peqlab
tank electroblotter PerfectBlue Web S, M	Peqlab
thermal cycler MJ Mini	Bio-Rad
vertical electrophoresis systems PerfectBlue Twin S, ExW S, L	Peqlab
vertical Sequencing gel system CBS SG-400-20	C.B.S. Scientific
Victor3 1420 multilabel counter	Perkin-Elmer
Vortex-Genie 2	Scientific Industries

6.2 Consumables

Table 6.2 Consumables.

Consumables	Manufacturer
G-25, G-50 MicroSpin columns	GE Healthcare
Hybond-XL membrane for nucleic acid transfer	GE Healthcare
inoculation loops 10 µl	VWR
L-shape bacteriology loops	VWR
microtiter plates (96-well)	Nunc
PCR tubes 0.2 ml	Thermo
Phase Lock Gel tubes 2 ml	5 Prime
pipette tips	Sarstedt
PolyScreen PVDF Transfer Membrane	PerkinElmer
reagent and centrifuge tubes 15, 50 ml	Sarstedt
safe-lock tubes 1.5 ml, 2.0 ml	Eppendorf
spectrophotometer cuvettes	Sarstedt
sterile fiters (0.25 µm pore size)	Whatman
conjugation filters (0.45 µm pore size)	Whatman
electroporation cuvettes (2 mm gap width)	Cell projects
SALSA microarrays	IFR, Norwich, UK
Agilent AMADID microarrays (Designcode: 026881)	Agilent Technologies

6.3 Chemicals and commercially available systems

Table 6.3 Chemicals and commercially available systems.

Chemicals and commercially available systems	Manufacturer
AffinityScript multi-temperature reverse transcriptase	Stratagene
albumin Fraktion V	Roth
ampicillin sodium salt	Roth
BioPrime DNA Labeling System	Bioprime
chloramphenicol	Roth
Cy3-dCTP	GE Healthcare
Cy5-dCTP	GE Healthcare
D(+)-Glucose	Merck
Difco Agar	BD
dimethyl sulfoxide (DMSO)	Roth
DL-serine hydroxamate (SHX)	Sigma
EDTA	Roth
EGTA	Roth
ethanol	Roth
ethanol (absolute for analysis)	Merck

formamide (99.5%)	Roth
glycerol (99%)	Sigma
glycine	Roth
GlycoBlue	Ambion
H_2O_2 30%	AppliChem
isopropanol	Roth
kanamycin sulfate	Roth
L(+)-Arabinose	Roth
lead acetate	Roth
luminol	Sigma-Aldrich
Masterpure DNA purification kit	Epicentre
MAXIScript T7 *in vitro* transcription kit	Ambion
MEGAScript T7 *in vitro* transcription kit	Ambion
methanol	Roth
milk powder (blotting grade)	Roth
MinElute PCR purification kit	Qiagen
NucleoSpin Plasmid Quick Pure Kit	Macherey-Nagel
Nutrient broth Difco	BD
o-Nitrophenyl β-D-galactopyranoside (ONPG)	AppliChem
cas-amino acids Difco	BD
p-Coumaric acid	Sigma
PAGE Blue staining solution	Fermentas
phenol	Roth
polymyxin B	Sigma
Precipitation/Inactivation buffer	Ambion
QIAquick Gel Extraction Kit	Qiagen
QIAquick PCR Purification kit	Qiagen
random hexamers	Invitrogen
random primer/reaction buffer mix	BioPrime
RedSafe	ChemBio
rifampicin	Fluka
Roti-Aqua-P/C/I	Roth
Roti-Hybri-Quick	Roth
Rotiphorese gel 40 (19:1)	Roth
Rotiphorese gel 40 (37.5:1)	Roth
Sequi Therm EXCELII DNA Sequencing Kit	Epicentre
StainsAll	Sigma
SUPERscriptII reverse transcription kit	Invitrogen
SUPERscriptIII reverse transcription kit	Invitrogen
SV40 Total RNA Isolation kit	Promega

SYBR Gold Nucleic Acid Gel Stain	Invitrogen
SYBR Green Mix	Qiagen
tetracycline	Roth
TOPO TA Cloning Kit	Invitrogen
Transposome kit EZ-Tn5 <DHFR-1>	Epicentre
Triton-X100	Sigma
TRIzol Reagent	Invitrogen
$tRNA^{fMet}$	Sigma
yeast RNA	Ambion
γ-^{32}P-ATP (222TBq (6000Ci)/mmol 370MBq (10mCi)/ml)	Hartmann Analytic
γ-^{32}P-UTP (29,6TBq (800Ci)/mmol 740MBq (20mCi)/ml)	Hartmann Analytic

Additional chemicals were purchased from Sigma, Roth and Merck.

6.4 Enzymes and size markers

Table 6.4 Enzymes and size markers.

Enzymes*	**Manufacturer**
calf intestinal phosphatase (CIP)	NEB
DNase I	Fermentas
Klenow enzyme	BioPrime
polynucleotide kinase (PNK)	Fermentas
Phusion High-Fidelity DNA polymerase	Fermentas
RNase H	NEB
SUPERaseIn RNase Inhibitor	Ambion
RNase T1	Ambion
T4 DNA ligase	Fermentas
Taq polymerase	NEB
lysozyme	Roth
shrimp alkaline phosphatase (SAP)	Fermentas
terminator exonuclease (TEX)	Epicentre
tobacco acid pyrophosphatase (TAP)	Epicentre
T4 RNA ligase	Fermentas
Size markers	**Manufacturer**
pUC Mix Marker 8	Fermentas
Gene Ruler 1kB Plus	Fermentas
RNA ladder High Range	Fermentas
RNA ladder Low Range	Fermentas
prestained protein marker	Fermentas

*All restriction enzymes were purchased from NEB.

6.5 Purified proteins and antibodies

Table 6.5 Purified proteins/ribosomes.

Purified protein	storage	provided by
E. coli Hfq	Hfq dilution buffer	K. Bandyra (Cambridge University)
E. coli RNase E N-terminal domain (NTD)	RNase E buffer	K. Bandyra (Cambridge University)
30S ribosomal subunit	Tico Buffer	K. Nierhaus (MPI for Molecular Genetics, Berlin)

Table 6.6 Antibodies.

Antibody/antisera	origin	source	working dilution
anti-RpoS	mouse	Neoclone	1:1,000
anti-GFP	mouse	Roche	1:3,000
anti-FLAG M2	mouse	Sigma	1:1,000
anti-OMP	rabbit	R. Misra (Tempe)	1:10,000
anti-S1	rabbit	M. Springer (Paris)	1:1,000
anti-GroEL	rabbit	Sigma	1:10,000
anti-mouse; HRP-conjugated	donkey	GE Healthcare	1:10,000
anti-rabbit; HRP-conjugated	goat	GE Healthcare	1:10,000

6.6 Synthetic oligonucleotides

Table 6.7 Synthetic oligonucleotides.

name	sequence 5'-3'
JVO-0048	TTTCGAGGAATTTCGAGGGGAAACACATAACCCATTGATTTATAATCTAAGTGTAGGCTGGAGCTGCTTC
JVO-0049	TTTTATCTCTGATAACAGACAAAACGCCAGGTTTTTTCAATCACCTTCGTGGTCCATATGAATATCCTCCTTAG
JVO-0051	GTTTTTCTCGAGCATCCGGATGGATTGACA
JVO-0052	GTTTTTTCTAGAGTCTGGCRCCGTTTAT
JVO-0176	GTTTTTCTCGAGCTAACAACGTCAACACC
JVO-0216	GACTGGCTTTCTACGTGTTC
JVO-0222	GATAAATGCAACGTAAGAGACAAATG
JVO-0322	CTACGGCGTTTCACTTCTGAGTTC
JVO-0358	GTTTTTTGCTAGCAAACAGATGCTCAAGC
JVO-0374	GGCAAACAAGGCATCTATCAGAGGGGATGGCGTATTCCATGGTCCATATGAATATCCTCCTTAG
JVO-0375	GTTTTTCTCGAGCAGCGTGTTGGACGAA
JVO-0376	GTTTTTTCTAGAGGATGATGCCGCGTA
JVO-0396	TTCATCGCTGAAAACAGG
JVO-0802	GTTTTGACGTCAAATCAATATTGAAACGG
JVO-0862	GTTTTTCTCGAGTCGACCCGCTGTACCT
JVO-0874	CCTGGCTTTCAGTACGGT
JVO-0902	5'Phosphate-GCAAGGCGATTTAGCC
JVO-0903	TTTTTCTAGAAACACATAACCCATTGATT
JVO-0905	5'Phosphate-GTTATATGCCTTTATTGTCACAT
JVO-0925	GTGACGCAGGCGAAG
JVO-0975	5'Phosphate-GCTTCCGATGTAGACCC
JVO-0986	GTTTTTTTTTTAATACGACTCACTATAGGGAGGCGTTCGGGCTTGTCA
JVO-0991	GACAGGGAGTCGTACAACG
JVO-0997	GTTTTTTTTAATACGACTCACTATAGGCCTGTATTCGGTCCAGG
JVO-1009	GTTTACCGTGCGCGATATCTCCGAACTGGTGCGTCAGGGACAGGATCGTGTAGGCTGGAGCTGCTTC
JVO-1010	CGCGCGCCTTTCGTGCCGAGCGGATCTTTCACTACCTGCACCATCAGGTCCATATGAATATCCTCCTTAG

JVO-1032	GGCTCTTGGGAGAGAGC
JVO-1043	GTTTTTTCTCGAGCACATAATCTTAACAAGAATGTT
JVO-1205	GTTGATGGGCTCCACAA
JVO-1472	GAATCGTCTCTGTCGGCATGT
JVO-1473	CAGGAAAAGACCATCCGGTTT
JVO-1977	AGTACGGCCGCAAGGTTAAAA
JVO-1978	GTTCTTCGCGTTGCATCGA
JVO-2192	GTCACCATCACTTCCGTTATCA
JVO-2223	GAAACTTATTATTGAACTTATGCCACTCCGTCATTTAAAAATAGTCCAAGCGAGCTCGATATCAAA
JVO-2309	GCACAGGTTCAAGCCG
JVO-2390	CTGGCGTCGTCATCTA
JVO-2475	GTTTTTGTTGTGATGTAGGCAT
JVO-2484	ATGAAACTTAAGTTAGTGGCAG
JVO-2678	GTTTTATGCATGCCATTGACAAACGCC
JVO-3493	GTACTTCAGCGGTATCAATATC
JVO-3540	AAATCATTTAGGATTTGCTATCTTAACTGCGTGCGGCCTGGTGTAGGCTGGAGCTGCTTC
JVO-3541	CACGATGTCGCGGTGCTGAAAGCCTGGGTGGCAAACGCGGGGTCCATATGAATATCCTCCTTAG
JVO-3622	GTTTTTTGACGTCGCGTTGTGGTCTTTTCCAT
JVO-3707	GGCCATCCATGGTGAATCG
JVO-3986	ACGCTAAACCGGAGGCGTAGCGCCTCCGGTGAAAGCACCCCATATGAATATCCTCCTTAG
JVO-4055	GTTTTTATGCATGGTTGTTTATATTACGATAATTATTAG
JVO-4056	GTTTTTATGCATAAGGTTCTGATCACCGTCC
JVO-4057	GTTTTTGCTAGCGTTATCATCCGGTACGCTG
JVO-4186	GCGGCGTTGAAAACGGACTGCGCGTTCCTCGCGACTACAAAGACCATGACGG
JVO-4187	CGGAAAATAAGATTCCCCCGCATGAAATGCGGCCATATGAATATCCTCCTTAG
JVO-4188	AGCTATTATCTCAACGCCTG
JVO-4189	TGAGCGTGTGAATATCGAG
JVO-4262	5'Phosphate-TCATGTATTCTTAAAGGGCAAG
JVO-4263	5'Phosphate-TCATATATTCTTAAAGGGCAAG
JVO-4264	5'Phosphate-TCATTTATTCTTAAAGGGCAAG
JVO-4265	CGACGCCAGGTTTTCC
JVO-4314	TGCCACTAACTTAAGTTTCAT
JVO-4363	AGAAAACGCCTGCGTC
JVO-4364	ACCAGTTATCATCCGGTACG
JVO-4378	GTTTTTTTTTTAATACGACTCACTATAGGGAGGTAACCAGGACCCGTGACG
JVO-4420	CTTCCGATGTAGATCATCCCTGTTTTCAGCG
JVO-4433	TATTTTATTTGTCATACAAATAAGTATAATACCCGCTTCCGTGTAGGCTGGAGCTGCTTC
JVO-4531	5'Phosphate-GGAGAAACAGTAGAGAGTTGC
JVO-4532	TTCCGATGTAGACCCGTC
JVO-4536	5'Phosphate-ACCGCTCCTGGTTAGACG
JVO-4537	GACGCAGGCGAAGGAG
JVO-4558	GTTTTTTTTAATACGACTCACTATAGGTTGTTTATATTACGATAATT
JVO-4573	GTTTTTATGCATAAATGCGCGTCTTTCATAT
JVO-4721	GTTTTTTTTTTTAATACGACTCACTATAGGTTCCGATGTAGACCCGTCC
JVO-4722	AGAAAACGCCTGCGTCTAAC
JVO-4731	5'Phosphate-ACTTTTAGCGCACGGCTC
JVO-4828	TTAGCGAGGAACGCGCAGTCCGTTTTCAACGCCGCGCGTAGGTCCATATGAATATCCTCCTTAG
JVO-4956	CGCGCCAGTATTCTCATCTATACATAATGAGGGTCGATATGTGTAGGCTGGAGCTGCTTC
JVO-5081	5'Phosphate-CTCCTTCGCCTGCGTC
JVO-5082	GACCGCTCTACATCGGAA
JVO-5165	GTTTTTTTTTTAATACGACTCACTATAGGTTCCGATGTAGAGCGGTCC
JVO-5236	TACCGAGCTCGAATTCATCG
JVO-5237	TGCAGGCATGCAAGCTTCA
JVO-5738	CGGCGCTAATAGCGACGGGCGGGCCGATATTGATATTAAACTTACTGTCCCTAGTGCTTGG
JVO-5739	TAAAATGGCTCTGTCCGCAAAGACAACGACCAGTGAACGTCTGCACGGCATACTCCTTAT
JVO-5773	CGGTTGTTTATATTACGATAATTATTAGGCATTAACGGGAGTGTAGGCTGGAGCTGCTTC
JVO-5990	GACTCTGAAATTACCCCGCGACAATATATCGCCTGCTAAGCCGTCTTACTGTCCCTAGTG
JVO-6516	TTGTAATATCCGCGCGACT
JVO-6533	CTGGAAAACCTGGCGTCGTCATCTATTCTTAAAGGGCAAGGTGTAGGCTGGAGCTGCTTC
JVO-6534	TTTCGAGGGGAAACACATAACCCATTGATTTATAATCTAAGGTCCATATGAATATCCTCCTTAG
JVO-7022	ACAATTCGTTGGCGATTCGGTACCAGTTATCAT
JVO-7023	GTTTTTTTTAATACGACTCACTATAGGCAAGGCGATTTAGCC

JVO-7025	AGAGACCGAATACGATTCC
JVO-7026	CATGCATTAACGGGAACCGGA
JVO-7033	ACGTGGGATAACTGGCTCA
JVO-7034	TCCCACGTAGAACAGAGGA
JVO-7035	TTCCCATGTAGACCCGTC
JVO-7048	GTTTTTCTCGAGTGGATTTAAATCCGGATAG
JVO-7049	AACCGCTGGTAATTAGCACGCTAACAATTTTCGGTTGAATGTGTAGGCTGGAGCTGCTTC
JVO-7053	GTTTTTTTTAATACGACTCACTATAGGTTCCCATGTAGACCCGTC
JVO-7072	CATGGAACCGGAGCGTTCC
JVO-7074	CATGATTCACCATGGATGGCC
JVO-7101	CTAGAAAGTATAGGAACTTCGAAGCAGCTCCAGCCTACACCGGAAGCGGGTATTATACT
JVO-7109	GTTTTTATGCATGGTTCATATAAATACGATAAAT
JVO-7110	GTTTTTATGCATAAGGTTCTGATCACATCAGG
JVO-7111	GTTTTTGCTAGCATTGTCGTCCCGAAGGC
JVO-7159	CGATTTAGCCTGCATTAATG
JVO-7161	CATTAATGCCAACTTTTAGCG
JVO-7163	TGGGATTAATGCAGGCTAA
JVO-7224	GCCTGCATTAATGCCAACTCATCCCTGTTTTCAGCG
JVO-7225	TTGGGAGCAGGCGTTGT
JVO-7328	5'Phosphate-CAGGGAAGTCACTGCCACTG
JVO-7692	ATGCCTGTTCAATGCGTG
JVO-7693	GTTTTTTTTTTAATACGACTCACTATAGGGAGGTTTCGGTTCCGCTTTG
JVO-7742	GCTTACGTGATGCTCTGATTTTGTTGTAAAAGAAATGTTAGGTCCATATGAATATCCTCCTTAG
JVO-7743	GTGTTTCCCCTCGAAATTCCTCGAAATTTCCTCGAATTTCGTGTAGGCTGGAGCTGCTTC
JVO-7859	AGATCACATAATCTTAACAAGAATGTTAAAAAACGCTGGAGGTCCATATGAATATCCTCCTTAG
JVO-7860	TTTATCTGTTAAAAGCCAGAAGCATTTCCTTCGCTGACTTGTGTAGGCTGGAGCTGCTTC
JVO-7861	CATGGTCATAGCTGTTTCCTGTGTGAAATCATCGGAAGCGCCTATTATATTTATTTGTATG
JVO-8022	GTAATTTTCTTAGCGTGACCCGTCCTCCTTCG
JVO-8321	TTTTCCCGGGCAGCGTGTTGGACGAA
JVO-8322	TTTTTCTAGACGGAAGCGGGTATTATACT
JVO-8360	AGGATCTCGCGTCTGACG
JVO-8361	AGATTTCGACTTCCGCCAG
JVO-8689	TTTTATGCATTGTGAGAAATCCCACGG
JVO-9009	AGACTTGTTAACCGCTGGTAATTAGCACGCTAACAATTTTTACACATCTCAACCATCATC
JVO-9010	TCCCGTTAATGCCTAATAATTATCGTAATATAAACAACCGGTGCTCAGTATCTCTATCACTGAT
JVO-9044	CCCACGGACAATTCCGT
E1	5'Phosphate-UUCACUGUUCUUAGCGGCCGCAUGCUC-idT[1]
E3 RACE	GGCCGCTAAGAACAGTGAA
lac promoter fusion rev	TCCCAGTCACGACGTTGTAAAACGACGGCCAGTGAATCCGTAATCATGGTCATAGCTGTTTCCTGTGTG
M13 fwd	GTAAAACGACGGCCAG
M13 rev	CAGGAAACAGCTATGAC
PBAD-FW	ATGCCATAGCATTTTTATCC
PBAD-REV	TTATCAGACCGCTTCTGC
p_LLacO C	5'Phosphate-GTGCTCAGTATCTTGTTATCCG
p_LLacO D	GTGCTCAGTATCTTGTTATCCG
pLlacoB	CGCACTGACCGAATTCATTAA
pMC847 lac rev	CGGGCCTCTTCGCTATTAC
pZE-A	GTGCCACCTGACGTCTAAGA
pZE-Cat	TGGGATATATCAACGGTGGT
pZE-T1	CGGCGGATTTGTCCTACT
pZE-TetB	5'P-CATGTGCTCAGTATCTCTATCACTGA
pZE-Xba	TCGTTTTATTTGATGCCTCTAGA
REV	TTCACACAGGAAACAGCTATGAC
single copy kan rev	CACCATGATATTCGGCAAGCAGGC
UNI-61	ACGACGTTGTAAAACGACGG

[1] idT: 3' inverted

6.7 Bacterial strains and plasmids

Table 6.8 Bacterial strains.

***Salmonella* Typhimurium**					
Trivial name in the manuscript	**Stock name**	**Genotype; relevant markers**	**Details on strain construction**	**Source/reference**	**used in Fig.**
wild-type	SL1344 JVS-0007	Str^R *hisG rpsL xyl*		laboratory stock	2.1; 2.3; 2.6; 2.7; 2.10; 2.11; 2.12; 2.17; 2.20; 2.21; 3.2; 3.7; 3.22; used for dRNA-seq
	JVS-0028	SL1344 Δ*sdsR*::Kan^R		(Papenfort et al, 2008)	
	JVS-0051	SL1344 Δ*micC*::Kan^R		(Papenfort et al, 2008)	
	14028S JVS-0078			laboratory stock	used for dRNA-seq
	JVS-0127	SL1344 Δ*rybB*::Kan^R		(Papenfort et al, 2008)	
	JVS-0175	SL1344 Δ*invR*::Kan^R		(Papenfort et al, 2008)	
Δ*hfq*	JVS-0255	SL1344 Δ*hfq*::Cm^R		(Pfeiffer et al, 2007)	2.17
Δ*rydC*	JVS-0291	SL1344 Δ*rydC*::Kan^R		(Papenfort et al, 2008)	3.1; 3.5; 3.8; 4.5
Δ*cyaR*	JVS-0410	SL1344 Δ*cyaR*::Kan^R		(Papenfort et al, 2008)	4.5
	JVS-0487	SL1344 Δ*invR*	derivative of JVS-0175; cured from Kan^R cassette using pCP20	This study	
	JVS-0673	SL1344 Δ*rpoS*::Kan^R		K. Tedin (KT2846)	
Δ*ompD*	JVS-0735	SL1344 Δ*ompD*::Kan^R		(Pfeiffer et al, 2007)	2.12
ΔRNase III	JVS-0938	SL1344 Δ*rnc*::Kan^R		(Viegas et al, 2007)	3.22
rne701	JVS-1238	SL1344 *rne701*::Kan^R		(Pfeiffer et al, 2009)	3.22
Δ*relA Δspo*T	JVS-1505	SL1344 Δ*relA*		K. Tedin (KT4478)	2.3
	JVS-3387	SL1344 Δ*micC*	derivative of JVS-0051; cured from Kan^R cassette using pCP20	This study	
	JVS-3541	SL1344 Δ*micC* Δ*rybB*::Kan^R	P22 transduction (lysate of JVS-0127) into JVS-3387	This study	
	JVS-3859	SL1344 Δ*arcZ*	λRED mutant (KO: JVO-3540*JVO-3541 on pKD4 in JVS-0007+pKD46; verification: JVO-0176*JVO-3493); cured from Kan^R cassette using pCP20	(Papenfort et al, 2008)	
Δ*rydC*	JVS-4584	SL1344 Δ*rydC*	derivative of JVS-0291; cured from Kan^R cassette using pCP20	This study	3.7
	JVS-4690	SL1344 *cfa::3xFLAG*::Kan^R	λRED mutant (integration: JVO-4186*JVO-4187 on pSUB11 in JVS-0007+pKD46; verification: JVO-4188*JVO-4189)	This study	
	JVS-4738	SL1344 *cfa::3xFLAG*::Kan^R	P22 transduction (lysate of JVS-4690) into JVS-0007	This study	
cfa-3xFLAG	JVS-4767	SL1344 *cfa::3xFLAG*	derivative of JVS-4690; cured from Kan^R cassette using pCP20	This study	3.9; 3.28
Δ*rydC* *cfa*-3xFLAG	JVS-4807	SL1344 Δ*rydC*::Kan^R *cfa::3xFLAG*	P22 transduction (lysate of JVS-0291) into JVS-4767	This study	3.10
	JVS-4862	SL1344 Δ*rydC*::Kan^R	λRED mutant (KO: JVO-4433*JVO-0374 on pKD4 in JVS-0007 +pKD46; verification: JVO-0375*JVO-0376)	This study	
Δ*rydC* *cfa*-3xFLAG	JVS-4938	SL1344 Δ*rydC* *cfa::3xFLAG*	derivative of JVS-0291; cured from Kan^R cassette using pCP20	This study	3.9; 3.28
Δ*rpoS* *cfa*-3xFLAG	JVS-4957	SL1344 *cfa::3xFLAG* Δ*rpoS*::Kan^R	P22 transduction (lysate of JVS-0673) into JVS-4767	This study	3.28
Δ*rydC* Δ*rpoS* *cfa*-3xFLAG	JVS-4958	SL1344 Δ*rydC* *cfa::3xFLAG* Δ*rpoS*::Kan^R	P22 transduction (lysate of JVS-0673) into JVS-4938	This study	3.9; 3.10; 3.28

	JVS-5098	SL1344 Δ*rydC*	derivative of JVS-4862; cured from Kan^R cassette using pCP20	This study	
	JVS-5179	SL1344 P*rydC'::lacZ*$^+$ *::*Kan^R	λRED mutant (integration of pKG136 in JVS-5098 + pCP20; verification: JVO-0375*pMC847 lac rev)	This study	
	JVS-5180	SL1344 P*arcZ'::lacZ*$^+$*::*Kan^R	λRED mutant (integration of pKG136 in JVS-3859 + pCP20; verification: JVO-3493*pMC847 lac rev)	This study	
P*rydC'::lacZ*$^+$	JVS-5195	SL1344 P*rydC'::lacZ*$^+$ *::*Kan^R	P22 transduction (lysate of JVS-5179) into JVS-0007	This study	
P*sraH'::lacZ*$^+$	JVS-5197	SL1344 P*arcZ'::lacZ*$^+$*::*Kan^R	P22 transduction (lysate of JVS-5180) into JVS-0007	This study	
	JVS-5457	SL1344 ΔSTM4242	λRED mutant (KO: JVO-3986*JVO-4956 on pKD4 in JVS-0007+pKD46; verification: JVO-0216*JVO-3622)	This study	
	JVS-5482	SL1344 PSTM4242*'::lacZ*$^+$*::*Kan^R	λRED mutant (integration of pKG136 in JVS-5098 + pCP20; verification: JVO-3622*pMC847 lac rev)	This study	
	JVS-5483	SL1344 PSTM4242*'::lacZ*$^+$*::*Kan^R	P22 transduction (lysate of JVS-5482) into JVS-0007	This study	
Δ*rpoS*	JVS-5487	SL1344 Δ*rpoS::*Cm^R		K. Tedin (KT4676)	2.3; 2.6; 2.7; 2.11
	JVS-5988	SL1344 Δ*ompD*	derivative of JVS-0735; cured from Kan^R cassette using pCP20	This study	
	JVS-6999	SL1344 [*rluC-rne*]IG::*cat*		L. Bossi; (Figueroa-Bossi et al, 2009)	
	JVS-7000	SL1344 [*rluC-rne*]IG::*cat rne-3071* (ts)		L. Bossi; (Figueroa-Bossi et al, 2009)	
Δ*sdsR* Δ*ompD*	JVS-8434	SL1344 Δ*sdsR*::Kan^R Δ*ompD*	P22 transduction (lysate of JVS-0028) into JVS-5988	This study	2.14; 2.15; 2.18
	JVS-8435	SL1344 Δ*cfa::*Kan^R	λRED mutant (KO: JVO-5773*JVO-4828 on pKD4 in JVS-0007 +pKD46; verification: JVO-4055*JVO-4189)	This study	
	JVS-8475	SL1344 Δ*micC* Δ*rybB*	derivative of JVS-3541; cured from Kan^R cassette using pCP20	This study	
	JVS-8491	SL1344 Δ*sdsR*::Kan^R Δ*invR*	P22 transduction (lysate of JVS-0028) into JVS-0487	This study	
	JVS-8494	SL1344 Δ*sdsR*::Kan^R Δ*micC* Δ*rybB*	P22 transduction (lysate of JVS-0028) into JVS-8475	This study	
	JVS-8716	SL1344 Δ*sdsR::*Kan^R	λRED mutant (KO: JVO-6533*JVO-6534 on pKD4 in JVS-0007+pKD46; verification: JVO-0052*JVO-0903)	This study	
sdsR::lacZ	JVS-8717	SL1344 *sdsR'::lacZ*$^+$*::*Kan^R	λRED mutant (integration of pKG136 in JVS-8827 carrying pCP20; verification: JVO-0052*pMC847 lac rev)	This study	2.8
	JVS-8724	SL1344 Δ*sdsR* Δ*invR*	derivative of JVS-8491; cured from Kan^R cassette using pCP20	This study	
	JVS-8725	SL1344 Δ*sdsR* Δ*micC* Δ*rybB*	derivative of JVS-8494; cured from Kan^R cassette using pCP20	This study	
	JVS-8726	SL1344 Δ*micC* Δ*rybB* Δ*invR*	derivative of JVS-5399; cured from Kan^R cassette using pCP20	This study	
Δ*rydC* Δ*rpoS*	JVS-8731	SL1344 Δ*rydC* Δ*rpoS::*Kan^R	P22 transduction (lysate of JVS-0673) into JVS-4584	This study	3.11; 3.13; 3.14; 3.16; 3.17; 3.18
	JVS-8732	SL1344 Δ*rydC* Δ*cfa::*Kan^R	P22 transduction (lysate of JVS-8435) into JVS-4584	This study	

Δ*rydC* Δ*rpoS*	JVS-8733	SL1344 Δ*rydC* Δ*rpoS*::Cm^R	P22 transduction (lysate of JVS-5487) into JVS-4584	This study	3.21
	JVS-8798	SL1344 Δ*sdsR* Δ*micC* Δ*invR*	P22 transduction (lysate of JVS-0052) into JVS-8724; cured from Kan^R cassette using pCP20	This study	
Δ*sdsR* Δ*micC* Δ*rybB* Δ*invR*	JVS-8799	SL1344 Δ*sdsR* Δ*micC* Δ*rybB* Δ*invR*	P22 transduction (lysate of JVS-0175) into JVS-8725; cured from Kan^R cassette using pCP20	This study	2.17
Δ*sdsR*	JVS-8827	SL1344 Δ*sdsR*	derivative of JVS-0028; cured from Kan^R cassette using pCP20	This study	2.4; 2.5; 2.6; 2.7; 2.12; 2.13; 2.14; 2.18
osmY::lacZ	JVS-9145	SL1344 *osmY'::lacZ*$^+$*::*Kan^R		J. Casadesus (SV6068)	2.8
	JVS-9152	SL1344 Cm^R::*ompD*	λRED mutant (KO: JVO-5738*JVO-5739 on pVP42 in JVS-0735+pKD46; verification: JVO-0802*JVO-2192)	This study	
	JVS-9153	SL1344 Cm^R::*ompD**	λRED mutant (KO: JVO-5738*JVO-5739 on pKF109 in JVS-0735+pKD46; verification: JVO-0802*JVO-2192)	This study	
Δ*sdsR ompD*	JVS-9154	SL1344 Δ*sdsR* Cm^R*::ompD*	P22 transduction (lysate of JVS-9152) into JVS-8827	This study	2.19
Δ*sdsR ompD**	JVS-9155	SL1344 Δ*sdsR* Cm^R*::ompD**	P22 transduction (lysate of JVS-9153) into JVS-8827	This study	2.19
	JVS-9158	SL1344 *hns_trunc::*Kan^R		Jay Hinton; (Dillon et al, 2010)	
	JVS-9187	SL1344 Δ*sdsR* Δ*rpoS*::Cm^R	P22 transduction (lysate of JVS-5487) into JVS-8827	This study	
Δ*sdsR hns_trunc*	JVS-9198	SL1344 Δ*sdsR hns_trunc::* Kan^R	P22 transduction (lysate of JVS-9158) into JVS-8827	This study	2.5
Δ*sdsR* Δ*rpoS hns_trunc*	JVS-9199	SL1344 Δ*sdsR* Δ*rpoS*::Cm^R *hns_trunc::* Kan^R	P22 transduction (lysate of JVS-9158) into JVS-9187	This study	2.5
	JVS-9215	SL1344 ΔP*sraC::*Kan^R	λRED mutant (KO: JVO-7742*JVO-7743 on pKD4 in JVS-0007+pKD46; verification: JVO-0051*JVO-0902)	This study	
Δ*sraC*	JVS-9251	SL1344 Δ*sraC*	derivative of JVS-9215; cured from Kan^R cassette using pCP20	This study	2.11
P$_{tet}$ *ompD*	JVS-9488	SL1344 Cm^R::P$_{Ltet0-1}$ *ompD*	λRED mutant (integration: JVO-2223*JVO-2192 on pVP192 in JVS-0007+pKD46; verification: JVO-0802*JVO-2192)	This study	2.22; 2.23
P$_{tet}$ *ompD* Δ*micC* Δ*rybB* Δ*invR*	JVS-9491	SL1344 Δ*micC* Δ*rybB* Δ*invR* Cm^R::P$_{Ltet0-1}$-*ompD*	P22 transduction (lysate of JVS-9488) into JVS-8726	This study	2.22; 2.23
rne-ctrl.	JVS-9549	SL1344 [*rluC-rne*]IG::*cat* Δ*sdsR* Δ*micC* Δ*rybB* Δ*invR*	P22 transduction (lysate of JVS-6999) into JVS-8799	This study	2.16
rne-TS	JVS-9550	SL1344 [*rluC-rne*]IG::*cat rne-3071* (ts) Δ*sdsR* Δ*micC* Δ*rybB* Δ*invR*	P22 transduction (lysate of JVS-7000) into JVS-8799	This study	2.16
Δ*sdsR* Δ*rpoS*	JVS-9551	SL1344 Δ*sdsR* Δ*rpoS::*Kan^R	P22 transduction (lysate of JVS-0673) into JVS-8827	This study	2.4
ΔRNase G	JVS-9559	SL1344 Δ*cafA::*Kan^R	λRED mutant (KO: JVO-1009*JVO-1010 on pKD4 in JVS-0007+pKD46; verification: JVO-8360*JVO-8361)	This study	3.22
P$_{tet}$ *ompD* Δ*sdsR* Δ*micC* Δ*invR*	JVS-9655	SL1344 Δ*sdsR* Δ*micC* Δ*invR* Cm^R::P$_{Ltet0-1}$-*ompD*	P22 transduction (lysate of JVS-9488) into JVS-8798	This study	2.22; 2.23
Δ*rydC* Δ*cfa*	JVS-9675	SL1344 Δ*rydC* Δ*cfa*	derivative of JVS-8732; cured from Kan^R cassette using pCP20	This study	3.10
Δ*rydC* Δ*cfa* Δ*rpoS*	JVS-9713	SL1344 Δ*rydC* Δ*cfa* Δ*rpoS::*Kan^R	P22 transduction (lysate of JVS-0673) into JVS-9675	This study	3.20

Δ*rydC* Δ*hfq* Δ*rpoS* *cfa*-3xFLAG	JVS-9798	SL1344 Δ*rydC rpoS::*Kan^R *cfa::3xFLAG* Δ*hfq::*Cm^R	P22 transduction (lysate of JVS-0255) into JVS-4958	This study	3.9
	JVS-9901	SL1344 DHFR^R::$P_{Ltet0-1}$ *cfa::3xFLAG::*Kan^R	λRED mutant (integration: JVO-9009*JVO-9010 on EZ-Tn5 transposon in JVS-0007+pKD46; verification: JVO-5237*JVO-4364); P22 transduction into JVS-4738	This study	
	JVS-9902	SL1344 DHFR^R::$P_{Ltet0-1}$ *cfa::3xFLAG::*Kan^R Δ*rydC*	P22 transduction (lysate of JVS-9901) into JVS-4584	This study	
	JVS-9904	SL1344 DHFR^R::$P_{Ltet0-1}$ *cfa::3xFLAG* Δ*rydC*	derivative of JVS-9902; cured from Kan^R cassette using pCP20	This study	
	JVS-9906	SL1344 DHFR^R::$P_{Ltet0-1}$ *cfa::3xFLAG* Δ*rydC* Δ*rpoS::*Kan^R	P22 transduction (lysate of JVS-0673) into JVS-9904	This study	
P_{tet} *cfa::3xFLAG* Δ*rydC* Δ*rpoS* *rne*-ctrl.	JVS-9908	SL1344 DHFR^R::$P_{Ltet0-1}$ *cfa::3xFLAG* Δ*rydC* Δ*rpoS::*Kan^R [*rluC-rne*]IG::*cat*	P22 transduction (lysate of JVS-6999) into JVS-9906	This study	3.23; 3.24
P_{tet} *cfa::3xFLAG* Δ*rydC* Δ*rpoS* *rne*-TS	JVS-9909	SL1344 DHFR^R::$P_{Ltet0-1}$ *cfa::3xFLAG* Δ*rydC* Δ*rpoS::*Kan^R [*rluC-rne*]IG::*cat rne-3071* (ts)	P22 transduction (lysate of JVS-7000) into JVS-9906	This study	3.23; 3.24
P*rydC'::lacZ*$^+$		SL1344 Cm^R::P*rydC'::lacZ*$^+$ *::*Kan^R	λRED mutant (integration: JVO-5990*JVO-7101 on pKF88-1 in JVS-5483+pKD46; verification: JVO-5237*JVO-4364); P22 transduction into JVS-0007	This study	

Escherichia coli

Trivial name in the manuscript	**Stock name**	**Genotype; relevant markers**	**Details on strain construction**	**Source/reference**	**used in Fig.**
TOP10		F$^-$ *mcrA* Δ(*mrr-hsdRMS-mcrBC*) Φ80*lacZΔM15* Δ*lacX74 recA1 araD139* Δ(*ara-leu*)7697 *galU galK rpsL endA1 nupG λ*$^-$		Invitrogen	
		MG1655 Δ*mhpA-lacI::(kan<<-cat)*+pKD46		A. Böhm (AB3025)	
Δ*ptsI*		MG1655 P*rydC'::lacZ*$^+$ Δ*ptsI::*Kan^R	P1 transduction (lysate of JW2409) into JVS-9438	This study	3.30
Δ*ptsG*		MG1655 P*rydC'::lacZ*$^+$ Δ*ptsI::*Kan^R	P1 transduction (lysate of JW1087) into JVS-9438	This study	3.30
Δ*crr*		MG1655 P*rydC'::lacZ*$^+$ Δ*crr::*Kan^R	P1 transduction (lysate of JW2410) into JVS-9438	This study	3.30
	JVS-1382	MC4100 Δ*rpoS::*Tn*10*		S. Altuvia	
wild-type	MC4100 JVS-5105	*relA+* derivative of MC4100 (*araD139* (*argF-lac*)*205 flb-5301 pstF25 rpsL150 deoC1 relA1*)		T. Nyström; (Sanden et al, 2003)	2.10; 2.11
	MC4100 JVS-0965	*relA+* derivative of MC4100 (*araD139* (*argF-lac*)*205 flb-5301 pstF25 rpsL150 deoC1 relA1*)		T. Nyström; (Sanden et al, 2003)	used for dRNA-seq
	JVS-9311	MC4100 *relA+* Δ*sraC*	λRED mutant (KO: JVO-7859*JVO-7860 on pKD4 in JVS-5105+pKD46; verification: JVO-1043*JVO-2390)	This study	
Δ*sraC*	JVS-9312	MC4100 *relA+* Δ*sraC*	derivative of JVS-9311; cured from Kan^R cassette using pCP20	This study	2.11
Δ*rpoS*	JVS-9322	MC4100 *relA+* Δ*rpoS::*Tn*10*	P1 transduction (lysate of JVS-1382) into JVS-5105	This study	2.11

	JVS-9436	MG1655 P*rydC'::lacZ*$^{+}$*::*Kan^{R}	λRED mutant (integration in AB3025 of JVO-7861*'single copy kan rev' on J1416; re-amplification by 'lac promoter fusion rev'*'single copy kan rev'; verification: 'single copy kan rev'*pMC847 lac rev)	This study	
ctrl.	JVS-9438	MG1655 P*rydC'::lacZ*$^{+}$	derivative of JVS-9436; cured from Kan^{R} cassette using pCP20	This study	3.30
	JVS-9452	*RP4-2(Km::Tn7, Tc::Mu-1) leu-163::IS10 uidA3(del)::pir+ recA1 endA1 thiE1 hsdR17 creC510*	conjugation competent strain carrying pAB540	Barry Wanner (BW20767); (Metcalf et al 1996); provided by A. Böhm	
wild-type	MG1655 JVS-9709	MG1655 F^{-} λ^{-} *rph-1*		(Blattner et al, 1997); provided by A. Böhm	3.30
Δ*ptsG*	JW1087	BW25113 Δ*ptsG::*Kan^{R}		KEIO collection; (Baba et al, 2006)	3.30
	JW1416	BW25113 Δ*ydcA::*Kan^{R}		KEIO collection; (Baba et al, 2006)	
Δ*ptsI*	JW2409	BW25113 Δ*ptsI::*Kan^{R}		KEIO collection; (Baba et al, 2006)	3.30
Δ*crr*	JW2410	BW25113 Δ*crr::*Kan^{R}		KEIO collection; (Baba et al, 2006)	3.30
Shigella flexneri					
Trivial name in the manuscript	**Stock name**	**Genotype; relevant markers**	**Details on strain construction**	**Source/reference**	**used in Fig.**
wild-type	BS176 JVS-0012	BS 176; plasmid cured derivative of *S. flexneri* M90T		Arturo Zychlinsky, Berlin; (Zychlinsky et al, 1992)	2.10
	M90T JVS-0013	*S. flexneri* M90T; carrying virulence plasmid		Arturo Zychlinsky, Berlin; (Zychlinsky et al, 1992)	used for dRNA-seq
Enterobacter					
Trivial name in the manuscript	**Stock name**	**Genotype; relevant markers**	**Details on strain construction**	**Source/reference**	**used in Fig.**
	Entero-bacter spp. 638 JVS-4308			D. van der Lelie, Brookhaven	
Citrobacter					
Trivial name in the manuscript	**Stock name**	**Genotype; relevant markers**	**Details on strain construction**	**Source/reference**	**used in Fig.**
	C. rodentium JVS-8970			laboratory stock	used for dRNA-seq

Table 6.9 Plasmids.

Plasmid trivial name	Plasmid stock name	Expressed fragment	Comment	Details on construction	Origin, Marker	Reference
pP_L-TMA	pFS135	TMA	ColE1 plasmid based on pZE12-luc; expresses truncated *Salmonella* MicA (starting at +23) from constitutive P_{Llac0} promoter		ColE1, Amp^{R}	(Bouvier et al, 2008)
	pJV300		pP_L control plasmid, expresses a ~50 nt nonsense transcript derived from *rrnB* terminator		ColE1, Amp^{R}	(Sittka et al, 2007)

pBAD-RydC-2	pJV766-21	RydC-2	expresses *Salmonella* RydC + two additional nt at the 5' end from arabinose-inducible P_{BAD} promoter	amplification of *Salmonella rydC* with JVO-0376*JVO-0975 from gDNA; ligation into pBAD Myc-His A via XbaI	oriV, Amp^R	This study
gfp	pJV859-8	*gfp*	Control plasmid, expresses *gfp* from constitutive $P_{LtetO-1}$ promoter		pSC101*, Cm^R	(Sittka et al, 2007)
TSS1-*cfa::gfp*	pKF30-1	TSS1-*cfa::gfp*	expresses *cfa::gfp* translational fusion (TSS1 of *cfa* + 15 aa) from constitutive $P_{LtetO-1}$ promoter	amplification of *Salmonella cfa* with JVO-4055*JVO-4057 from gDNA; ligation into pXG10 via NheI/BfrBI	pSC101*, Cm^R	This study
TSS2-*cfa::gfp*	pKF31-1	TSS2-*cfa::gfp*	expresses *cfa::gfp* translational fusion (TSS2 of *cfa* + 15 aa) from constitutive $P_{LtetO-1}$ promoter	amplification of *Salmonella cfa* with JVO-4056*JVO-4057 from gDNA; ligation into pXG10 via NheI/BfrBI	pSC101*, Cm^R	This study
pP_L-RydC-TMA	pKF38	RydC-TMA	ColE1 plasmid based on pZE12-luc; expresses truncated *Salmonella* RydC (nt 1-12) fused to +23 of *Salmonella* MicA from constitutive P_{Llac0} promoter	derivative of pFS135-1; ligation of PCR product of JVO-4420*pLLacOC	ColE1, Amp^R	This study
pBAD-RydC	pKF41-2	RydC	expresses *Salmonella* RydC from arabinose-inducible P_{BAD} promoter	derivative of pJV766-21; ligation of PCR product of JVO-4531*JVO-4532	oriV, Amp^R	This study
pP_L-RydC	pKF42-1	RydC	ColE1 plasmid based on pZE12-luc; expresses *Salmonella* RydC from constitutive P_{Llac0} promoter	derivative of pVP142; ligation of PCR product of JVO-4532*pLLacOC	ColE1, Amp^R	This study
luxS::gfp	pKF58-2	*luxS::gfp*	expresses *luxS::gfp* translational fusion from constitutive $P_{LtetO-1}$ promoter	amplification of *Salmonella luxS* with JVO-4573*JVO-0358 from gDNA; ligation into pXG10 via NheI/BfrBI	pSC101*, Cm^R	This study
pP_L-RydC-K1	pKF60-1	RydC-K1	ColE1 plasmid based on pZE12-luc; expresses *Salmonella* RydC-K1 (SNEs G37C; G39C) from constitutive P_{Llac0} promoter	derivative of pKF42-1; ligation of PCR product of JVO-4536*JVO-4537	ColE1, Amp^R	This study
pP_L-RydC-K2	pKF61-1	RydC-K2	ColE1 plasmid based on pZE12-luc; expresses *Salmonella* RydC-K2 (SNEs C13G; C15G) from constitutive P_{Llac0} promoter	derivative of pKF42-1; ligation of PCR product of JVO-5081*JVO-5082	ColE1, Amp^R	This study
pP_L-RydC-K1/2	pKF62-1	RydC-K1/2	ColE1 plasmid based on pZE12-luc; expresses *Salmonella* RydC-K1/2 (SNEs C13G; C15G; G37C; G39C) from constitutive P_{Llac0} promoter	derivative of pKF61-1; ligation of PCR product of JVO-4536*JVO-4537	ColE1, Amp^R	This study
pP_L-SdsR	pKF68-3	SdsR	ColE1 plasmid based on pZE12-luc; expresses *Salmonella* SdsR from constitutive P_{Llac0} promoter	amplification of *Salmonella sdsR* with JVO-0902*JVO-0903 from gDNA; ligation into pZE12 via XbaI	ColE1, Amp^R	This study
pP_L-SdsR proc.	pKF73-1	SdsR proc.	ColE1 plasmid based on pZE12-luc; expresses truncated *Salmonella* SdsR (starting at processing site +31) from constitutive P_{Llac0} promoter	derivative of pKF68-3; ligation of PCR product of JVO-4731*pLLacOD	ColE1, Amp^R	This study
-183*cfa::gfp*	pKF79-2	-183*cfa::gfp*	expresses *cfa::gfp* translational fusion (-183 rel. to AUG of *cfa* + 15 aa) from constitutive $P_{LtetO-1}$ promoter	derivative of pKF31-1; ligation of PCR product of JVO-7026*pZETetB	pSC101*, Cm^R	This study

TSS1-*cfa*::gfp*	pKF83-1	TSS1-*cfa*::gfp*	expresses *cfa*::gfp* translational fusion (TSS1 of *cfa* + 15 aa with SNE C-102G) from constitutive $P_{Ltet0-1}$ promoter	derivative of pKF31-1; ligation of PCR product of JVO-7033*JVO-7034	pSC101*, Cm^R	This study
pP_L-RydC*	pKF86-1	RydC*	ColE1 plasmid based on pZE12-luc; expresses *Salmonella* RydC* (SNE G5C) from constitutive P_{LlacO} promoter;	derivative of pKF42-1; ligation of PCR product of JVO-7035*pLLacOC	ColE1, Amp^R	This study
p*rydC*	pKF88-1	RydC	*rydC* complementation plasmid (low copy plasmid); expresses RydC from its own promoter	amplification of *Salmonella rydC* with JVO-7048*JVO-0376 from gDNA; ligation into pXG10 via XhoI/XbaI	pSC101*, Cm^R	This study
-174*cfa::gfp*	pKF89-1	-174*cfa::gfp*	expresses *cfa::gfp* translational fusion (-174 rel. to AUG of *cfa* + 15 aa) from constitutive $P_{Ltet0-1}$ promoter	derivative of pKF31-1; ligation of PCR product of JVO-7072*pZETetB	pSC101*, Cm^R	This study
-157*cfa::gfp*	pKF91-1	-157*cfa::gfp*	expresses *cfa::gfp* translational fusion (-157 rel. to AUG of *cfa* + 15 aa) from constitutive $P_{Ltet0-1}$ promoter	derivative of pKF31-1; ligation of PCR product of JVO-7074*pZETetB	pSC101*, Cm^R	This study
TSS1-*cfa(Ent)::gfp*	pKF93-2	TSS1-*cfa(Ent)::gfp*	expresses *Enterobacter 638 cfa::gfp* translational fusion (TSS1 of *cfa* + 15 aa) from constitutive $P_{Ltet0-1}$ promoter	amplification of *Enterobacter 638 cfa* with JVO-7109*JVO-7111 from gDNA; ligation into pXG10 via NheI/BfrBI	pSC101*, Cm^R	This study
TSS2-*cfa(Ent)::gfp*	pKF94-1	TSS2-*cfa(Ent)::gfp*	expresses *Enterobacter 638 cfa::gfp* translational fusion (TSS2 of *cfa* + 15 aa) from constitutive $P_{Ltet0-1}$ promoter	amplification of *Salmonella cfa* with JVO-7110*JVO-7111 from gDNA; ligation into pXG10 via NheI/BfrBI	pSC101*, Cm^R	This study
pP_L-SdsR +7	pKF97-1	SdsR +7	ColE1 plasmid based on pZE12-luc; expresses truncated *Salmonella* SdsR (starting at +7) from constitutive P_{LlacO} promoter	derivative of pKF68-3; ligation of PCR product of JVO-7159*pLLacOD	ColE1, Amp^R	This study
pP_L-SdsR +19	pKF99-1	SdsR +19	ColE1 plasmid based on pZE12-luc; expresses truncated *Salmonella* SdsR (starting at +19) from constitutive P_{LlacO} promoter	derivative of pKF68-3; ligation of PCR product of JVO-7161*pLLacOD	ColE1, Amp^R	This study
pP_L-SdsR*	pKF101-26	SdsR*	ColE1 plasmid based on pZE12-luc; expresses *Salmonella* SdsR* (SNE G26C) from constitutive P_{LlacO} promoter;	derivative of pKF68-3; ligation of PCR product of JVO-7163*pLLacOD	ColE1, Amp^R	This study
pP_L-SdsR-TMA	pKF105-1	SdsR-TMA	ColE1 plasmid based on pZE12-luc; expresses truncated *Salmonella* SdsR (+14-32) fused to +23 of *Salmonella* MicA from constitutive P_{LlacO} promoter	derivative of pFS135-1; ligation of PCR product of JVO-7224*pLLacOC	ColE1, Amp^R	This study
p*sdsR* C-13G	pKF106-2	SdsR; SraC	pSC101* plasmid based on pZE12-luc; expresses *Salmonella* SdsR from endogenous promoter with SNE (C-13G)	derivative of pVP203; ligation of PCR product of JVO-4262*JVO-4265	pSC101*, Amp^R	This study
p*sdsR* C-13A	pKF107-1	SdsR; SraC	pSC101* plasmid based on pZE12-luc; expresses *Salmonella* SdsR from endogenous promoter with SNE (C-13A)	derivative of pVP203; ligation of PCR product of JVO-4263*JVO-4265	pSC101*, Amp^R	This study
p*sdsR* C-13T	pKF108-3	SdsR; SraC	pSC101* plasmid based on pZE12-luc; expresses *Salmonella* SdsR from endogenous promoter with SNE (C-13T)	derivative of pVP203; ligation of PCR product of JVO-4264*JVO-4265	pSC101*, Amp^R	This study

p*ompD**	pKF109-1	*ompD**	*ompD** complementation plasmid; expresses *ompD** (SNE C44G) from its own promoter	derivative of pVP42-3; ligation of PCR product JVO-7328*JVO-7225	pSC101*, Cm^R	This study
pP_L-antiD-TMA	pKF131-1	antiD-TMA	ColE1 plasmid based on pZE12-luc; expresses synthetic RNA antisense to nt -14 to -29 of *Salmonella ompD* mRNA fused to +23 of *Salmonella* MicA from constitutive P_{LlacO} promoter	derivative of pFS135-1; ligation of PCR product of JVO-8022*pLLacOC	ColE1, Amp^R	This study
pP_{rydC}*::gfp*	pKF132	*gfp*	ColE1 plasmid based on pZEP08; expresses *gfp* under the control of *Salmonella rydC* promoter	amplification of *Salmonella rydC* promoter with JVO-8321*JVO-8322; ligation into pZEP08 via SmaI/XbaI	ColE1, Amp^R, Cm^R	This study
TSS1-*cfa-X::gfp*	pKF133-1	TSS1-*cfa-X::gfp*	expresses chimeric *cfa-ompX::gfp* translational fusion (encompassing nt 1-147 of *cfa* UTR and UTR + 10 aa of *ompX*) from constitutive $P_{LtetO-1}$ promoter	amplification of *Salmonella cfa* UTR with pZECat*JVO-8689 from pKF31; ligation into pKP60 via BfrBI	pSC101*, Cm^R	This study
-183*cfa-X::gfp*	pKF134	-183*cfa-X::gfp*	expresses chimeric *cfa-ompX::gfp* translational fusion (encompassing nt 30-147 of *cfa* UTR and UTR + 10 aa of *ompX*) from constitutive $P_{LtetO-1}$ promoter	amplification of *Salmonella cfa* UTR with pZECat*JVO-8689 from pKF79; ligation into pKP60 via BfrBI	pSC101*, Cm^R	This study
pBAD	pKP8-35		pP_{BAD} control plasmid, expresses a ~50 nt nonsense transcript derived from *rrnB* terminator		pBR322, Amp^R	(Papenfort et al, 2006)
pBAD-SdsR	pKP19-8	SdsR	expresses *Salmonella* SdsR from arabinose-inducible P_{BAD} promoter	amplification of *Salmonella rydC* with JVO-0902*JVO-0903 from gDNA; ligation into pBAD Myc-His A via XbaI	oriV, Amp^R	This study
pP_L-CyaR	pKP39-3	CyaR	ColE1 plasmid based on pZE12-luc; expresses *Salmonella* CyaR from constitutive P_{LlacO} promoter		ColE1, Amp^R	(Papenfort et al, 2008)
ompX::gfp	pKP60	*ompX::gfp*	expresses *ompX::gfp* translational fusion (-33 rel. to AUG of *cfa* + 10 aa) from constitutive $P_{LtetO-1}$ promoter		pSC101*, Cm^R	(Papenfort et al, 2008)
	pRH800		pP_{tac} control plasmid		pBR322, Amp^R	(Lange & Hengge-Aronis, 1994)
pP_{tac}-RpoS	pRL40.1	*rpoS*	*E. coli rpoS* expressed from constitutive P_{tac} promoter		pBR322, Amp^R	(Lange & Hengge-Aronis, 1994)
p*ompD*	pVP42-3	*ompD*	*ompD* complementation plasmid; expresses *ompD* from its own promoter		pSC101*, Cm^R	(Pfeiffer et al, 2009)
pP_L-MicC-TMA	pVP94-1	MicC16-TMA	ColE1 plasmid based on pZE12-luc; expresses nt 1-16 of *Salmonella* MicC fused to +15 of *Salmonella* MicA from constitutive P_{LlacO} promoter		ColE1, Amp^R	(Pfeiffer et al, 2009)
p*rydC*	pVP112	RydC	*rydC* complementation plasmid (high copy plasmid); expresses RydC from its own promoter	amplification of *Salmonella rydC* with JVO-0375*JVO-0376 from gDNA; ligation into pXG10 via XhoI/XbaI	ColE1, Amp^R	This study

pP_L-RydC-2	pVP142	RydC-2	ColE1 plasmid based on pZE12-luc; expresses *Salmonella* RydC + 2 nt at the 5' from constitutive P_{LlacO} promoter	amplification of *Salmonella rydC* with JVO-0376*JVO-0975 from gDNA; ligation into pZE12 via XbaI	ColE1, Amp^R	This study
D+45::*gfp*	pVP188-1	*ompD*+45::*gfp*	expresses *ompD+45::gfp* translational fusion from constitutive $P_{LtetO-1}$ promoter		pSC101*, Cm^R	(Pfeiffer et al, 2009)
D+3::*gfp*	pVP192-1	*ompD*+3::*gfp*	expresses *ompD+3::gfp* translational fusion from constitutive $P_{LtetO-1}$ promoter		pSC101*, Cm^R	(Pfeiffer et al, 2009)
p*sdsR*	pVP203-1	SdsR; SraC	pSC101* plasmid based on pZE12-luc; expresses *Salmonella* SdsR from endogenous promoter	amplification of *Salmonella sdsR* with JVO-0051*JVO-0052 from gDNA; ligation into pVP003 via XhoI/XbaI	pSC101*, Amp^R	This study
D+78::*gfp*	pVP206-1	*ompD*+78::*gfp*	expresses *ompD+78:: gfp* translational fusion from constitutive $P_{LtetO-1}$ promoter		pSC101*, Cm^R	(Pfeiffer et al, 2009)
D+99::*gfp*	pVP207-1	*ompD*+99::*gfp*	expresses *ompD+99::gfp* translational fusion from constitutive $P_{LtetO-1}$ promoter		pSC101*, Cm^R	(Pfeiffer et al, 2009)
STM3820 *::gfp*		STM3820 *::gfp*	expresses STM3820*::gfp* (TSS at -84 to +35aa) translational fusion from constitutive $P_{LtetO-1}$ promoter		pSC101*, Cm^R	K. Händler; J. Hinton
	pAB540	Tn*mariner::*Kan^R	Tn*mariner::*Kan^R transposon delivery vector; for conjugation		oriR6K, Amp^R	(Boehm et al, 2010)
	pBAD Myc-His A		pBAD expression plasmid		oriV, Amp^R	Invitrogen
	pCP20	FLP - ci857	Temperature-sensitive Flp recombinase expression plasmid		pSC101, Amp^R, Cm^R	(Cherepanov & Wackernagel, 1995)
	pKD4		template plasmid Kan^R for λRED mutants		oriRγ, Amp^R	(Datsenko & Wanner, 2000)
	pKD46	*γ-β-exo*	Temperature-sensitive λRED recombinase expression plasmid; expresses λRED-recombinase from arabinose-inducible P_{araB} promoter		oriR101, AmpR	(Datsenko & Wanner, 2000)
	pKG136		For FLP-mediated *lacZ-Y* integration to construct transcriptional *lac* fusions		oriR6K, Kan^R	J.M. Slauch
	pVP003	*luc*	general cloning plasmid; low copy version of pZE12-*luc*		pSC101*, Amp^R	(Sittka et al, 2007)
	pZE12-*luc*	*luc*	general cloning plasmid		ColE1, Amp^R	(Lutz & Bujard, 1997)
	pZEP08	*gfp+*	cloning plasmid for transcriptional *gfp* reporter fusions		ColE1, Amp^R, Cm^R	(Hautefort et al, 2003)

unpublished plasmids prepared by others
pJV series: Jörg Vogel (lab stock)
pKP series: Kai Papenfort (lab stock)
pVP series: Verena Pfeiffer (lab stock)

6.8 Media and media stocks

Lennox-broth (LB)	10 g tryptone 5 g yeast extract 5 g NaCl H_2O ad 1 l
LB agar	10 g tryptone 5 g yeast extract 5 g NaCl 1.2% (w/v) agar H_2O ad 1 l
M9 minimal medium	1X M9 salts 2 mM $MgSO_4$ 0.1 mM $CaCl_2$ 0.5 µg/ml thiamine 40 µg/ml L-histidine 0.2-0.4 % glucose/glycerol
5X M9 salts	85.7 g Na_2HPO_4x12 H_2O 15 g KH_2PO_4 2.5 g NaCl 5 g NH_4Cl H_2O ad 1 l
Nutrient broth	8 g/l Difco Nutrient broth
SPI-1 medium	10 g tryptone 5 g yeast extract 0.3 M NaCl
PCN1 medium (SPI-2 MES medium; pH=5.8)	1X MES buffer 1X Phosphate buffer 0.4 % (w/v) glucose 15 mM NH_4Cl 1 mM $MgSO_4$ 10 µM $CaCl_2$ 0.04 % (w/v) L-histidine 0.001 % (w/v) thiamine 10X Micronutrients

MES buffer stock solution (10x)	800 mM MES
	40 mM tricine; adjust to pH=5.8 with KOH
	1 mM $FeCl_3$
	3.76 mM K_2SO_4
	500 mM NaCl
Phosphate buffer stock solution	200 mM K_2HPO_4
(200x; pH=5.8)	50 mM KH_2PO_4
Micronutrients (10,000x)	10 µM Na_2MoO_4 x 2 H_2O
	10 µM $NaSeO_3$ x 5 H_2O
	4 µM H_3BO_3
	0.3 mM $CoCl_2$ x 6 H_2O
	0.1 mM $CuSO_4$ x 5 H_2O
	0.8 mM $MnCl_2$ x 4 H_2O
	0.1 mM $ZnSO_4$ x 7 H_2O

6.9 Media supplements

Table 6.10 Antibiotics and media supplements.

antibiotic	**solvent**	**stock concentration**	**working concentration**
ampicillin	H_2O	100 mg/ml	100 µg/ml
chloramphenicol	ethanol (abs.)	20 mg/ml	20 µg/ml
kanamycin	H_2O	50 mg/ml	50 µg/ml
trimethoprim	DMF	10 mg/ml	5 µg/ml
streptomycin	H_2O	50 mg/ml	50 µg/ml
rifampicin	DMSO	50 mg/ml	500 µg/ml
tetracycline	ethanol (abs.)	5 mg/ml	15 µg/ml
supplement	**solvent**	**stock concentration**	**working concentration**
X-Gal	DMF	20 mg/ml	40 µg/ml
cas-amino acids	H_2O	10 % (w/v)	0.2 % (w/v)
L-Arabinose	H_2O	20 % (w/v)	0.2 % (w/v)
serine hydroxamate (SHX)	H_2O	20 mg/ml (166 mM)	1 µM to 1 mM
polymyxin B	H_2O	5 mg/ml	5 µg/ml
sodium citrate	H_2O	1 M	20-100 mM

6.10 Buffers and solutions

agarose gel solution	0.8-4% (w/v) agarose in 1X TAE
chemiluminescence solution	2 ml chemiluminescence solution A 200 µl chemiluminescence solution B 5 µl 3% (v/v) H_2O_2
chemiluminescence solution A	0.1 M Tris-Cl (pH=8.6) 0.025% (w/v) luminol
chemiluminescence solution B	0.11% (w/v) *p*-coumaric acid in DMSO
DNA loading buffer (5X)	10 mM Tris-Cl (pH=7.6) 60% (v/v) glycerol 60 mM EDTA (pH=8.0) 0.025% (w/v) bromophenol blue
GLII (RNA loading buffer II; 2X)	0.025% (w/v) bromophenol blue 0.025% (w/v) xylene cyanol 18 µM EDTA (pH=8.0) 0.13% (w/v) SDS 95% formamide
Hfq dilution buffer	1X structure buffer 1% (v/v) glycerol 0.1% Triton-X100
native loading buffer (5X)	50% (v/v) glycerol 0.5X TBE 0.02% (w/v) bromophenol blue
PAA solution denaturing RNA gel	100 ml 10X TBE 420 g Urea (7 M) 4% 6% 10% 12% 15% 100 150 250 300 375 ml Rotiphorese gel 40 (19:1) H_2O ad 1 l
PAA solution native gel	50 ml 10X TBE 150 ml Rotiphorese gel 40 (19:1) H_2O ad 1 l

PAA solution stacking gel (4%)	1.25 ml Tris solution (upper buffer) 1 ml Rotiphorese gel 40 (37.5:1) 7.5 ml H_2O 75 µl 10% (w/v) APS 7.5 µl TEMED
PAA solution resolving gel (10-15%)	3.75 ml Tris solution (lower buffer) 10% 11% 12% 15% 2.5 2.75 3.0 3.75 ml Rotiphorese gel 40 (37.5:1) 3.75 3.5 3.25 3.0 ml H_2O 150 µl 10% (w/v) APS 15 µl TEMED
RNA elution buffer	0.1 M sodium acetate 0.1% (w/v) SDS 10 mM EDTA (pH=8.0)
RNase E reaction buffer (2X)	50 mM Tris-Cl (pH=7.6) 100 mM NaCl 100 mM KCl 20 mM $MgCl_2$ freshly supplemented with 2 mM DTT
RNase E storage buffer	20 mM Tris-Cl (pH=7.9) 5% (v/v) glycerol 500 mM NaCl 10 mM $MgSO_4$ 0.5 mM EDTA (pH=8.0) 10 mM DTT
SB 5X -Mg	50 mM Tris-acetate (pH=7.6) 500 mM potassium acetate 5 mM DTT
SB 1X Mg10	10 mM Tris-acetate (pH=7.6) 100 mM potassium acetate 1 mM DTT 10 mM magnesium acetate

SB 1X Mg60	10 mM Tris-acetate (pH=7.6) 100 mM potassium acetate 1 mM DTT 60 mM magnesium acetate
SDS running buffer (10X)	30.275 g Tris base 144 g glycin 10 g SDS H_2O ad 1 l
SSC buffer (20X)	3 M NaCl 0.3 M sodium citrate adjust to pH=7 with HCl
StainsAll solution	0.015% (w/v) StainsAll 60% formamide
structure buffer (10X)	100 mM Tris-HCl (pH=7) 1M KCl 100 mM $MgCl_2$
TAE (50X)	242 g Tris base 51.7 ml acetic acid 10 mM EDTA (pH=8.0) H_2O ad 1 l
TBE (10X)	108 g Tris base 55 g boric acid 20 mM EDTA (pH=8.0) H_2O ad 1 l
TBS (10X)	24.11 g Tris base 72.6 g NaCl adjust to pH=7.4 with HCl H_2O ad 1 l
TBST (1X)	1X TBS 0.1% (v/v) Tween20

TE buffer (1X)	100 mM Tris-Cl (pH=8.0) 10 mM EDTA (pH=8.0)
Tico buffer	20 mM HEPES-KOH (pH=7.6) 6 mM magnesium acetate 30 mM ammonium acetate 4 mM 2-mercaptoethanol
Toeprint Stop Solution	50 mM Tris-Cl (pH=7.5) 0.1% (w/v) SDS 10 mM EDTA (pH=8.0)
transfer buffer (1X)	100 ml transfer buffer stock (10X) 200 ml methanol H_2O ad 1 l
transfer buffer stock (10X)	30 g Tris base 144 g glycin H_2O ad 1 l
Tris solution (lower buffer)	1.5 M Tris-HCl (pH=8.8) 0.4% (w/v) SDS
Tris solution (upper buffer)	0.5 M Tris-HCl (pH=6.8) 0.4% (w/v) SDS
Z-buffer	8.54 g Na_2HPO_4 5.5 g $NaH_2PO_4*H_2O$ 0.75 g KCl 0.25 g $MgSO_4*7H_2O$ adjust to pH=7.0 H_2O ad 1 l freshly supplement with 0.28% (v/v) 2-mercaptoethanol

6.11 Sterilization

All media and solutions used throughout this study were sterilized prior to use by autoclaving for 20 min at 120°C and 1 bar. If necessary, solutions were sterile filtered. Glassware was sterilized by heating to 180°C for a minimum of three hours.

6.12 Microbiological Methods

6.12.1 Standard growth conditions

Unless stated otherwise, bacteria were grown on LB agar plates or in LB at 37°C, 220 rpm with normal aeration throughout this study. Cultures were inoculated from a single colony of strains grown o/n on plates at 37°C, or from o/n cultures (inoculated from a single colony) which were diluted 1:100 into fresh medium. Where appropriate, media were supplemented (Table 6.10).

6.12.2 Growth under SPI-1-inducing conditions

For growth under SPI-1 inducing conditions, bacteria were inoculated from a single colony in 5 ml SPI-1 medium in 15 ml tubes. Growth was carried out for 12 h at 37°C, 220 rpm with tightly closed lids to ensure oxygen limitation.

6.12.3 Growth under SPI-2-inducing conditions

For growth under SPI-2 inducing conditions, bacteria were grown o/n in SPI-2 medium (inoculated from single colony) and diluted 1:100 into fresh medium. Cells were grown at 37°C, 220 rpm to an OD_{600} of 0.4.

6.12.4 Growth in M9 minimal medium

For growth in M9 minimal medium, bacteria were inoculated from a single colony in LB and grown for 3h at 37°C, 220 rpm. M9 o/n cultures were inoculated 1:500 with pre-cultured cells. Main cultures were inoculated 1:100 from o/n cultures.

6.12.5 Induction of heat-shock

To apply heat shock, cells were grown in LB at 30°C to an OD_{600} of 0.3 or, alternatively, at 37°C to an OD_{600} of 0.5. Cultures were split and growth was continued either as before (control) or at 44°C.

6.12.6 Induction of osmotic shock

To apply osmotic shock, cells were cultured at 37°C in M9 minimal medium containing 0.4% glycerol and supplemented with cas-amino acids (0.2%) to an OD_{600} of 0.3. Cultures were split and NaCl was added to one batch at a final concentration of 0.3 M.

6.12.7 Induction of amino acid starvation

Stringent response was induced by addition of serine hydroxamate (1 µM to 1 mM) to cells during exponential growth (OD_{600} of 0.15) in Nutrient broth supplemented with 0.75 mM L-serine.

6.12.8 Induction of envelope stress

Envelope stress was induced by addition of polymyxin B (final concentration: 5 µg/ml) to cells grown in LB to late exponential phase (OD_{600} of 1.5).

6.12.9 Induction of acetate stress

To induce acetate shock, cells were grown at 37°C in LB medium to an OD_{600} of 0.4, when cultures were split and either supplemented with H_2O (control) or neutral acetate (final concentration 50 or 100 mM), and growth was continued for additional 20 min.

6.12.10 Transformation of chemically competent *E. coli*

DNA (1 µl of plasmid DNA or 5 µl of ligation reactions) was mixed with 25 µl of chemically competent *E. coli* TOP10 cells. Upon incubation on ice for 20 min, cells were heat-shocked at 42°C for 35 sec. Cells were chilled on ice for 1 min and resuspended in 300 µl LB medium. Recovery was carried out for 60 min at 37°C, 220 rpm.

6.12.11 Transformation of electrocompetent *E. coli*

For preparation of electrocompetent *E. coli*, cultures inoculated from single colonies or o/n cultures were grown at 37°C, 220 rpm to an OD_{600} of 0.5. Cells were chilled on ice for 30 min and collected by centrifugation (20 min; 4,000 rpm; 4°C). Bacteria were washed three times with ice-cold H_2O (first wash) or 10% (v/v) glycerol (second and third wash). Pellets were resuspended in ice-cold H_2O (1 OD/100 µl). 100 µl of cells were mixed with DNA in electroporation cuvettes (2 mm gap size) and transformed by electroporation (200 Ω; 25 µF; 2.5 kV). Cells were resuspended in 300 µl LB and recovered for 60 min at 37°C, 220 rpm.

6.12.12 P1 transduction

Chromosomal mutations were moved in *E. coli* with the help of P1 transduction. For lysate preparation, strains of interest were grown in 5 ml LB at 37°C, 220 rpm to an OD_{600} of 0.3. Upon addition of $CaCl_2$ (final concentration: 10 mM) and 10 µl P1 phage lysate, incubation was continued for 3-4 h until the culture significantly lessened in its turbidity. 250 µl of chloroform were added, lysates were vortexed and cell debris was collected by centrifugation (15 min; 5,000 rpm; 4°C). The supernatant was transferred to a fresh glass storage tube and supplemented with 200 µl chloroform. Phage lysates were stored at 4°C.

For transduction, recipient cells were grown to an OD_{600} of 0.5-0.8 and adjacently supplemented with $CaCl_2$ (final concentration: 10 mM). 1 ml culture was mixed with P1 lysate (10-100 µl) and incubated at RT for 15 min. Phage transduction was stopped by the addition of sodium citrate (final concentration: 100 mM) and cells were recovered for 1 h at 37°C. Transductants were selected on LB plates supplemented with the appropriate antibiotic and sodium citrate (final concentration: 20 mM). Clones were restreaked twice on plates containing sodium citrate.

6.12.13 Transformation of *Salmonella*

For preparation of electrocompetent *Salmonella*, cultures inoculated from single colonies or o/n cultures were grown at 37°C, 220 rpm to an OD_{600} of 0.5. Cells were chilled on ice for 30 min and

collected by centrifugation (20 min; 4,000 rpm; 4°C). Bacteria were washed twice with ice-cold H_2O. Pellets were resuspended in ice-cold H_2O (1 OD/100 µl). 100 µl of cells were mixed with DNA in electroporation cuvettes (2 mm gap size) and transformed by electroporation (200 Ω; 25 µF; 2.5 kV). Cells were resuspended in 300 µl LB and recovered for 60 min at 37°C, 220 rpm.

6.12.14 P22 transduction

Phage P22 transduction was employed to transfer each single chromosomal modification to a fresh *Salmonella* wild-type background, as well as to obtain strains carrying multiple mutations. P22 lysates of strains of interest were prepared using soft agar plates following standard protocols (Sternberg & Maurer, 1991). *Salmonella* donor strains were grown to OD_{600} of 1.0 and 100 µl of culture was added to 2.5 ml Top Agar (supplemented with 20 mM $MgSO_4$ and 10 mM $CaCl_2$). The mix was poured on a pre-warmed LB plate and 100 µl P22 lysate prepared from *Salmonella* wild-type cells was spread on the Top Agar. Plates were incubated o/n at 37°C. Subsequently, Top Agar was scraped from the plates and resuspended in 5 ml LB broth (supplemented with 20 mM $MgSO_4$ and 10 mM $CaCl_2$). Upon addition of 400 µl chloroform, the suspension was vigorously vortexed and incubated on a turning wheel at 4°C o/n. Cell debris was collected by centrifugation (15 min; 4,000 rpm; 4°C). The supernatant was transferred to a fresh glass storage tube and supplemented with 200 µl chloroform. Phage lysates were stored at 4°C.

For transduction, recipient cells were grown to an OD_{600} of 1.0. 100 µl culture were mixed with P22 lysate (1-50 µl) and incubated at RT for 20 min. Phage transduction was stopped by the addition of EGTA (final concentration: 10 mM) and transductants were selected on LB plates supplemented with the appropriate antibiotic.

6.12.15 One-step integration into the chromosome

Single mutant derivatives in *Salmonella* and *E. coli* strains were constructed by the λRED recombinase one-step inactivation method according to (Datsenko & Wanner, 2000) with modifications. Competent cells were prepared from strains carrying the helper plasmid pKD46 and which were grown at 28°C to an OD_{600} of 0.5 in LB supplemented with ampicillin and L-arabinose (0.2%) to induce λRED recombinase expression. Cells were electroporated in the presence of 200-500 ng of the DNA fragment to be integrated. For disruption of genes, a Kan^R cassette flanked by FRT sites was amplified from pKD4 using oligos carrying gene-specific sequences corresponding to the chromosomal region to be deleted. Likewise, promoter elements or point mutations linked to different resistance cassettes were amplified from plasmids carrying the respective sequences and integrated by recombination. N-terminal 3xFLAG-tagged strains were obtained by replacing the stop codon of the respective gene by a 3xFLAG::Kan^R-encoding sequence amplified from pSUB11 (Uzzau et al, 2001). Mutants were

selected on LB plates supplemented with the appropriate antibiotics and screened by colony PCR.

To eliminate the Kan^R cassette flanked by FRT sites of λRed-derived mutants, cells were transformed with the FLP recombinase expression plasmid pCP20 (Datsenko & Wanner, 2000). Mutant susceptibility to kanamycin and loss of the temperature-sensitive FLP expression plasmid were tested by streaking strains on LB plates and LB plates supplemented with ampicillin or kanamycin. Clones only able to grow in the absence of antibiotics were selected.

6.12.16 Construction of *Salmonella* chromosomal *rydC'::lacZ*$^+$ reporter fusions

The single copy transcriptional *lacZ* fusions in the *Salmonella* chromosome were constructed as in (Ellermeier et al, 2002). Mutant strains deleted for the sequences to be replaced by the *lacZ* fusion were obtained by the λRED recombinase protocol using a DNA fragment generated by PCR amplification on pKD4. The Kan^R cassette was removed by pCP20 and mutants were transformed with pKG136 in the presence of pCP20. Transformants were screened for the integration of *lacZY* on LB plates supplemented with kanamycin and X-Gal and verified by colony PCR.

6.12.17 Construction of a *E.coli* chromosomal P*rydC'::lacZ*$^+$ reporter fusion

The single copy transcriptional P*rydC'::lacZ*$^+$ fusion in the *E. coli* chromosome was constructed as in (Mahr, 2012). Briefly, a single-mutant of *ydcA* (Keio collection strain JW1416; replacement by Kan^R), the 5' flanking gene of *rydC* in *E. coli* located on the opposite strand, served as template to amplify a fragment comprising the 5' end of the Kan^R cassette and the promoter region of *rydC* including the first five nucleotides of the sRNA (oligo set JVO-7861*'single copy kan rev'). The resulting product was re-amplified (oligo set 'lac promoter fusion rev'*'single copy kan rev') and integrated using the λRED recombinase protocol into AB3025. Obtained clones were screened by colony PCR (oligo set 'single copy kan rev'*pMC847 lac rev), and moved in between strains by P1 transduction.

6.12.18 Screening for transcriptional regulators by transposon insertion

To obtain transposon insertion mutants, *Salmonella rydC'::lacZ*$^+$ reporter strains were either transduced with P22 donor lysates (Tn10::Tet^R library; provided by J. Casadesus, University of Seville) or transformed with the Ez-Tn5 transposome according to the manufacturer's instructions.

In *E. coli*, insertion mutants were generated by conjugation of a Tn*mariner::*Kan^R transposon from a conjugation-competent donor into the *rydC'::lacZ*$^+$ reporter strain. Briefly, both donor (JVS-9452) and recipient (JVS-9438 + pKF132-1) were grown in LB to an OD_{600} of 1.3. For mating, the donor strain (250 µl or 2.5 ml) was collected by vacuum filtration on a 0.45 µm sterile filter and cells were washed twice with LB to remove medium containing ampicillin. Adjacently, the acceptor strain was added (2.5 ml), and filters were incubated on a prewarmed

LB plate at 37°C for 5h. Cells were recovered from the filter in 2.5 ml LB, and conjugants were selected on plates containing X-Gal, kanamycin and chloramphenicol.

Transposon insertions in selected clones were mapped by sequencing of genomic DNA prepared with the Masterpure DNA purification Kit using a oligo specific for the integrated resistance cassette (Tet^R: JVO-2475; $DHFR^R$: JVO-5236; Kan^R: JVO-0216)

6.12.19 Determination of *lacZ* activity (β-galactosidase assay)

Levels of ß-galactosidase expressed from single-copy transcriptional *lacZ* fusions were assayed from three biological replicates as follows: at selected time-points, cells were collected by centrifugation (2 min; 16,000 rcf; 4°C) and resuspended in Z-Buffer to a final concentration of 1 OD/ml. After the addition of 0.15 vol. equiv. chloroform and 0.1 vol. equiv. 0.1% SDS, samples were vigorously vortexed for 15 sec and stored on ice. In a microtiter plate, 200 µl of each cell lysate were mixed with 40 µl ONPG (40 mg/ml) and the absorbances at OD_{405} and OD_{600} were determined at 28°C over time (0-45 min) with a Victor3 plate reader. Relative ß-galactosidase levels were calculated at time-points at which the absorbance of *o*-nitrophenol (OD_{405}) increased linearly with time and was within the linear response range of the detector. Absorbance at OD_{600} was measured to control for the amounts of cell debris.

6.13 Molecular biological methods

6.13.1 Determination of concentration of nucleic acids

DNA and RNA concentrations were determined using a NanoDrop2000.

6.13.2 Preparation of plasmid DNA

Plasmid DNA was extracted from bacterial cells using the NucleoSpin Plasmid QuickPure kits (Mini and Midi scale) according to the manufacturer's instructions.

6.13.3 Polymerase chain reaction (PCR)

DNA fragments of interest were amplified by PCR using *Taq* DNA polymerase or Phusion polymerase and the DNA oligonucleotides listed in Table 6.7. For screening of bacterial transformants, cells were picked from plates and streaked into tubes to serve as template in colony PCR. PCR products were purified using the QIAquick PCR Purification kit according to he manufacturer's instructions. Single-nucleotide exchanges, the deletion or addition of sequence stretches were introduced by amplification of the original plasmids and self-ligation of purified PCR products.

	Taq polymerase			Phusion polymerase		
Reagents						
DNA template	~ 100 ng			< 100 ng		
Reaction buffer	5 µl (10X)			10 µl (5X)		
dNTPs	100 µM			200 µM		
Primer forward	1 µM			1 µM		
Primer reverse	1 µM			1 µM		
DNA polymerase	1.25 U			0.5 U		
Water	ad 50 µl			ad 50 µl		
Program	Temp.	Time	Cycles	Temp.	Time	Cycles
Initialization:	95°C	5’	1	98°C	3‘	1
Denaturation:	95°C	30’’	30-35 x	98°C	20’’	30-35 x
Primer annealing:	55-60°C	30’’		55-60°C	20’’	
Elongation:	72°C	1’ – 3’30		72°C	1’ – 3’30	
Final Elongation:	72°C	5’	1	72°C	5’	1

6.13.4 Agarose gel electrophoresis of DNA

DNA fragments of different sizes were separated using 0.8 to 4% (w/v) agarose gels in 1X TAE buffer as described in (Sambrook, 2001). Prior to loading, samples were mixed with DNA loading buffer (ratio 4:1) and separated at 100 V for 20-100 min. GeneRuler 1kB DNA ladder or pUC Mix Marker 8 served as size standards. DNA fragments were visualized by the addition of RedSafe (0.02% (v/v)) to agarose gel solutions or stained post running with ethidium bromide (0.5 µg/ml in TAE). If desired, DNA fragments were excised from gels under UV light and recovered using the QIAquick Gel Extraction Kit.

6.13.5 Restriction digest and DNA ligation

PCR fragments amplified to obtain plasmid variants were incubated with DpnI for 1h at 37°C to digest template DNA. All other restriction enzyme digests were performed in the buffers and under the conditions suggested by the manufacturer.

Digested DNA fragments and linearized vectors were ligated by T4 DNA ligase and reactions as described in (Sambrook, 2001) prior to transformation into chemically competent *E. coli*.

6.14 RNA techniques

6.14.1 RNA purification using TRIzol

To obtain total RNA samples for Northern blot analysis, 0.2 vol. equiv. Stop-Mix (95% ethanol, 5% phenol) were mixed with culture aliquots corresponding to an OD_{600} of 4, and samples were shock-frozen in liquid nitrogen. In case RNA was to be prepared from cells grown in M9 minimal medium, samples were collected without Stop-Mix, spun immediately (10 min; 4,000 rpm; 4°C), and pellets were frozen in liquid nitrogen.

For RNA preparation, cells were collected by centrifugation (15 min; 4,000 rpm; 4°C), the supernatant was removed and the pellet was resuspended in 1 ml TRIzol. The sample was transferred to a phase lock tube and 400 µl chloroform were added. The mixture was vigorously shaken, incubated for 5 min at RT and adjacently centrifuged (15 min; 13,000 rpm; 4°C). The aqueous layer was transferred into a fresh tube and RNA was precipitated by addition of 450 µl of isopropanol for 30 minutes at RT. Samples were centrifuged (30 min; 13,000 rpm; 4°C) and the supernatant was removed. RNA pellets were washed with 75 % ethanol and air-dried. RNA pellets were resuspended in sterile water. For RNA analysis by denaturing PAGE, RNA was diluted in H_2O and 1X GLII.

6.14.2 Hot Phenol method for RNA purification

RNA was prepared by the Hot Phenol method for primer extension analysis and RNA sequencing. To this end, bacterial cell pellets (obtained as in 2.5.6) were resuspended in 600 µl lysozyme solution (0.5 mg/ml lysozyme in TE buffer, pH 8.0) and 60 µl of 10% (w/v) SDS were added. The suspension was mixed by inversion and incubated at 64 °C in a water bath for 1 to 2 minutes. The pH was equilibrated by addition of 66 µl of sodium acetate (pH 5.2), and samples were mixed with 750 µl phenol. Tubes were incubated at 64 °C for 6 minutes and frequently mixed. Upon 1 min chilling on ice, samples were centrifuged (10 min; 13,000 rpm; 4°C) to ensure phase separation. The aqueous layer was transferred to a phase lock tube, mixed with 750 µl chloroform and centrifuged again (10 min; 13,000 rpm; 4°C). RNA was precipitated from the aqueous layer by addition of 1.4 ml of a 30:1 ethanol:sodium acetate (pH 6.5) mix. RNA pellets were washed with 75% ethanol and air-dried. RNA was resuspended in sterile water. For RNA analysis by denaturing PAGE, RNA was diluted in H_2O and 1X GLII.

6.14.3 RNA purification using SV Total RNA Isolation System

RNA purified using the SV Total RNA Isolation System was employed in RT-PCR and microarray experiments. Bacterial cell pellets (obtained as in 2.5.6) were resuspended in 100 µl lysozyme solution (50 mg/ml in H_2O) and samples were incubated for 4 min at room temperature. The samples were mixed with 75 µl of lysis reagent and 350 µl RNA dilution buffer were added. The lysates were incubated for 3 min at 70°C and adjacently, cell debris was collected by

centrifugation (10 min; 13,000 rpm; RT). In a fresh tube, the supernatant was mixed with 200 µl 95% ethanol and loaded on a spin column provided with the kit. After centrifugation (1 min; 13,000 rpm; RT) the eluate was discarded and the column was washed with 600 µl wash buffer. After an additional centrifugation step (1 min; 13,000 rpm; RT), 50 µl of a DNase I mix (5 µl 90 mM $MnCl_2$, 40 µl DNase I core buffer and 5 µl DNase I; all provided with the kit) was applied to the membrane and samples were incubated for 15 min at room temperature. Digestion was stopped by the addition of 200 µl DNase I stop mix and the columns were centrifuged (1 min; 13,000 rpm; RT). Following two wash steps with 600 µl and 250 µl wash buffer, respectively (1 min and 2 min; 13,000 rpm; RT), the column was transferred to a sterile tube and 100 µl RNase-free water were added. After incubation for 1 min at room temperature the RNA was eluted by centrifugation (2 min; 13,000 rpm; RT).

6.14.4 DNase I digest

To remove residual DNA from RNA preparations, 10 µg of RNA were treated with 1 U DNase I in the presence of 1X reaction buffer (+$MgCl_2$), at 37°C for 30 min. RNA was purified by P:C:I extraction and precipitated with 3 vol. equiv. of 30:1 ethanol:sodium acetate (pH 6.5) mix.

6.14.5 5'RACE

Rapid amplification of cDNA ends (RACE) to determine RNA 5' ends was performed as in (Argaman et al, 2001) with modifications. 5 µg of DNA-free RNA (in 5 µl H_2O) were mixed with 5 µl of 10X TAP buffer and 0.25 µl SUPERaseIn RNase inhibitor. Reactions were split in two, and either supplemented with 2.5 U tobacco acid pyrophosphatase (TAP) or H_2O (negative control) before being incubated at 37°C for 30 min. 150 pmol of RNA-linker A4 were added to both reactions prior to P:C:I extraction and precipitation with 3 vol. equiv. of 30:1 ethanol:sodium acetate (pH 6.5) mix (-20°C, 3 h). The RNA pellet was dissolved in 13.5 µl H_20, denatured for 5 min at 95°C and chilled on ice for 5 min. The RNA-linker ligation was performed o/n at 16°C in the presence of 10 U T4 RNA ligase, 1X RNA ligase buffer, 10% (v/v) DMSO and 10 U SUPERaseIn RNase Inhibitor. Following P:C:I extraction and precipitation with 3 vol. equiv. of 30:1 ethanol:sodium acetate (pH 6.5) mix (-20°C, 3 h), 2 µg linker-ligated RNA were denatured at 65°C for 5 min and adjacently converted to cDNA using 100 pmol random hexamer primers and 200 U Superscript III reverse transcriptase according to the manufacturer's instructions. Prior to enzyme addition, samples were incubated at 25°C for 10 min. Reverse transcription was carried out in a series of incubation steps (41°C for 15 min; 50°C for 15 min; 55°C for 15 min; 60°C for 15 min). The enzyme was inactivated at 85°C for 5 min and RNA was digested in the presence of 1 U RNase H at 37°C for 20 min.

5' fragments of RNAs were amplified with Taq polymerase by PCR from the cDNA templates (1 µl in 50 µl reactions) using a gene-specific primer (SdsR: JVO-0997; RydC: JVO-0925; *cfa* mRNA: JVO-7022) in combination with JVO-0367 (antisense to the RNA linker). Cycling

conditions were as follows: 95°C for 5 min; 35 cycles of 95°C for 40 sec, 56°C for 40 sec, 72°C for 40 sec; and 72°C for 8 min). The PCR products were separated on 3% agarose gels. Selected bands were purified and subcloned using the TOPO TA Cloning Kit as recommended by the manufacturer. Inserts of obtained clones were amplified by PCR (M13fwd/M13rev) and analyzed by sequencing.

6.14.6 3'RACE

3'RACE experiments were carried out following the protocols in (Argaman et al, 2001) and (Pfeiffer et al, 2009) with a few modifications. Briefly, 7.5 µg of total DNA-free RNA was dephosphorylated with 10 U calf intestine alkaline phosphatase (CIP) in the presence of 1X NEB buffer 3 in a total volume of 25 µl at 37°C for 1 h. Following P:C:I extraction, the RNA was precipitated from the aqueous phase together with 250 pmol of RNA adapter E1 and 15 µg GlycoBlue using 3 vol. equiv. of 30:1 ethanol:sodium acetate (pH 6.5) mix. For ligation of the RNA linker, the pellet was resuspended in H_2O and dissolved at 65°C for 10 min. Hereafter, a 20 µl reaction containing 20 U T4 RNA ligase, 1X T4 RNA ligase buffer, 10% (v/v) DMSO and 10 U SUPERaseIn RNase Inhibitor was incubated at 16° overnight. The ligated RNA was P:C:I-extracted and precipitated with 3 vol. equiv. of 30:1 ethanol:sodium acetate (pH 6.5) mix. The RNA was reverse transcribed for 5 min at 50°C and 60 min at 55°C in the presence of adapter E1-specific oligo E3 RACE (39 pmol) using 200 U SuperscriptIII reverse transcriptase in a 20 µl reaction mix (1X FS buffer, 2 mM dNTPs, 5 mM DTT, and 10 U SUPERaseIn RNase Inhibitor). Template RNA was digested by RNase H. To identify *ompD*-specific fragments, 1 µl aliquots of the RT reaction were used as the template in a PCR reaction with 1 mM each linker-specific primer, E3 RACE, and gene-specific primer, JVO-2678 (binding at the transcriptional start of *ompD* mRNA), 1.25 U Taq-DNA polymerase, 1X ThermoPol buffer, and 1.5 mM dNTPs. Cycling conditions were as follows: 95°C for 5 min; 35 cycles of 95°C for 40 sec, 58°C for 40 sec, and 72°C for 50 sec; and 72°C for 5 min. The PCR products were resolved on 3.5% agarose gels. Selected bands were purified and subcloned using the TOPO TA Cloning Kit as recommended by the manufacturer. Inserts of obtained clones were amplified by PCR (M13fwd/M13rev) and analyzed by sequencing.

6.14.7 Quantitative RT-PCR

Quantitative real-time PCR (qRT-PCR) was described previously (Papenfort et al, 2006). Briefly, RNA was isolated using the SV40 Total RNA Isolation kit. Expression of *cfa* mRNA was quantitatively assessed by qRT-PCR in a CFX96 RealTime System (Biorad), with the *rrsA* gene as reference. For each reaction (25 µL final vol.), 1 µl of RNA sample (100 ng/reaction) was mixed with 0.25 µl of primer pairs (0.5 µM final) and 12.5 µL of SYBR Green mix (Qiagen). For coupled cDNA synthesis and target gene amplification, 0.25µl of Quantitect RT mix was added. Each sample was assayed in triplicate for each run. Reaction conditions were: 30 min 50°C, 15 min

95°C, and 45 cycles at 94°C for 20 sec, 60°C for 40 sec, and 72°C for 40 sec. Primer sets used in this experiment: JVO-1472*JVO-1473 (*cfa*), JVO-1977*JVO-1978 (*rrsA*).

6.14.8 Denaturing PAGE

To prepare gels used for separation of RNA in denaturating polyacrylamide gel electrophoresis (PAGE), PAA gel solution was mixed with 0.01 vol. equiv. ammonium persulfate (APS; 10% (w/v)) as well as 0.001 vol. equiv. vol. of TEMED to initiate polymerization. Prior to loading, RNA samples (in 1X GLII) were denatured at 95°C for 5 min and chilled on ice for 5 min. Gels were run in the presence of 1X TBE at 300 V (Northern blots) or at 40 W (sequencing gels) at room temperature.

6.14.9 Native PAGE

Preformed RNA-protein complexes were analyzed by native PAGE using gels prepared from 6% PAA solution lacking urea, and the PAA gel solution was mixed with 0.01 vol. equiv. APS (10% (w/v) as well as 0.001 vol. equiv. volume of TEMED to initiate polymerization. Samples were diluted in 1X Native sample loading buffer and separated in the presence of 0.5X TBE at 300 V. To avoid heating, the gel apparatus was connected to a water cooling system that maintained the gel at a constant temperature of 4°C.

6.14.10 Northern blot analysis

For sRNA and mRNA detection, 5 or 10 µg of total RNA (in 1X GLII) and γ-^{32}P-labelled pUC Mix Marker 8 were resolved on 4-12%/7M urea polyacrylamide gels. RNA was transferred to Hybond-XL membranes by electro-blotting (1 h, 50 V, 4°C) in a tank electroblotter in the presence of 1X TBE. RNA was cross-linked to the membrane by UV light (120 mJ) and the membranes were pre-hybridized in 15 ml RotiHybriQuick at 42°C for 1 h prior to addition of gene-specific 5' end-labelled DNA-oligonucleotides or riboprobes (Table 6.11). Hybridization conditions and SSC concentrations of the three subsequent washing steps (15 min each) are summarized in Table 6.12. Membranes were sealed and exposed to imaging plates. Signals were determined on a Typhoon FLA 7000 phosphorimager and band intensities quantified with AIDA software.

Table 6.11 Probes for Northern blot detection.

recognized RNA	probe	comment	used in Fig.
5S rRNA	oligo JVO-0322		2.1; 2.3; 2.4; 2.5; 2.6; 2.7; 2.10; 2.11; 2.12; 2.13; 2.14; 2.16; 2.17; 2.19; 2.20; 2.21; 2.22; 2.23; 3.2; 3.5; 3.8; 3.9; 3.11; 3.14; 3.16; 3.30
cfa mRNA	oligo JVO-3707	specific for *cfa* mRNA initiating from distal start site	3.8; 3.26
InvR	oligo JVO-0222		2.21
MicC	riboprobe	template: JVO-0905*JVO-0986	2.21

ompD mRNA	oligo JVO-4314		2.12; 2.13; 2.14; 2.16; 2.17; 2.19; 2.22; 2.23
osmY mRNA	riboprobe	template: JVO-7692*JVO-7693	2.6; 2.7
RybB	oligo JVO-1205		2.21; 2.22; 2.23
RydC	oligo JVO-4363		3.5; 3.8; 3.14; 3.16
RydC	riboprobe	template: JVO-0975*JVO-4378	3.2; 3.9; 3.11; 3.30
SdsR	riboprobe	template: JVO-0902*JVO-0997	2.1; 2.6; 2.7; 2.21; 2.22; 2.23
SdsR	oligo JVO-1032		2.3; 2.4; 2.5; 2.10; 2.11; 2.12; 2.13; 2.14; 2.16; 2.19
SraC	oligo JVO-2309		2.10; 2.11
TMA	oligo JVO-0396		2.13; 2.20; 3.16

Table 6.12 Washing conditions used for the different radiolabelled probes.

Radiolabelled probe	Hybridization temperature	SSC concentration for washing steps	Washing temperature
Oligonucleotide	42°C	5X, 1X, 0.5X	42°C
Riboprobe	68°C	2X, 1X, 0.5X	42°C, 68°C, 68°C

6.14.11 Generation of radiolabelled DNA oligonucleotides for RNA detection

For labelling, 1 pmol of the oligo was incubated with 25 µCi of γ-^{32}P-ATP in the presence of 1 U polynucleotide kinase (PNK) and 1X PNK buffer for 1 h at 37°C in a 20 µl reaction. Unincorporated nucleotides were removed using Microspin G-25 Columns.

6.14.12 Generation of radiolabelled RNA transcripts (riboprobes) for RNA detection

DNA templates for T7 *in vitro* transcription of riboprobes were amplified by PCR from template plasmids or genomic DNA using gene specific primer sets. *In vitro* transcription was performed with the MAXIscript kit using 200 ng of template DNA in the presence of 25 µCi α-^{32}P-UTP at 37°C for 1 h. Following DNase I digestion (1 U; 15 min; 37°C), the riboprobes were purified over a MicroSpin G50 column.

6.14.13 Determination of RNA stability

To determine RNA stability, cultures were grown in triplicates to appropriate growth phases when transcription was inhibited by the addition of rifampicin (final concentration: 500 µg/ml). Prior to, and at 2, 4, 8, 16 as well as 32 min post rifampicin treatment, culture aliquots were mixed with 0.2 vol. equiv. Stop-Mix (95% ethanol, 5% phenol) and samples were frozen in liquid nitrogen. RNA was prepared, and either quantified on Northern blots or by qRT-PCR.

6.14.14 Primer extension analysis

For primer extension, 10 µg of RNA samples (in 8 µl H_2O) prepared by the Hot Phenol method were denaturated in the presence of 1 pmol 5' end-labelled primer at 70°C for 2 min and adjacently chilled on ice for 5 min. Next, 5 µl of reaction mix (3 µl 5X First strand buffer, 5 mM

DTT, 0.5 mM each dATP, dGTP, dCTP and dTTP) were mixed with the samples at 42°C, and 1 µl SuperScript III (100 U; diluted 1:1 in H_2O) were added. cDNA synthesis was performed at 50°C for 60 min, followed by incubation at 70°C for 15 min to inactivate the enzyme. Samples were RNase H-treated (1 µl; 2.5 U) for 15 minutes at 37 °C and the reaction was stopped by the addition of 10 µl GLII loading buffer. 12 µl of the samples were separated electrophoretically together with 10 µl of 1:10-diluted template-specific ladder (prepared using the SequiTherm EXCELII DNA Sequencing Kit; Table 6.13) on 6-8 % sequencing constant power of 40 W. Gels were dried and signals were determined on a Typhoon FLA 7000 phosphorimager.

Table 6.13 Gene specific ladders for primer extension and 30S toeprint analysis.

sequencing ladder	template preparation
P_{own} *cfa*	JVO-7049*JVO-7022 on gDNA
$DHFR^R$::P_{LTetO1} *cfa*	JVO-5237*JVO-7022 on JVS-9908
Cm^R::P_{LTetO1} *cfa*	JVO-4055*JVO-0155 on pKF31-1
Cm^R::P_{LTetO1} TSS1-*cfa-X::gfp*	pZE-Cat*JVO-0155 on pKF133-1

6.14.15 *In vitro* transcription and 5' end-labelling of RNA

For RNA *in vitro* synthesis, ~200 ng of template DNA carrying a T7 promoter sequence were amplified by PCR (see Table 6.14) were reverse transcribed employing the T7 MEGAscript kit according to the manufacturer's instructions. Following P:C:I extraction and precipitation by 3 vol. equiv. 30:1 ethanol:sodium acetate (pH 6.5) mix, the correct size and integrity of the RNA were confirmed by denaturing PAGE. Gels were stained using StainsAll solution.

For 5' end-labelling, 20 pmol RNA were dephophorylated by CIP-treatment (10 U) at 37°C for 1 h. Following P:C:I extraction, the RNA was precipitated by 3 vol. equiv. 30:1 ethanol:sodium acetate (pH 6.5) mix in the presence of 20 µg GlycoBlue at -20°C o/n. Next, the RNA was 5' phosphorylated at 37°C for 1 h by 1 U PNK in the presence of 20 µCi γ-^{32}P-ATP. Unincorporated nucleotides were removed using Microspin G-50 columns, and labelled RNA was separated by denaturing PAGE. Upon exposure of the gel to imaging plates and determination of signals by phosphorimaging, RNA was cut and recovered from the gel by elution at 4°C o/n in RNA elution buffer. Labeled RNA was purified by P:C:I extraction, and quantified by NanoDrop measurement.

Table 6.14 Templates for T7 *in vitro* synthesis.

RNA	template preparation
RydC	JVO-4721*JVO-4722 on pKF42-1
RydC*	JVO-7053*JVO-4722 on pKF86-1
RydC-K1	JVO-5165*JVO-4722 on pKF60-1
SdsR	JVO-7023*JVO-7025 on pKF68-3
cfa mRNA (TSS1-CDS+70)	JVO-4558*JVO-6516 on gDNA
cfa mRNA (TSS1 to -72)	JVO-4558*JVO-9044 on pKF31-1
TSS1-*cfa-X::gfp* mRNA	JVO-4558*pZE-T1 on pKF133-1
ompX::gfp mRNA	JVO-9004*pZE-T1 on pKP60-1

6.14.16 Determination of sRNA *in vivo* copy number

To determine sRNA copy numbers over growth, RNA was prepared from culture aliquots corresponding to exactly an OD_{600} of 4. RNA pellets were resuspended in 20 µl of H_2O, and 5 µl RNA (corresponding to an OD_{600} of 1.0) were mixed with 5 µl GLII and subjected to Northern blot analysis. Signals were compared to serial dilutions of sRNA *in vitro* transcripts (0.5/1/2.5/5/10/20 ng for SdsR; 0.05/0.1/0.5/1/2.5/5 ng for RydC) on Northern blots hybridized with gene-specific riboprobes. Calculations of RNA levels per cell were based on determination of viable cell counts per OD_{600} in (Sittka et al, 2007).

6.14.17 Electrophoretic mobility shift assay (EMSA)

Formation of complexes between sRNAs and Hfq *in vitro* was analyzed by gel shift assays. 5' end-labelled RNA (4 pmol) was denatured (95°C, 2 min), chilled on ice for 5 min and supplemented with 1X structure buffer and 1 µg yeast RNA. Upon addition of purified Hfq (concentration as indicated in the figure legends) or Hfq dilution buffer (control), samples were incubated at 37°C for 10 min. Prior to loading, reactions were mixed with Native loading buffer, and separated by native PAGE. Gels were dried and signals were determined on a Typhoon FLA 7000 phosphorimager.

6.14.18 *In vitro* structure probing

In vitro structure probing and mapping of RNA/Hfq footprints was conducted on *in vitro* synthesized and 5' end-labelled mRNA. Upon denaturation at 70°C for 2 min, RNA was chilled on ice. Next, 0.2 pmol 5' end-labelled mRNA were mixed with Hfq (0.2 pmol) or Hfq dilution buffer in the presence of 1X structure buffer and 1 µg yeast RNA and samples were incubated at 37°C for 10 min. Subsequently, unlabelled sRNA (2 pmol) or water were added, and reactions were kept at 37°C for additional 10 min. For digestion, samples were treated with 0.1 U RNase T1 for 2 min or with lead(II) acetate (final concentration: 5mM) for 1.5 min. Reactions were stopped by

addition of 2 vol equiv. Precipitation/Inactivation buffer and precipitated at -20°C for 1h. Pellets were washed with 70% ethanol, and resuspended in GLII.

To prepare RNase T1 sequencing ladders, 0.4 pmol 5' end-labelled mRNA were denatured (95°C, 2 min) in the presence of 1X sequencing buffer and chilled on ice. 0.1 U RNase T1 was added, and RNA was digested for 5' at 37°C. Alkaline (OH) sequencing ladders were prepared by incubating 0.4 pmol 5' end-labelled mRNA at 95°C for 5 min in the presence of alkaline hydrolysis buffer. Reactions were stopped by addition of 1 vol equiv. GLII.

Samples were denatured prior to loading (95°C, 2 min) and separated by denaturing PAGE on 6-10 % sequencing gels at constant power of 40 W. Gels were dried and signals were determined on a Typhoon FLA 7000 phosphorimager.

6.14.19 30S toeprint analysis

In vitro 30S toeprint experiments were carried out as in (Hartz et al 1988; Udekwu 2005) with few modifications. For annealing of the primer, an unlabelled mRNA fragment (0.2 pmol) and 0.5 pmol 5' end-labelled oligo (JVO-0155; binding ~120 nt downstream of AUG in *gfp*) were denatured in the presence of 0.8 µl SB 5X -Mg in a total volume of 3 µl at 90°C for 1 min and adjacently chilled on ice for 5 min. Next, 1 µl dNTPs (5 mM each) and 1 µl SB 1X Mg60 were added, and samples were shifted to 37°C. Reactions were supplemented with Hfq (0.2 pmol) or Hfq dilution buffer, and incubated for 10 min when either unlabelled sRNA (2 pmol) or water were added. Upon an additional incubation time of 10 min, samples were mixed with 2 pmol purified 30S ribosomal subunit (or SB 1X Mg10 for the control). After 5 min, 10 pmol uncharged $tRNA^{fMet}$ (or SB 1X Mg10 for the control) was added to the samples and reactions were incubated for additional 15 min before reverse transcription was initiated by addition of 100 U SuperScriptII. Following cDNA synthesis for 20 min, reactions were stopped with 100 µl Toeprint Stop Solution. RNA was digested by alkaline hydrolysis in the presence of KOH at 90°C for 5 min, and cDNA was precipitated in the presence of 1 µg GlycoBlue at -20°C o/n. Samples were denatured prior to loading (95°C, 2 min) and separated in the presence of gene specific sequencing ladders (prepared using the SequiTherm EXCELII DNA Sequencing Kit; see Table 6.13) by denaturing PAGE on 6-8 % sequencing gels at constant power of 40 W. Gels were dried and signals were determined on a Typhoon FLA 7000 phosphorimager.

6.14.20 *In vitro* RNase E cleavage assay

For *in vitro* RNase E cleavage assays of unlabelled *cfa* mRNA (TSS1-CDS+70), *in vitro* transcribed RNA was denatured at 70°C for 2 min and adjacently incubated on ice for 3 min and at room temperature for additional 3 min. 2 pmol mRNA (in 2 µl H_2O) were mixed with 4 µl 2X RNase E reaction buffer, and either Hfq (2 pmol), or Hfq dilution buffer was added to the samples. Upon incubation at 37°C for 10 min, sRNA (20 pmol) or water were added, and reactions were kept at 37°C for additional 10 min. Next, samples were incubated in the presence of 3 pmol purified

RNase E NTD (N-terminal domain; kindly provided by K. Bandyra, Luisi lab, University of Cambridge) at 37°C. Samples were withdrawn prior to and at various time-points after RNase E addition, and reactions were stopped by addition of 25 µl Precipitation/Inactivation buffer and 5µl 100 mM EDTA and precipitated at -20°C for 1h. Samples were collected by centrifugation (30 min; 16,000 rcf; 4°C), washed with 70% ethanol, and pellets were resuspended in GLII.

The time-course RNase E cleavage assay with 5' end-labelled *cfa* mRNA was performed following the same protocol, but with modifications in employed RNA and protein amounts: *cfa* mRNA (TSS1-CDS+70): 0.2 pmol; Hfq: 0.2 pmol; RydC and RydC* sRNA: 2 pmol; RNase E NTD: 0.5 pmol.

6.15 Transcriptome analyses

6.15.1 Microarray experiments

The first microarray dataset analyzed in this study based on pulse expression of RydC (carrying two additional nucleotides at the 5' end; chapter 4.2) from pJV766-21 was performed by K. Papenfort. Data were obtained using chips including PCR products of all the genes present in the sequenced *S.* Typhimurium strain LT2 and additional 229 genes specific to *S.* Typhimurium strain SL1344. Details of all the amplicons can be found at http://www.ifr.ac.uk/Safety/MolMicro/pubs.html.

In contrast, custommade arrays from Agilent Technologies (Agilent AMADID Designcode: 026881) were employed in the second microarray experiment of this study comparing transcriptome changes upon pulse over-expression of RydC from pKF41-2 (chapter 3.3). These chips comprise 13,268 60-mer *S.* Typhimurium strain SL1344-specific oligonucleotides supplemented with 360 60-mer oligonucleotides specific for 149 *Salmonella* sRNAs.

The experimental design of both microarray studies involved the use of *Salmonella* serovar Typhimurium genomic DNA as the co-hybridized control for one channel on all microarrays. This method has the advantage of allowing the direct comparison of multiple samples. Total RNA and chromosomal DNA were labelled by random priming according to the protocols described at IFR (Instiute for Food Research, Norwich, UK) website (http://www.ifr.bbsrc.ac.uk/safety/microarrays/protocols.html) with few modifications.

RNA samples were collected (in duplicates) from JVS-0291 carrying either control plasmid pKP8-35 or pKF42-1. Cells were grown in LB to OD_{600} of 1.5 when expression from the pBAD promoter was induced by addition of arabinose. Samples collected prior to and 10 min post arabinose-treatment were used in the microarray experiment

10 µg of DNaseI-digested RNA (purification by the SV Total RNA Isolation System) were mixed with 5 µg of random hexamers in a total volume of 9.4 µl, incubated at 70 °C for 5 min and adjacently chilled on ice for 10 min. 4.6 µl of reaction mix (2.0 µl 10X RT buffer, 2.0 µl 0.1 M DTT,

0.6 µl 50X dNTPs, 2 µl Cy3-dCTP, 4 µl Stratagene AffinityScript multi-temperature Reverse Transcriptase) were added. Samples were incubated at 25°C for 10 min and adjacently at 42°C o/n. Next, RNA was hydrolyzed by incubation of samples for 10 min at 70°C in the presence of 0.1 M NaOH. The solution was neutralized by the addition of 15 µl of 0.1 M HCl and purified using the QIAquick PCR Purification kit following the manufacturer's instructions.

To label reference DNA, 2 µg of chromosomal DNA (in a final volume of 21 µl) were added to 20 µl of 2.5X Random primer/reaction buffer mix, incubated at 95°C for 5 min and then placed on ice for 5 min. Next, 5 µl 10X dNTP mix (1.2 mM each dATP, dGTP, dTTP, 0.6 mM dCTP, 10 mM Tris pH 8.0, 1 mM EDTA), 3 µl Cy5 dCTP and 1 µl Klenow enzyme were added to the sample. The reaction mixture was incubated at 37 °C overnight. Labeled DNA samples purified using the QIAquick PCR Purification kit.

Each Cy3-labelled cDNA sample was mixed with Cy5-labelled chromosomal DNA. Hybridization and raw data generation were performed by the microarray core facility of the Max Planck Institute for Infection Biology (Berlin). Samples were hybridized to the arrays overnight at 65°C according to the manufacturer's instruction. After hybridization, slides were washed and scanned by a G2565CA high resolution laser microarray scanner (Agilent Technologies). Raw microarray image data were analyzed with the Image Analysis/Feature Extraction software G2567AA (Version A.10.5.1, Agilent Technologies). For each array feature both MedianSignals were background corrected by appropriate BGMedianSignal subtraction while signals <10 were adjusted to 10. To compensate for unequal dye incorporation, data centring to zero was performed for each single microarray on one slide. Microarray data were analysed using GeneSpring 7.3 (Agilent) and genes were considered to be differentially expressed if they displayed at least 3-fold changes in both replicates and were statistically significantly different (Student's t-test; $P < 0.15$).

6.15.2 Whole transcriptome sequencing

Differential RNA sequencing was performed as in (Sharma et al, 2010) with modifications. Total RNA was prepared by the Hot Phenol method from *S.* Typhimurium SL1344 (JVS-1574), *S.* Typhimurium 14028S (JVS-0078), *E. coli* MC4100 *relA+* (JVS-0965), *S. flexneri* M90T (JVS-0013) and *Citrobacter rodentium* (JVS-8970) grown in LB to early stationary (OD_{600} of 2.0). Upon DNaseI digestion, integrity of the samples was determined by staining of total RNA separated on denaturing PAA gels. In two separate reactions, 10 µg of RNA (in 34.5 µl H_2O) each were denatured at 90°C for 2 min and adjacently chilled on ice for 5 min. Samples were mixed with 5 µl 10X TDE buffer, 0.5 µl SUPERaseIn and either 10 µl TEX (1 U/µl; TEX+) or 10 µl H_2O (TEX-). Samples were incubated at 30°C for 60 min, and reactions were stopped by addition of 0.5 µl 0.5 M EDTA and 50 µl H_2O. RNA was P:C:I extracted, and precipitated in the presence of 30 µg GlycoBlue with 3 vol. equiv. of 30:1 ethanol:sodium acetate (pH 6.5) mix at -20°C o/n. RNA

samples were collected by centrifugation (30 min; 13,000 rpm; 4°C) and the pellet was resuspended in 16 µl H_2O. RNA concentration was determined by NanoDrop measurement, and both samples were adjacently TAP-treated to enable linker ligation during cDNA library preparation. 15 µl RNA sample were mixed with 2 µl of 10X TAP buffer, 0. 5 µl SUPERaseIn RNase inhibitor, 0.75 µl TAP (10 U/µl) and 1.75 µl H_2O. Samples were incubated at 37°C for 60 min, extracted by P:C:I and precipitated as before in the presence of 10 µg GlycoBlue. RNA pellets were resuspended in 31 µl H_2O, RNA concentration was determined by NanoDrop measurement and RNA integrity was controlled by staining of total RNA separated on denaturing PAA gels.

cDNA libraries for Solexa sequencing were prepared at Vertis Biotechnology AG (Freising, Germany) as described before (Sittka et al, 2008) and sequencing was performed on a Illumina Genome Analyzer IIx machine. cDNA libraries were mapped to the *S.* Typhimurium SL1344, *S.* Typhimurium 14028S, *E. coli* MC4100 *relA+*, *S. flexneri* M90T and *C. rodentium* genomes by K. Förstner (Sharma group/Vogel group; University of Würzburg) as previously described using the segemehl software (Hoffmann et al, 2009; Sharma et al, 2010). For each library, graphs representing the number of mapped reads per nucleotide were calculated and coverage values were normalized by the total number of mapped reads. Graphs were visualized using the Integrated Genome Browser as described previously (Sittka et al, 2008).

6.16 Protein techniques

6.16.1 Preparation of total protein samples

To prepare total protein samples, cells were collected by centrifugation (2 min; 16,000 rcf; 4°C). The supernatant was removed and pellets were resuspended in 1X PLB to a final concentration of 0.01 OD/µl. Protein samples were denatured at 95°C for 5 min.

6.16.2 One-dimensional SDS-PAGE

Total proteins samples were separated according to their electrophoretic mobility by one-dimensional sodium dodecyl sulfate polyacrylamide gel electrophoresis (SDS-PAGE). Samples corresponding to 0.01 to 0.1 OD were loaded on gels consisting of a 4% PAA stacking gel on top of a 10-15% PAA resolving gel, and gels were run at 0.02 to 0.04 A in the presence of 1X TBE buffer. Gels were either stained overnight by PAGE Blue staining solution or subjected to Western blotting.

6.16.3 Western blot analysis

Proteins were transferred onto a polyvinylidene fluoride (PVDF) membrane by semidry blotting. Prior to assembly of the blotting sandwich, the PVDF membrane was equilibrated in methanol

and transfer buffer. Likewise, Whatman paper as well as the gel were wetted in transfer buffer. Transfer was carried out in a semidry blotter at 2 mA/cm^2 membrane for 1.5 h.

Subsequently, immunoblots were blocked with 5% (w/v) non-fat dry milk in 1X TBST for 1 h. Blots were rinsed with 1X TBST and hybridized with antibodies or antisera (diluted in 3% (w/v) BSA in 1X TBST) on a shaker for 1 h at room temperature or at 4°C overnight. After three washing steps (10 min; TBST), membranes were incubated with secondary antibodies conjugated to horseradish peroxidase (HRP; diluted in 3% (w/v) BSA in 1X TBST) on a shaker for 1 h at room temperature. Blots were again washed with TBST as before and (3 times 15 minutes each) the membrane was developed using chemiluminescence detection solution. Signals were detected with an ImageQuant LAS 4000 CCD camera and subsequently analyzed with AIDA software.

6.17 Bioinformatic tools

6.17.1 Sequence retrieval

Information for sequence alignments was collected using BlastN searches (http://www.ncbi.nlm.nih.gov/sutils/genom_table.cgi) of the following genome sequences (accession numbers are given in parentheses): *Citrobacter koseri* ATCC BAA-895 (NC_009792), *Citrobacter rodentium* ICC168 (NC_013716), *Cronobacter turicensis* z30232 (NC_013282), *Dickeya dadantii* Ech 703 (NC_012880), *Escherichia coli* K12 substr. MG1655 (NC_000913), *Enterobacter aerogenes* KCTC 2190 (NC_015663), *Enterobacter* Sp.638 (NC_009436), *Escherichia coli* K12 substr. MC4100(MuLac) BW2952 (NC_012759), *Escherichia fergusonii* ATCC 35469 (NC_011740), *Erwinia pyrifoliae* Ep1/96 (NC_003197), *Klebsiella pneumoniae* 342 (NC_011283), *Pantoea ananatis* LMG 20103 (NC_013956), *Photorhabdus luminescens subsp. laumondii* TT01 (NC_005126), *Salmonella bongori* NCTC 12419 (NC_015761), *Salmonella typhi* Ty2 (NC_004631), *Salmonella* Typhimurium LT2 (NC_003197), *Serratia proteamaculans 568* (NC_009832), *Shigella flexneri* 2a str 301 (NC_004337), *Shigella flexneri* 5 str 8401 (NC_008258), *Sodalis glossinidius str. 'morsitans'* (NC_007712), *Yersinia enterocolitica subsp. enterocolitica* 8081 (NC_008800), *Yersinia pestis* KIM (NC_005088), *Xenorhabdus nematophila* ATCC 19061 (NC_014228).

6.17.2 Alignments

Alignments were calculated using MultAlin (Corpet, 1988): http://multalin.toulouse.inra.fr/multalin/multalin.html

6.17.3 Hybrid predictions

Potential interactions between two RNA molecules were predicted using RNAhybrid (Rehmsmeier et al, 2004): http://bibiserv.techfak.uni-bielefeld.de/rnahybrid/

6.17.4 Secondary structure predictions

RNA secondary structures were predicted using *RNAfold* (Gruber et al, 2008) and pknotsRG (Reeder et al, 2007):

http://rna.tbi.univie.ac.at/cgi-bin/RNAfold.cgi

http://bibiserv.techfak.uni-bielefeld.de/pknotsrg/submission.html

6.17.5 Melting temperature oligos

Melting temperature of oligos was calculated according to (Rychlik et al, 1990)

http://bioinformatics.weizmann.ac.il/blocks/oligo_melt.html

6.17.6 Software

Table 6.15 Employed software.

Software	Manufacturer
Adobe Acrobate X Pro	Adobe Systems
Aida	Raytest
Chromas LITE	Technelysium
CorelDraw X5	Corel
Endnote	Thompson Reuters
Gene Spring 7.3	Agilent
Integrated Genome Browser	Affymetrix
Microsoft Windows and Office	Microsoft

7 References

Aiba H (2007) Mechanism of RNA silencing by Hfq-binding small RNAs. *Curr Opin Microbiol* **10**(2)**:** 134-139

Alba BM, Gross CA (2004) Regulation of the Escherichia coli sigma-dependent envelope stress response. *Mol Microbiol* **52**(3)**:** 613-619

Altuvia S (2007) Identification of bacterial small non-coding RNAs: experimental approaches. *Curr Opin Microbiol* **10**(3)**:** 257-261

Altuvia S, Weinstein-Fischer D, Zhang A, Postow L, Storz G (1997) A small, stable RNA induced by oxidative stress: role as a pleiotropic regulator and antimutator. *Cell* **90**(1)**:** 43-53

Andersen J, Delihas N (1990) micF RNA binds to the 5' end of ompF mRNA and to a protein from Escherichia coli. *Biochemistry* **29**(39)**:** 9249-9256

Andrade JM, Pobre V, Matos AM, Arraiano CM (2012) The crucial role of PNPase in the degradation of small RNAs that are not associated with Hfq. *RNA* **18**(4)**:** 844-855

Antal M, Bordeau V, Douchin V, Felden B (2005) A small bacterial RNA regulates a putative ABC transporter. *J Biol Chem* **280**(9)**:** 7901-7908

Apirion D (1978) Isolation, Genetic-Mapping and Some Characterization of a Mutation in Escherichia-Coli That Affects Processing of Ribonucleic-Acid. *Genetics* **90**(4)**:** 659-671

Argaman L, Altuvia S (2000) fhlA repression by OxyS RNA: kissing complex formation at two sites results in a stable antisense-target RNA complex. *J Mol Biol* **300**(5)**:** 1101-1112

Argaman L, Hershberg R, Vogel J, Bejerano G, Wagner EG, Margalit H, Altuvia S (2001) Novel small RNA-encoding genes in the intergenic regions of Escherichia coli. *Curr Biol* **11**(12)**:** 941-950

Baba T, Ara T, Hasegawa M, Takai Y, Okumura Y, Baba M, Datsenko KA, Tomita M, Wanner BL, Mori H (2006) Construction of Escherichia coli K-12 in-frame, single-gene knockout mutants: the Keio collection. *Mol Syst Biol* **2:** 2006 0008

Babitzke P, Granger L, Olszewski J, Kushner SR (1993) Analysis of mRNA decay and rRNA processing in Escherichia coli multiple mutants carrying a deletion in RNase III. *J Bacteriol* **175**(1)**:** 229-239

Babitzke P, Romeo T (2007) CsrB sRNA family: sequestration of RNA-binding regulatory proteins. *Curr Opin Microbiol* **10**(2)**:** 156-163

Backofen R, Hess WR (2010) Computational prediction of sRNAs and their targets in bacteria. *RNA Biol* **7**(1)**:** 33-42

Baker KE, Mackie GA (2003) Ectopic RNase E sites promote bypass of 5'-end-dependent mRNA decay in Escherichia coli. *Mol Microbiol* **47**(1)**:** 75-88

Balbontin R, Figueroa-Bossi N, Casadesus J, Bossi L (2008) Insertion hot spot for horizontally acquired DNA within a bidirectional small-RNA locus in Salmonella enterica. *J Bacteriol* **190**(11)**:** 4075-4078

Balbontin R, Fiorini F, Figueroa-Bossi N, Casadesus J, Bossi L (2010) Recognition of heptameric seed sequence underlies multi-target regulation by RybB small RNA in Salmonella enterica. *Mol Microbiol* **78**(2)**:** 380-394

Bandyra KJ, Said N, Pfeiffer V, Gorna MW, Vogel J, Luisi BF (2012) The Seed Region of a Small RNA Drives the Controlled Destruction of the Target mRNA by the Endoribonuclease RNase E. *Mol Cell*

Barrick JE, Sudarsan N, Weinberg Z, Ruzzo WL, Breaker RR (2005) 6S RNA is a widespread regulator of eubacterial RNA polymerase that resembles an open promoter. *RNA* **11**(5)**:** 774-784

Barth M, Marschall C, Muffler A, Fischer D, Hengge-Aronis R (1995) Role for the histone-like protein H-NS in growth phase-dependent and osmotic regulation of sigma S and many sigma S-dependent genes in Escherichia coli. *J Bacteriol* **177**(12)**:** 3455-3464

Battesti A, Majdalani N, Gottesman S (2011) The RpoS-mediated general stress response in Escherichia coli. *Annu Rev Microbiol* **65:** 189-213

Battesti A, Tsegaye YM, Packer DG, Majdalani N, Gottesman S (2012) H-NS regulation of IraD and IraM antiadaptors for control of RpoS degradation. *J Bacteriol* **194**(10)**:** 2470-2478

Becker G, Hengge-Aronis R (2001) What makes an Escherichia coli promoter sigma(S) dependent? Role of the -13/-14 nucleotide promoter positions and region 2.5 of sigma(S). *Mol Microbiol* **39**(5)**:** 1153-1165

Beisel CL, Storz G (2011) Base pairing small RNAs and their roles in global regulatory networks. *FEMS Microbiol Rev* **34**(5)**:** 866-882

Beisel CL, Updegrove TB, Janson BJ, Storz G (2012) Multiple factors dictate target selection by Hfq-binding small RNAs. *EMBO J* **31**(8)**:** 1961-1974

Bensing BA, Meyer BJ, Dunny GM (1996) Sensitive detection of bacterial transcription initiation sites and differentiation from RNA processing sites in the pheromone-induced plasmid transfer system of Enterococcus faecalis. *Proc Natl Acad Sci U S A* **93**(15)**:** 7794-7799

Berghoff BA, Glaeser J, Sharma CM, Zobawa M, Lottspeich F, Vogel J, Klug G (2011) Contribution of Hfq to photooxidative stress resistance and global regulation in Rhodobacter sphaeroides. *Mol Microbiol* **80**(6)**:** 1479-1495

Blattner FR, Plunkett G, 3rd, Bloch CA, Perna NT, Burland V, Riley M, Collado-Vides J, Glasner JD, Rode CK, Mayhew GF, Gregor J, Davis NW, Kirkpatrick HA, Goeden MA, Rose DJ, Mau B, Shao Y (1997) The complete genome sequence of Escherichia coli K-12. *Science* **277**(5331)**:** 1453-1462

Boehm A, Kaiser M, Li H, Spangler C, Kasper CA, Ackermann M, Kaever V, Sourjik V, Roth V, Jenal U (2010) Second messenger-mediated adjustment of bacterial swimming velocity. *Cell* **141**(1)**:** 107-116

Bos MP, Robert V, Tommassen J (2007) Biogenesis of the gram-negative bacterial outer membrane. *Annu Rev Microbiol* **61:** 191-214

Bouvier M, Sharma CM, Mika F, Nierhaus KH, Vogel J (2008) Small RNA binding to 5' mRNA coding region inhibits translational initiation. *Mol Cell* **32**(6)**:** 827-837

Boysen A, Moller-Jensen J, Kallipolitis B, Valentin-Hansen P, Overgaard M (2010) Translational regulation of gene expression by an anaerobically induced small non-coding RNA in Escherichia coli. *J Biol Chem* **285**(14)**:** 10690-10702

Brantl S (2007) Regulatory mechanisms employed by cis-encoded antisense RNAs. *Curr Opin Microbiol* **10**(2)**:** 102-109

Brennan RG, Link TM (2007) Hfq structure, function and ligand binding. *Curr Opin Microbiol* **10**(2)**:** 125-133

Brenner M, Tomizawa J (1989) Rom transcript of plasmid ColE1. *Nucleic Acids Res* **17**(11)**:** 4309-4326

Browning DF, Busby SJ (2004) The regulation of bacterial transcription initiation. *Nat Rev Microbiol* **2**(1)**:** 57-65

Burgin AB, Parodos K, Lane DJ, Pace NR (1990) The excision of intervening sequences from Salmonella 23S ribosomal RNA. *Cell* **60**(3)**:** 405-414

Callaghan AJ, Marcaida MJ, Stead JA, McDowall KJ, Scott WG, Luisi BF (2005) Structure of Escherichia coli RNase E catalytic domain and implications for RNA turnover. *Nature* **437**(7062)**:** 1187-1191

Carpousis AJ (2007) The RNA degradosome of Escherichia coli: an mRNA-degrading machine assembled on RNase E. *Annu Rev Microbiol* **61:** 71-87

Chang YY, Cronan JE, Jr. (1999) Membrane cyclopropane fatty acid content is a major factor in acid resistance of Escherichia coli. *Mol Microbiol* **33**(2)**:** 249-259

Chang YY, Eichel J, Cronan JE, Jr. (2000) Metabolic instability of Escherichia coli cyclopropane fatty acid synthase is due to RpoH-dependent proteolysis. *J Bacteriol* **182**(15)**:** 4288-4294

Chao Y, Papenfort K, Reinhardt R, Sharma CM, Vogel J (2012) An atlas of Hfq-bound transcripts reveals 3' UTRs as a genomic reservoir of regulatory small RNAs. *EMBO J*

Chao Y, Vogel J (2010) The role of Hfq in bacterial pathogens. *Curr Opin Microbiol* **13**(1)**:** 24-33

Chen D, Patton JT (2001) Reverse transcriptase adds nontemplated nucleotides to cDNAs during 5'-RACE and primer extension. *Biotechniques* **30**(3)**:** 574-580, 582

Chen S, Zhang A, Blyn LB, Storz G (2004) MicC, a second small-RNA regulator of Omp protein expression in Escherichia coli. *J Bacteriol* **186**(20)**:** 6689-6697

Cherepanov PP, Wackernagel W (1995) Gene disruption in Escherichia coli: TcR and KmR cassettes with the option of Flp-catalyzed excision of the antibiotic-resistance determinant. *Gene* **158**(1)**:** 9-14

Clarke EJ, Voigt CA (2011) Characterization of combinatorial patterns generated by multiple two-component sensors in E. coli that respond to many stimuli. *Biotechnol Bioeng* **108**(3)**:** 666-675

Corcoran CP, Podkaminski D, Papenfort K, Urban JH, Hinton JC, Vogel J (2012) Superfolder GFP reporters validate diverse new mRNA targets of the classic porin regulator, MicF RNA. *Mol Microbiol* **84**(3)**:** 428-445

Corpet F (1988) Multiple sequence alignment with hierarchical clustering. *Nucleic Acids Res* **16**(22)**:** 10881-10890

Cronan JE, Jr. (2002) Phospholipid modifications in bacteria. *Curr Opin Microbiol* **5**(2)**:** 202-205

Crump JA, Luby SP, Mintz ED (2004) The global burden of typhoid fever. *Bull World Health Organ* **82**(5)**:** 346-353

Darfeuille F, Unoson C, Vogel J, Wagner EG (2007) An antisense RNA inhibits translation by competing with standby ribosomes. *Mol Cell* **26**(3)**:** 381-392

Datsenko KA, Wanner BL (2000) One-step inactivation of chromosomal genes in Escherichia coli K-12 using PCR products. *Proc Natl Acad Sci U S A* **97**(12)**:** 6640-6645

De la Cruz MA, Calva E (2010) The complexities of porin genetic regulation. *J Mol Microbiol Biotechnol* **18**(1)**:** 24-36

De Lay N, Gottesman S (2009) The Crp-activated small noncoding regulatory RNA CyaR (RyeE) links nutritional status to group behavior. *J Bacteriol* **191**(2)**:** 461-476

Desnoyers G, Masse E (2012) Noncanonical repression of translation initiation through small RNA recruitment of the RNA chaperone Hfq. *Genes Dev* **26**(7)**:** 726-739

Deutscher J, Francke C, Postma PW (2006) How phosphotransferase system-related protein phosphorylation regulates carbohydrate metabolism in bacteria. *Microbiol Mol Biol Rev* **70**(4)**:** 939-1031

Dillon SC, Cameron AD, Hokamp K, Lucchini S, Hinton JC, Dorman CJ (2010) Genome-wide analysis of the H-NS and Sfh regulatory networks in Salmonella Typhimurium identifies a plasmid-encoded transcription silencing mechanism. *Mol Microbiol* **76**(5)**:** 1250-1265

Dobrindt U, Hochhut B, Hentschel U, Hacker J (2004) Genomic islands in pathogenic and environmental microorganisms. *Nat Rev Microbiol* **2**(5)**:** 414-424

Dufourc EJ, Smith IC, Jarrell HC (1984) The role of cyclopropane moieties in the lipid properties of biological membranes: a deuterium NMR structural and dynamical approach. *Biochemistry* **23**(10)**:** 2300-2309

Durand S, Storz G (2010) Reprogramming of anaerobic metabolism by the FnrS small RNA. *Mol Microbiol* **75**(5)**:** 1215-1231

Durfee T, Hansen AM, Zhi H, Blattner FR, Jin DJ (2008) Transcription profiling of the stringent response in Escherichia coli. *J Bacteriol* **190**(3)**:** 1084-1096

Ellermeier CD, Janakiraman A, Slauch JM (2002) Construction of targeted single copy lac fusions using lambda Red and FLP-mediated site-specific recombination in bacteria. *Gene* **290**(1-2)**:** 153-161

Falconi M, McGovern V, Gualerzi C, Hillyard D, Higgins NP (1991) Mutations altering chromosomal protein H-NS induce mini-Mu transposition. *New Biol* **3**(6)**:** 615-625

Fender A, Elf J, Hampel K, Zimmermann B, Wagner EG (2010) RNAs actively cycle on the Sm-like protein Hfq. *Genes Dev* **24**(23)**:** 2621-2626

Figueroa-Bossi N, Lemire S, Maloriol D, Balbontin R, Casadesus J, Bossi L (2006) Loss of Hfq activates the sigmaE-dependent envelope stress response in Salmonella enterica. *Mol Microbiol* **62**(3)**:** 838-852

Figueroa-Bossi N, Valentini M, Malleret L, Fiorini F, Bossi L (2009) Caught at its own game: regulatory small RNA inactivated by an inducible transcript mimicking its target. *Genes Dev* **23**(17)**:** 2004-2015

Foster JW, Spector MP (1995) How Salmonella survive against the odds. *Annu Rev Microbiol* **49:** 145-174

Franze de Fernandez MT, Eoyang L, August JT (1968) Factor fraction required for the synthesis of bacteriophage Qbeta-RNA. *Nature* **219**(5154)**:** 588-590

Fröhlich KS, Papenfort K, Berger AA, Vogel J (2012) A conserved RpoS-dependent small RNA controls the synthesis of major porin OmpD. *Nucleic Acids Res* **40**(8)**:** 3623-3640

Fröhlich KS, Vogel J (2009) Activation of gene expression by small RNA. *Curr Opin Microbiol* **12**(6)**:** 674-682

Gaal T, Ross W, Estrem ST, Nguyen LH, Burgess RR, Gourse RL (2001) Promoter recognition and discrimination by EsigmaS RNA polymerase. *Mol Microbiol* **42**(4)**:** 939-954

Galan JE (2009) Common themes in the design and function of bacterial effectors. *Cell Host Microbe* **5**(6)**:** 571-579

Gerdes K, Maisonneuve E (2012) Bacterial persistence and toxin-antitoxin Loci. *Annu Rev Microbiol* **66:** 103-123

Giedroc DP, Theimer CA, Nixon PL (2000) Structure, stability and function of RNA pseudoknots involved in stimulating ribosomal frameshifting. *J Mol Biol* **298**(2)**:** 167-185

Gogol EB, Rhodius VA, Papenfort K, Vogel J, Gross CA (2011) Small RNAs endow a transcriptional activator with essential repressor functions for single-tier control of a global stress regulon. *Proc Natl Acad Sci U S A* **108**(31)**:** 12875-12880

Goodrich AF, Steege DA (1999) Roles of polyadenylation and nucleolytic cleavage in the filamentous phage mRNA processing and decay pathways in Escherichia coli. *RNA* **5**(7)**:** 972-985

Göpel Y, Luttmann D, Heroven AK, Reichenbach B, Dersch P, Gorke B (2011) Common and divergent features in transcriptional control of the homologous small RNAs GlmY and GlmZ in Enterobacteriaceae. *Nucleic Acids Res* **39**(4)**:** 1294-1309

Gottesman S (2005) Micros for microbes: non-coding regulatory RNAs in bacteria. *Trends Genet* **21**(7)**:** 399-404

Green NJ, Grundy FJ, Henkin TM (2010) The T box mechanism: tRNA as a regulatory molecule. *FEBS Lett* **584**(2)**:** 318-324

Grogan DW, Cronan JE, Jr. (1984) Cloning and manipulation of the Escherichia coli cyclopropane fatty acid synthase gene: physiological aspects of enzyme overproduction. *J Bacteriol* **158**(1)**:** 286-295

Grogan DW, Cronan JE, Jr. (1997) Cyclopropane ring formation in membrane lipids of bacteria. *Microbiol Mol Biol Rev* **61**(4)**:** 429-441

Gruber AR, Lorenz R, Bernhart SH, Neubock R, Hofacker IL (2008) The Vienna RNA websuite. *Nucleic Acids Res* **36**(Web Server issue)**:** W70-74

Grundy FJ, Henkin TM (2004) Regulation of gene expression by effectors that bind to RNA. *Curr Opin Microbiol* **7**(2)**:** 126-131

Hajnsdorf E, Regnier P (2000) Host factor Hfq of Escherichia coli stimulates elongation of poly(A) tails by poly(A) polymerase I. *Proc Natl Acad Sci U S A* **97**(4)**:** 1501-1505

Hammer BK, Bassler BL (2007) Regulatory small RNAs circumvent the conventional quorum sensing pathway in pandemic Vibrio cholerae. *Proc Natl Acad Sci U S A* **104**(27)**:** 11145-11149

Hansen-Wester I, Hensel M (2001) Salmonella pathogenicity islands encoding type III secretion systems. *Microbes Infect* **3**(7)**:** 549-559

Haraga A, Ohlson MB, Miller SI (2008) Salmonellae interplay with host cells. *Nat Rev Microbiol* **6**(1)**:** 53-66

Hartz D, McPheeters DS, Traut R, Gold L (1988) Extension inhibition analysis of translation initiation complexes. *Methods Enzymol* **164:** 419-425

Hautefort I, Proenca MJ, Hinton JC (2003) Single-copy green fluorescent protein gene fusions allow accurate measurement of Salmonella gene expression in vitro and during infection of mammalian cells. *Appl Environ Microbiol* **69**(12)**:** 7480-7491

Hebrard M, Kroger C, Srikumar S, Colgan A, Handler K, Hinton J (2012) sRNAs and the virulence of Salmonella enterica serovar Typhimurium. *RNA Biol* **9**(4)

Hengge-Aronis R (1996) Back to log phase: sigma S as a global regulator in the osmotic control of gene expression in Escherichia coli. *Mol Microbiol* **21**(5)**:** 887-893

Hensel M (2004) Evolution of pathogenicity islands of Salmonella enterica. *Int J Med Microbiol* **294**(2-3)**:** 95-102

Hernandez VJ, Bremer H (1991) Escherichia coli ppGpp synthetase II activity requires spoT. *J Biol Chem* **266**(9)**:** 5991-5999

Hershberg R, Altuvia S, Margalit H (2003) A survey of small RNA-encoding genes in Escherichia coli. *Nucleic Acids Res* **31**(7)**:** 1813-1820

Hoffmann S, Otto C, Kurtz S, Sharma CM, Khaitovich P, Vogel J, Stadler PF, Hackermuller J (2009) Fast mapping of short sequences with mismatches, insertions and deletions using index structures. *PLoS Comput Biol* **5**(9)**:** e1000502

Hoiseth SK, Stocker BA (1981) Aromatic-dependent Salmonella typhimurium are non-virulent and effective as live vaccines. *Nature* **291**(5812)**:** 238-239

Holmqvist E, Reimegard J, Sterk M, Grantcharova N, Romling U, Wagner EG (2010) Two antisense RNAs target the transcriptional regulator CsgD to inhibit curli synthesis. *EMBO J* **29**(11)**:** 1840-1850

Hopkins JF, Panja S, Woodson SA (2011) Rapid binding and release of Hfq from ternary complexes during RNA annealing. *Nucleic Acids Res* **39**(12)**:** 5193-5202

Humphreys S, Stevenson A, Bacon A, Weinhardt AB, Roberts M (1999) The alternative sigma factor, sigmaE, is critically important for the virulence of Salmonella typhimurium. *Infect Immun* **67**(4)**:** 1560-1568

Hussein R, Lim HN (2011) Disruption of small RNA signaling caused by competition for Hfq. *Proc Natl Acad Sci U S A* **108**(3)**:** 1110-1115

Hüttenhofer A, Noller HF (1994) Footprinting mRNA-ribosome complexes with chemical probes. *EMBO J* **13**(16)**:** 3892-3901

Hwang W, Arluison V, Hohng S (2011) Dynamic competition of DsrA and rpoS fragments for the proximal binding site of Hfq as a means for efficient annealing. *Nucleic Acids Res* **39**(12)**:** 5131-5139

Ikeda Y, Yagi M, Morita T, Aiba H (2011) Hfq binding at RhlB-recognition region of RNase E is crucial for the rapid degradation of target mRNAs mediated by sRNAs in Escherichia coli. *Mol Microbiol* **79**(2)**:** 419-432

Ishihama A (2000) Functional modulation of Escherichia coli RNA polymerase. *Annu Rev Microbiol* **54:** 499-518

Ishikawa H, Otaka H, Maki K, Morita T, Aiba H (2012) The functional Hfq-binding module of bacterial sRNAs consists of a double or single hairpin preceded by a U-rich sequence and followed by a 3' poly(U) tail. *RNA* **18**(5)**:** 1062-1074

Jacques N, Dreyfus M (1990) Translation initiation in Escherichia coli: old and new questions. *Mol Microbiol* **4**(7)**:** 1063-1067

Johansen J, Eriksen M, Kallipolitis B, Valentin-Hansen P (2008) Down-regulation of outer membrane proteins by noncoding RNAs: unraveling the cAMP-CRP- and sigmaE-dependent CyaR-ompX regulatory case. *J Mol Biol* **383**(1)**:** 1-9

Johansen J, Rasmussen AA, Overgaard M, Valentin-Hansen P (2006) Conserved small non-coding RNAs that belong to the sigmaE regulon: role in down-regulation of outer membrane proteins. *J Mol Biol* **364**(1)**:** 1-8

Jorgensen MG, Nielsen JS, Boysen A, Franch T, Moller-Jensen J, Valentin-Hansen P (2012) Small regulatory RNAs control the multi-cellular adhesive lifestyle of Escherichia coli. *Mol Microbiol* **84**(1)**:** 36-50

Kalamorz F, Reichenbach B, Marz W, Rak B, Gorke B (2007) Feedback control of glucosamine-6-phosphate synthase GlmS expression depends on the small RNA GlmZ and involves the novel protein YhbJ in Escherichia coli. *Mol Microbiol* **65**(6)**:** 1518-1533

Kawamoto H, Koide Y, Morita T, Aiba H (2006) Base-pairing requirement for RNA silencing by a bacterial small RNA and acceleration of duplex formation by Hfq. *Mol Microbiol* **61**(4)**:** 1013-1022

Kim BH, Kim S, Kim HG, Lee J, Lee IS, Park YK (2005) The formation of cyclopropane fatty acids in Salmonella enterica serovar Typhimurium. *Microbiology* **151**(Pt 1)**:** 209-218

Kingsford CL, Ayanbule K, Salzberg SL (2007) Rapid, accurate, computational discovery of Rho-independent transcription terminators illuminates their relationship to DNA uptake. *Genome Biol* **8**(2)**:** R22

Kortmann J, Narberhaus F (2012) Bacterial RNA thermometers: molecular zippers and switches. *Nat Rev Microbiol* **10**(4)**:** 255-265

Kröger C, Dillon SC, Cameron AD, Papenfort K, Sivasankaran SK, Hokamp K, Chao Y, Sittka A, Hebrard M, Handler K, Colgan A, Leekitcharoenphon P, Langridge GC, Lohan AJ, Loftus B, Lucchini S, Ussery DW, Dorman CJ, Thomson NR, Vogel J, Hinton JC (2012) The transcriptional landscape and small RNAs of Salmonella enterica serovar Typhimurium. *Proc Natl Acad Sci U S A* **109**(20)**:** E1277-1286

Kusano S, Ding Q, Fujita N, Ishihama A (1996) Promoter selectivity of Escherichia coli RNA polymerase E sigma 70 and E sigma 38 holoenzymes. Effect of DNA supercoiling. *J Biol Chem* **271**(4)**:** 1998-2004

Kushner SR (2002) mRNA decay in Escherichia coli comes of age. *J Bacteriol* **184**(17)**:** 4658-4665; discussion 4657

Kvint K, Farewell A, Nystrom T (2000) RpoS-dependent promoters require guanosine tetraphosphate for induction even in the presence of high levels of sigma(s). *J Biol Chem* **275**(20)**:** 14795-14798

Lan R, Reeves PR, Octavia S (2009) Population structure, origins and evolution of major Salmonella enterica clones. *Infect Genet Evol* **9**(5)**:** 996-1005

Lange R, Hengge-Aronis R (1991) Identification of a central regulator of stationary-phase gene expression in Escherichia coli. *Mol Microbiol* **5**(1)**:** 49-59

Lange R, Hengge-Aronis R (1994) The cellular concentration of the sigma S subunit of RNA polymerase in Escherichia coli is controlled at the levels of transcription, translation, and protein stability. *Genes Dev* **8**(13)**:** 1600-1612

Lee DR, Schnaitman CA (1980) Comparison of outer membrane porin proteins produced by Escherichia coli and Salmonella typhimurium. *J Bacteriol* **142**(3)**:** 1019-1022

Lee SJ, Gralla JD (2001) Sigma38 (rpoS) RNA polymerase promoter engagement via -10 region nucleotides. *J Biol Chem* **276**(32)**:** 30064-30071

Lee T, Feig AL (2008) The RNA binding protein Hfq interacts specifically with tRNAs. *RNA* **14**(3)**:** 514-523

Lenz DH, Mok KC, Lilley BN, Kulkarni RV, Wingreen NS, Bassler BL (2004) The small RNA chaperone Hfq and multiple small RNAs control quorum sensing in Vibrio harveyi and Vibrio cholerae. *Cell* **118**(1)**:** 69-82

Li Z, Pandit S, Deutscher MP (1999) RNase G (CafA protein) and RNase E are both required for the 5' maturation of 16S ribosomal RNA. *EMBO J* **18**(10)**:** 2878-2885

Link TM, Valentin-Hansen P, Brennan RG (2009) Structure of Escherichia coli Hfq bound to polyriboadenylate RNA. *Proc Natl Acad Sci U S A* **106**(46)**:** 19292-19297

Lutz R, Bujard H (1997) Independent and tight regulation of transcriptional units in Escherichia coli via the LacR/O, the TetR/O and AraC/I1-I2 regulatory elements. *Nucleic Acids Res* **25**(6)**:** 1203-1210

Lux R, Jahreis K, Bettenbrock K, Parkinson JS, Lengeler JW (1995) Coupling the phosphotransferase system and the methyl-accepting chemotaxis protein-dependent chemotaxis signaling pathways of Escherichia coli. *Proc Natl Acad Sci U S A* **92**(25)**:** 11583-11587

Maciag A, Peano C, Pietrelli A, Egli T, De Bellis G, Landini P (2011) In vitro transcription profiling of the sigmaS subunit of bacterial RNA polymerase: re-definition of the sigmaS regulon and identification of sigmaS-specific promoter sequence elements. *Nucleic Acids Res* **39**(13)**:** 5338-5355

Mackie GA (1998) Ribonuclease E is a 5'-end-dependent endonuclease. *Nature* **395**(6703)**:** 720-723

Madan Babu M, Teichmann SA, Aravind L (2006) Evolutionary dynamics of prokaryotic transcriptional regulatory networks. *J Mol Biol* **358**(2)**:** 614-633

Mahr R (2012) A new method for fast and easy generation of single copy chromosomal reporter gene fusions in E. coli. *Master Thesis Julius-Maximilians-University Würzburg*

Majdalani N, Chen S, Murrow J, St John K, Gottesman S (2001) Regulation of RpoS by a novel small RNA: the characterization of RprA. *Mol Microbiol* **39**(5)**:** 1382-1394

Majdalani N, Cunning C, Sledjeski D, Elliott T, Gottesman S (1998) DsrA RNA regulates translation of RpoS message by an anti-antisense mechanism, independent of its action as an antisilencer of transcription. *Proc Natl Acad Sci U S A* **95**(21)**:** 12462-12467

Majdalani N, Hernandez D, Gottesman S (2002) Regulation and mode of action of the second small RNA activator of RpoS translation, RprA. *Mol Microbiol* **46**(3)**:** 813-826

Majowicz SE, Musto J, Scallan E, Angulo FJ, Kirk M, O'Brien SJ, Jones TF, Fazil A, Hoekstra RM (2010) The global burden of nontyphoidal Salmonella gastroenteritis. *Clin Infect Dis* **50**(6)**:** 882-889

Maki K, Morita T, Otaka H, Aiba H (2010) A minimal base-pairing region of a bacterial small RNA SgrS required for translational repression of ptsG mRNA. *Mol Microbiol* **76**(3)**:** 782-792

Mandin P, Gottesman S (2010) Integrating anaerobic/aerobic sensing and the general stress response through the ArcZ small RNA. *EMBO J* **29**(18)**:** 3094-3107

Marcaida MJ, DePristo MA, Chandran V, Carpousis AJ, Luisi BF (2006) The RNA degradosome: life in the fast lane of adaptive molecular evolution. *Trends Biochem Sci* **31**(7)**:** 359-365

Masse E, Escorcia FE, Gottesman S (2003) Coupled degradation of a small regulatory RNA and its mRNA targets in Escherichia coli. *Genes Dev* **17**(19)**:** 2374-2383

Masse E, Gottesman S (2002) A small RNA regulates the expression of genes involved in iron metabolism in Escherichia coli. *Proc Natl Acad Sci U S A* **99**(7)**:** 4620-4625

Masse E, Vanderpool CK, Gottesman S (2005) Effect of RyhB small RNA on global iron use in Escherichia coli. *J Bacteriol* **187**(20)**:** 6962-6971

McDowall KJ, Lin-Chao S, Cohen SN (1994) A+U content rather than a particular nucleotide order determines the specificity of RNase E cleavage. *J Biol Chem* **269**(14)**:** 10790-10796

Mika F, Busse S, Possling A, Berkholz J, Tschowri N, Sommerfeldt N, Pruteanu M, Hengge R (2012) Targeting of csgD by the small regulatory RNA RprA links stationary phase, biofilm formation and cell envelope stress in Escherichia coli. *Mol Microbiol* **84**(1)**:** 51-65

Mizuno T, Chou MY, Inouye M (1984) A unique mechanism regulating gene expression: translational inhibition by a complementary RNA transcript (micRNA). *Proc Natl Acad Sci U S A* **81**(7)**:** 1966-1970

Mohanty BK, Maples VF, Kushner SR (2004) The Sm-like protein Hfq regulates polyadenylation dependent mRNA decay in Escherichia coli. *Mol Microbiol* **54**(4)**:** 905-920

Moller T, Franch T, Hojrup P, Keene DR, Bachinger HP, Brennan RG, Valentin-Hansen P (2002) Hfq: a bacterial Sm-like protein that mediates RNA-RNA interaction. *Mol Cell* **9**(1)**:** 23-30

Moon K, Gottesman S (2009) A PhoQ/P-regulated small RNA regulates sensitivity of Escherichia coli to antimicrobial peptides. *Mol Microbiol* **74**(6)**:** 1314-1330

Morfeldt E, Taylor D, von Gabain A, Arvidson S (1995) Activation of alpha-toxin translation in Staphylococcus aureus by the trans-encoded antisense RNA, RNAIII. *EMBO J* **14**(18)**:** 4569-4577

Morita T, Maki K, Aiba H (2005) RNase E-based ribonucleoprotein complexes: mechanical basis of mRNA destabilization mediated by bacterial noncoding RNAs. *Genes Dev* **19**(18)**:** 2176-2186

Morita T, Mochizuki Y, Aiba H (2006) Translational repression is sufficient for gene silencing by bacterial small noncoding RNAs in the absence of mRNA destruction. *Proc Natl Acad Sci U S A* **103**(13)**:** 4858-4863

Muffler A, Barth M, Marschall C, Hengge-Aronis R (1997) Heat shock regulation of sigmaS turnover: a role for DnaK and relationship between stress responses mediated by sigmaS and sigma32 in Escherichia coli. *J Bacteriol* **179**(2)**:** 445-452

Muller C, Bang IS, Velayudhan J, Karlinsey J, Papenfort K, Vogel J, Fang FC (2009) Acid stress activation of the sigma(E) stress response in Salmonella enterica serovar Typhimurium. *Mol Microbiol* **71**(5)**:** 1228-1238

Mutalik VK, Nonaka G, Ades SE, Rhodius VA, Gross CA (2009) Promoter strength properties of the complete sigma E regulon of Escherichia coli and Salmonella enterica. *J Bacteriol* **191**(23)**:** 7279-7287

Navarre WW, Porwollik S, Wang Y, McClelland M, Rosen H, Libby SJ, Fang FC (2006) Selective silencing of foreign DNA with low GC content by the H-NS protein in Salmonella. *Science* **313**(5784)**:** 236-238

Navarro Llorens JM, Tormo A, Martinez-Garcia E (2010) Stationary phase in gram-negative bacteria. *FEMS Microbiol Rev* **34**(4)**:** 476-495

Nicholson AW (1999) Function, mechanism and regulation of bacterial ribonucleases. *FEMS Microbiol Rev* **23**(3)**:** 371-390

Nudler E, Gottesman ME (2002) Transcription termination and anti-termination in E. coli. *Genes Cells* **7**(8)**:** 755-768

Nystrom T (2004) Stationary-phase physiology. *Annu Rev Microbiol* **58:** 161-181

Obana N, Shirahama Y, Abe K, Nakamura K (2010) Stabilization of Clostridium perfringens collagenase mRNA by VR-RNA-dependent cleavage in 5' leader sequence. *Mol Microbiol* **77**(6)**:** 1416-1428

Opdyke JA, Kang JG, Storz G (2004) GadY, a small-RNA regulator of acid response genes in Escherichia coli. *J Bacteriol* **186**(20)**:** 6698-6705

Oppenheim DS, Yanofsky C (1980) Translational coupling during expression of the tryptophan operon of Escherichia coli. *Genetics* **95**(4)**:** 785-795

Otaka H, Ishikawa H, Morita T, Aiba H (2011) PolyU tail of rho-independent terminator of bacterial small RNAs is essential for Hfq action. *Proc Natl Acad Sci U S A* **108**(32)**:** 13059-13064

Overgaard M, Johansen J, Moller-Jensen J, Valentin-Hansen P (2009) Switching off small RNA regulation with trap-mRNA. *Mol Microbiol* **73**(5)**:** 790-800

Padalon-Brauch G, Hershberg R, Elgrably-Weiss M, Baruch K, Rosenshine I, Margalit H, Altuvia S (2008) Small RNAs encoded within genetic islands of Salmonella typhimurium show host-induced expression and role in virulence. *Nucleic Acids Res* **36**(6)**:** 1913-1927

Papenfort K, Bouvier M, Mika F, Sharma CM, Vogel J (2010) Evidence for an autonomous 5' target recognition domain in an Hfq-associated small RNA. *Proc Natl Acad Sci U S A* **107**(47)**:** 20435-20440

Papenfort K, Pfeiffer V, Lucchini S, Sonawane A, Hinton JC, Vogel J (2008) Systematic deletion of Salmonella small RNA genes identifies CyaR, a conserved CRP-dependent riboregulator of OmpX synthesis. *Mol Microbiol* **68**(4)**:** 890-906

Papenfort K, Pfeiffer V, Mika F, Lucchini S, Hinton JC, Vogel J (2006) SigmaE-dependent small RNAs of Salmonella respond to membrane stress by accelerating global omp mRNA decay. *Mol Microbiol* **62**(6)**:** 1674-1688

Papenfort K, Podkaminski D, Hinton JC, Vogel J (2012) The ancestral SgrS RNA discriminates horizontally acquired Salmonella mRNAs through a single G-U wobble pair. *Proc Natl Acad Sci U S A* **109**(13)**:** E757-764

Papenfort K, Said N, Welsink T, Lucchini S, Hinton JC, Vogel J (2009) Specific and pleiotropic patterns of mRNA regulation by ArcZ, a conserved, Hfq-dependent small RNA. *Mol Microbiol* **74**(1)**:** 139-158

Papenfort K, Vogel J (2009) Multiple target regulation by small noncoding RNAs rewires gene expression at the post-transcriptional level. *Res Microbiol* **160**(4)**:** 278-287

Papenfort K, Vogel J (2010) Regulatory RNA in bacterial pathogens. *Cell Host Microbe* **8**(1)**:** 116-127

Peer A, Margalit H (2011) Accessibility and evolutionary conservation mark bacterial small-rna target-binding regions. *J Bacteriol* **193**(7)**:** 1690-1701

Perez-Rueda E, Collado-Vides J (2000) The repertoire of DNA-binding transcriptional regulators in Escherichia coli K-12. *Nucleic Acids Res* **28**(8)**:** 1838-1847

Pfeiffer V, Papenfort K, Lucchini S, Hinton JC, Vogel J (2009) Coding sequence targeting by MicC RNA reveals bacterial mRNA silencing downstream of translational initiation. *Nat Struct Mol Biol* **16**(8)**:** 840-846

Pfeiffer V, Sittka A, Tomer R, Tedin K, Brinkmann V, Vogel J (2007) A small non-coding RNA of the invasion gene island (SPI-1) represses outer membrane protein synthesis from the Salmonella core genome. *Mol Microbiol* **66**(5)**:** 1174-1191

Pizarro-Cerda J, Tedin K (2004) The bacterial signal molecule, ppGpp, regulates Salmonella virulence gene expression. *Mol Microbiol* **52**(6)**:** 1827-1844

Platt T (1986) Transcription termination and the regulation of gene expression. *Annu Rev Biochem* **55:** 339-372

Potrykus K, Cashel M (2008) (p)ppGpp: still magical? *Annu Rev Microbiol* **62:** 35-51

Prevost K, Desnoyers G, Jacques JF, Lavoie F, Masse E (2011) Small RNA-induced mRNA degradation achieved through both translation block and activated cleavage. *Genes Dev* **25**(4)**:** 385-396

Prevost K, Salvail H, Desnoyers G, Jacques JF, Phaneuf E, Masse E (2007) The small RNA RyhB activates the translation of shiA mRNA encoding a permease of shikimate, a compound involved in siderophore synthesis. *Mol Microbiol* **64**(5)**:** 1260-1273

Raina S, Missiakas D, Georgopoulos C (1995) The rpoE gene encoding the sigma E (sigma 24) heat shock sigma factor of Escherichia coli. *EMBO J* **14**(5)**:** 1043-1055

Ramirez-Pena E, Trevino J, Liu Z, Perez N, Sumby P (2010) The group A Streptococcus small regulatory RNA FasX enhances streptokinase activity by increasing the stability of the ska mRNA transcript. *Mol Microbiol* **78**(6)**:** 1332-1347

Rankin JD, Taylor RJ (1966) The estimation of doses of Salmonella typhimurium suitable for the experimental production of disease in calves. *Vet Rec* **78**(21)**:** 706-707

Rasmussen AA, Johansen J, Nielsen JS, Overgaard M, Kallipolitis B, Valentin-Hansen P (2009) A conserved small RNA promotes silencing of the outer membrane protein YbfM. *Mol Microbiol*

Reeder J, Steffen P, Giegerich R (2007) pknotsRG: RNA pseudoknot folding including near-optimal structures and sliding windows. *Nucleic Acids Res* **35**(Web Server issue)**:** W320-324

Rehmsmeier M, Steffen P, Hochsmann M, Giegerich R (2004) Fast and effective prediction of microRNA/target duplexes. *RNA* **10**(10)**:** 1507-1517

Reichenbach B, Gopel Y, Gorke B (2009) Dual control by perfectly overlapping sigma 54- and sigma 70-promoters adjusts small RNA GlmY expression to different environmental signals. *Mol Microbiol* **74**(5)**:** 1054-1070

Reitzer L (2003) Nitrogen assimilation and global regulation in Escherichia coli. *Annu Rev Microbiol* **57:** 155-176

Rice JB, Vanderpool CK (2011) The small RNA SgrS controls sugar-phosphate accumulation by regulating multiple PTS genes. *Nucleic Acids Res* **39**(9)**:** 3806-3819

Rivas E, Klein RJ, Jones TA, Eddy SR (2001) Computational identification of noncoding RNAs in E. coli by comparative genomics. *Curr Biol* **11**(17)**:** 1369-1373

Rosenthal AZ, Kim Y, Gralla JD (2008) Regulation of transcription by acetate in Escherichia coli: in vivo and in vitro comparisons. *Mol Microbiol* **68**(4)**:** 907-917

Rouviere PE, De Las Penas A, Mecsas J, Lu CZ, Rudd KE, Gross CA (1995) rpoE, the gene encoding the second heat-shock sigma factor, sigma E, in Escherichia coli. *EMBO J* **14**(5)**:** 1032-1042

Rychlik W, Spencer WJ, Rhoads RE (1990) Optimization of the annealing temperature for DNA amplification in vitro. *Nucleic Acids Res* **18**(21)**:** 6409-6412

Sambrook J, Russel D. W. (2001) Molecular Cloning: A Laboratory Manual. **1-3**

Sanden AM, Prytz I, Tubulekas I, Forberg C, Le H, Hektor A, Neubauer P, Pragai Z, Harwood C, Ward A, Picon A, De Mattos JT, Postma P, Farewell A, Nystrom T, Reeh S, Pedersen S, Larsson G (2003) Limiting factors in Escherichia coli fed-batch production of recombinant proteins. *Biotechnol Bioeng* **81**(2)**:** 158-166

Sands MK, Roberts RB (1952) The effects of a tryptophan-histidine deficiency in a mutant of Escherichia coli. *J Bacteriol* **63**(4)**:** 505-511

Santiviago CA, Toro CS, Hidalgo AA, Youderian P, Mora GC (2003) Global regulation of the Salmonella enterica serovar typhimurium major porin, OmpD. *J Bacteriol* **185**(19)**:** 5901-5905

Sauer E, Schmidt S, Weichenrieder O (2012) Small RNA binding to the lateral surface of Hfq hexamers and structural rearrangements upon mRNA target recognition. *Proc Natl Acad Sci U S A* **109**(24)**:** 9396-9401

Sauer E, Weichenrieder O (2011) Structural basis for RNA 3'-end recognition by Hfq. *Proc Natl Acad Sci U S A* **108**(32)**:** 13065-13070

Scheibe M, Bonin S, Hajnsdorf E, Betat H, Morl M (2007) Hfq stimulates the activity of the CCA-adding enzyme. *BMC Mol Biol* **8:** 92

Schumacher MA, Pearson RF, Moller T, Valentin-Hansen P, Brennan RG (2002) Structures of the pleiotropic translational regulator Hfq and an Hfq-RNA complex: a bacterial Sm-like protein. *EMBO J* **21**(13)**:** 3546-3556

Schümperli D, McKenney K, Sobieski DA, Rosenberg M (1982) Translational coupling at an intercistronic boundary of the Escherichia coli galactose operon. *Cell* **30**(3)**:** 865-871

Sharma CM, Darfeuille F, Plantinga TH, Vogel J (2007) A small RNA regulates multiple ABC transporter mRNAs by targeting C/A-rich elements inside and upstream of ribosome-binding sites. *Genes Dev* **21**(21)**:** 2804-2817

Sharma CM, Hoffmann S, Darfeuille F, Reignier J, Findeiss S, Sittka A, Chabas S, Reiche K, Hackermuller J, Reinhardt R, Stadler PF, Vogel J (2010) The primary transcriptome of the major human pathogen Helicobacter pylori. *Nature* **464**(7286)**:** 250-255

Sharma CM, Papenfort K, Pernitzsch SR, Mollenkopf HJ, Hinton JC, Vogel J (2011) Pervasive post-transcriptional control of genes involved in amino acid metabolism by the Hfq-dependent GcvB small RNA. *Mol Microbiol* **81**(5)**:** 1144-1165

Sharma CM, Vogel J (2009) Experimental approaches for the discovery and characterization of regulatory small RNA. *Curr Opin Microbiol* **12**(5)**:** 536-546

Shuman HA, Silhavy TJ (2003) The art and design of genetic screens: Escherichia coli. *Nat Rev Genet* **4**(6)**:** 419-431

Sittka A, Lucchini S, Papenfort K, Sharma CM, Rolle K, Binnewies TT, Hinton JC, Vogel J (2008) Deep sequencing analysis of small noncoding RNA and mRNA targets of the global post-transcriptional regulator, Hfq. *PLoS Genet* **4**(8)**:** e1000163

Sittka A, Pfeiffer V, Tedin K, Vogel J (2007) The RNA chaperone Hfq is essential for the virulence of Salmonella typhimurium. *Mol Microbiol* **63**(1)**:** 193-217

Sittka A, Sharma CM, Rolle K, Vogel J (2009) Deep sequencing of Salmonella RNA associated with heterologous Hfq proteins in vivo reveals small RNAs as a major target class and identifies RNA processing phenotypes. *RNA Biol* **6**(3)**:** 266-275

Song T, Mika F, Lindmark B, Liu Z, Schild S, Bishop A, Zhu J, Camilli A, Johansson J, Vogel J, Wai SN (2008) A new Vibrio cholerae sRNA modulates colonization and affects release of outer membrane vesicles. *Mol Microbiol* **70**(1)**:** 100-111

Sonnleitner E, Abdou L, Haas D (2009) Small RNA as global regulator of carbon catabolite repression in Pseudomonas aeruginosa. *Proc Natl Acad Sci U S A* **106**(51)**:** 21866-21871

Sonnleitner E, Gonzalez N, Sorger-Domenigg T, Heeb S, Richter AS, Backofen R, Williams P, Huttenhofer A, Haas D, Blasi U (2011) The small RNA PhrS stimulates synthesis of the Pseudomonas aeruginosa quinolone signal. *Mol Microbiol* **80**(4)**:** 868-885

Soper T, Mandin P, Majdalani N, Gottesman S, Woodson SA (2010) Positive regulation by small RNAs and the role of Hfq. *Proc Natl Acad Sci U S A* **107**(21)**:** 9602-9607

Staple DW, Butcher SE (2005) Pseudoknots: RNA structures with diverse functions. *PLoS Biol* **3**(6)**:** e213

Stent GS, Brenner S (1961) A genetic locus for the regulation of ribonucleic acid synthesis. *Proc Natl Acad Sci U S A* **47:** 2005-2014

Sternberg NL, Maurer R (1991) Bacteriophage-mediated generalized transduction in Escherichia coli and Salmonella typhimurium. *Methods Enzymol* **204:** 18-43

Stoebel DM, Free A, Dorman CJ (2008) Anti-silencing: overcoming H-NS-mediated repression of transcription in Gram-negative enteric bacteria. *Microbiology* **154**(Pt 9)**:** 2533-2545

Storz G, Opdyke JA, Zhang A (2004) Controlling mRNA stability and translation with small, noncoding RNAs. *Curr Opin Microbiol* **7**(2)**:** 140-144

Storz G, Vogel J, Wassarman KM (2011) Regulation by small RNAs in bacteria: expanding frontiers. *Mol Cell* **43**(6)**:** 880-891

Surette MG, Miller MB, Bassler BL (1999) Quorum sensing in Escherichia coli, Salmonella typhimurium, and Vibrio harveyi: a new family of genes responsible for autoinducer production. *Proc Natl Acad Sci U S A* **96**(4)**:** 1639-1644

Takyar S, Hickerson RP, Noller HF (2005) mRNA helicase activity of the ribosome. *Cell* **120**(1)**:** 49-58

Taylor FR, Cronan JE, Jr. (1979) Cyclopropane fatty acid synthase of Escherichia coli. Stabilization, purification, and interaction with phospholipid vesicles. *Biochemistry* **18**(15)**:** 3292-3300

Tedin K, Norel F (2001) Comparison of DeltarelA strains of Escherichia coli and Salmonella enterica serovar Typhimurium suggests a role for ppGpp in attenuation regulation of branched-chain amino acid biosynthesis. *J Bacteriol* **183**(21)**:** 6184-6196

Thiennimitr P, Winter SE, Baumler AJ (2012) Salmonella, the host and its microbiota. *Curr Opin Microbiol* **15**(1)**:** 108-114

Thomason MK, Fontaine F, De Lay N, Storz G A small RNA that regulates motility and biofilm formation in response to changes in nutrient availability in Escherichia coli. *Mol Microbiol* **84**(1)**:** 17-35

Thomason MK, Storz G (2010) Bacterial antisense RNAs: how many are there, and what are they doing? *Annu Rev Genet* **44:** 167-188

Thompson KM, Rhodius VA, Gottesman S (2007) SigmaE regulates and is regulated by a small RNA in Escherichia coli. *J Bacteriol* **189**(11)**:** 4243-4256

Tomizawa J, Itoh T, Selzer G, Som T (1981) Inhibition of ColE1 RNA primer formation by a plasmid-specified small RNA. *Proc Natl Acad Sci U S A* **78**(3)**:** 1421-1425

Tosa T, Pizer LI (1971) Biochemical bases for the antimetabolite action of L-serine hydroxamate. *J Bacteriol* **106**(3)**:** 972-982

Tramonti A, Visca P, De Canio M, Falconi M, De Biase D (2002) Functional characterization and regulation of gadX, a gene encoding an AraC/XylS-like transcriptional activator of the Escherichia coli glutamic acid decarboxylase system. *J Bacteriol* **184**(10)**:** 2603-2613

Traxler MF, Zacharia VM, Marquardt S, Summers SM, Nguyen HT, Stark SE, Conway T (2011) Discretely calibrated regulatory loops controlled by ppGpp partition gene induction across the 'feast to famine' gradient in Escherichia coli. *Mol Microbiol* **79**(4)**:** 830-845

Trotochaud AE, Wassarman KM (2005) A highly conserved 6S RNA structure is required for regulation of transcription. *Nat Struct Mol Biol* **12**(4)**:** 313-319

Tu KC, Bassler BL (2007) Multiple small RNAs act additively to integrate sensory information and control quorum sensing in Vibrio harveyi. *Genes Dev* **21**(2)**:** 221-233

Typas A, Becker G, Hengge R (2007) The molecular basis of selective promoter activation by the sigmaS subunit of RNA polymerase. *Mol Microbiol* **63**(5)**:** 1296-1306

Udekwu KI, Wagner EG (2007) Sigma E controls biogenesis of the antisense RNA MicA. *Nucleic Acids Res* **35**(4)**:** 1279-1288

Unoson C, Wagner EG (2007) Dealing with stable structures at ribosome binding sites: bacterial translation and ribosome standby. *RNA Biol* **4**(3)**:** 113-117

Urban JH, Papenfort K, Thomsen J, Schmitz RA, Vogel J (2007) A conserved small RNA promotes discoordinate expression of the glmUS operon mRNA to activate GlmS synthesis. *J Mol Biol* **373**(3)**:** 521-528

Urban JH, Vogel J (2007) Translational control and target recognition by Escherichia coli small RNAs in vivo. *Nucleic Acids Res* **35**(3)**:** 1018-1037

Urban JH, Vogel J (2008) Two seemingly homologous noncoding RNAs act hierarchically to activate glmS mRNA translation. *PLoS Biol* **6**(3)**:** e64

Urban JH, Vogel J (2009) A green fluorescent protein (GFP)-based plasmid system to study post-transcriptional control of gene expression in vivo. *Methods Mol Biol* **540:** 301-319

Uzzau S, Figueroa-Bossi N, Rubino S, Bossi L (2001) Epitope tagging of chromosomal genes in Salmonella. *Proc Natl Acad Sci U S A* **98**(26)**:** 15264-15269

Valentin-Hansen P, Eriksen M, Udesen C (2004) The bacterial Sm-like protein Hfq: a key player in RNA transactions. *Mol Microbiol* **51**(6)**:** 1525-1533

van Vliet AH (2011) Next generation sequencing of microbial transcriptomes: challenges and opportunities. *FEMS Microbiol Lett* **302**(1)**:** 1-7

Vecerek B, Moll I, Blasi U (2007) Control of Fur synthesis by the non-coding RNA RyhB and iron-responsive decoding. *EMBO J* **26**(4)**:** 965-975

Viegas SC, Pfeiffer V, Sittka A, Silva IJ, Vogel J, Arraiano CM (2007) Characterization of the role of ribonucleases in Salmonella small RNA decay. *Nucleic Acids Res* **35**(22)**:** 7651-7664

Vogel J (2009) A rough guide to the non-coding RNA world of Salmonella. *Mol Microbiol* **71**(1)**:** 1-11

Vogel J, Bartels V, Tang TH, Churakov G, Slagter-Jager JG, Huttenhofer A, Wagner EG (2003) RNomics in Escherichia coli detects new sRNA species and indicates parallel transcriptional output in bacteria. *Nucleic Acids Res* **31**(22)**:** 6435-6443

Vogel J, Luisi BF (2011) Hfq and its constellation of RNA. *Nat Rev Microbiol* **9**(8)**:** 578-589

Vogel J, Papenfort K (2006) Small non-coding RNAs and the bacterial outer membrane. *Curr Opin Microbiol* **9**(6)**:** 605-611

Vogel J, Wagner EG (2007) Target identification of small noncoding RNAs in bacteria. *Curr Opin Microbiol* **10**(3)**:** 262-270

Vytvytska O, Moll I, Kaberdin VR, von Gabain A, Blasi U (2000) Hfq (HF1) stimulates ompA mRNA decay by interfering with ribosome binding. *Genes Dev* **14**(9)**:** 1109-1118

Wang AY, Cronan JE, Jr. (1994) The growth phase-dependent synthesis of cyclopropane fatty acids in Escherichia coli is the result of an RpoS(KatF)-dependent promoter plus enzyme instability. *Mol Microbiol* **11**(6)**:** 1009-1017

Wassarman KM (2007) 6S RNA: a regulator of transcription. *Mol Microbiol* **65**(6)**:** 1425-1431

Wassarman KM, Repoila F, Rosenow C, Storz G, Gottesman S (2001) Identification of novel small RNAs using comparative genomics and microarrays. *Genes Dev* **15**(13)**:** 1637-1651

Wassarman KM, Zhang A, Storz G (1999) Small RNAs in Escherichia coli. *Trends Microbiol* **7**(1)**:** 37-45

Waters LS, Storz G (2009) Regulatory RNAs in bacteria. *Cell* **136**(4)**:** 615-628

Weber H, Polen T, Heuveling J, Wendisch VF, Hengge R (2005) Genome-wide analysis of the general stress response network in Escherichia coli: sigmaS-dependent genes, promoters, and sigma factor selectivity. *J Bacteriol* **187**(5)**:** 1591-1603

Westhof E (2010) The amazing world of bacterial structured RNAs. *Genome Biol* **11**(3)**:** 108

Wilusz CJ, Wilusz J (2005) Eukaryotic Lsm proteins: lessons from bacteria. *Nat Struct Mol Biol* **12**(12)**:** 1031-1036

Wood JM (2011) Bacterial osmoregulation: a paradigm for the study of cellular homeostasis. *Annu Rev Microbiol* **65:** 215-238

Xiao H, Kalman M, Ikehara K, Zemel S, Glaser G, Cashel M (1991) Residual guanosine 3',5'-bispyrophosphate synthetic activity of relA null mutants can be eliminated by spoT null mutations. *J Biol Chem* **266**(9)**:** 5980-5990

Yakhnin AV, Babitzke P (2002) NusA-stimulated RNA polymerase pausing and termination participates in the Bacillus subtilis trp operon attenuation mechanism invitro. *Proc Natl Acad Sci U S A* **99**(17)**:** 11067-11072

Zhang A, Altuvia S, Tiwari A, Argaman L, Hengge-Aronis R, Storz G (1998) The OxyS regulatory RNA represses rpoS translation and binds the Hfq (HF-I) protein. *EMBO J* **17**(20)**:** 6061-6068

Zhang A, Wassarman KM, Rosenow C, Tjaden BC, Storz G, Gottesman S (2003) Global analysis of small RNA and mRNA targets of Hfq. *Mol Microbiol* **50**(4)**:** 1111-1124

Zhang H, Switzer RL (2003) Transcriptional pausing in the Bacillus subtilis pyr operon in vitro: a role in transcriptional attenuation? *J Bacteriol* **185**(16)**:** 4764-4771

Zhang YM, Rock CO (2008) Membrane lipid homeostasis in bacteria. *Nat Rev Microbiol* **6**(3)**:** 222-233

Zychlinsky A, Prevost MC, Sansonetti PJ (1992) Shigella flexneri induces apoptosis in infected macrophages. *Nature* **358**(6382)**:** 167-169

8 Abbreviation index

% (v/v)	% (volume/volume)
% (w/v)	% (weight/volume)
°C	degree Celsius
A	adenosine
aa	amino acid
Amp	ampicillin
APS	ammonium persulfate
Ara	L-arabinose
ATP	adenosine triphosphate
AUG	start codon
bp	base pair
C	cytosine
cDNA	complementary DNA
CDS	coding sequence
Ci	Curie
CIP	calf intestinal phosphatase
Cm	chloramphenicol
Da	Dalton
DMSO	dimethylsulfoxide
DNA	deoxyribonucleic acid
dNTP	deoxyribonucleotide
dRNA-seq	differential RNA sequencing
DTT	dithiothreitol
EDTA	ethylene diamine tetraacetic acid
EGTA	ethylene glycol tetraacetic acid
EMSA	electrophoretic mobility shift assay
G	guanosine
gDNA	genomic DNA
GFP	green fluorescent protein
IGR	intergenic region
Kan	kanamycin
K_D	dissociation constant
LB	Lennox-broth
M	molar
M-cells	microfold cell
MFE	minimum free energy
min	minute
miRNA	microRNA
mRNA	messenger RNA
N	any nucleotide
n.d.	not determined
NaCl	sodium chloride
NSB	non-specific band
nt	nucleotide
NTD	RNase E N-terminal domain
o/n	overnight
OD_{600}	optical density at 600 nm
OMP	outer membrane porin
ORF	open reading frame

P:C:I	phenol:chloroform:isoamyl alcohol
PAA	polyacrylamide
PCR	polymerase chain reaction
PMB	polymyxin B
PNK	polynucleotide kinase
poly(U)	poly-uridine
ppGpp	guanosine tetraphosphate
PTS	phosphoenolpyruvate (PEP):carbohydrate phosphotransferase system
qRT-PCR	quantitative real-time PCR
R	purine nucleotide
RACE	rapid amplification of cDNA ends
RBS	ribosome binding site
rcf	relative centrifugal force
RNA	ribonucleic acid
RNAP	RNA polymerase
RNase	ribonuclease
RNase	ribonuclease
rpm	revolutions per minute
rRNA	ribosomal RNA
SAM	*S*-adenosyl methionine
SD	Shine-Dalgarno
SDS	sodium dodecyl sulfate
SDS-PAGE	sodium dodecyl sulfate polyacrylamide gel electrophoresis
sec	second
SHX	sodium hydroxamate
SPI	*Salmonella* pathogenicity island
sRNA	small regulatory RNA
SSC	saline-sodium citrate
t	time
T	tyrosine
$t_{1/2}$	half-life
T3SS	type III secretion system
TAP	tobacco acid phosphatase
TEMED	N,N,N,N,-Tetramethylethylendiamin
TEX	terminator exonuclease
TMA	truncated MicA
tRNA	transfer RNA
TSS	transcriptional start site
U	unit
U	uridine
UTP	uridine triphosphate
UTR	untranslated region
vol	volume

9 List of Figures

Figure 1.1 Post-transcriptional repression of gene expression by sRNAs. 5
Figure 1.2 Mechanisms of target gene activation by sRNAs. 7
Figure 1.3 Profiles of Hfq-associated sRNAs over growth. 9
Figure 1.4 Schematic structure of RNase E and organization of the degradosome. 11
Figure 1.5 Conservation analysis of the two core sRNAs SdsR and RydC. 14
Figure 2.1 Genomic localization, expression and secondary structure of SdsR. 17
Figure 2.2 Non-redundant alignment of the *sdsR* gene and its upstream promoter region. 19
Figure 2.3 SdsR expression is dependent on σ^S and the alarmone ppGpp. 20
Figure 2.4 Permutation of cytosine at position -13 in the *sdsR* promoter. 21
Figure 2.5 σ^S-dependency of the *sdsR* promoter is independent of H-NS. 22
Figure 2.6 Rapid induction of SdsR sRNA and *osmY* mRNA during heat stress. 23
Figure 2.7 σ^S-dependent induction of SdsR during osmotic stress. 24
Figure 2.8 Activity of *sdsR* and *osmY* promoters during heat and osmotic shock. 24
Figure 2.9 Non-redundant alignment of the *sraC* promoter region. 26
Figure 2.10 Expression patterns of SdsR and SraC in *Salmonella*, *E. coli* and *Shigella*. 27
Figure 2.11 Interdependence of SdsR and SraC expression in *Salmonella* and *E. coli*. 28
Figure 2.12 SdsR down-regulates the *Salmonella* OmpD protein. 29
Figure 2.13 The SdsR 5' end is required for *ompD* regulation 31
Figure 2.14 Pulse expression of SdsR sRNA results in a rapid decrease of *ompD* mRNA levels. 32
Figure 2.15 Regulation of *ompD::gfp* reporter fusions by SdsR. 33
Figure 2.16 RNase E is essential for post-transcriptional repression of *ompD* mRNA by SdsR. 35
Figure 2.17 Hfq-dependent regulation of *ompD* under heat-shock. 36
Figure 2.18 3'RACE analysis of *ompD* mRNA fragments enriched upon SdsR expression. 37
Figure 2.19 Compensatory base-pair exchanges validate the SdsR-*ompD* mRNA interaction. 38
Figure 2.20 Repression of OmpD by an sRNA targeting the 5' UTR. 40
Figure 2.21 Expression of sRNAs regulating *ompD*. 41
Figure 2.22 The stringent response triggers SdsR-specific *ompD* mRNA decay. 42
Figure 2.23 RybB facilitates *ompD* mRNA repression during membrane stress. 43
Figure 3.1 Conservation and 5' end mapping of RydC. 45
Figure 3.2 Expression of *rydC* over growth. 46
Figure 3.3 Predicted secondary structures of RydC in different enterobacteria. 47
Figure 3.4 Predicted secondary structure of RydC and RydC mutants. 48
Figure 3.5 Stability of RydC and RydC variants. 49
Figure 3.6 RydC and RydC-K1 association with Hfq *in vitro*. 50

Figure 3.7 Whole cell protein patterns of wild-type and *rydC* mutant *Salmonella*. 51
Figure 3.8 Transcriptomic experiments identify *cfa* mRNA as a putative target of RydC. 52
Figure 3.9 Cfa::3xFLAG expression is activated by RydC. 53
Figure 3.10 Cfa is expressed from two independent promoters. 55
Figure 3.11 Regulation of *cfa::gfp* reporter gene fusions by RydC. 56
Figure 3.12 Conservation of the *cfa* gene in enterobacteria 57
Figure 3.13 Regulation of *Salmonella* and *Enterobacter cfa::gfp* fusions. 58
Figure 3.14 Analysis of the RydC-*cfa* mRNA interaction *in vivo*. 59
Figure 3.15 *In vitro* structure probing confirms RydC interaction site on *cfa* mRNA 60
Figure 3.16 A chimera carrying the RydC 5' end as a *cfa* mRNA regulator. 61
Figure 3.17 Regulation of mutant *cfa::gfp* reporter fusions in the presence of RydC. 62
Figure 3.18 Regulation of translational *cfa::ompX::gfp* fusion variants by RydC. 63
Figure 3.19 Toeprint formation on TSS1-*cfa-X::gfp* and *ompX* mRNAs. 65
Figure 3.20 Primer extension analysis of *cfa::gfp* mRNA in the presence of RydC. 66
Figure 3.21 Stability of *cfa* mRNA in the presence of RydC. 67
Figure 3.22 Effect of RNases on *cfa::gfp* expression in the presence of RydC. 68
Figure 3.23 Effect of RNase E on *cfa::gfp* expression in the presence of RydC. 70
Figure 3.24 5'RACE analysis of *cfa* mRNA fragments in the presence and absence of RydC. 71
Figure 3.25 *In vitro* cleavage of *cfa* mRNA by RNase E. 72
Figure 3.26 Specific inhibiton of *in vitro* cleavage of *cfa* mRNA by RydC. 73
Figure 3.27 Mapping of *cfa* mRNA cleavage sites *in vitro* 74
Figure 3.28 Regulation of Cfa::3xFLAG under stress. 75
Figure 3.29 Transcriptional *rydC* reporter fusions. 77
Figure 3.30 Activity of *rydC::gfp* reporter fusions in different mutants of the PTS. 80
Figure 4.1 Read coverage across the reference genomes. 84
Figure 4.2 cDNAs mapped onto the *sraC*/*sdsR* locus. 85
Figure 4.3 cDNAs mapped onto the *rydC* locus. 86
Figure 4.4 cDNAs mapped onto the *cfa* locus. 87
Figure 4.5 Regulation of translational *luxS::gfp* fusions by RydC-2 91
Figure 4.6 Determination of SdsR 5' ends. 93
Figure 4.7 Alignment of SdsR, truncated SdsR variants and SdsR chimera. 93
Figure 4.8 Regulation of STM3820*::gfp* 94
Figure 4.9 Alignment of *cfa* and *ompX* mRNAs 94
Figure 4.10 Alignment of RydC, TMA and RydC-TMA. 94
Figure 5.1 Distribution of targeting sites in the processed sRNAs SdsR, ArcZ and RprA 99
Figure 5.2 sRNAs under the control of alternative σ factors 102
Figure 5.3 Network of Hfq-dependent sRNA regulating outer membrane protein synthesis 104

10 List of Tables

Table 3.1 Transcripts deregulated 3-fold or more upon RydC pulse-expression. 52
Table 3.2 Screening experiments to identify a transcriptional regulator of *rydC*. 78
Table 4.1 Mapping of sequencing reads to the reference genomes. 82
Table 4.2 Annotation of 5' and 3' ends of SdsR, SraC, RydC and *cfa* mRNA. 88
Table 4.3 Transcripts deregulated 3-fold or more upon RydC-2 pulse-expression. 89
Table 6.1 Equipment and instruments. 118
Table 6.2 Consumables. 119
Table 6.3 Chemicals and commercially available systems. 119
Table 6.4 Enzymes and size markers. 121
Table 6.5 Purified proteins/ribosomes. 122
Table 6.6 Antibodies. 122
Table 6.7 Synthetic oligonucleotides. 122
Table 6.8 Bacterial strains. 125
Table 6.9 Plasmids. 129
Table 6.10 Antibiotics and media supplements. 135
Table 6.11 Probes for Northern blot detection. 149
Table 6.12 Washing conditions used for the different radiolabelled probes. 150
Table 6.13 Gene specific ladders for primer extension and 30S toeprint analysis. 151
Table 6.14 Templates for T7 *in vitro* synthesis. 152
Table 6.15 Employed software. 158

11 Curriculum vitae

12 Publications

Fröhlich KS, Papenfort K, Berger AA, Vogel J (2012) A conserved RpoS-dependent small RNA controls the synthesis of major porin OmpD. *Nucleic Acids Res* **40**(8)**:** 3623-3640

Papenfort K, Corcoran CP, Gupta SG, Miyakoshi M, Heidrich N, Chao Y, **Fröhlich KS**, Sharma CM, Ziebuhr W, Böhm A, Vogel J (2012) Regulatory Mechanisms of Special Significance: Role of Small RNAs in Virulence Regulation. In "Regulation of Bacterial Virulence". ASM Press, Washington, DC *doi:10.1128/9781555818528*

Eulalio A, **Fröhlich KS**, Mano M, Giacca M, Vogel J (2011) A candidate approach implicates the secreted Salmonella effector protein SpvB in P-body disassembly. *PLoS One* **6**(3)**:** e17296

Fröhlich KS, Vogel J (2009) Activation of gene expression by small RNA. *Curr Opin Microbiol* **12**(6)**:** 674-682

Manuscript in preparation:

Fröhlich KS, Papenfort K, Vogel J The conserved 5' end of RydC sRNA activates one of two isoforms of *cfa* mRNA.

13 Acknowledgements

Erklärung

gemäß § 4 Abs. 3 S. 3, 5 und 8 der Promotionsordung der Falkultät für Biologie der Bayerischen Julius-Maximilians-Universität Würzburg

Hiermit erkläre ich, dass ich die vorliegende Dissertation

"**Assigning functions to Hfq-dependent small RNAs in the model pathogen *Salmonella* Typhimurium**"

selbständig angefertigt habe und keine anderen als die von mir angegebenen Quellen oder Hilfsmittel benutzt habe.

Ich erkläre außerdem, dass diese Dissertation weder in gleicher noch in anderer Form bereits in einem Prüfungsverfahren vorgelegen hat.

Ich habe früher, außer den mit dem Zulassungsgesuch urkundlich vorgelegten Graden keine weiteren akademischen Grade erworben oder zu erwerben versucht.

Würzburg, den 02.10.2012 _____

Kathrin Fröhlich